University of New Hampshire
University of New Hampshire Scholars' Repository

Doctoral Dissertations | Student Scholarship

Spring 2015

Survey of the charge properties of phospholipids using Nanodiscs and Membrane-confined electrophoresis

Cheng Her
University of New Hampshire, Durham

Follow this and additional works at: https://scholars.unh.edu/dissertation

Recommended Citation
Her, Cheng, "Survey of the charge properties of phospholipids using Nanodiscs and Membrane-confined electrophoresis" (2015). *Doctoral Dissertations*. 2194.
https://scholars.unh.edu/dissertation/2194

This Dissertation is brought to you for free and open access by the Student Scholarship at University of New Hampshire Scholars' Repository. It has been accepted for inclusion in Doctoral Dissertations by an authorized administrator of University of New Hampshire Scholars' Repository. For more information, please contact nicole.hentz@unh.edu.

SURVEY OF THE CHARGE PROPERTIES OF PHOSPHOLIPIDS USING NANODISCS AND MEMBRANE-CONFINED ELECTROPHORESIS

BY

Cheng Her
B.A., Chemistry, Assumption College, 2009
B.A., Biology, Assumption College, 2009

DISSERTATION

Submitted to the University of New Hampshire
in partial fulfillment
of the Requirements for the Degree of

Doctor of Philosophy

in

Biochemistry

May, 2015

This dissertation has been examined and approved in partial fulfillment of the requirements for the degree of Doctor of Philosophy in Biochemistry by:

Dissertation Director, Thomas M. Laue
Professor of Biochemistry and Molecular Biology

Rick H. Cote
Professor of Biochemistry and Molecular Biology

Feixia Chu
Assistant Professor of Biochemistry and Molecular Biology

David B. Hayes, Principal Scientist
Boehringer Ingelheim

Walter F. Stafford, Senior Scientist (retired)
Boston Biomedical Research Foundation

April 9, 2015

Original approval signatures are on file with the University of New Hampshire Graduate School.

DEDICATION

To my parents, who in their darkest hours, still worried more about me than themselves. None of this would be possible without you and your support. With all the sacrifices you have made for my sake, this accomplishment is as much yours, as it is mine. To my grandmother, who would, without fail, wait at the corner of my elementary school to walk me home in one of the most dangerous neightborhoods of South Providence, RI. May you be smiling down upon me wherever it is you are now.

ACKNOWLEDGEMENTS

"I find I'm so excited that I can barely sit still or hold a thought in my head. I think it's the excitement only a free man can feel. A free man at a start of a long journey whose conclusion is uncertain. I hope I can make it across the border. I hope to see my friend and shake his hand. I hope the pacific is as blue as it has been in my dreams. I hope."

- Ellis Boyd "Red" Redding *The Shawshank Redemption (1994)*

I imagine this is what every graduate student feels after their defense; it's certainly how I felt after six years. In graduate school, most people will remember the large milestones: 1) the acceptance, 2) passing all the qualifying exams, 3) the defense, and, 4) the graduation. However, the people I've met, the friends I've made, the experiences I've had, the mentors I've learned from and the students I've taught in these six years is what I'll remember the most. People always say, "you'll find yourself, one day", and I think I found myself in graduate school. I certainly do have some regrets in my high school and undergraduate college experience. My focus was solely on getting good grades, that I let some opportunities pass me by. But I leave graduate school with no regrets. I took far more chances than I normally would have and it paid off in spades. Not that every risk resulted in success, because there were plenty of failures as well. However, even in the face of failure, taking that first step is the most difficult and rewarding. I rediscovered my love of cycling and one day woke up, found an ad on craigslist and then drove 3 hours to Bethlehem, NH to buy the bike. I improved my musicianship considerably by rededicating myself to playing guitar and piano and one day woke up and decided to start a video game orchestra; something I'd wanted to do for a long time, but never had the courage to do so. I finally took Ms. Frizzle's advice to heart, I stopped waiting for others and jumping on their bandwagons and initiated things myself.

When I started graduate school, I had no expectations of success or failure. I do not consider myself particularly smart or intelligent, and am not necessarily the hardest working

graduate student. I mean, I've had my share of being in the lab for 24+ hours at a time, but there have been other graduate students that have put in a greater number of hours in the lab than I. However, being supremely intelligent or putting in an incredible amount of work into a research project does not guarantee success. In graduate school, as in life, you will fail, it is an inevitability. The most important thing, is how you deal with failure. Failure is always an incredibly humbling experience and can often times cripple our confidence and shake us to our very core. I am very lucky to be surrounded by such wonderful people, and it is no exaggeration to say that without all my friends and family supporting me on my journey through graduate school, my failures would remain just that, failures.

I would first like to thank Tom. Why he took a chance on a "hot-shot punk" like me, I'll never know, but I am grateful. If ever there were a lab that fit my style and personality, I don't think I could find a better on than the Laue Lab. Tom's enthusiasm and energy is incredible and without his guidance, I would have been hopeless. Because of Tom, I took a detour in my scientific career that I otherwise would normally have avoided. I generally hate travel and once I am in a comfort zone, I tend to go on cruise control. But Tom suggesting that I uproot everything (and after only being in the lab for one semester) and apply for an internship position in Gaithersburg, MD resulted in one of the best experiences of my life. It greatly improved some skills that I lacked as a scientist and a person. It was one of the most humbling experiences in my life. Thank you Tom!

The Laue lab also would not be the Laue lab without the two Sues, both who helped me so much and treated me like your own son. Both of you chastised me for getting into trouble, such as a speeding ticket that forced me to miss a lab meeting, and gave me words of encouragement when I needed them. Sue Chase lost her battle with cancer, but her influence

will live on. She was the reason I initially chose to work with Tom. During the presentations of potential advisors for first-year graduate students, Sue, in Tom's stead, made a couple *Back to the Future* references during her talk. I knew then that I would fit in just fine with the wonderful people in the Laue lab. She also made a comment during one of my presentations that I did not have enough *Back to the Future* references. This is why I try to include as many as I can in future talks. Sue Lucius was the glue that held together the Laue Lab. It was because of her that all of us graduate students were able to solely focus on the science. I always thought of Sue as the Pauly Cicero (from *Goodfellas*) of our lab. Everything would go through her, and when something needed to be done, she was the person to go to, and it would be done. Even through some of her darkest times, she was still taking care of us. That sort of kindness is immeasurable and something I have never forgotten and will never forget. How she put up with us I will never know. We literally could not function without her. Thank you.

I would also like to thank the rest of the members of the Laue lab. There have been quite a few undergraduates and graduates that have worked in the Laue lab since I've been here. We may not have worked on the same projects, but the camaraderie was second to none. I hope that each one of you finds success and happiness. Thank you, Katie, Andraya, Feier, Anthony, Kiara, Joe Kadina, Jack, Alex, Carrie, Dana, Rae, Danlin and Ron.

In addition, I am indebted to Dr. Stephen G. Sligar and Dr. Mark McLean, without whom, this project would still be stuck in first gear. They took a chance on us and sent us our first Nanodisc^{TM} samples that sent us on our way. Their enthusiasm as this project started really inspired us to take this project as far as we could, which it seems now has no end in sight.

To my committee members, Rick Cote, David Hayes, Walter Stafford, Clyde Denis and Feixia Chu. Thank you for all the comments, criticisms, words of encouragement and help. The

truth hurts sometimes (well, mostly all the time), but it helped me focus my research and write my dissertation. In addition, my qualifying exams were some of the best worst experiences of my life, but what I learned from those shortcomings was immense. It is true what they say, you do learn much more from your failures, than you do from your successes.

I would also like to thank my friends, especially Wes, Kristina and Olivia, whose support and confidence was unwavering (even in the face of the truth!). Thank you for keeping me sane with our crazy email chains, cards of support and for playing some great music together. I only hope that I have been as good a friend to you, as you have been to me.

To the Cote lab members, especially Karyn for putting up with me early on while I worked on the recombinant MSP expressions. To Laurie Westover, for helping me out immensely, even though we did not get off on the right foot, as I was pretty cavalier early on. But you scolded me when you should have and never let me off the hook, which I appreciated, because I thoroughly deserved it. To all my students, you inspired me more than you could ever know.

To Alan Eaton, Patty Bedkar, Ed Tillinghast and the rest of the faculty on the second floor of Spaulding Hall. Whether it was giving me fruit that was farm fresh, giving me reassurance and advice, or just engaging in a friendly conversation, it made me feel welcome to have such friendly people to talk to on a daily basis.

To the St. Michael's Hmong and lay community in Rhode Island, who helped us get on our feet when my family and I first arrived in the United States. This is dedicated in particular, to Sr. Ann Keefe, who lost her battle with cancer in January, and Fr. Bill Tanguay.

To my family, especially my parents. We may not be the perfect singing kumbaya by the fireplace family, but I wouldn't trade you for the world.

This acknowledgements section may have dragged on, but it isn't only about the people who helped me in graduate school. This is a thank you to everyone that has helped me in my 28 years of life, not just the last 6 years of graduate school.

"Everything that has a beginning, has an end"

- The Oracle *The Matrix Revolutions (2003)*

Table of Contents

LIST OF ABBREVIATIONS

$10PIP_2$	10% PIP_2 Nanodiscs
10POPA	10% POPA Nanodiscs
10POPS	10% POPS Nanodiscs
10POPE	10% POPE Nanodiscs
30POPA	30% POPA Nanodiscs
30POPS	30% POPS Nanodiscs
70POPA	70% POPA Nanodiscs
70POPS	70% POPS Nanodiscs
AU	Absorbance units
AUC	Analytical ultracentrifugation
BSA	Bovine serum albumin
CE	Capillary electrophoresis
COG	Center of gravity
DLS	Dynamic Light Scattering
DMPC	1,2-dimyristoyl-***sn***-glycero-3-phosphocholine
DMPE	1,2-dimyristoyl-***sn***-glycero-3-phosphoethanolamine
dsDNA	Double stranded DNA
DOPC	1,2-dioleoyl-***sn***-glycero-3-phosphocholine
DOPS	1,2-dioleoyl-***sn***-glycero-3- phospho-L-serine
DPPC	1,2-dipalmitoyl-*sn*-glycero-3-phosphocholine
DSPC	1,2-distearoyl-***sn***-glycero-3-phosphocholine
DSPE	1,2-distearoyl-***sn***-glycero-3-phosphoethanolamine
ELS	Electrophoretic light scattering
EM	Electrophoretic mobility
ER	Endoplasmic reticulum
FVIIa	Factor VIIa
GC	Gas Chromatography
HDL	High density lipoproteins
HEPES	4-(2-hydroxyethyl)-1-piperazineethanesulfonic acid
ITC	Isothermal titration calorimetry
K_{IR}	Inwardly rectifying potassium channels
MCE	Membrane-confined electrophoresis
MOPS	3-(N-morpholino)propansulfonic acid
MS	Mass Spectrometry
MSP	Membrane scaffolding protein
MWCO	Molecular weight cutoff
ND	Not determined
NMR	Nuclear magnetic resonance
PA	Phosphatidic Acid

PBS	Phosphate buffered saline
PC	Phosphatidylcholine
PE	Phosphatidylethanolamine
PEG	Polyethylene glycol
PG	Phopshatidylglycerol
PI	Phosphatidylinositol
PIP	Phosphatidylinositol 4-phosphate
PIP_2	Phosphatidylinositol 4,5-bisphoshate
PIP_3	Phosphatidylinositol (3,4,5)-trisphosphate
PS	Phosphatidylserine
PL	Phospholipid
POPA	1-palmitoyl-2-oleoyl-*sn*-glycerco-3-phosphate
POPC	1-palmitoyl-2-oleoyl-*sn*-glycerco-3-phosphocholine
POPE	1-palmitoyl-2-oleoyl-*sn*-glycerco-3-phosphoethanolamine
POPS	1-palmitoyl-2-oleoyl-*sn*-glycerco-3-phospho-L-serine
ssDNA	Single stranded DNA
SOPC	1-stearoyl-2-oleoyl-***sn***-glycero-3-phosphocholine
TLC	Thin-Layer Chromatography
TF	Tissue factor
TNPh	2,4,6-trinitrophenol or picric acid
Tris	Tris(hydroxymethyl)aminomethane
UV	Ultraviolet
Z_{DHH}	Debye-Huckel Henry charge

LIST OF SCIENTIFIC TERMS

k_B	Boltzmann's constant
T	Temperature
Å	Angstrom
R_s	Stokes Radius
μ	Electrophoretic mobility
f	Frictional coefficient
D	Debye
f(κa)	Henry's Function
Q_p	Fundamental proton charge
$\bar{\upsilon}$	Partial specific volume
esu	Electrostatic units
c-c	Center -to-center
M_b	Buoyant molecular weight
mS	millisiemens
cρ	centipoise
V	Volts
κ	Inverse Debye Length
K^{-1}	Binding constant
$S_{20,w}$	Corrected sedimentation coefficient to a standard of water at 20^oC

ABSTRACT

SURVEY OF THE CHARGE PROPERTIES OF PHOSPHOLIPIDS USING NANODISCS AND MEMBRANE-CONFINED ELECTROPHORESIS

by

Cheng Her

University of New Hampshire, May, 2015

Phospholipids (PL) are a major, diverse constituent of cell membranes. PL diversity arises from the nature of the fatty acid chains, as well as the head group structure. The head group charge is thought to contribute to both the strength, and specificity of protein-membrane interactions. Furthermore, the divalent cations Ca^{2+} and Mg^{2+}, have been shown to be essential for optimal binding for some of these interactions. Because it has been difficult to measure membrane charge, it has been impossible to quantitate the role charge plays in these interactions. However, Nanodiscs provide a stable, planar membrane bilayer suitable for biophysical studies. Here we present the first measurements of the charge on Nanodiscs containing neutral (POPC and POPE) and anionic (POPS, POPA, and PIP_2) PLs in varying ratios, and in different solvent conditions. The data reveal that: 1) Nanodiscs provide high-quality charge data using membrane-confined electrophoresis (MCE), and; 2) Nanodiscs exhibit polyelectrolyte behavior. Therefore, the technique of MCE combined with the technology of Nanodiscs give us the ability to develop a simple, reproducible way to analyze lipid charge under physiological conditions; which can clarify inconsistencies between data obtained using various analytical techniques, membrane systems, and experimental conditions.

INTRODUCTION

Charge is a fundamental property that directly influences the structure, stability, solubility and interactions of macromolecules [Edsall and Wyman, 1958; O'Brien and White, 1978]. Since the solution electrostatic properties of a molecule are affected by the solvent composition (i.e. ionic strength, ion type, etc.), pH, dielectric constant and temperature, charge is a system property. Charge estimates based on amino acid sequences [Scatchard and Black, 1948; Gokarn et al., 2011], nucleotide sequences [Wooll, 1996; May, 2007] and lipid head groups [Roy et al., 1998] are typically higher in magnitude than their experimental counterparts. The discrepancy between calculation and measurement seems to result from the failure of calculations to consider ion binding aside from H^+ [Gokarn et al. 2011]. While there are good charge measurement data for proteins and nucleic acids [Durant, 2003; May, 2007], charge measurement of lipids have posed experimental difficulties. This lack of knowledge is unfortunate because membrane composition, including charge, is of fundamental importance to a variety of cellular and physiological functions [Tavoosi et al., 2011]. The research in this dissertation provides the first systematic measurement of lipid charge. These charge measurements will provide the information needed to test hypotheses and models for lipid membrane structure and function [Saiz and Klein, 2002; Gurtovenko and Vattulainen, 2008].

For proteins and DNA, charge measurements using different methods are straight forward and provide similar results [Schwartz and Guttman, 1995]. The reason for the relative ease of measurements, is that near physiological conditions may be found where these molecules do not interact with the container in which the measurement is made (i.e. capillaries, cuvettes, etc.), whereas lipids tend to bind tightly to glass surfaces [Owens et al., 2005]. As a consequence,

proteins and DNA usually do not require non-aqueous solvent phases in analytical electrophoretic techniques, such as capillary electrophoresis (CE) and electrophoretic light scattering (ELS) for charge measurements; whereas lipids often do [Krylov and Dovichi., 2000]. Charge measurements of proteins and nucleic acids made in a CE apparatus can be compared with measurements made using other electrophoretic techniques, such as MCE and ELS run in the same solvent [Krylov and Dovichi., 2000; Filoti et al., 2015]. This allows for more accurate measured charge quantities (i.e. electrophoretic mobility, zeta potential, Z_{DHH}) when a direct comparison of these quantities can be made across different electrophoretic techniques in the same solvent conditions.

Because of their high charge density, some proteins and nucleic acids, in general, exhibit polyelectrolyte behavior. Polyelectrolytes have seemingly counterintuitive properties; for a 100-base ssDNA, the expected charge is about -20, whereas a dsDNA will have an expected charge of only -12, even though there are more phosphate groups in the dsDNA [Record et al. 1987; Manning, 1969]. The cause of the reduced charge in dsDNA, is the higher charge density of the phosphate groups in dsDNA in comparison to ssDNA. As a result of the higher charge density, more counter-ion binding is required to minimize the electrostatic potential that gives rise to the lowered expected charge for dsDNA. This effect is more pronounced in dsDNA due to the rigid nature of its structural backbone and the closer proximity of the phosphate groups [May, 2007; Dessinges et al., 2002]. Polyelectrolyte behavior also is observed in a variety of proteins [Durant, 2003; Collins, 2012].

The relevant parameter for polyelectrolyte behavior is the Bjerrum length [l_B; Manning, 1969], which is the effective distance between charge groups that yield an electrostatic potential energy that is equal in magnitude to the thermal energy (k_BT). In an aqueous system at 298K, the

Bjerrum length ($l_{B\text{aqueous}}$) is 7.0 Å [Morfin et al. 2004]. For a dsDNA molecule, the distance between phosphate groups is ~ 1.7 Å, significantly shorter than the $l_{B\text{aqueous}}$, giving rise to its high charge density [van der Maarel, 2008]. As a result of this high charge density, counter-ions will adsorb onto the phosphate groups of dsDNA until the effective distance between the charged groups is increased to $l_{B\text{aqueous}}$. In a membrane, the closest approach of lipid head groups is on the order of $l_{B\text{aqueous}}$ [Levental et al., 2008]. Therefore, if anionic lipids cluster on the membrane leaflet, polyelectrolyte behavior may be observed.

Lipids, in the form of liposomes, have been much more difficult to analyze electrophoretically due to their relative instability and tendency to aggregate and interact with glass [Heiger, 1992]. In CE, liposome interactions with a glass capillary are usually remedied using two methods. First, the capillary is coated with non-polar hydrophobic groups [Heiger, 1992]. Unfortunately, the resultant hydrophobic surfaces may interact with neutral lipids and prevent the liposomes from migrating. Consequently, a second remedy is to add an organic solvent to the aqueous solution to prevent liposomes from sticking to the capillary walls [Schmitt-Koplin, 2008]. While organic-containing solvents allow the migration of liposomes in CE, the solvent also may interact with the liposomes and affect the charge, thus making it difficult to compare charge estimates made in CE with those from methods that use solely aqueous conditions (e.g. NMR and native gels). Furthermore, the addition of an organic solvent also lowers the solvent dielectric constant, which will impact the measured charge [Heiger, 1992]. Liposomes provide two other challenges. First, they tend to be heterogeneous with respect to size and composition [Antonelli and Forster, 2003]. Second, they are unstable due to liposome fusion. Two recent advances have made lipid charge measurements feasible.

First, the development of lipid Nanodiscs has provided science with a stable membrane platform suitable for electrophoretic charge measurements [Bayburt and Sligar, 2011]. Nanodiscs provide a phospholipid bilayer system stabilized by a pair of membrane scaffolding proteins (MSP) that act like a belt around the lipid bilayer [Nath et al. 2007]; these scaffolding proteins provide two significant advantages over liposomes. First, the MSPs are negatively charged and provide enough electrostatic repulsion to prevent the Nanodiscs from self-associating. Second, these proteins allow us to track the migration of the Nanodiscs with UV optics. Using membrane confined-electrophoresis (MCE) in addition to lipid Nanodiscs should allow us to make meaningful charge measurements in physiologically relevant conditions.

Second, MCE has been shown to provide accurate charge measurements on molecules rapidly, using small quantities of material and in physiological solvents [Ridgeway et al., 1998; Durant, 2003; Filoti et al., 2015]. MCE is a primary technique that relies on first principle methods, and does not require appropriate markers or standards for data analysis. In contrast, other electrophoretic techniques such as CE and native gel analysis do require standards for estimation of the charge. By using lipid Nanodiscs and MCE, it is possible to characterize lipid charge systematically.

Liposomes versus Nanodiscs: Liposomes are generally difficult to prepare [Ritchie et al., 2009]. Furthermore, liposomes have been difficult to use in biophysical experiments due to their relative instability and size heterogeneity [Ritchie et al., 2009]. In order to stabilize liposome preparations, the lipids often are modified (e.g. PEG coating, head group derivitization), making them fundamentally different in structure and, ultimately, function from cellular membranes [Immordino et al., 2006]. Another impediment to working with liposomes is that, unless chemically modified, lipids typically lack structural elements that can be detected by UV

spectroscopy. Often, gas chromatography (GC) and mass spectrometry (MS) are required for quantification and identification. For non-volatile lipids, thin-layer chromatography (TLC) may be used [Wilson and Poole, 2000].

Nanodiscs have been shown to be very stable [Bayburt and Sligar, 2010]. The data indicate that at 4^{o}C they remain generally monodisperse over a period of four years. Nanodiscs, are smaller in diameter (~ 10 nm) than liposomes and their size can easily be managed by simply modifying the length of the MSPs [Ritchie et al., 2009]. Because the MSPs are part of the Nanodisc^{TM} structure, Nanodiscs can easily be tracked using the UV absorbance of the protein.

Charge estimates by other techniques: In the past, lipid:ion behavior has been explored using methods other than analytical electrophoresis. For example, one widely accepted model for Ca^{2+} interactions with phosphatidylcholine (PC) lipids, consists of one Ca^{2+} ion binding and bridging two phosphate groups on PC membranes [Altenbach and Seelig, 1984]. This model was developed from a combination of nuclear magnetic resonance spectroscopy (NMR) and atomic absorbance spectroscopy (AA) measurements made in solutions with 0.005 - 8 M Ca^{2+} using heterogeneous (10 – 100 nm diameter) liposome mixtures. With rare exception, lipids never experience Ca^{2+} concentrations exceeding 5 mM [Takahashi et al. 1999]. Therefore, the relevance of the NMR data to lipid charge *in vivo* is questionable. Furthermore, the authors' assertion that the shift in NMR signal provides a measure of the charge is based on calculations made using unsubstantiated assumptions concerning the nature and meaning of the chemical shift observed in NMR. For example, the authors assume that the mode of Ca^{2+} binding remains constant (i.e. Ca^{2+} forms specific complexes with the phosphocholine portion of PC lipids). A consequence of this assumption is that signal shifts observed in NMR spectra are attributed solely to Ca^{2+}- lipid binding and any considerations of preferential solvation effects, monovalent

ion adsorption, proximity effects, etc. are ignored. This is problematic, as the observed signal splitting of the NMR spectra of POPC liposomes occurred when Ca^{2+} concentrations were greater than 2 M, where preferential solvation and proximity effects can have a greater influence on the position of the phosphocholine group due to the c-c distance of Ca^{2+} ions being less than $l_{B\text{aqueous}}$ at these high concentrations [Manning, 1969; Morfin et al. 2004].

Another technique used to address lipid charge is capillary electrophoresis (CE). As previously stated, CE often requires addition of an organic solvent or special treatment to the capillary [Schmitt-Koplin, 2008]. Since charge is a system property, solvent changes, particularly the inclusion of organic components may impact the physiological relevance of the data. Both the technique of real-time electrophoretic mobility and Nanodisc^{TM} lipid membrane models are relatively new technologies [Jordan, 2014; Ridgeway, 1998; Ritchie et al., 2009]. Having a stable and well characterized membrane model [Nath et al. 2007], as well as the ability to rapidly conduct analytical real-time electrophoretic mobility analysis can give us better insight to the charge properties of lipids.

SIGNIFICANCE

Importance of membrane charge to biological processes: Membrane electrostatics plays an important role in many biological processes. In the blood coagulation cascade, tissue factor (TF) cannot bind factor VIIa (FVIIa) unless anionic lipids and Ca^{2+} are both present [Tavoosi et al. 2011]. In metabolism, the membrane phospholipids of both the inner and outer membrane of mitochondria play an important role in the energy transduction pathways of the electron transport chain found in eukaryotes. The inner membrane contains a higher protein:lipid (80:20 versus 50:50) ratio, twice the amount of anionic lipids and three times the amount of cardiolipin than the outer membrane [van Meer et al., 2008]. Membranes containing phosphatidyl 4,5-bisphospate (PIP_2) act in concert with Ca^{2+} playing an important role in the signal transduction cascades of protein kinase C [Newton, 2010]. Anionic lipids also have an important role in bone formation and repair as they bind Ca^{2+} and stabilize amorphous calcium phosphate as it is converted to hydroxyapatite [Merolli and Satin, 2009].

Importance of this work: The dissertation represents the first systematic measurements of membrane charge using analytical electrophoretic techniques. These lipid studies will complement those done with proteins [Durant, 2003] and nucleic acids [May, 2008]. Lipid bilayers in Nanodiscs are fluid, allowing the charge elements to arrange themselves in the lipid monolayer. Membrane lipids are known to cluster into microdomains ("rafting"), and such clustering is known to be important to membrane function [Thomas et al., 2004]. In particular, the increased density of anionic lipids in microdomains is thought to be important in modulating

activation and interactions in blood coagulation, receptor-ligand interactions and signal transduction [Tavoosi et al. 2011; Owen et al. 2005; Scherer and Seelig, 1989].

Theoretical work with respect to describing charge on membranes has mostly relied on models and molecular dynamics simulations that use incomplete experimental work that is difficult to interpret [Manning, 2007; Collins, 2012]. Furthermore, while many experiments have shown the necessity for ion-mediated lipid-lipid, lipid-protein and protein-protein interactions, not much is known about the mechanisms by which these interactions occur. For example, it's been observed that Ca^{2+} and Mg^{2+} can induce both membrane fusion and aggregation [Martin-Molina et al., 2012]. The proposed mechanism for these interactions is that Mg^{2+} and Ca^{2+} can interact with groups on the membrane surface, neutralizing the charges on anionic lipids or proteins at the membrane surface, thereby decreasing the electrostatic repulsion between cellular membranes and allowing them to aggregate and potentially undergo fusion [Roy et al, 1998]. However, most of these aggregation/fusion studies focus on the success or failure of aggregation/fusion, not an underlying cause.

This dissertation addresses the underlying cause by measuring the charge on a variety of lipids in different solvents. In the proximity energy framework, it is observed that charge-charge repulsion is the only electrostatic interaction that benefits solubility [Majhi et al., 2005]. In accord with this observation, it has been shown that proteins tend to aggregate at their isoelectric point, and that solubility generally correlates with charge [Majhi et al., 2005]. However, other solvent conditions can lead to aggregation, and correlating the charge on molecules with the changes in the buffer conditions can provide insight as to why this aggregation occurs

when anionic lipids interact with divalent cations Mg^{2+} and Ca^{2+}.

It is known that the simple calculation of charge made by summing the charges on ionizable groups is not a reasonable first approximation for charge. It has already been shown with proteins and DNA that the measured charge is lower in magnitude than that of the expected charge [Durant, 2003; May, 2008]. However, while there has been a lot of research done on protein and DNA charge, there has not been much physical data on lipids in physiologically relevant solvent conditions. Combining moving-boundary electrophoretic instrumentation (MCE) and stable lipid membrane models (Nanodisc^{TM}) will provide insights into the effect charge has on lipid assembly interactions.

RESEARCH OBJECTIVES

The objectives of this work are: 1) to measure Nanodisc^{TM} charge for different lipid compositions in different solvents using MCE, 2) to compare these direct charge measurements with estimates using other indirect methods, and 3) integrate these charge data into theoretical and molecular models. These objectives will be addressed using the following specific aims.

Aim 1: Measure the charge of lipid Nanodiscs using MCE in physiologically relevant buffers. Historically, lipid charge has been difficult to measure, and there are few first principle measurements reported [Schmitt-Koplin, 2008]. Nanodisc^{TM} charge will be measured using: 1) two different sizes of Nanodisc^{TM}, 2) Nanodiscs containing different mole ratios of neutral (phosphatidylcholine- PC, phosphatidylethanolamine- PE) lipids and 3) Nanodiscs containing anionic lipids (phosphatidic acid- PA, phophatidylserine- PS, and phosphatidyl 4,5-bisphosphate- PIP_2 and 4) in solvents containing different co-ions and counterions. In all cases, the phospholipids will have 1-palmitoyl-2-oleoyl-*sn*-glycerco-3-X (denoted PO-X, with X

representing the head group), as the fatty acids so that the membranes will generally be above their phase transition temperature. This aim will assess the extent of Nanodisc^{TM} heterogeneity with respect to charge. Furthermore, the data will provide standards that can be duplicated in other laboratories.

Aim 2: Observe solvent ion type, salt concentration and pH effects on lipid Nanodisc^{TM} charge. Charge is a system property and therefore dependent on the solvent composition. In this aim, the solvent composition will be varied as follows:

Ion Type. Different ion types may interact differently with Nanodiscs due to ion-specific variations in charge density, electronegativity, orbital orientation and the presence of interaction sites on the Nanodiscs [Klasczyk et al., 2013] These ionic interactions will affect the electrophoretic mobility and subsequent Z_{DHH} calculations. Nanodisc^{TM} mobility and Z_{DHH} will be determined for several Nanodisc^{TM} lipid compositions in 50 mM Tris, pH 7.4, containing varying concentrations of Na^+, K^+, Li^+, Mg^{2+}, Ca^{2+}, and SO_4^{2-}. Measurements will be made with Nanodiscs containing varying mole ratios of PA, PS, PE, PC, and PIP_2.

Salt concentration. Excluding the Debye-Huckel cloud, which is a solvent response to the charge on a macromolecule, ion binding may take two forms. One form is specific binding, in which an ion interacts with a well-defined site on the lipid surface. When bound in this manner, the ion will be visible as part of the structure in X-ray crystallography and NMR spectroscopy [Altenbach and Seelig, 1984]. The second form is territorial binding, in which an ion is held by electrostatics in an area adjacent to a highly charged region on a macromolecule, but does not bind to a particular site [Manning, 1969]. This sort of binding is common in polyelectrolytes such as protein and DNA [O'Shaughnessy and Yang, 2005]. An ion bound in this manner may

exchange readily with ions in the solvent, but cannot dissociate to leave the charged patch exposed. Though part of the charge structure, territorially bound ions are mobile over the charged surface and do not appear in X-ray or NMR structures. In order to determine whether Nanodiscs bind counterions territorially (i.e. act as polyelectrolytes), the charge on Nanodiscs of varying lipid compositions will be determined as a function of salt concentration.

pH. Lipid head groups may contain multiple charge groups which ionize at different pHs. Phosphatidic acid is of particular interest, because it contains two ionizable groups, one with a pKa ~ 3.0 and another with a pKa ~ 8.0, with the latter near physiological pH [Marsh, 1990]. Mobility and Z_{DHH} data will be obtained on PA-containing Nanodiscs to determine the dependence of charge on pH. Similar studies will be conducted on PC, PE, PS, PA and PIP_2 Nanodiscs to distinguish head-group-specific from belt-protein specific contributions to any charge change.

MATERIALS AND METHODS

Nanodiscs — Nanodiscs were obtained from Dr. Mark McLean of the Sligar group at the University of Illinois at Urbana-Champaign and Dr. Sandy Ross of the University of Montana. Initial concentrations of POPC, 10% POPS, 30% POPS and 70% POPS (referred to as 10POPS, 30POPS and 70POPS, respectively) MSP1D1 and MSP1E3D1 Nanodiscs were ~ 20 uM. Initial concentrations of MSP1D1 10% POPA, 30% POPA and 70% POPA Nanodiscs (referred to as 10POPA, 30POPA and 70POPA respectively) were ~ 10 uM. Initial concentrations of MSP1D1 10% POPE and 10% PIP2 (referred to as 10POPE and 10PIP_2, respectively) Nanodiscs were ~ 8 uM. Nanodisc^{TM} formulation buffer was as follows: 100 mM NaCl, 50 mM Tris(hydroxymethyl)aminomethane) [Tris], 0.1% NaN_3 at pH 7.4. Nanodiscs were initially stored in a -20^{o}C freezer. Stock samples were aliquoted in 50 uL amounts into Fisherbrand microcentrifuge tubes (Premium, 500 uL, mixed, Cat No. 05-408-137, Lot 10210771) and stored at -20^{o}C. When samples were taken out and thawed for analysis, they were re-stored at 4^{o}C.

Buffers—Standard buffer consisted of 100 mM NaCl (Sigma-Aldrich, S7653, BioXtra ≥ 99% (AT), Lot # SLBJ2691V, CAS: 7647-14-15), 50 mM Trizma®base (Sigma-Aldrich, Primary Standard and Buffer ≥99%(titration), crystalline, T1503, Lot # SLBH5708V, CAS: 77-86-1) at pH 7.4. In buffers consisting of different monovalent ions, the concentration of the salt was kept constant: 100 mM KCl (Sigma-Aldrich, P9541, for molecular biology, ≥ 99.0%, Lot # SLBD2274V, CAS: 7447-40-70 and 100 mM LiCl (Aldrich, 99+% A.C.S. Reagent, CAS: 7447-41-8). PBS buffer prepared from constituent component consisted of: 137 mM NaCl, 2.7 mM KCl, 10 mM Na_2HPO_4 (Sigma, S-0876, Dibasic, Anhydrous, Minimum 99%, Lot 29H0002, EC No. 231-448-7) and 1.7 mM KH_2PO_4 (Fisher Scientific, P-285, Certified A.C.S, Lot 784276) at pH 7.4. In divalent cation experiments, 3 mM of either $MgCl_2$ (Sigma-Aldrich, M2670, BioXtra

≥ 99.0%, Lot # SLBD6918V, CAS: 7791-18-6) or $CaCl_2$ (Baker Analyzed REAGENT, Granular, Actual Analysis Lot # 646135) was added to standard buffer. Experiments using 0.007 - 10 mM $MgCl_2$ and $CaCl_2$ were also conducted to determine whether or not similar interactions were seen at minimal and saturated Mg^{2+} and Ca^{2+} concentrations (**Figures B2 - B5**). For dilution experiments, the total combined NaCl and Tris concentrations used were 50, 75, 100, 125, 150 and 225 mM, with the ratio of salt to buffer maintained at 2:1. Experiments were run at lower salt concentrations, however it was determined that salt concentrations below 50 mM were not sufficient for MCE analysis. For experiments where pH was varied, the standard buffer was used and titrated to the desired pHs (7.00, 7.40, 8.00 and 8.50 ± 1.0 x 10^{-3}) with a 6N solution of HCl (Sigma-Aldrich, 37%, 258148-2.5 L-GL, A.C.S Reagent, Pcode 4100462796, Lot # SHBB1294V, CAS: 7647-01-0) using a Corning pH/ion analyzer 355 (Serial C1139) with an Orion Triode™ pH electrode (Model: 91-57BN). Initially, water obtained from a NANOpure™ system was used to make all buffers. However, on April 24th, 2014, water from a Milli-Q system was used thereafter. All buffers were filtered using a sterile Autofil PES bottle top filtration device (500 mL, 0.22 um PES unit, PN 1102-RLS, Lot # 400011496) and then stored at 4°C until use.

Membrane confined-electrophoresis—All measurements were initially carried out in an MCE apparatus (Spin-Analytical, [Laue et al., 1989]) in standard buffer. Membranes used were Spectra/Por molecularporous membrane tubing with a MWCO of 6-8 kDa (Serial: 26872). Membranes were prepped according to Laue et al. (1989). Biotech grade membranes from Spectrapor were also used, but due to inconsistent run-to-run variability, were eschewed in favor of normal dialysis Spectrapor membranes. Like all electrophoretic techniques that use glass surfaces, MCE cuvettes are typically silanized to minimize electroendoosmosis [Ridgeway et al.

1998]. A single silanization treatment can last a long time (>6 months) with no loss in data quality. Thoroughly washing and rinsing the cuvette with alternating water, 1% Hellmanax and isopropyl alcohol was sufficient to prepare the cuvette for another experiment. This simple protocol was used for extended periods of time without requiring re-silanization. Furthermore, there was no observed "sticking" of the Nanodiscs to the cuvette wall. After the sample was loaded and the cell assembled, each sample was dialyzed for 24 hours before the experimental run. A total of three sequential runs were performed per sample, with a 24 hour period used to re-equilibrate the Nanodisc^{TM} concentration. After three sequential runs, we observed fluctuations in the data, presumably due to material build up at the bottom membrane, and the resultant deterioration of membranes as neutral porous structures. In order to increase throughput, after 9 runs (triplicate runs of 3 per sample); dialysis time was cut to 12 hours. No significant changes to the electrophoretic mobility were observed when the dialysis time was shortened. All measurements were made using absorbance detection of the moving boundary at 230 nm and 20^{o}C for standard experiments. The number of scans was initially set to 350, but was variable across the different Nanodisc^{TM} samples due to the differing electrophoretic mobilities. Conductivity measurements were made using a Bio-Rad pump system connected to a conductivity monitor (Biologic LP System 731-8300 as part of the BioLogic DuoFlow detector kit #750-0240.) and a VWR EC meter (model-1056, S/N 198310020) in conjunction with a NESLAB RTE-111 temperature controlled water bath set to 20 ^{o}C.

Data analysis was performed according to MCE protocol (Spin Analytical). A stokes radius (R_s) of ~ 4.8 nm for MSP1D1 Nanodiscs and ~ 5.6 nm for MSP1E3D1 Nanodiscs (**Table 2)** were calculated from sedimentation velocity and agree with R_s values calculated from DLS measurements by Inagaki et al. (2013). These R_s values were used in the data analysis. Values

of the solvent viscosities used in calculating the Debye-Huckel Henry charge (Z_{DHH}) can be found in **Table 3** and were calculated with Sednterp [Laue et al., 1992]. All Nanodiscs were run at their stock concentrations (~18-20 uM for POPC and POPC/POPS Nanodiscs and ~10-12 uM for POPA Nanodiscs), at 230 nm, 20 ^{o}C and at an electric field of ~ -2 V/cm. POPC and POPE Nanodiscs also were run at electric fields of -4 and -6 V/cm due the lower magnitude of their electrophoretic mobilities in order to increase the resolution between the moving boundaries. Z_{DHH} was calculated from the electrophoretic mobility as: $Z_{DHH} = \mu f/Qp(1+\kappa a)/f(\kappa a)$ where μ is the electrophoretic mobility, *f* is the translational friction coefficient, κ is the inverse Debye length, a is the sum of the Stokes radius of the macromolecule and its counterion, Q_p is the fundamental proton charge, and $f(\kappa a)$ is Henry's function [Durant, 2003].

Analytical Ultracentrifugation using Sedimentation Velocity—All Nanodisc^{TM} samples were run at wavelengths of 280 and 230 nm with sample absorbances in the range of 0.2-0.7 AU (with respect to the solvent). For POPC and POPS Nanodiscs, a five-fold dilution of the stock solution was sufficient. Each sample was run at a 1:5, 1:10 and 1:20 dilution at 280 and 230 nm. POPA and POPE Nanodiscs were run at their stock concentration, 1:5 and 1:10 dilutions at 280 and 230 nm. All samples were run at 45000 RPM, 20 ^{o}C, acquiring 150 scans per analysis in a Beckman-Coulter XLA Ultracentrifuge. The data were analyzed using Sedfit, SedAnal, and DC/DT+ [Schuck, 2000; Stafford, 2003; Philo, 2000].

Analytical Ultracentrifugation using Sedimentation Equilibrium— All Nanodisc^{TM} samples were run at 15, 20, 25 and 30-thousand RPM with scans acquired at 1 hour intervals for 20 hours per rotor speed at 20 ^{o}C, using both 280 and 230 nm detection in a Beckman-Coulter XLA Ultracentrifuge. Samples were diluted until the absorbance fell into the range of 0.2-0.7 AU.

Prior to loading, each sample was dialyzed for a period of 48 hours, with buffer exchange every 12 hours. The data were analyzed using Hetero-Analysis [Cole and Hansen, 1999].

RESULTS

Survey of Nanodisc^{TM} charge using membrane confined electrophoresis (Aim 1). In order to characterize lipid effects on protein charge properties within the Nanodisc^{TM} system, foundational studies must be done on the Nanodiscs' themselves in order to: 1) generate comparative charge data on pure lipid Nanodiscs that allows us to better interpret charge data with protein-embedded Nanodiscs and 2) develop well defined experimental conditions in order to optimize resolution and precision with respect to the charge measurements.

Figure 1A shows the raw intensity scan of a 30POPS Nanodisc^{TM} sample in standard buffer using MCE. When monodisperse with respect to size and charge, Nanodiscs form a single distinct moving boundary in the presence of an electric field. **Figure 1B** shows the transformed Z_{DHH} distribution curve (from the raw data of **Figure 1A**) of 30POPS Nanodiscs. Nanodiscs are well behaved in MCE as seen by the symmetric Z_{DHH} distribution.

Table 1 summarizes the hydrodynamic properties of Nanodiscs used to calculate R_s. For sedimentation equilibrium data, the program Hetero-Analysis was used to acquire the buoyant molecular weight (M_b). For sedimentation velocity experiments, Sedfit [Schuck, 2000], SedAnal [Stafford, 2003] and DC/DT+ [Philo, 2000] were used to acquire the $S_{20,w}$. Due to lack of sample, sedimentation velocity and equilibrium experiments were not run on 10PIP$_2$ Nanodiscs. **Table 2** shows the calculated Stokes radius (R_s) and partial specific volume ($\bar{\upsilon}$) of various Nanodisc^{TM} samples. The R_s was used in calculating Z_{DHH} from the electrophoretic mobility

obtained from MCE. The R_s was calculated using information from both sedimentation velocity and sedimentation equilibrium data as described by Cole et al. (2008). The partial specific volume ($\bar{\upsilon}$) was obtained using a molecular weight calculated from the MSPs and 125 lipids for a single Nanodisc^{TM}, the calculated R_s, experimental $S_{20,w}$ and the frictional coefficient *f*, calculated from the M_b obtained via sedimentation equilibrium experiments.

Table 3 shows the properties of the different solvent conditions used in determining the electrophoretic mobility and Z_{DHH} of Nanodiscs by MCE. Due to slight variations in the measured conductivity (that have been accounted for in the calculations of both the electrophoretic mobility and Z_{DHH}), ranges are given for the conductivities. The uncertainty of the conductivity meters were ± 0.5% (VWR EC meter) and ± 1.0% (Biologic LP System 731-8300). All viscosity values used were calculated using Sednterp [Laue et al. 1992].

Tables 4a and 4**b** show the charge estimated values of MSP1D1 (**Table 5a**) and MSP1E3D1 (**Table 5b**) Nanodiscs calculated from the summation of all ionizable groups, including: 1) those found in the MSP amino acid composition and 2) those found on the hydrophilic head groups of the specific embedded phospholipids at pH 7.4. MSP1D1 and MSP1E3D1 membrane scaffolding proteins differ at ~ 66 amino acids, with the MSP1E3D1 protein forming larger Nanodiscs. For neutral lipids such as PC and PE, the charge should come solely from the MSPs, as neutral lipids should not contribute to the overall charge on Nanodiscs. For POPS Nanodiscs, each lipid head group is assumed to contribute a charge of -1 per head group at pH 7.4. For POPA Nanodiscs, each lipid head group is assumed to contribute a charge of ~ -1.25 per lipid head group at pH 7.4. The estimated charge per lipid head group is calculated from the reported pKa value of ~ 8.0 for the second ionization event of the phosphate group on PA lipids [**Figures C7 and C8**; Marsh, 1990]. The expected charge per lipid head group of PIP_2 should be -3 and

therefore the expected charge should be similar to that of 30POPS Nanodiscs [Toner et al. 1988]. **Table 5** summarizes the electrophoretic mobility and Z_{DHH} data on Nanodiscs in standard buffer using MCE. For PIP_2 Nanodiscs, an R_s of 4.9 nm was used in the calculation for Z_{DHH}. This value was the average R_s for all MSP1D1 Nanodiscs analyzed using analytical ultracentrifugation.

MSP1D1 Nanodiscs versus MSP1E3D1 Nanodiscs. **Figure 2** compares the Z_{DHH} of MSP1D1 and MSP1E3D1 Nanodiscs. MSP1D1 and MSP1E3D1 Nanodiscs differ in size and number of lipids per bilayer area. MSP1D1 Nanodiscs typically have a bilayer area of ~ 4400$Å^2$ and ~ 126 total lipids (~ 63 per bilayer) [Ritchie et al., 2009]. MSP1E3D1 Nanodiscs typically have a bilayer area of ~ 8900$Å^2$ and ~ 250 total lipids (~ 125 per bilayer) [Ritchie et al., 2009]. Surface area constraints are important to consider, as Nanodisc^{TM} embedded proteins displace lipids within the bilayer, affecting both the charge and frictional properties of the protein and Nanodisc^{TM} [Ritchie et al., 2009]. Larger proteins cannot be embedded into smaller Nanodiscs, therefore, increasing the library of Nanodisc^{TM} charge to include larger Nanodiscs is important.

Figure 3 summarizes the comparative analysis of the measured Z_{DHH} with that of the calculated charge estimates of MSP1D1 (**Tables 5a)** and MSP1E3D1 (**Table 5b**) Nanodiscs. Note that as the charge magnitude of the Nanodisc^{TM} increases, the fractional charge decreases for both Nanodisc^{TM} sizes. The fractional charge depicted here is the ratio of the measured Z_{DHH} to the calculated charge estimates in **Tables 5a** and **5b**. It must be noted that after initial experiments using both MSP1D1 and MSP1E3D1 Nanodiscs, no significant differences were observed between MSP1D1 and MSP1E3D1 Nanodiscs with respect to different solvent conditions. Therefore it was assumed that any effects seen in MSP1D1 Nanodiscs would be duplicated with the MSP1E3D1 Nanodiscs.

Comparison of similarly charged phospholipids: phosphatidylcholine versus phosphatidylethanolamine. **Table 6** shows a comparison of the Z_{DHH} for POPC and POPE Nanodiscs. Both PC and PE lipids usually are considered neutral. For PC lipids, the general consensus is that the positively charged choline group at the surface and the negatively charged phosphate in the ester bond electrostatically cancel each other out, resulting in an electrically neutral molecule [Marsh, 1990]. However, PC lipids do posses a significant dipole ~ 10 D [Clarke, 1997]. It must be noted that while the measured dipole of PC lipids is relatively large and categorically makes it a "highly ionic" molecular species, a Debye unit is still only 1×10^{-10} charge units as expressed in electrostatic units · angstroms (esu·Å). Interestingly, studies on PC lipids using different electrophoretic techniques have observed non-zero mobilities and zeta potentials [McLaughlin et al., 1978; Woodle et al., 1992; Pincet et al., 1999; Klasczyk et al., 2010; Disalvo and Bouchet 2014]. This may be due to lipid impurities, heterogeneous liposome size distributions, chemical modifications, or electrophoresis-specific effects such as electroendosmosis. One major difference between the liposomes used in those studies and the Nanodiscs used in this study is the presence of the MSPs on the Nanodiscs. These proteins give a net negative charge overall and therefore non-zero electrophoretic mobilities on POPC Nanodiscs were expected.

PE lipids are also considered neutral due to the ammonium cation and the anionic phosphate ester group cancelling the charges electrostatically. In addition, at pH 7.4, the pH is not high enough to ionize the ammonium cation group, with its pKa ~ 11.25 [**Figure C4**; Marsh, 1990]. Like PC lipids, PE also has a dipole between the positively charged ammonium cation and the negatively charged phosphate; although measurements on the strength of that dipole cannot currently be found in the literature (although most agree that it should be on the same

order of the dipole moment found on PC lipids) [Clarke, 1997]. While the POPC Nanodiscs exhibit a charge that does not exceed the calculated charge of the MSP1D1 membrane scaffolding proteins (**Table 5a**), 10POPE Nanodiscs exhibit a charge significantly larger in magnitude than POPC Nanodiscs, demonstrating that POPE Nanodiscs should be considered anionic lipids in this system. The Z_{DHH} of 10POPE Nanodiscs is much closer to the Z_{DHH} of 10POPS Nanodiscs.

Figures 4a and **4b** show a comparison of the transformed Z_{DHH} distribution curves for POPC (**Figure 4a**) and POPE (**Figure 4b**) Nanodiscs. Notice that the POPC Nanodiscs provide a much narrower and more symmetrical charge distribution. However, 10POPE lipids also show a significantly higher electrophoretic mobility and Z_{DHH} than POPC Nanodiscs, even though PC and PE are considered "neutral" lipids.

Phosphatidylserine versus phosphatidic acid. **Figure 5** summarizes the charge data comparing POPS and POPA Nanodiscs in standard buffer. Both PS and PA lipids have a net charge of ~ -1 at physiologic pH. However, their head group structures are different, with PS lipids containing a serine group that includes a carboxylate anion and ammonium cation group, and PA lipids lacking a head group and having just the phosphate group. Thus, while both PS and PA lipids have similar expected net charges, the physical and chemical nature of the groups giving rise to that charge are quite different. For PS, there is a dipole between the ammonium and carboxyl group that is not present in PA. Furthermore, PA lipids contain an ionizable group with a pKa (~ 8.0) within physiologic range and can potentially exhibit a net charge of -1 to -2 depending on the local lipid microenvironment [Marsh, 1990]. Significant differences in the measured electrophoretic mobilities and Z_{DHH} could provide insight as to the local environmental

differences in similarly charged anionic lipids; which could explain why one lipid may be preferred over the other in specific ion-mediated reactions.

The Z_{DHH} of POPA Nanodiscs exhibit a significantly higher charge magnitude than those of equivalent POPS Nanodiscs, suggesting that the charge per lipid head group of each PA lipid is slightly greater than -1.

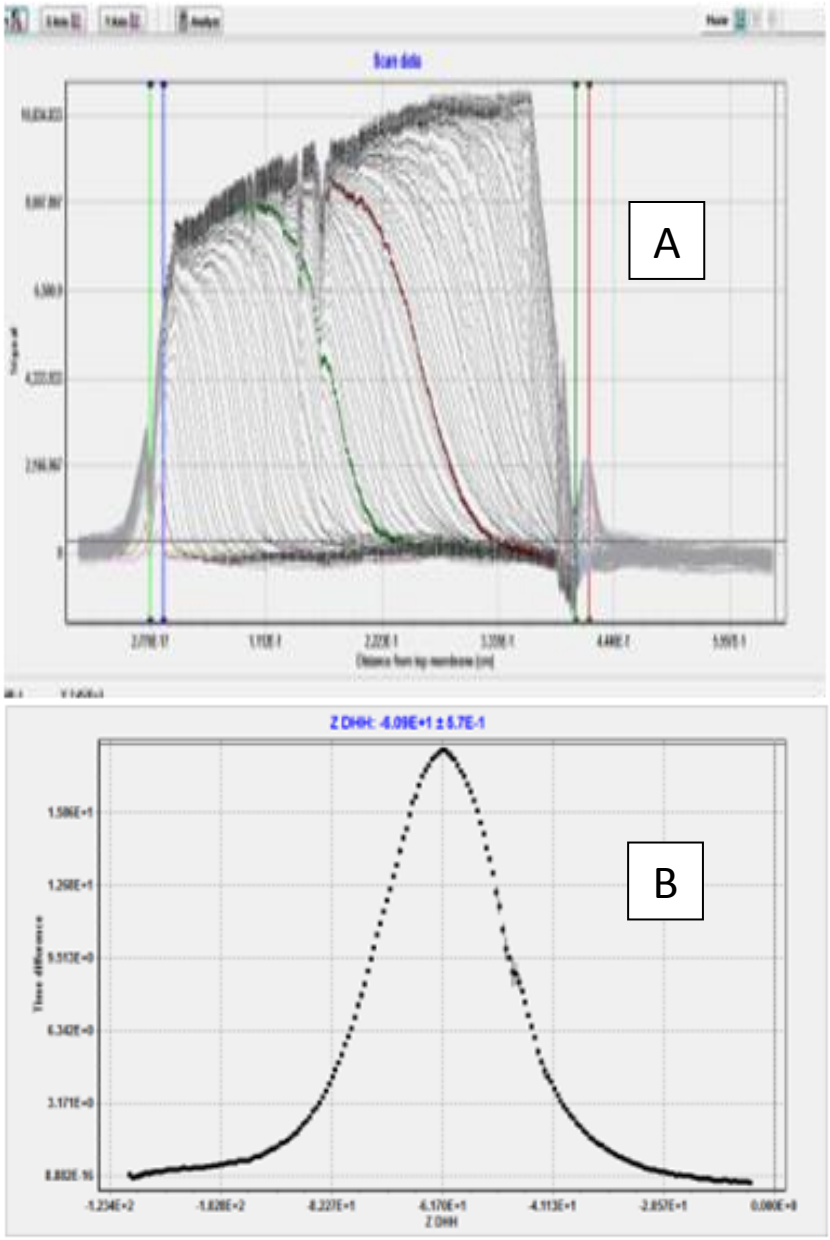

Figure 1 Free-boundary electrophoresis of 30 POPS Nanodiscs. **A**: Raw intensity scans shows boundary movement from left to right as an intensity increase where the boundary has passed, **B:** The distribution of Z_{DHH} calculated as $\mu f(1+ka)/(f(ka)Q_P)$, where μ is the electrophoretic mobility in $cm^2/V\text{-}s$, etc. [Ridgeway et al., 1989] The distribution width is due to the combined effects of diffusion, charge heterogeneity and conductance variation across the boundary, and not the charge heterogeneity alone. Although there are variations in light intensity due to dust and scratches on the optics, these do not obscure the boundary. Importantly, these intensity variations are spatially consistent with time, and therefore removed using the time difference method in manner analogous to the time difference methods used for sedimentation velocity [Stafford, 1992].

Nanodisc^{TM} Sample	Buoyant Molecular Weight (kDa)	Sedimentation coefficient ($S_{20,w}$)
MSP1D1 POPC	14.3 ± 0.4	$3.0_{52} \pm 5.0 \times 10^{-3}$
MSP1D1 10% POPS	15.5 ± 0.4	$3.1_{27} \pm 5.0 \times 10^{-3}$
MSP1D1 30% POPS	17.8 ± 0.6	$3.5_{09} \pm 3.0 \times 10^{-3}$
MSP1D1 70% POPS	21.6 ± 0.7	$4.4_{27} \pm 5.0 \times 10^{-3}$
MSP1E3D1 POPC	16.8 ± 1.2	$2.9_{37} \pm 4.0 \times 10^{-3}$
MSP1E3D1 10% POPS	19.0 ± 0.6	$3.2_{59} \pm 2.0 \times 10^{-3}$
MSP1E3D1 30% POPS	20.6 ± 0.6	$3.6_{21} \pm 4.0 \times 10^{-3}$
MSP1E3D1 70% POPS	26.7 ± 1.1	$4.6_{41} \pm 3.0 \times 10^{-3}$
MSP1D1 10% POPA	14.6 ± 0.8	$3.0_{22} \pm 3.0 \times 10^{-3}$
MSP1D1 30% POPA	15.7 ± 0.8	$3.1_{76} \pm 6.0 \times 10^{-3}$
MSP1D1 70% POPA	18.5 ± 1.0	$3.5_{95} \pm 8.0 \times 10^{-3}$
MSP1D1 10% POPE	14.6 ± 0.6	$3.0_{31} \pm 4.0 \times 10^{-3}$
MSP1D1 10% PIP_2	ND	ND

Table 1 Hydrodynamic properties of lipid Nanodiscs as acquired by sedimentation equilibrium (M_b) and sedimentation velocity ($S_{20,w}$) experiments using an analytical ultracentrifuge.

Nanodisc™ Sample	R_s (nm)	$\bar{\upsilon}$ (cm^3/g)
MSP1D1 POPC	$4.7 \pm 5.0 \times 10^{-2}$	$0.88_8 \pm 3.0 \times 10^{-3}$
MSP1D1 10% POPS	$4.9 \pm 3.0 \times 10^{-2}$	$0.89_2 \pm 4.0 \times 10^{-3}$
MSP1D1 30% POPS	$5.0 \pm 5.0 \times 10^{-2}$	$0.87_9 \pm 4.0 \times 10^{-3}$
MSP1D1 70% POPS	$4.8 \pm 4.0 \times 10^{-2}$	$0.88_6 \pm 3.0 \times 10^{-3}$
MSP1E3D1 POPC	$5.7 \pm 8.0 \times 10^{-2}$	$0.899 \pm 3.0 \times 10^{-3}$
MSP1E3D1 10% POPS	$5.8 \pm 1.0 \times 10^{-1}$	$0.88_9 \pm 2.0 \times 10^{-2}$
MSP1E3D1 30% POPS	$5.7 \pm 6.0 \times 10^{-2}$	$0.89_1 \pm 4.0 \times 10^{-3}$
MSP1E3D1 70% POPS	$5.7 \pm 1.0 \times 10^{-1}$	$0.88_9 \pm 3.0 \times 10^{-3}$
MSP1D1 10% POPA	$4.8 \pm 6.0 \times 10^{-2}$	$0.89_1 \pm 4.0 \times 10^{-3}$
MSP1D1 30% POPA	$4.9 \pm 6.0 \times 10^{-2}$	$0.88_9 \pm 4.0 \times 10^{-3}$
MSP1D1 70% POPA	$5.1 \pm 1.1 \times 10^{-1}$	$0.88_9 \pm 3.0 \times 10^{-3}$
MSP1D1 10% POPE	$4.8 \pm 4.0 \times 10^{-2}$	$0.88_9 \pm 2.0 \times 10^{-3}$
MSP1D1 10% PIP_2	ND	ND

Table 2 Hydrodynamic properties of Nanodiscs calculated from the data acquired via sedimentation equilibrium and sedimentation velocity experiments on an analytical ultracentrifuge.

Buffer	Conductivity (mS)	Viscosity (cρ)
100mM NaCl, 50mM Tris pH 7.4	12.0 - 12.4	1.02_{67}
34mM NaCl, 17mM Tris pH 7.4	3.9 - 4.1	1.01_{02}
50mM NaCl, 25mM Tris pH 7.4	5.6 - 6.0	1.01_{42}
68mM NaCl, 34mM Tris pH 7.4	8.1 - 8.3	1.01_{87}
84mM NaCl, 42mM Tris pH 7.4	10.1 - 10.4	1.02_{27}
150mM NaCl, 75mM Tris pH 7.4	17.5 - 18.0	1.03_{90}
100mM NaCl, 50mM Tris, 3mM $CaCl_2$ pH 7.4	10.0 - 10.5	1.02_{72}
100mM NaCl, 50mM Tris, 3mM MgCl pH 7.4	11.8 - 12.3	1.02_{80}
100mM KCl, 50mM Tris pH 7.4	14.3 - 14.7	1.01_{60}
100mM LiCl, 50mM Tris pH 7.4	9.8 - 10.4	1.04_{21}
1X PBS	13.5 - 13.8	1.02_{00}
100mM Na_2So_4, 50mM Tris pH 7.4	16.2 - 16.5	1.05_{50}
100mM NaCl, 50mM Tris pH 7.0	12.4 - 12.8	1.02_{67}
100mM NaCl, 50mM Tris pH 8.0	11.2 - 11.5	1.02_{67}
100mM NaCl, 50mM Tris pH 8.5	10.4 - 10.8	1.02_{67}
100mM NaCl, 50mM Tris pH 7.4[a]	13.8 - 14.0	0.89_{0}
100mM NaCl, 50mM Tris pH 7.4[b]	16.8 - 17.1	0.71_{9}

Table 3 Solvent properties of different buffers used to determine the electrophoretic mobility and Z_{DHH} (see **Material and Methods** for conductivity protocol) of Nanodiscs by MCE. Experiments, unless denoted, were performed at 20°C.

[a]Conductivity and viscosity values of standard buffer at 25°C

[b]Conductivity and viscosity values of standard buffer at 35°C

MSP1D1 Nanodiscs	Charge contribution from belt proteins	Charge contribution from phospholipids	Calculated Total Charge
POPC/POPE	-16	0	-16
10% POPS	-16	-13	-29
30% POPS	-16	-38	-54
70%POPS	-16	-88	-104
10% POPA	-16	-16	-32
30% POPA	-16	-47	-63
70% POPA	-16	-109	-125
10% PIP_2	-16	-38	-54

MSP1E3D1 Nanodiscs	Charge contribution from belt proteins	Charge contribution from phospholipids	Calculated Total Charge
POPC	-20	0	-20
10% POPS	-20	-25	-45
30% POPS	-20	-75	-95
70%POPS	-20	-175	-195

Tables 4a and **4b** show the calculated charge estimates of MSP1D1 and MSP1E3D1 Nanodiscs, respectively.

Nanodisc™ Sample	Electrophoretic Mobility ($cm^2/V \cdot s$)	Z_{DHH}
MSP1D1 POPC	$-4.2 \times 10^{-5} \pm 3.8 \times 10^{-6}$	-14.1 ± 1.0
MSP1D1 10% POPS	$-7.1 \times 10^{-5} \pm 2.9 \times 10^{-6}$	-24.6 ± 0.8
MSP1D1 30% POPS	$-1.2 \times 10^{-4} \pm 5.7 \times 10^{-6}$	-38.5 ± 1.4
MSP1D1 70% POPS	$-1.7 \times 10^{-4} \pm 3.8 \times 10^{-6}$	-56.4 ± 2.4
MSP1E3D1 POPC	$-3.8 \times 10^{-5} \pm 3.9 \times 10^{-6}$	-18.0 ± 0.7
MSP1E3D1 10% POPS	$-7.9 \times 10^{-5} \pm 3.9 \times 10^{-6}$	-37.0 ± 2.0
MSP1E3D1 30% POPS	$-1.2 \times 10^{-4} \pm 3.6 \times 10^{-6}$	-57.2 ± 2.5
MSP1E3D1 70% POPS	$-2.0 \times 10^{-4} \pm 5.0 \times 10^{-6}$	-92.3 ± 4.1
MSP1D1 10% POPA	$-7.5 \times 10^{-5} \pm 1.7 \times 10^{-6}$	-26.2 ± 1.7
MSP1D1 30% POPA	$-1.4 \times 10^{-4} \pm 1.6 \times 10^{-5}$	-45.0 ± 3.0
MSP1D1 70% POPA	$-2.1 \times 10^{-4} \pm 1.0 \times 10^{-5}$	-66.6 ± 4.7
MSP1D1 10% PIP_2	$1.2 \times 10^{-4} \pm 3.6 \times 10^{-6}$	-39.7 ± 1.1
MSP1D1 10% POPE	$6.5 \times 10^{-5} \pm 5.3 \times 10^{-6}$	-21.4 ± 1.5

Table 5 The measured electrophoretic mobility and Z_{DHH} values of various Nanodiscs in standard buffer containing various phospholipid ratios using MCE. The charge magnitude increases as more anionic lipids are incorporated into Nanodiscs. Note that the electrophoretic mobility measured resulted in a Z_{DHH} for POPC Nanodiscs that does not exceed the calculated charge of the membrane scaffolding proteins from the amino acid sequence.

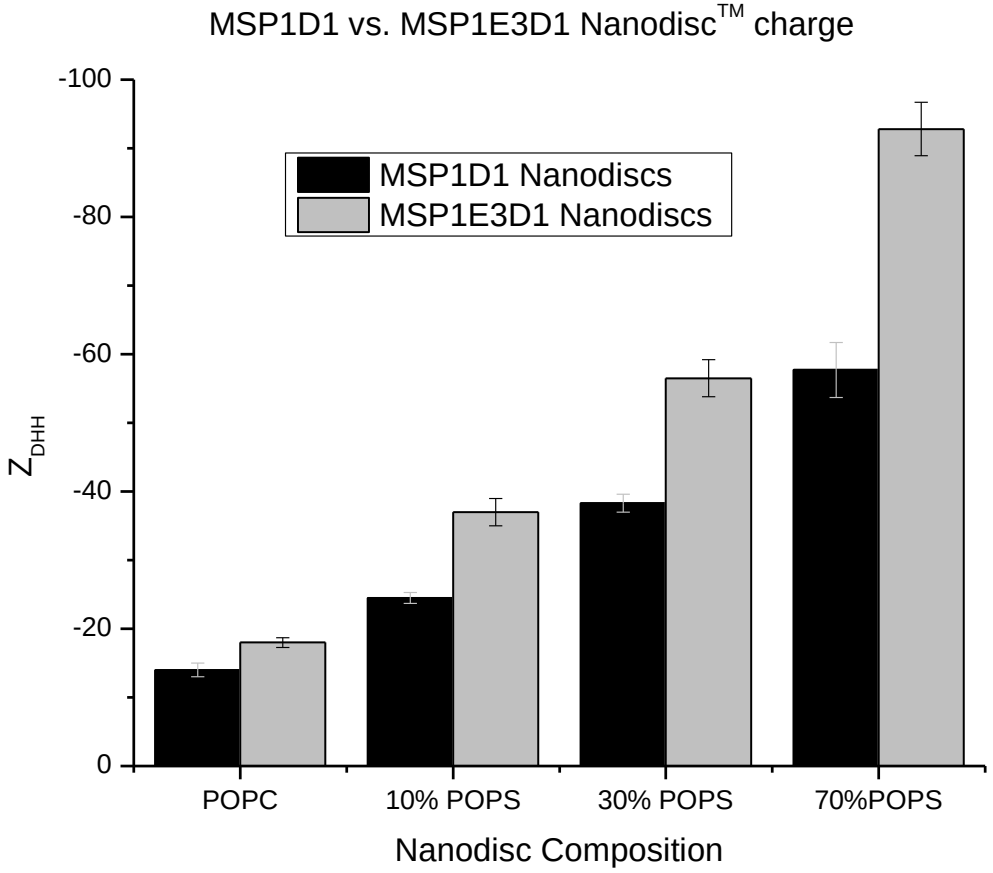

Figure 2 Z_{DHH} of MSP1D1 (black) and MSP1E3D1 (gray) Nanodiscs with varying PS content measured in standard buffer. In this and subsequent figures, the ordinate has been inverted, so that the amplitude reflects the anionic charge magnitude. The vertical bars in the figures represent the standard deviations.

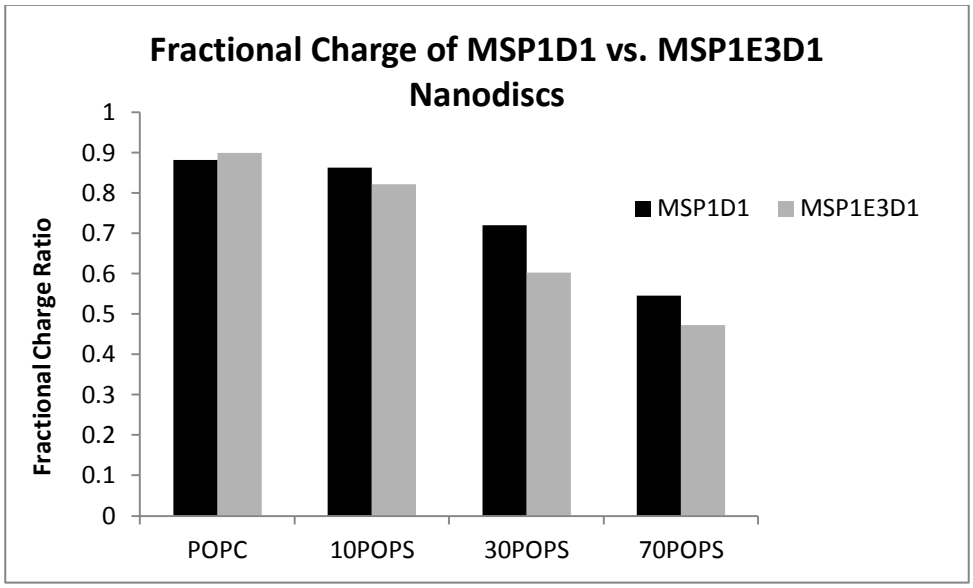

Figure 3 The fractional charge of MSP1D1 (black) and MSP1E3D1 (gray) Nanodiscs with varying PS content. The fractional charge was obtained from the ratio of the Z_{DHH} to the calculated charge estimates seen in **Tables 5a** and **5b**. A ratio of 1 means that the raw charge of the molecule is fully expressed in solution, with no neutralization from any counter-ions. Ratios below one mean that charge neutralization is occurring.

Neutral Lipids

Nanodisc™ Sample	Buffer	Z_{DHH}
MSP1D1 POPC	100 mM NaCl, 50 mM Tris, pH 7.4	-14.1 ± 1.0
MSP1D1 10POPE	100 mM NaCl, 50 mM Tris, pH 7.4	-21.4 ± 1.5

Table 6 A comparison of the Z_{DHH} of neutral lipids PC and PE.

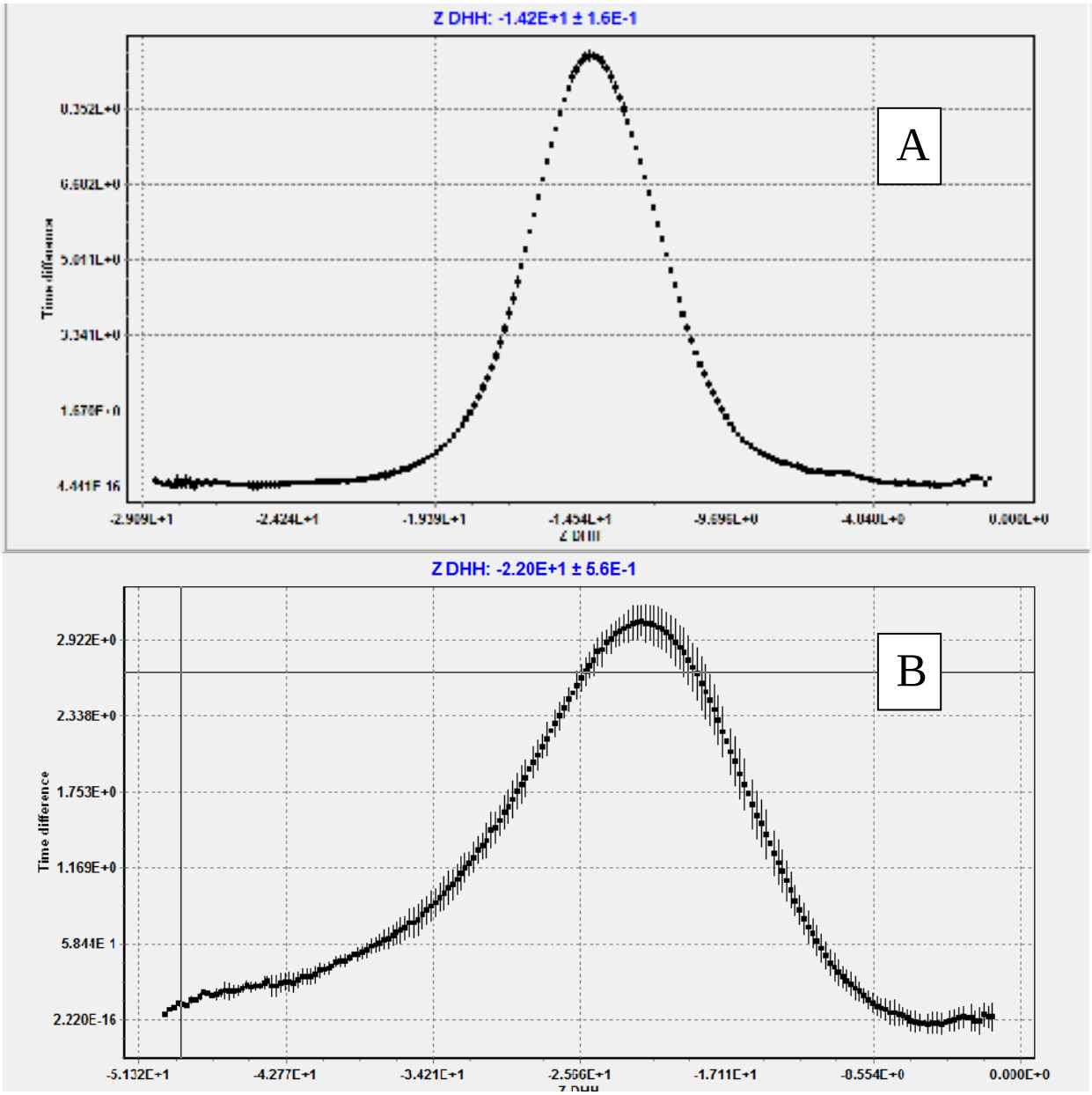

Figures 4a and **4b** The transformed Z_{DHH} distribution of MSP1D1 POPC (**a**) and POPE (**b**) Nanodiscs.

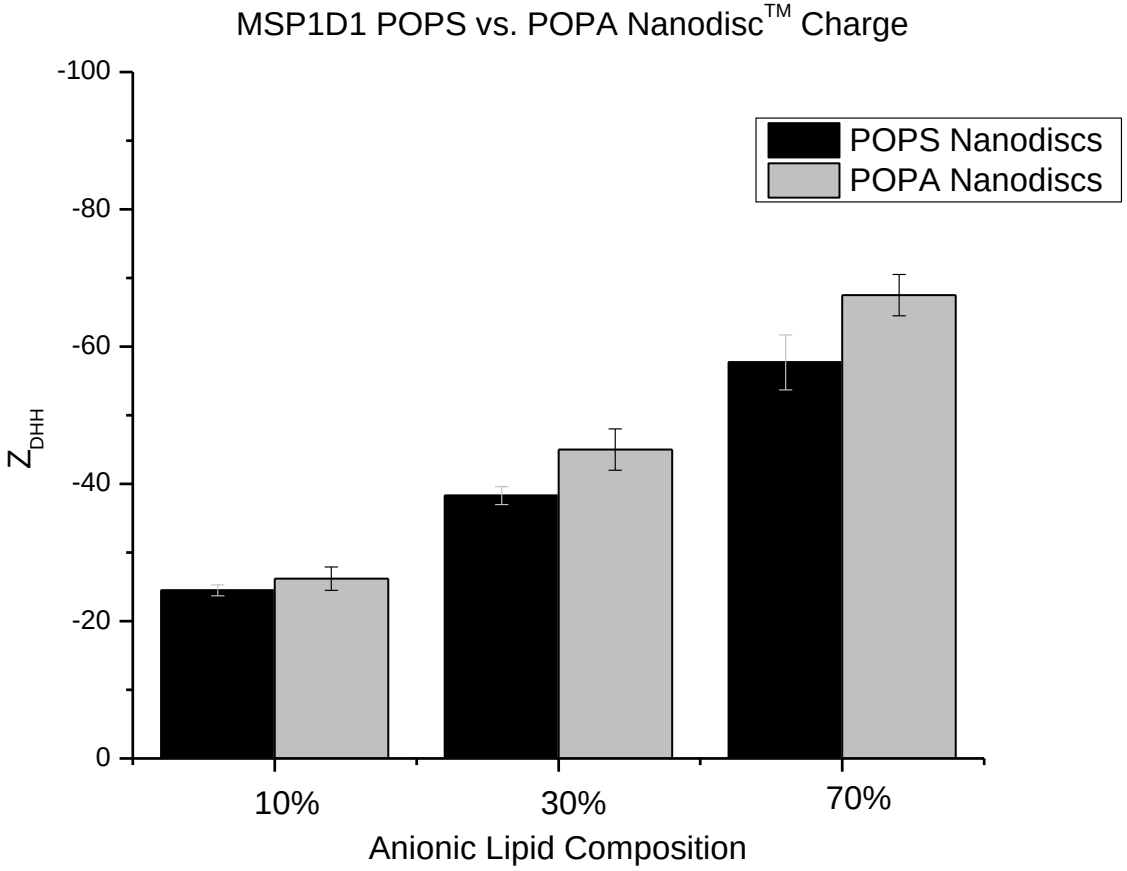

Figure 5 Comparison of Z_{DHH} for MSP1D1 POPS (black) and POPA (gray) Nanodiscs from their measured electrophoretic mobilities using MCE. As shown, the charge magnitudes between POPS and POPA Nanodiscs differ slightly at low lipid composition by ~ 8%. However, at higher anionic lipid composition the difference in charge magnitude between POPS and POPA increases to ~ 18%.

Survey of Nanodisc^{TM} charge in different monovalent cationic solvents. After establishing a baseline of Nanodisc^{TM} charge in standard buffer, it is important to observe Nanodiscs in different ionic environments. Since charge is a system property, it cannot be assumed that the charge it carries in one solvent is the same in another.

Figures 6 shows the Z_{DHH} of MSP1D1 POPC and MSP1D1 POPS Nanodiscs in PBS, and in the presence of different monovalent alkali cations Na^+, K^+, and Li^+. **Figure 7** shows the Z_{DHH} of MSP1D1 POPA Nanodiscs in PBS and in the presence of different monovalent alkali cations Na^+, K^+, and Li^+. **Figures 8** shows the Z_{DHH} of MSP1D1 10POPE and MSP1D1 10PIP_2 Nanodiscs in PBS and in the presence of different monovalent alkali cations Na^+, K^+, and Li^+.

Na^+, K^+, and Li^+ ions have been observed generally to have non-specific interactions with lipids [Tatulian, 1987; Binder and Zschornig, 2002; Klasczyk et al. 2010], allowing us to generate comparative studies differentiating non-specific ion adsorption from specific binding events. As seen, the different monovalent alkali cations did not show a significant difference in the electrophoretic mobilities and Z_{DHH} across all Nanodisc^{TM} samples.

Survey of Nanodisc^{TM} charge as a function of Na^+ concentration.

Figures 9 shows the Z_{DHH} for MSP1D1 POPC and MSP1D1 10POPE Nanodiscs as a function of Na^+ concentration. **Figures 10** shows the Z_{DHH} for MSP1D1 10POPS, 30POPS, and 70POPS Nanodiscs as a function of Na^+ concentration. **Figures 11** shows the Z_{DHH} for MSP1D1 10POPA, 30POPA, and 70POPA Nanodiscs as a function of Na^+ concentration. **Figures 12** shows the Z_{DHH} for MSP1D1 10PIP_2 Nanodiscs as a function of Na^+ concentration.

These measurements provide insights into the strength of interaction between Na^+ ions and Nanodiscs, since the calculation of Z_{DHH} takes into account the effects of salt concentration

on electrophoretic processes. Thus, changes in Z_{DHH} reflect changes in ion binding by Nanodiscs. It is seen in **Figure 9** that the charge on POPC Nanodiscs is rather insensitive to Na^+ concentration, whereas increasing levels of anionic lipids in POPE (**Figure 9**), POPS (**Figure 10**), POPA (**Figure 11**), and PIP_2 (**Figure 12**) Nanodiscs lead to increasing sensitivity to Na^+ concentration. However, at high Na^+ concentrations, even POPS, POPA, POPE and PIP_2 Nanodiscs become insensitive to changes in the salt concentration. This observation agrees well with polyelectrolyte theory. When enough counter-ions are adsorbed to a macromolecule to bring the free energy of the system (in this case, the lipid-water surface) under a particular energy threshold (in this case, the thermal energy k_BT), additional ions will not continue to adsorb onto the surface of the Nanodiscs [Manning, 1969].

Extrapolation of Z_{DHH} to zero salt concentration.

Figure 13 shows Z_{DHH} as a function of Na^+ concentration for MSP1D1 POPC Nanodiscs fitted to a 3rd order polynomial. **Figure 14** shows Z_{DHH} as a function of Na^+concentration for MSP1D1 10POPE Nanodiscs fitted to a 3rd order polynomial. **Figures 15, 16 and 17** show Z_{DHH} as a function of Na^+ concentration for MSP1D1 10POPS, 30POPS and 70POPS Nanodiscs, respectively, fitted to a 3rd order polynomial. **Figures 18, 19 and 20** show Z_{DHH} as a function of Na^+concentration for MSP1D1 10POPA, 30POPA and 70POPA Nanodiscs, respectively, fitted to a 3rd order polynomial. **Figure 21** shows Z_{DHH} as a function of Na^+ concentration for MSP1D1 10PIP_2 Nanodiscs fitted to a 3rd order polynomial. **Table** 7 summarizes and compares the extrapolated Z_{DHH} values at zero salt to that of the calculated charge estimates (**Tables 5a** and **5b**).

It is not surprising that the measured Z_{DHH} (**Table 5**) of pure lipid Nanodiscs is of a lower magnitude than the charge calculated estimates (**Tables 4a** and **4b**). In numerous studies of other macromolecules (proteins and DNA in particular), measured charges were also lower in magnitude than their calculated charges [Durant, 2003; May, 2007; Filoti et al., 2015]. However, while the measured charges reflect chemical and electrostatic interactions in solution, it is very difficult to get the raw charge on a molecule directly using electrophoretic methods. An inherent limitation of electrophoresis is the need for a sufficient amount of ions to carry the charge from one electrode to another [Filoti et al., 2015]. At higher salt concentrations, the solvent ion conducts the vast majority of the current, and the macro-ion carries only a small fraction of the total current. The amount of current carried is described by the repetition function. The repetition function is described and used by Ornstein and Davis (1964), with respect to gel electrophoresis. However, when there aren't enough ions in solution, the macromolecule must now carry a larger fraction of the current to satisfy electro-neutrality [Altria, 1996]. As a result, the electrophoretic mobility of the molecule is perturbed due to it influencing a greater fraction of the electric field.

What must be done therefore is to run samples at the lowest possible salt concentrations (having sufficient ions) and then extrapolate to zero salt in order to estimate the raw charge based off the electrophoretic mobility data. For lipid Nanodiscs, 34 mM (resulting in a solution with an ionic strength of ~ 50 mM) was the lowest salt concentration that did not result in asymmetric moving boundaries (that are commonly seen when there are not enough ions in solution).

A 3rd order polynomial model fit the charge data best and can provide some insight as to the raw charge of the Nanodiscs. **Table 7** shows that for POPC, 10POPE, 10POPS, 30POPS, 10POPA, and 30POPA the extrapolated Z_{DHH} to zero salt concentrations were slightly higher

than the calculated charge estimates. For 70POPS, 70POPA and 10PIP_2 Nanodiscs, the extrapolated Z_{DHH} to zero salt of was lower than the calculated charge estimate. While the extrapolated Z_{DHH} to zero salt of 10PIP_2 Nanodiscs was only slightly lower than the calculated charge (~ 3%), the extrapolated Z_{DHH} to zero salt of 70POPS (~ 16%) and 70POPA (~ 33%) were significantly lower in comparison.

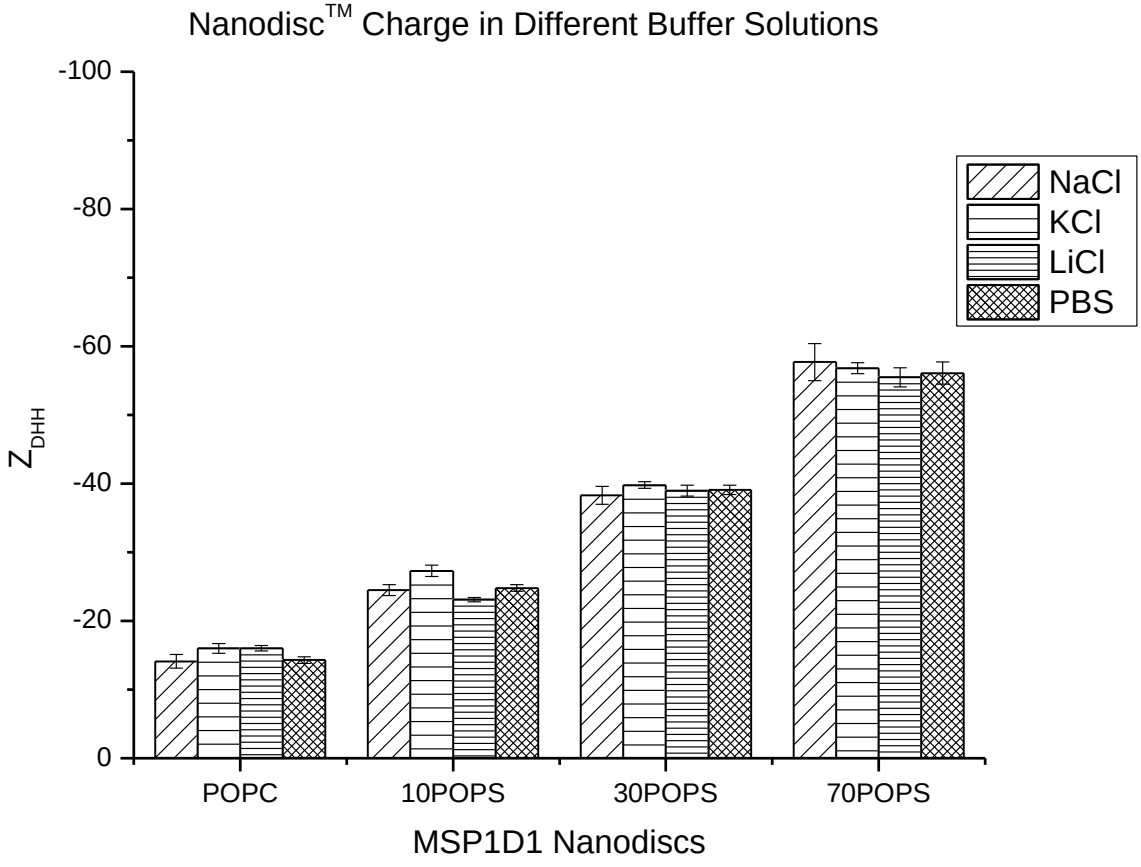

Figure 6 Z_{DHH} of MSP1D1 POPC and POPS Nanodiscs in different solvent conditions.

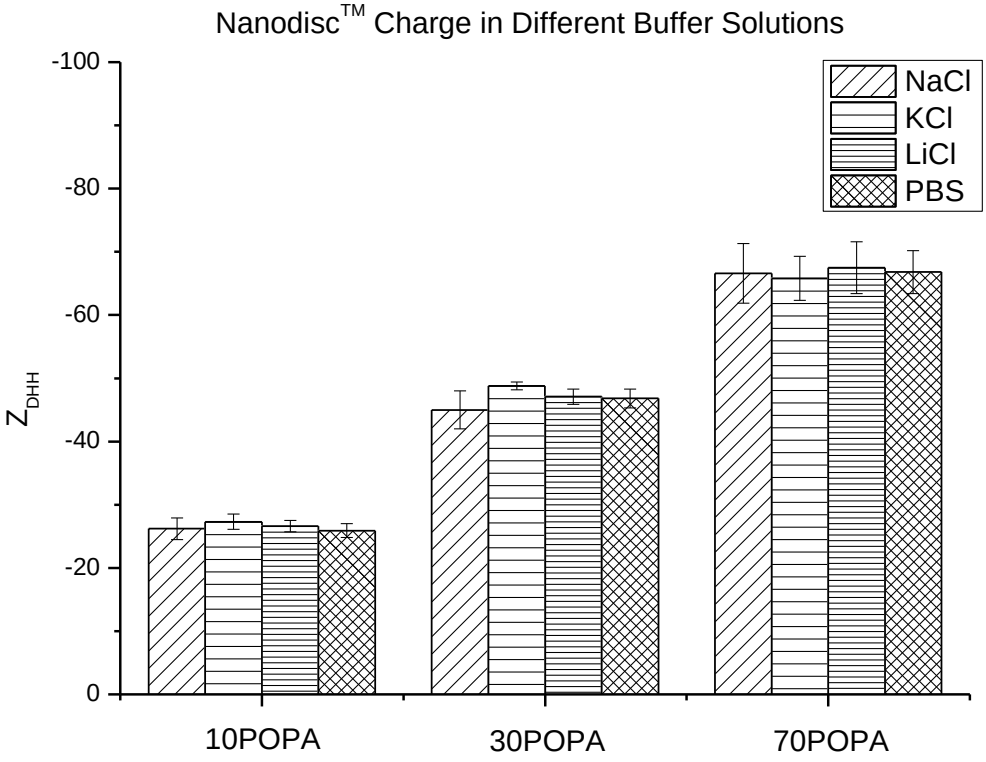

Figure 7 Z_{DHH} of MSP1D1 POPA Nanodiscs in different solvent conditions.

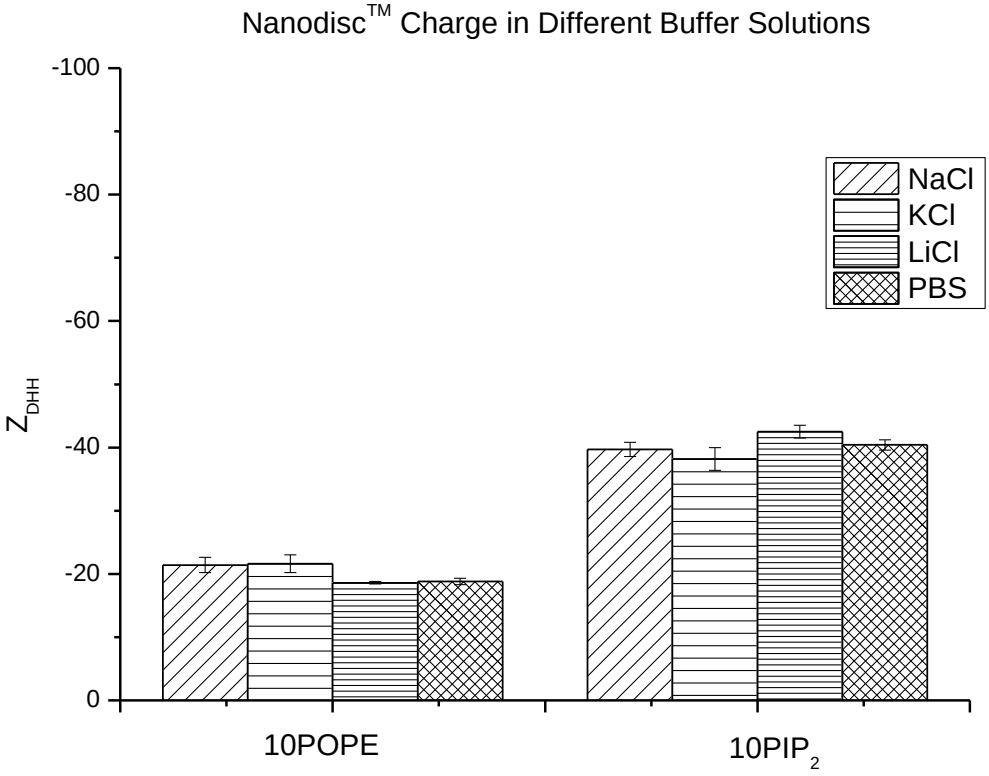

Figure 8 Z_{DHH} charges of MSP1D1 10POPE and 10PIP_2 Nanodiscs in different solvent conditions.

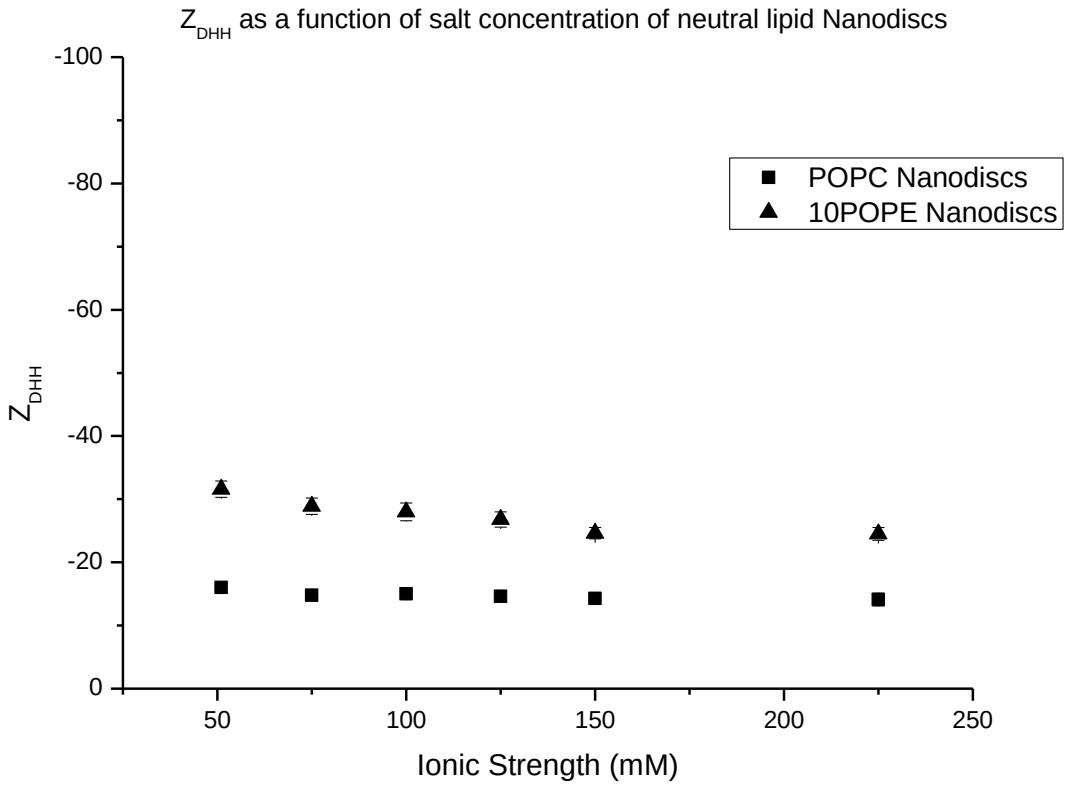

Figure 9 Z_{DHH} as a function of Na^+ concentration for neutral lipids PC (squares) and PE (triangles). MSP1D1 POPC Nanodisc™ charge magnitude remained constant independent of salt concentration. MSP1D1 POPE Nanodisc™ charge however, decreased in charge magnitude as the salt concentration of the buffer solution increased, although at Na^+ concentrations of 75 mM and higher, 10POPE Nanodisc™ charge plateaus.

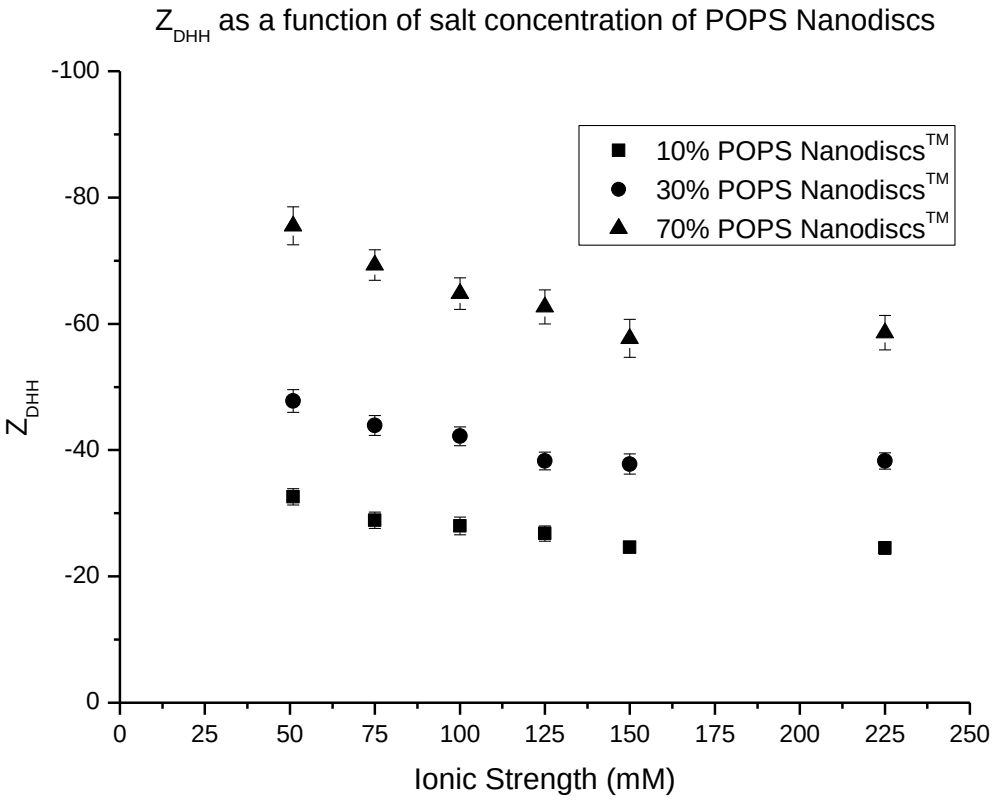

Figure 10 Z_{DHH} as a function of Na^+ concentration for MSP1D1 POPS Nanodiscs. Similar to POPE Nanodiscs, the charge magnitude of POPS Nanodiscs decreased as the salt concentration increased. For POPS Nanodiscs, the plateau threshold increases as POPS content increases, with 10POPS (squares) reaching a plateau at ~ 75 mM, 30POPS (circles) at ~ 100 mM and 70POPS (triangles) reaching a plateau at ~ 125 mM.

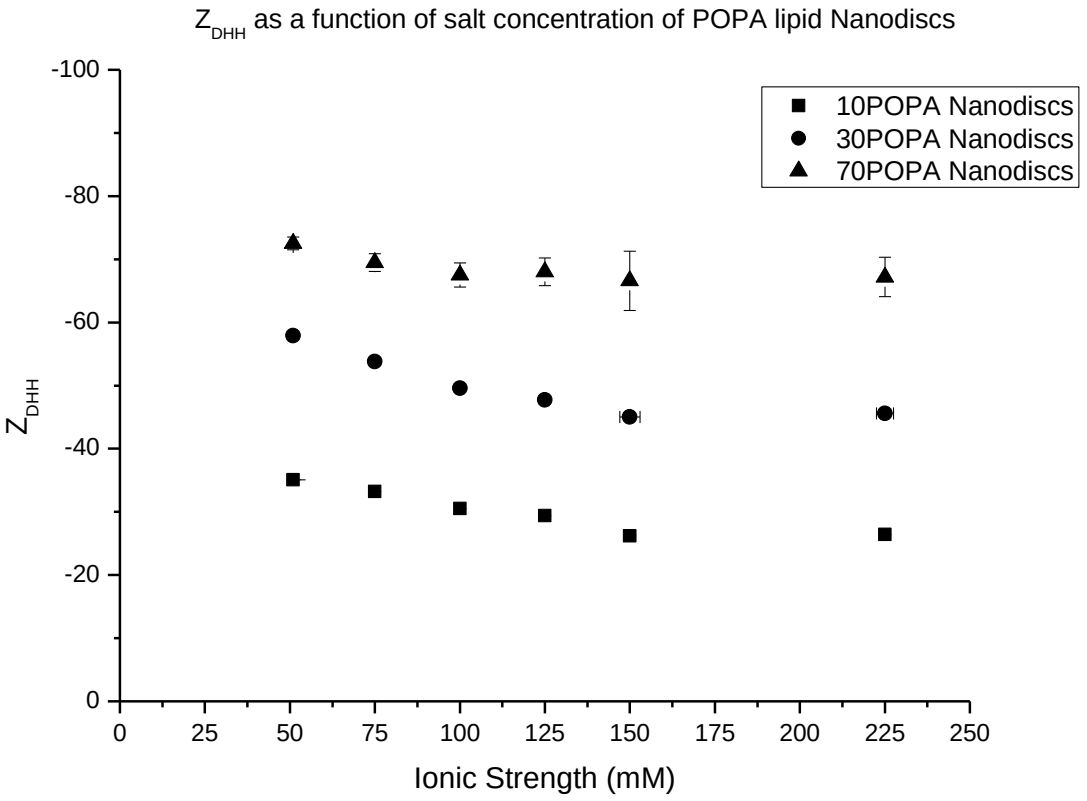

Figure 11 Z_{DHH} as a function of Na^+ concentration for MSP1D1 POPA Nanodiscs. Similar to other anionic Nanodiscs, the charge magnitude of POPA Nanodiscs decreased as the salt concentration increased. For POPA Nanodiscs, the plateau threshold increases as POPA content increases, with 10POPA (squares) reaching a plateau at ~ 100 mM, 30POPA (circles) at ~ 125 mM and 70POPA (triangles) reaching a plateau at ~ 150 mM.

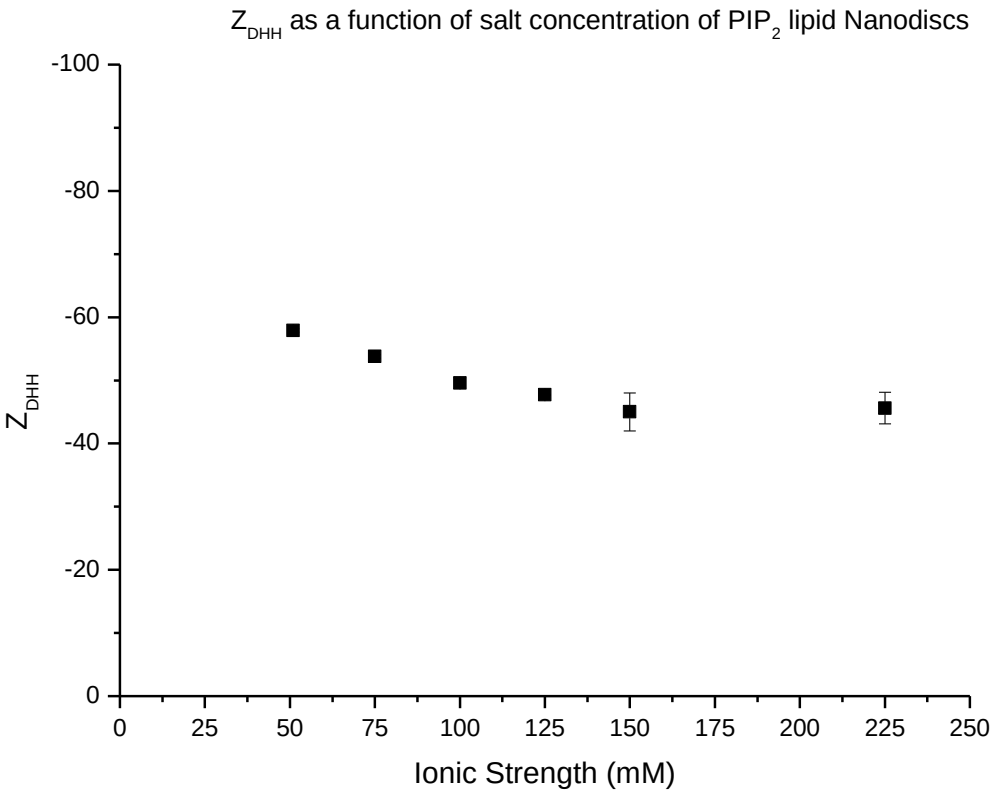

Figure 12 Z_{DHH} as a function of Na^+ concentration for MSP1D1 PIP2 Nanodiscs. Similar to other anionic Nanodiscs, the charge magnitude of PIP2 Nanodiscs decreased as the salt concentration increased. For PIP2 Nanodiscs, the plateau threshold was similar to that of 30POPS Nanodiscs at ~ 100 mM (**Figure 10**).

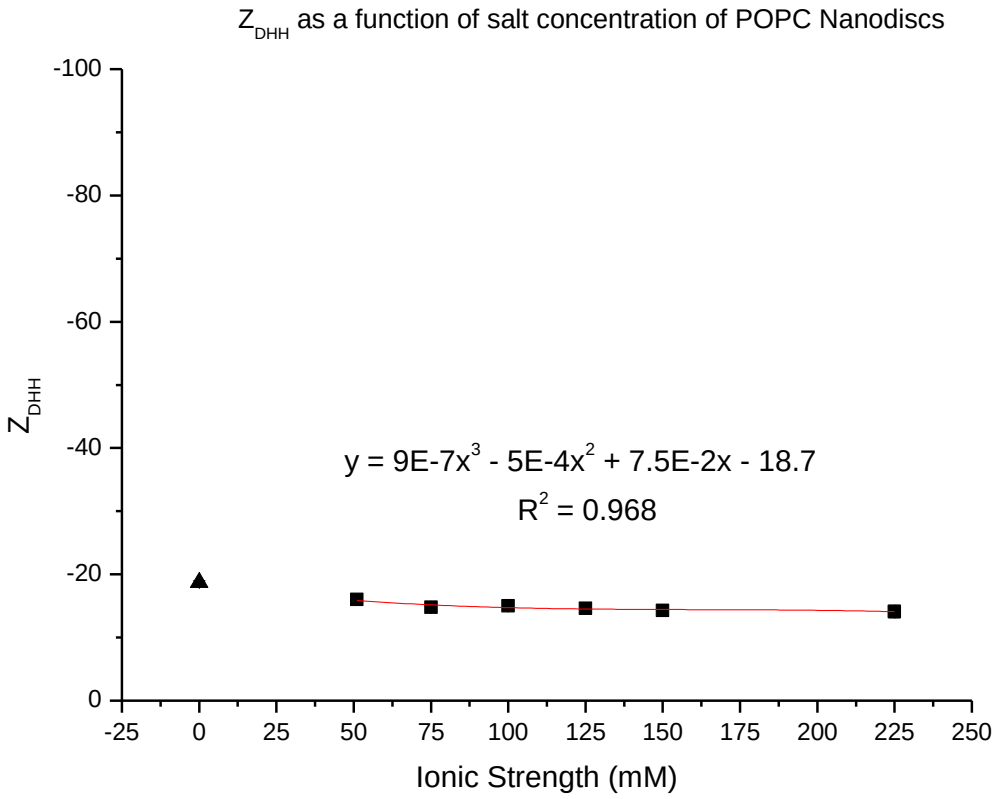

Figure 13 Z_{DHH} as a function of Na^+ concentration for MSP1D1 POPC Nanodiscs fitted to a 3rd order polynomial. The intercept of the 3rd order polynomial was -18.7 ± 0.3. In this and subsequent figures, the square data points represent the experimental Z_{DHH} values using MCE and the triangle data point represents the extrapolated intercept value at zero salt. The line represents the fit of the 3rd order polynomial to the experimental data points.

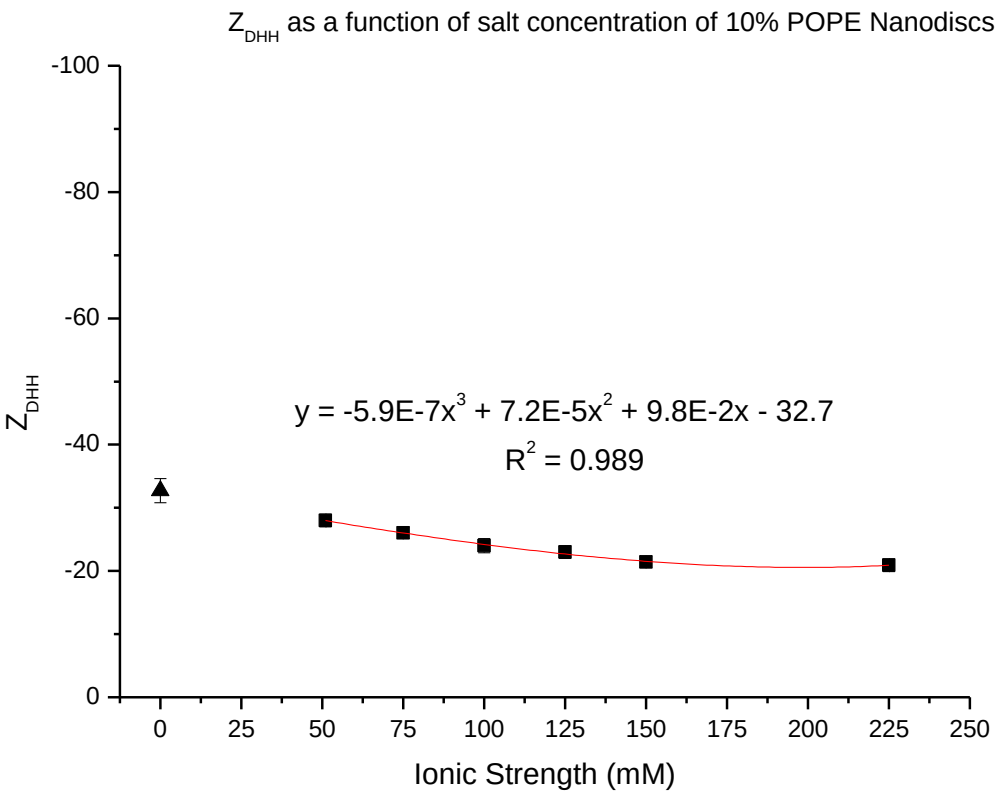

Figure 14 Z_{DHH} as a function of Na^+ concentration for MSP1D1 10POPE Nanodiscs fitted to a 3rd order polynomial. The intercept of the 3rd order polynomial was -32.7 ± 2.7.

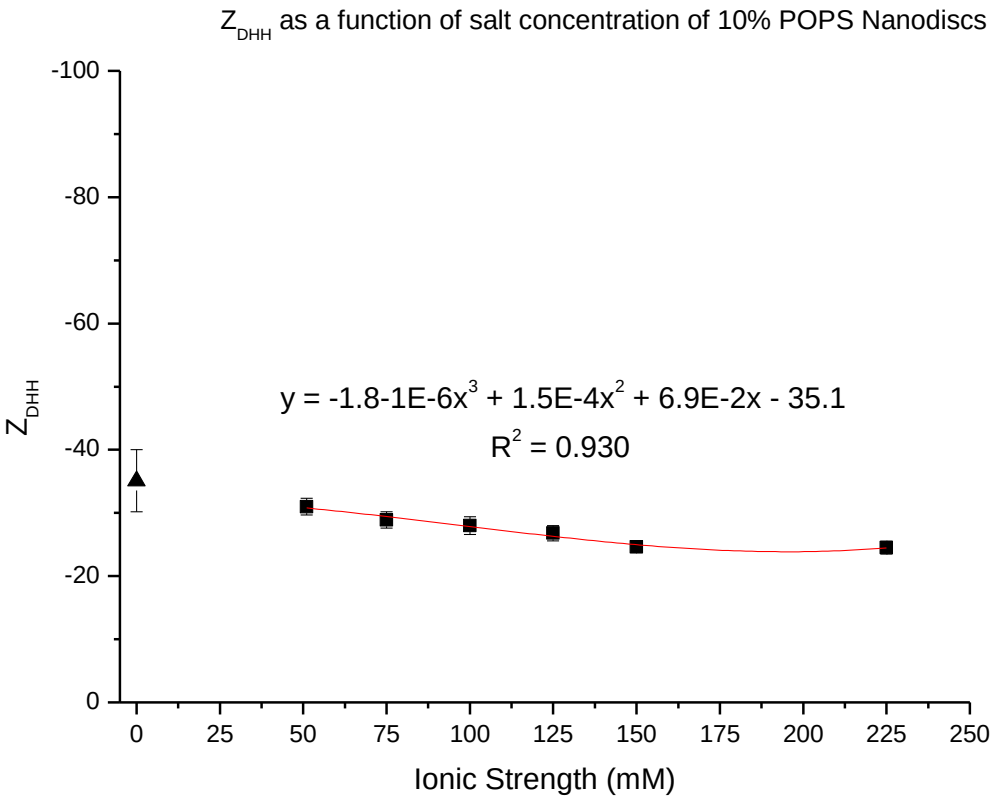

Figure 15 Z_{DHH} as a function of Na^+ concentration for MSP1D1 10POPS Nanodiscs fitted to a 3rd order polynomial. The intercept of the 3rd order polynomial was -35.1 ± 4.1.

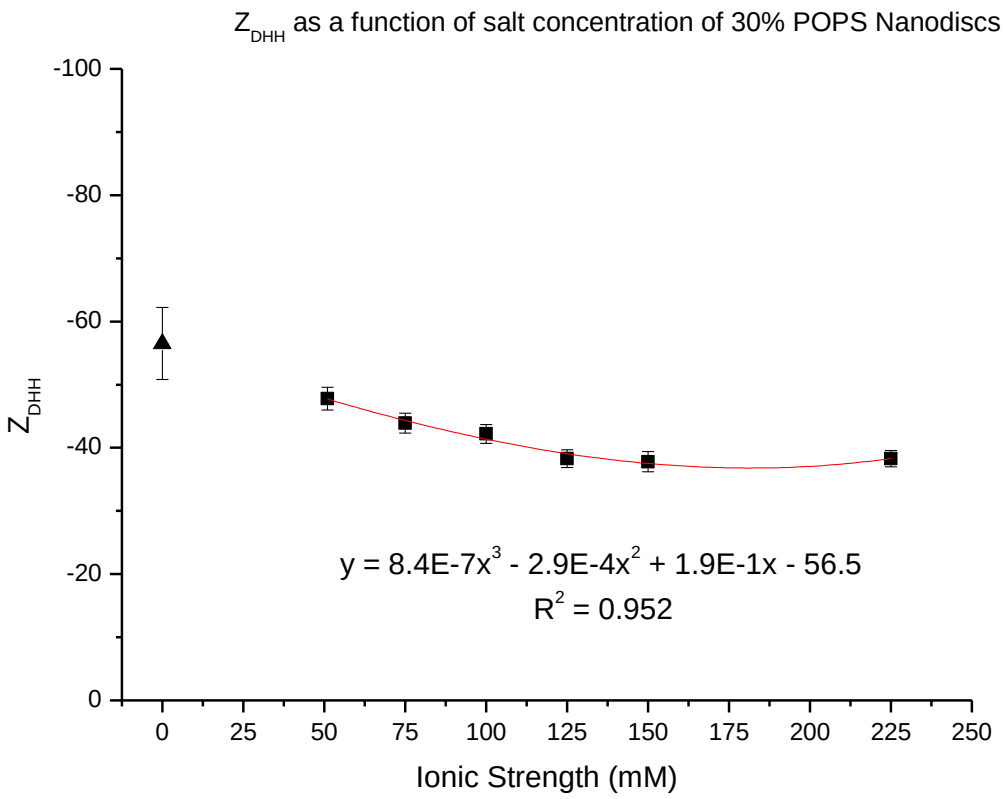

Figure 16 Z_{DHH} charge as a function of Na^+ concentration for MSP1D1 30POPS Nanodiscs fitted to a 3rd order polynomial. The intercept of the 3rd order polynomial was -56.5 ± 5.7.

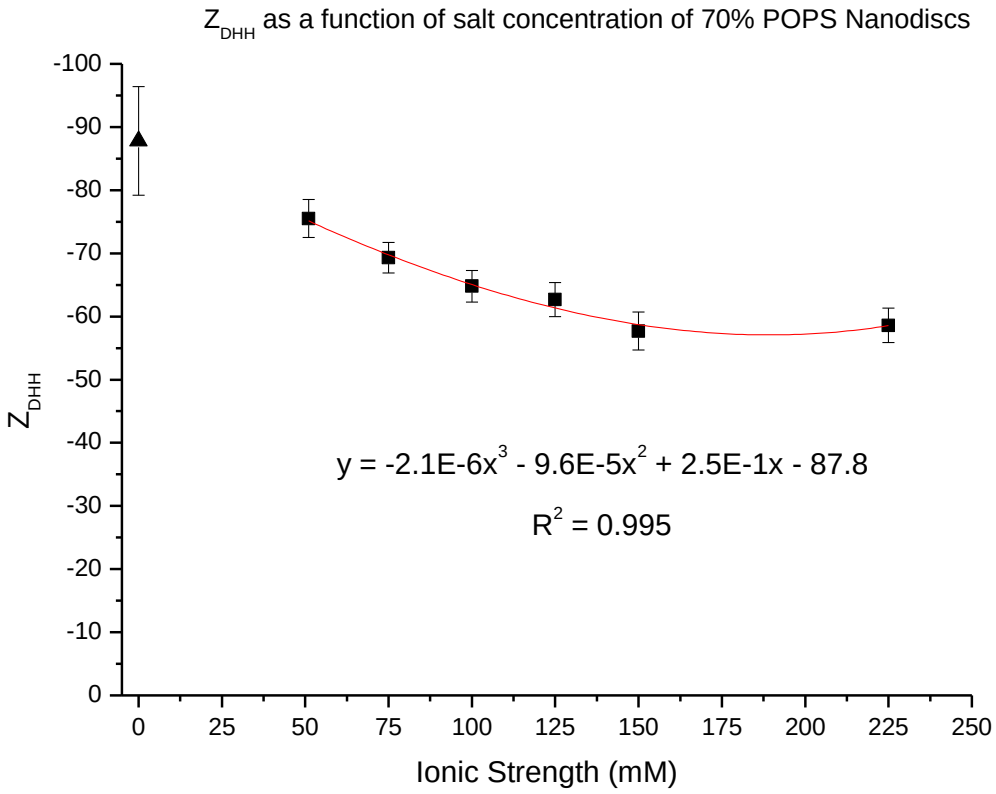

Figure 17 Z_{DHH} as a function of Na^+ concentration for MSP1D1 70POPS Nanodiscs fitted to a 3rd order polynomial. The intercept of the 3rd order polynomial was -87.8 ± 8.6.

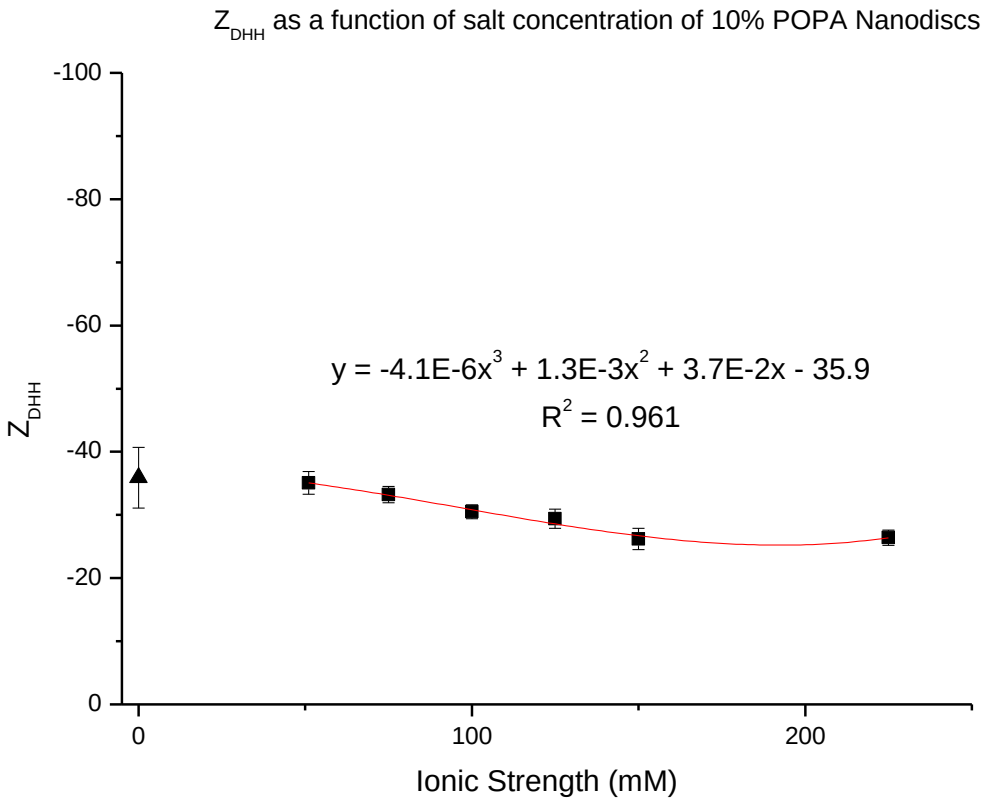

Figure 18 Z_{DHH} as a function of Na^+ concentration for MSP1D1 10POPA Nanodiscs fitted to a 3rd order polynomial. The intercept of the 3rd order polynomial was -35.9 ± 4.8.

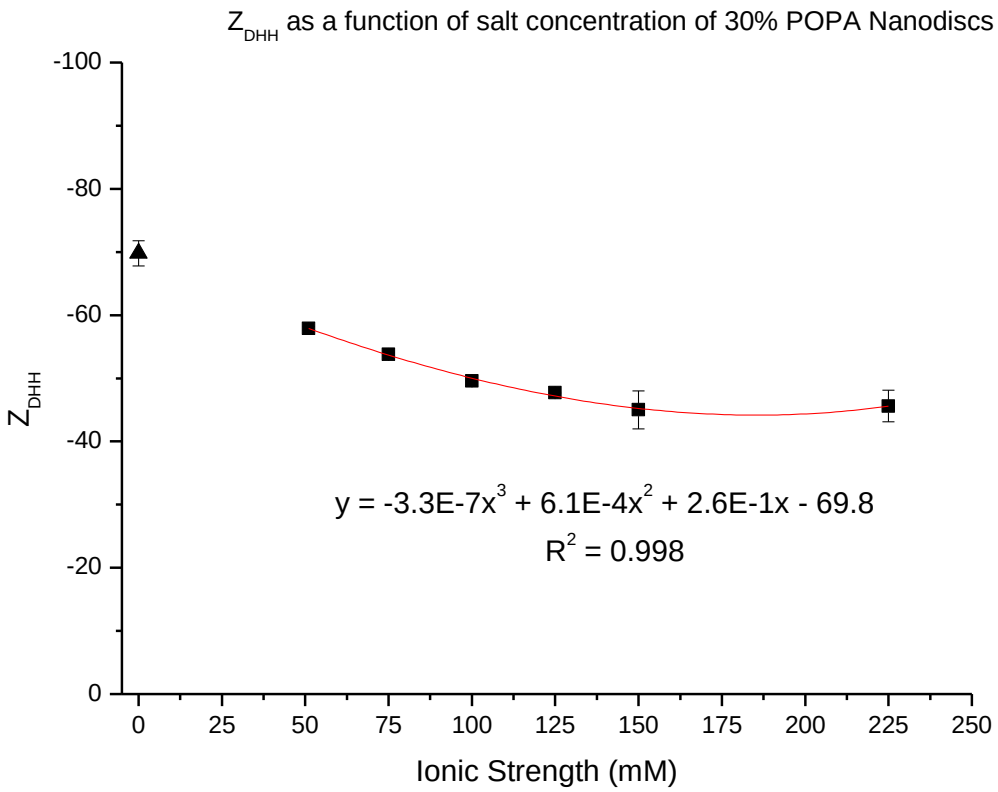

Figure 19 Z_{DHH} as a function of Na^+ concentration for MSP1D1 30POPA Nanodiscs fitted to a 3rd order polynomial. The intercept of the 3rd order polynomial was -69.8 ± 2.0.

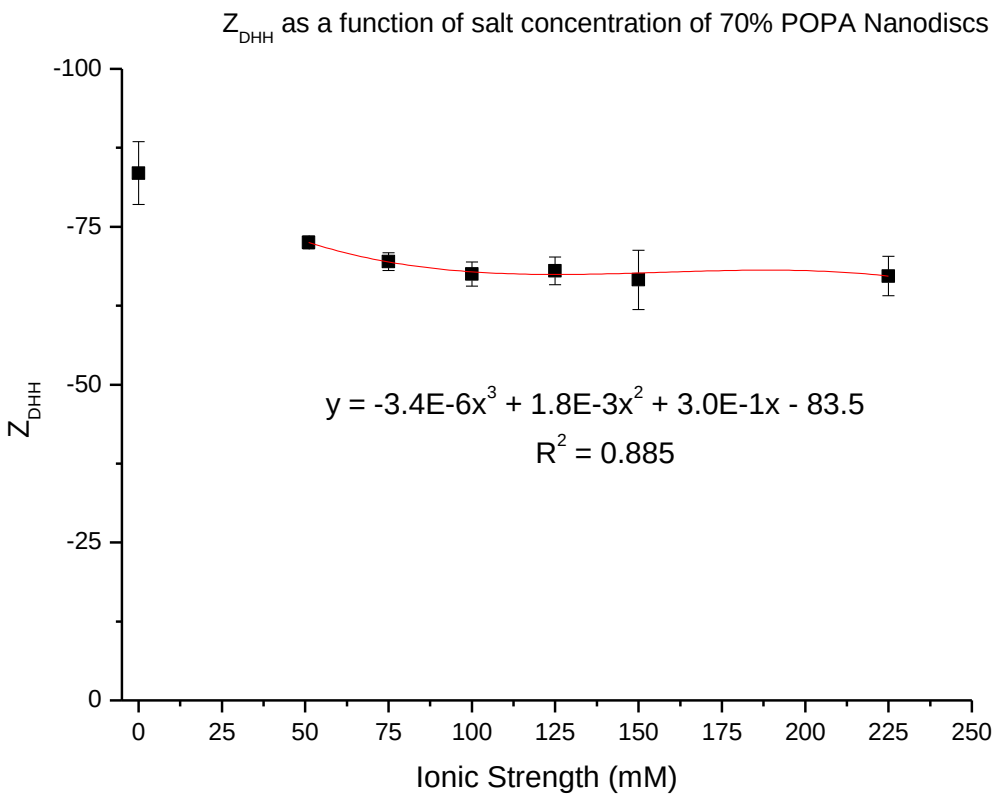

Figure 20 Z_{DHH} as a function of Na^+ concentration for MSP1D1 70POPA Nanodiscs fitted to a 3rd order polynomial. The intercept of the 3rd order polynomial was -83.5 ± 5.0.

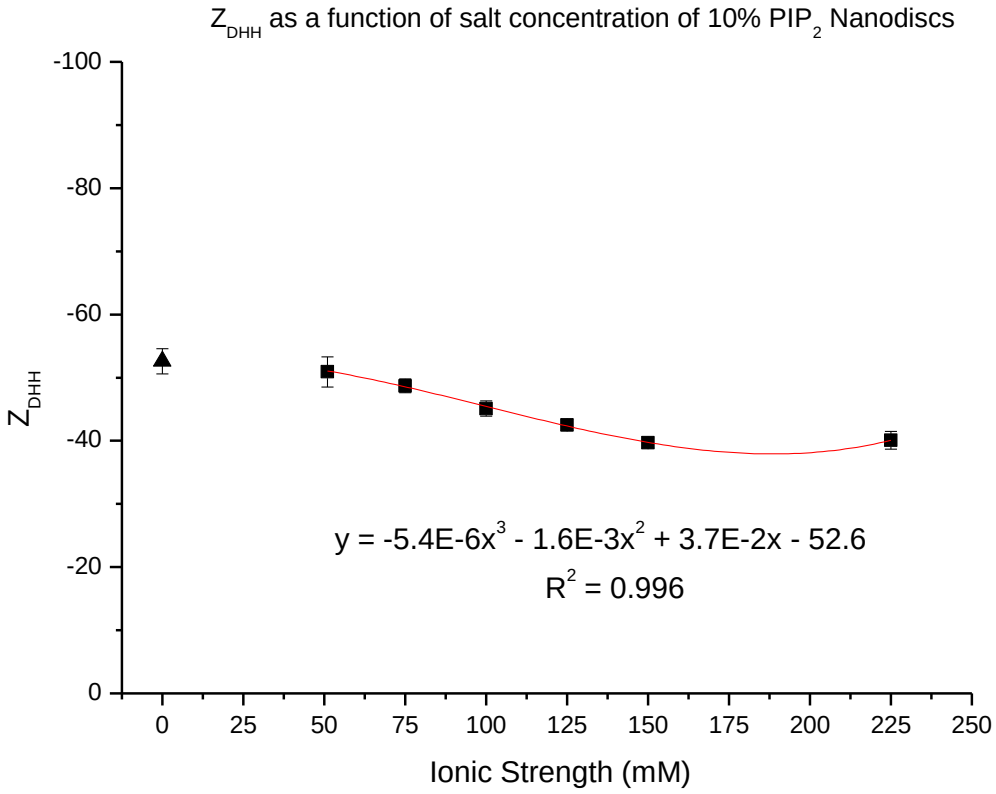

Figure 21 Z_{DHH} as a function of Na^+ concentration for MSP1D1 10PIP_2 Nanodiscs fitted to a 3rd order polynomial. The intercept of the 3rd order polynomial was -52.6 ± 2.0.

Nanodisc™ Sample	Extrapolated Z_{DHH} at zero salt concentration	Calculated total charge
MSP1D1 POPC	-18.7 ± 0.3	-16
MSP1D1 POPE	-32.7 ± 2.7	-29
MSP1D1 10POPS	-35.1 ± 4.1	-29
MSP1D1 30POPS	-56.5 ± 5.7	-54
MSP1D1 70POPS	-87.8 ± 8.6	-104
MSP1D1 10POPA	-35.9 ± 4.8	-32
MSP1D1 30POPA	-69.8 ± 2.0	-63
MSP1D1 70POPA	-83.5 ± 5.0	-125
MSP1D1 10PIP_2	-52.6 ± 2.0	-54

Table 7 Summary and comparison of the extrapolated Z_{DHH} values at zero salt to the calculated charge estimates seen in **Tables 5a** and **5b.**

Divalent Cations. Divalent cations have been shown to play direct roles in various lipid:lipid and lipid:protein interactions. In particular, there are numerous reactions that do not occur in the absence of a particular divalent cation [Tavoosi et al., 2009]. Ca^{2+} and Mg^{2+} are relevant with respect to lipids because the electrostatic properties of the lipids also play a role in ion-mediated reactions with proteins, lipid translocation and bilayer aggregation/fusion [Martin-Molina et al., 2012].

POPC and POPS Nanodiscs. **Figure 22a** shows the Z_{DHH} of MSP1D1 POPC and MSP1D1 10POPS, 30POPS and 70POPS Nanodiscs in the absence and presence of divalent cations Ca^{2+} and Mg^{2+}. In the presence of 3 mM Mg^{2+}, there is no significant change to the Z_{DHH} of POPC and POPS Nanodiscs. In the presence of 3 mM $CaCl_2$, Z_{DHH} decreases by ~ 20-25% for both POPC and POPS Nanodiscs. However, the absolute magnitude of the Z_{DHH} decrease in the presence of 3 mM Ca^{2+} increases with increasing PS content. **Figure 22b** shows the fractional charge of MSP1D1 POPC and MSP1D1 POPS Nanodiscs in the presence of 3 mM Ca^{2+}. In **Figure 22b**, the fractional charge depicted here, is the ratio of the Z_{DHH} in the presence of Ca^{2+} to the Z_{DHH} in the absence of Ca^{2+} (**Table 1**).

POPA Nanodiscs. **Figures 23a** and **23b** show the sedimentation velocity of MSP1D1 70POPA Nanodiscs in the absence (a) and presence (b) of Ca^{2+}. In the presence of 3 mM Ca^{2+}, multiple larger species to appear (**Figure 23b**). This was also observed in the MSP1D1 10 and 30POPA Nanodiscs (**Figures A12** and **A14**). Typical of all Nanodisc^{TM} samples is a peak at 0.5 S. It is currently unknown as to what that material is, but it is not an artifact. It is present in every Nanodisc^{TM} sample that has been analyzed by AUC using Sedfit analysis.

Figures 24a and **24b** show the Z_{DHH} distribution of MSP1D1 30POPA Nanodiscs in the presence of 3 mM Ca^{2+} (**Figure 24a**) and 3 mM Mg^{2+} (**Figure 24b**). In comparison to the Z_{DHH} distribution of MSP1D1 30POPS Nanodiscs, the population of MSP1D1 30POPA Nanodiscs contains a pronounced shoulder (indicated by arrow) and is heterogeneous in terms of size and charge in the presence of Ca^{2+}. It should be noted, that while aggregate formation was observed, the Z_{DHH} was not completely neutralized and a non-zero Z_{DHH} was observed. The Z_{DHH} of 30POPA Nanodiscs was ~ 50% less in the presence of Ca^{2+}, in comparison to the Z_{DHH} of POPA Nanodiscs in the absence of Ca^{2+}. The Z_{DHH} of 30POPA Nanodiscs was ~ 30% less in the presence of Ca^{2+}, in comparison to the Z_{DHH} of 30POPA Nanodiscs in the presence of 3 mM Mg^{2+}. Similar Z_{DHH} data was observed in 10POPA and 70POPA Nanodiscs.

Figure 25 shows the Z_{DHH} of POPA Nanodiscs in the absence and presence of Mg^{2+}. As seen in **Figure 23b** and **Figure 24**, POPA Nanodiscs aggregate in the presence of Ca^{2+}. However, in the presence of Mg^{2+}, Z_{DHH} decreases by ~ 25%. This is in contrast to POPC and POPS Nanodiscs, which do not see a change in Z_{DHH} in the presence of Mg^{2+} (**Figure 6**).

Figure 26a shows the fractional charge of MSP1D1 POPA Nanodiscs in the presence of 3 mM Mg^{2+}. In this graph, the fractional charge depicted, is the ratio of the Z_{DHH} of POPA Nanodiscs in the presence of 3 mM Mg^{2+} to the Z_{DHH} of POPA Nanodiscs in the absence of 3 mM Mg^{2+}. While the fractional charge does decrease slightly as more PA lipids are incorporated, the change is not significant (<10%) as more PA lipids are incorporated.

Figure 26b shows a comparison of the fractional charge of MSP1D1 POPS Nanodiscs in the presence of Ca^{2+} to the fractional charge of MSP1D1 POPA Nanodiscs in the presence of Mg^{2+}. Similar to the fractional charge of POPS Nanodiscs in the presence of Ca^{2+}, the fractional charge

of POPA Nanodiscs in the presence of Mg^{2+} decreases ~ 20-25% as more anionic lipids are incorporated into the Nanodiscs.

POPA Nanodiscs behave very differently in the presence of divalent cations and therefore is treated separately from POPC and POPS data **(Figures 24** and **25).** However, Mg^{2+} affects the electrophoretic mobility and Z_{DHH} of POPA Nanodiscs similarly to that of Ca^{2+} and POPC and POPS Nanodiscs as seen by the similar fractional charges (**Figure 26b**). At the current time, this observation cannot be explained. In addition, POPA Nanodiscs also exhibit a proclivity to aggregate irreversibly in the presence of Ca^{2+}. In the presence of Ca^{2+}, AUC (**Figure 23b**) and MCE (**Figure 24**) data show multiple peaks and shoulders that cannot be diluted out with multiple rounds of dialysis (up to a week of dialyzing with buffer exchanges every 12 hours).

PIP_2 Nanodiscs. **Figure 27** shows the Z_{DHH} distribution of $10PIP_2$ Nanodiscs in standard buffer in the absence of divalent cations. **Figure 28** shows the ZDHH distribution of $10PIP_2$ Nanodiscs in the presence of 3 mM Ca^{2+}. **Figure 29** shows the ZDHH distribution of $10PIP_2$ Nanodiscs in the presence of 3 mM Mg^{2+}. **Table 8** summarizes the Z_{DHH} of $10PIP_2$ Nanodiscs in the absence and presence of divalent cations Ca^{2+} and Mg^{2+}.

Table 9 summarizes the aggregation behavior of POPC, POPE, POPS, POPA and PIP_2 Nanodiscs in the presence of divalent cations Ca^{2+} and Mg^{2+}.

PIP_2 Nanodiscs behave oppositely that of POPA Nanodiscs. In the presence of Ca^{2+}, the Z_{DHH} of PIP_2 Nanodiscs is decreased by ~ 50% relative to the Z_{DHH} of PIP_2 Nanodiscs in the absence of Ca^{2+} (**Figure 28** and **Table 8**). In the presence of Mg^{2+}, aggregation behavior was observed (**Figure 29**). In addition, the fractional charge of PIP_2 Nanodiscs in the presence of Ca^{2+} is much lower in magnitude than that of POPC and POPS in the presence of Ca^{2+} (**Figure**

30). Like POPA Nanodiscs, the aggregation behavior of PIP_2 Nanodiscs cannot be diluted or dialyzed away, suggesting an irreversible interaction.

POPE Nanodiscs were well behaved in standard buffer and solvents containing different monovalent alkali cations. However MCE experiments in the presence of Mg^{2+} and Ca^{2+} were not successful. When Mg^{2+} or Ca^{2+} was dialyzed into the sample (from 24 hours to a maximum of 72 hours), mobility experiments resulted in no movement of the POPE Nanodiscs. It is not very likely the POPE Nanodiscs are completely neutral, as the membrane scaffolding protein should still contribute overall net negative charge to the Nanodiscs. If POPC Nanodiscs were not observed to be stationary in any capacity, neither should POPE Nanodiscs, unless sufficient cationic charge was added with Mg^{2+} and Ca^{2+} to make the Nanodiscs neutral.

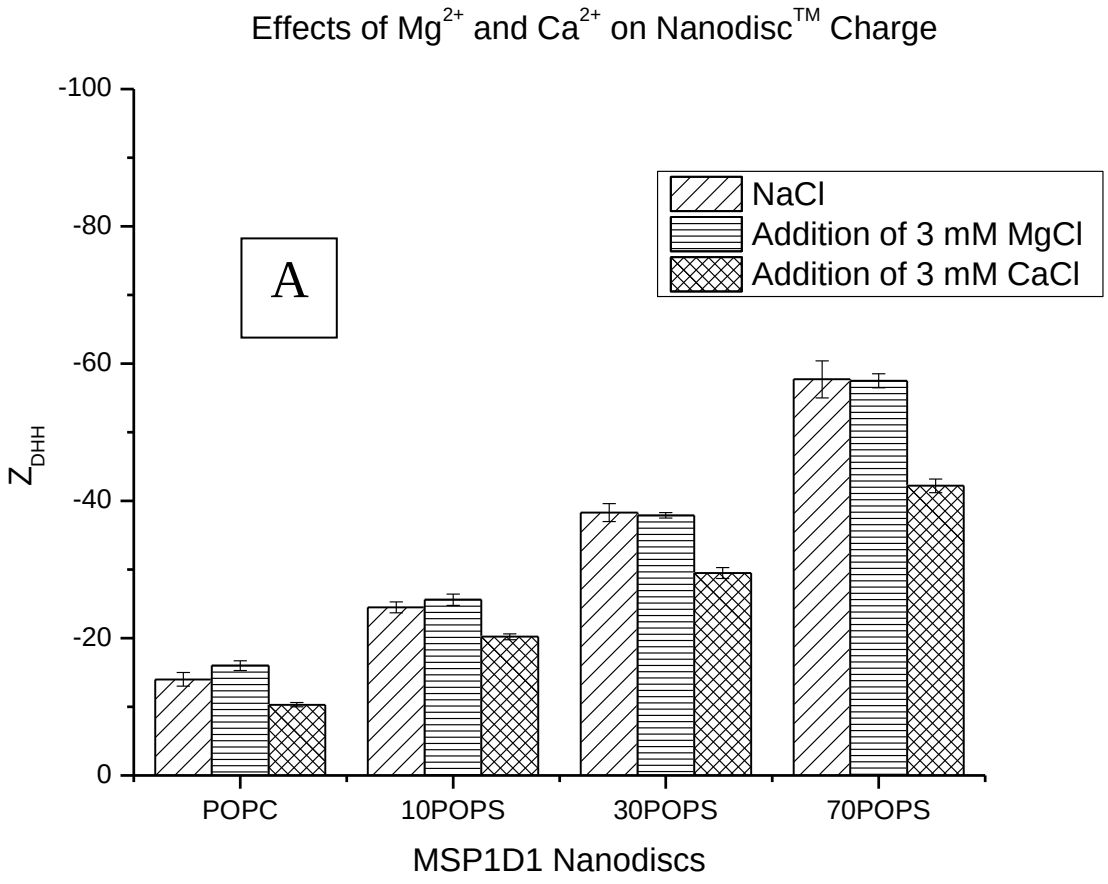

Figure 22a Z_{DHH} of MSP1D1 POPC and POPS Nanodiscs in the absence and presence of different divalent cations. When Mg^{2+} is added, there is no significant change to the Z_{DHH} of POPC and POPS Nanodiscs. When 3 mM $CaCl_2$ is added, the charge magnitude decreases by ~ 20-25% for both POPC and POPS.

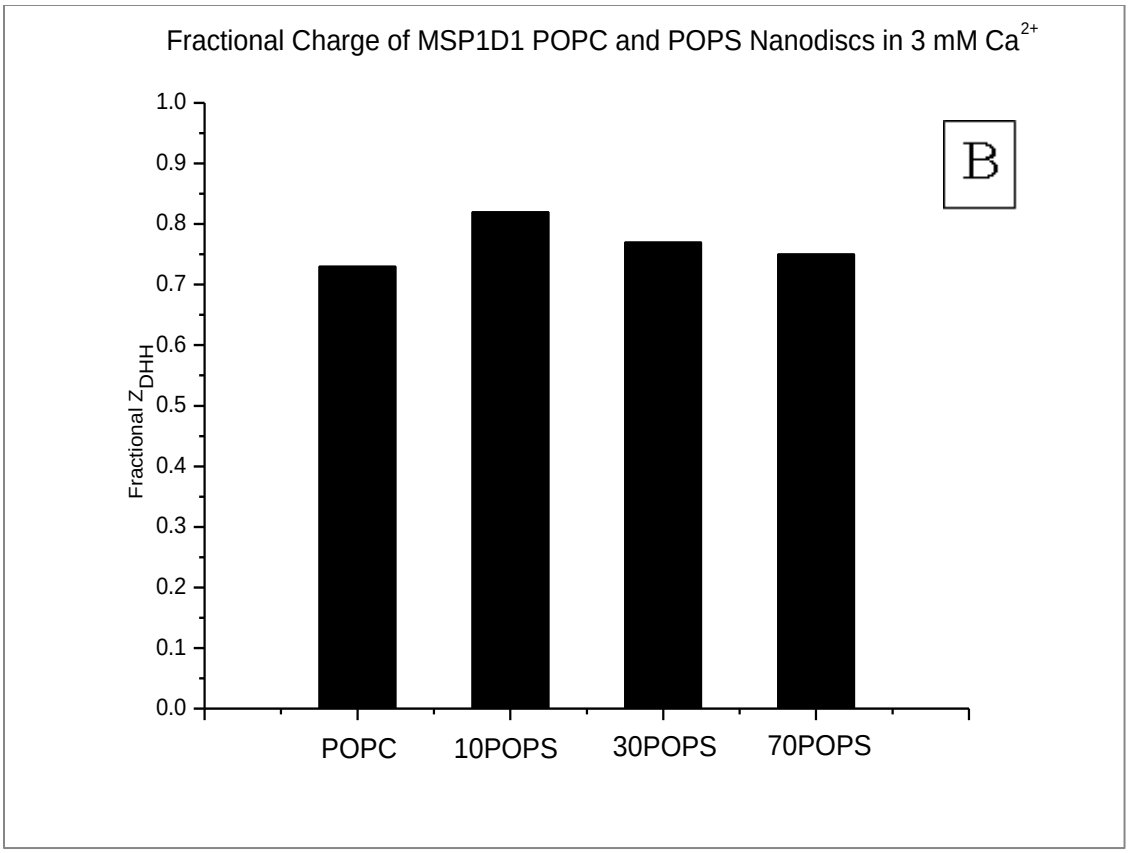

Figure 22b Fractional charge of MSP1D1 POPC and POPS Nanodiscs in standard buffer with 3 mM $CaCl_2$ added. In this graph, the fractional charge is the ratio of the Z_{DHH} in the presence of Ca^{2+} to the Z_{DHH} in the absence of Ca^{2+} **(Table 1).** The data show that there is a 20-25% decrease in the charge magnitude, in the presence of 3 mM Ca^{2+} regardless of PS content.

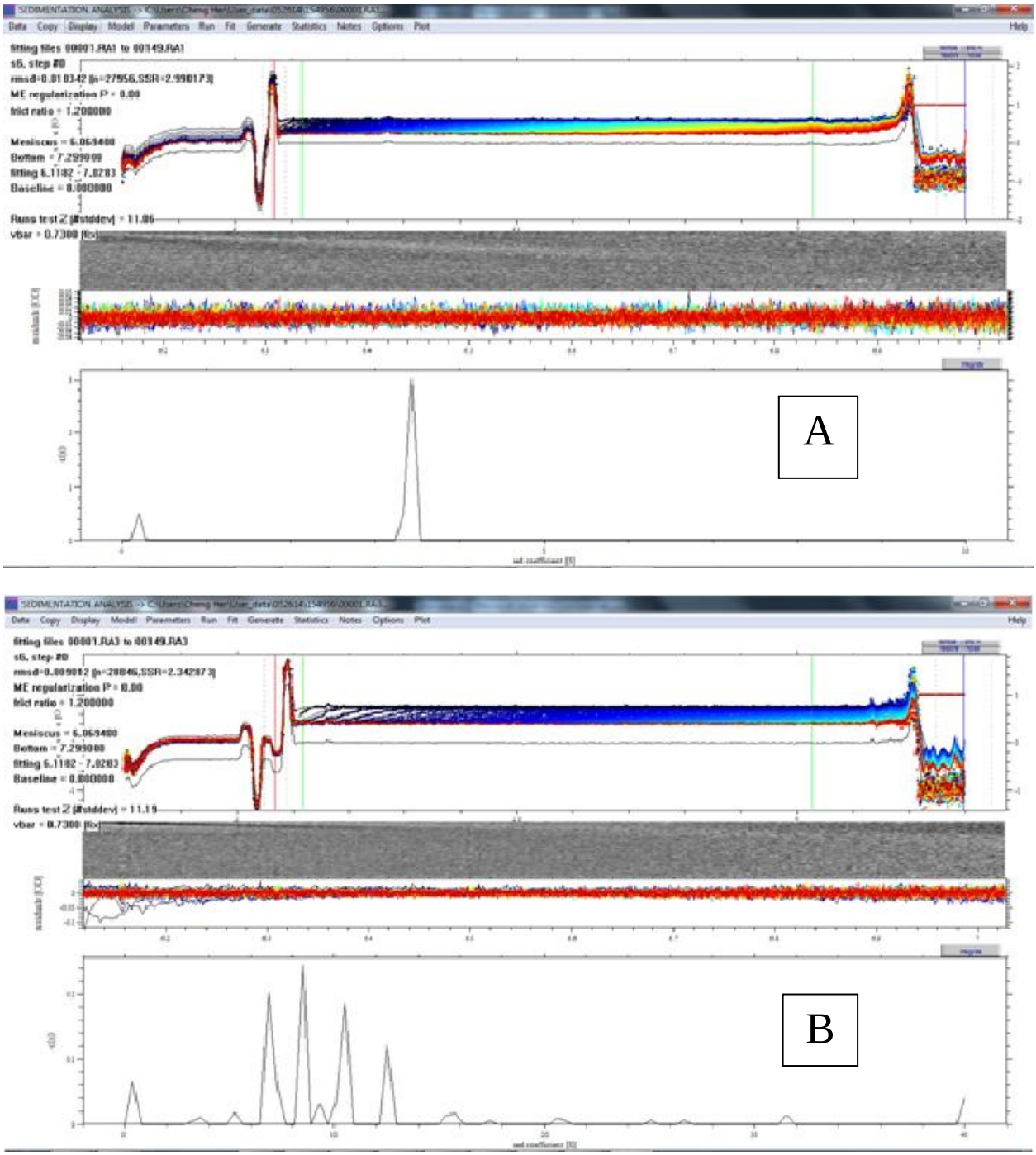

Figure 23a and 23b Sedimentation velocity data of MSP1D1 70POPA in the absence (a) and presence (b) of Ca^{2+}.

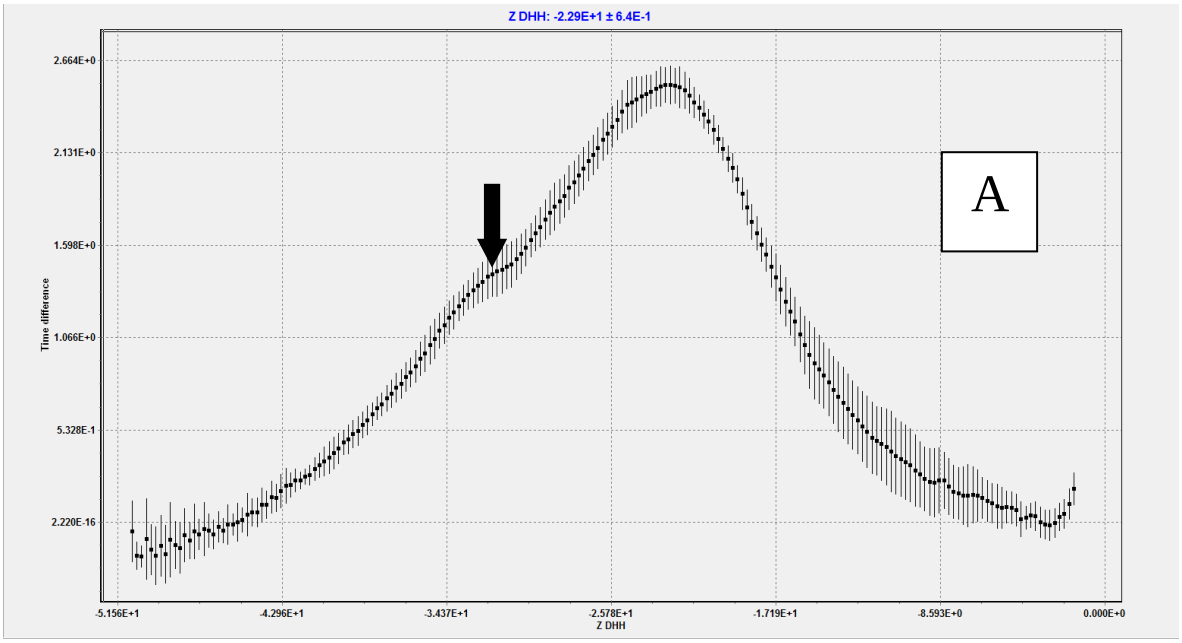

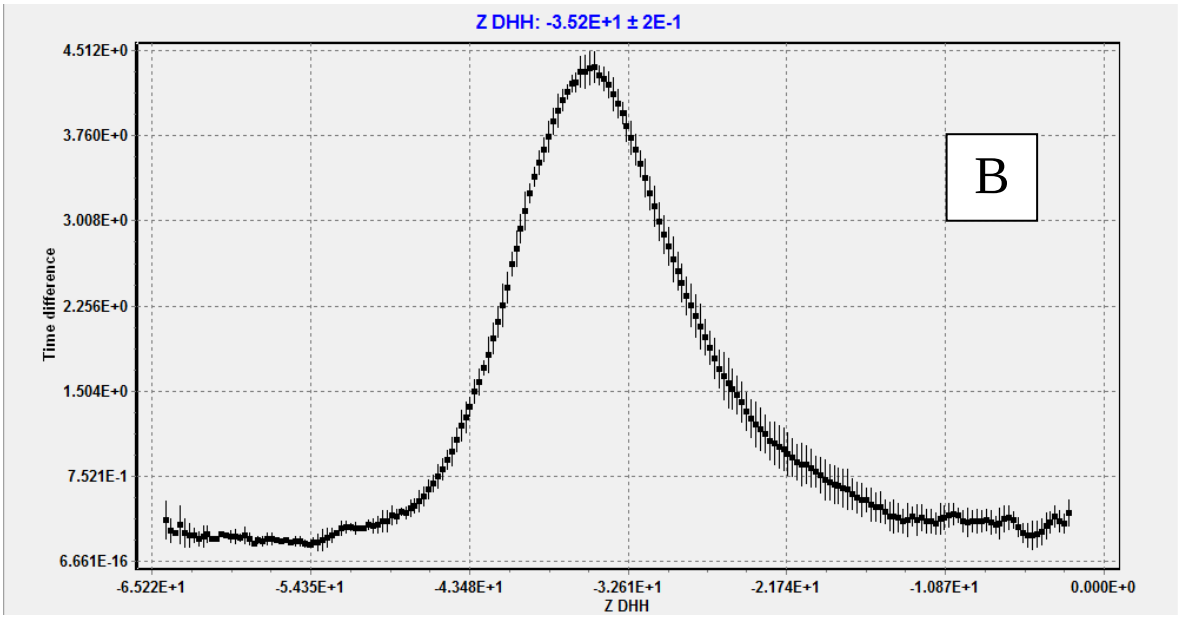

Figures 24a and **24b** MCE data for MSP1D1 30POPA Nanodiscs in the presence of 3 mM Ca^{2+} (a) and 3 mM Mg^{2+} (b). Unlike the distribution data seen in **Figure 1**, there is a pronounced shoulder (indicated by the arrow) in this data in accord with the aggregation characterized by sedimentation velocity (**Figure 23b)**. This peak mobility is considerably less than 30POPA in the absence of Ca^{2+} (**Table 4**) and in the presence of Mg^{2+}, but the distribution is very broad, indicating that there is aggregation as well as neutralization occurring. Similar Z_{DHH} distributions were also observed with 10 and 70POPA Nanodiscs in the presence of Ca^{2+}.

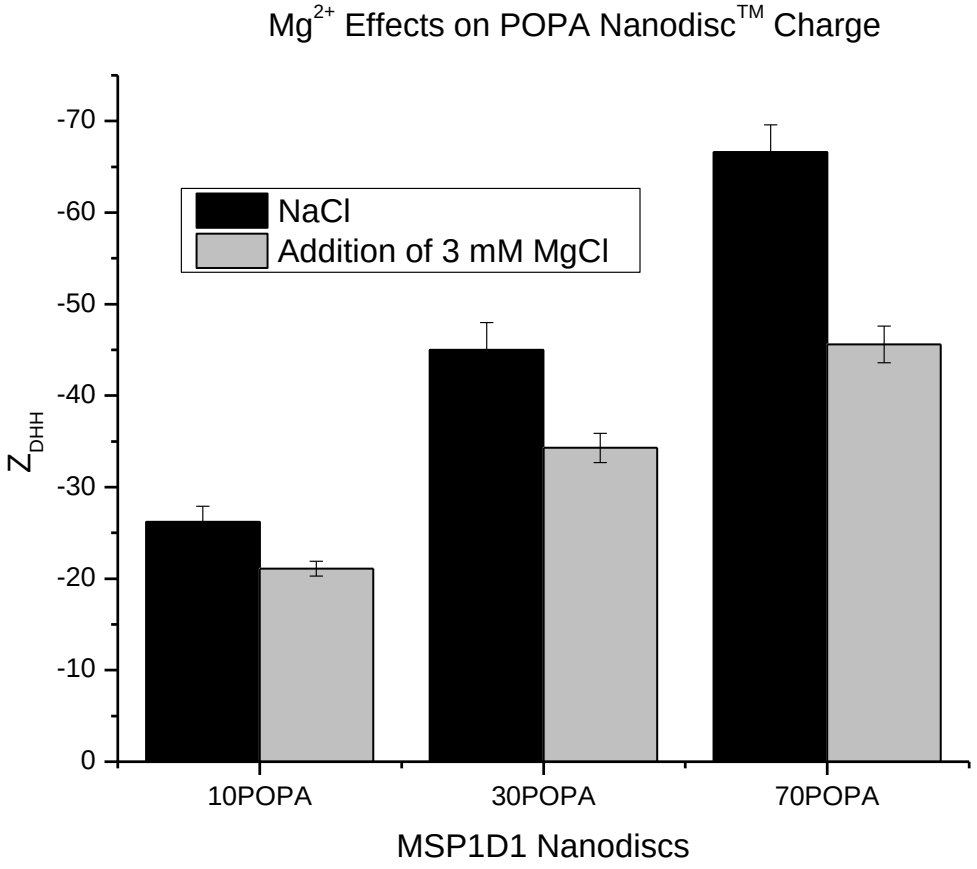

Figure 25 The Z_{DHH} of POPA Nanodiscs in the absence (black) and presence (gray) of Mg^{2+}.

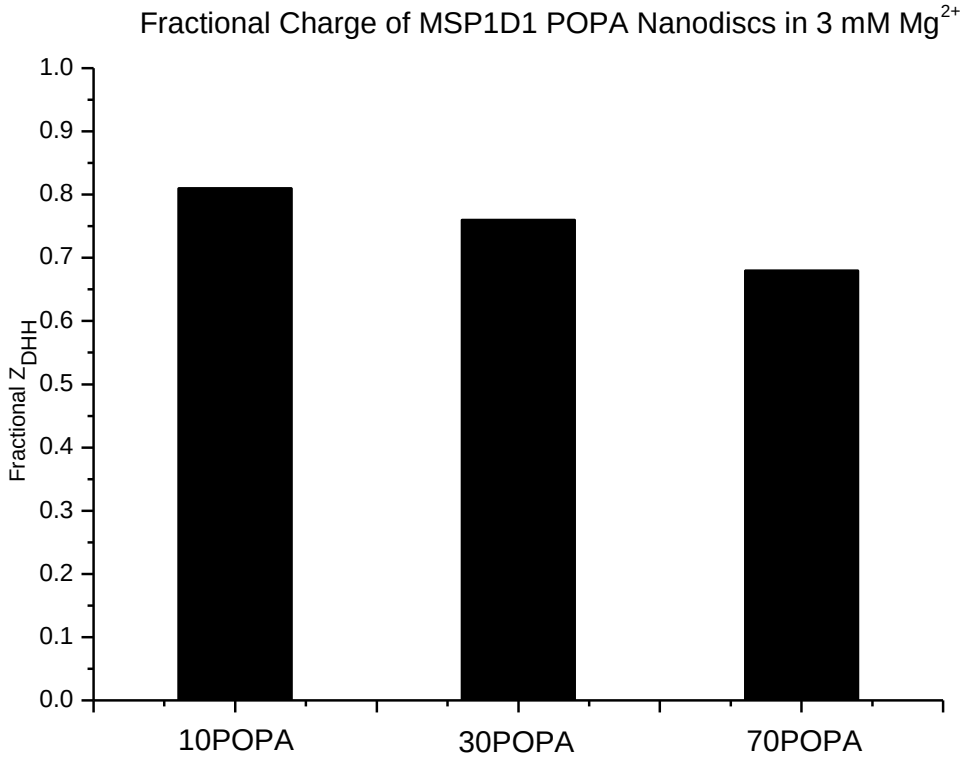

Figure 26a Fractional charge of MSP1D1 POPA Nanodiscs in the presence of 3 mM Mg^{2+}. In this graph, the fractional charge is the ratio of the Z_{DHH} in the presence of 3 mM Mg^{2+} to the Z_{DHH} in the absence of 3 mM Mg^{2+}.

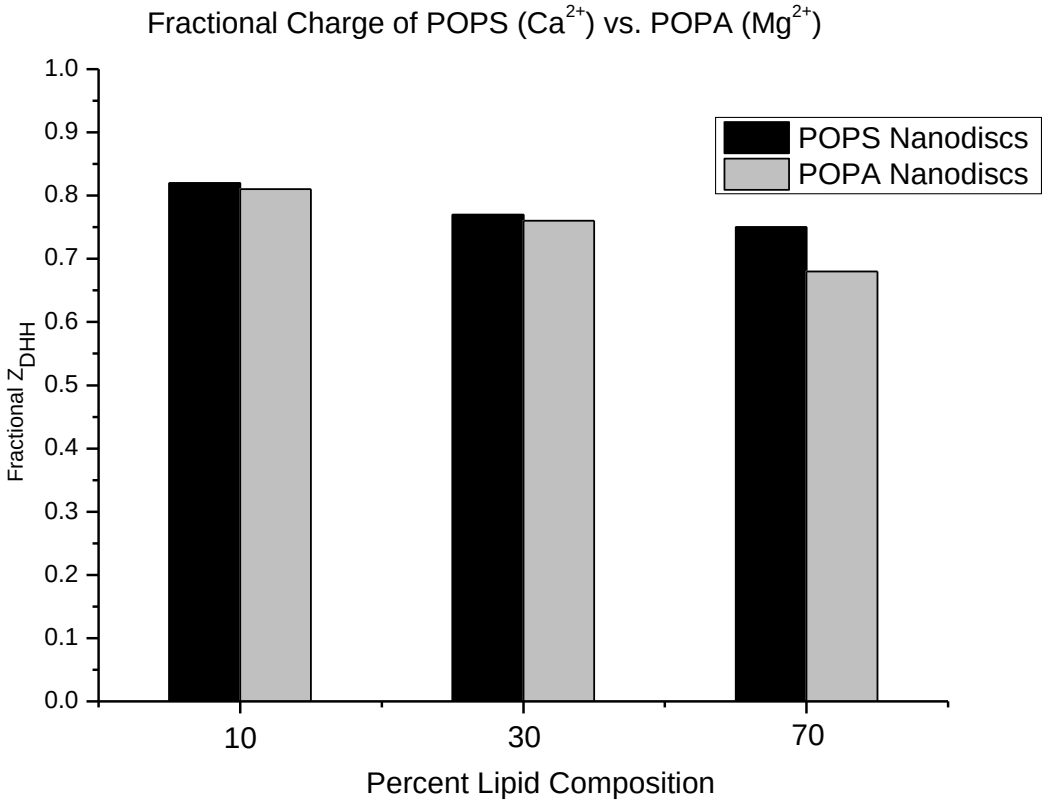

Figure 26b Comparison of the fractional charge between POPS Nanodiscs in the presence of 3mM Ca^{2+} (black) and POPA Nanodiscs in the presence of Mg^{2+} (gray). The fractional charges are similar for the different anionic lipids with the different divalent cations.

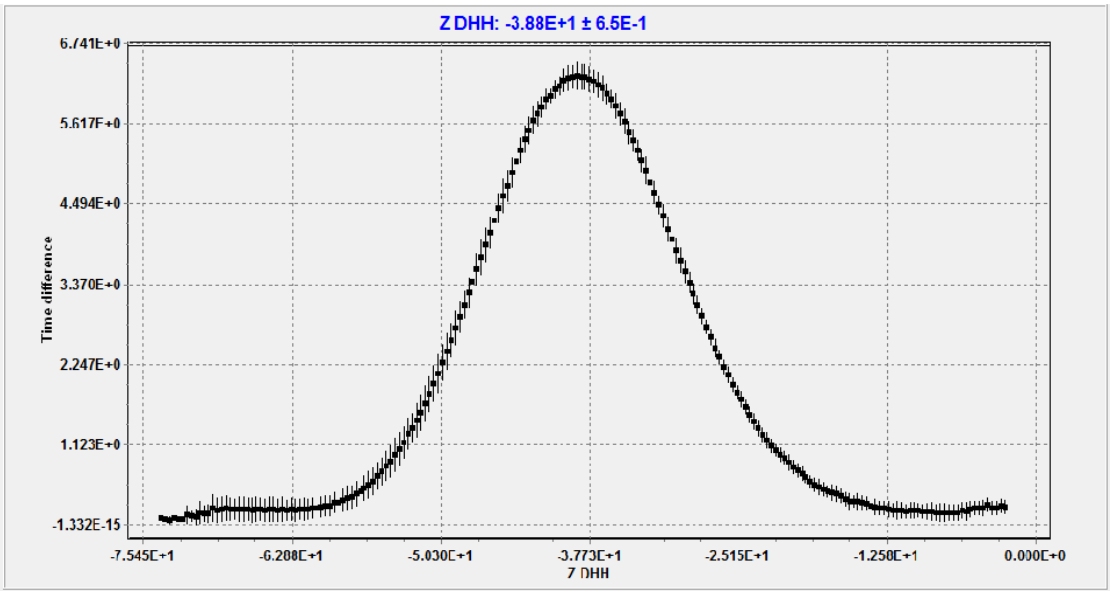

Figure 27 The Z_{DHH} distribution curve for MSP1D1 10PIP$_2$ Nanodiscs in the absence of divalent cations transformed from the raw intensity scans.

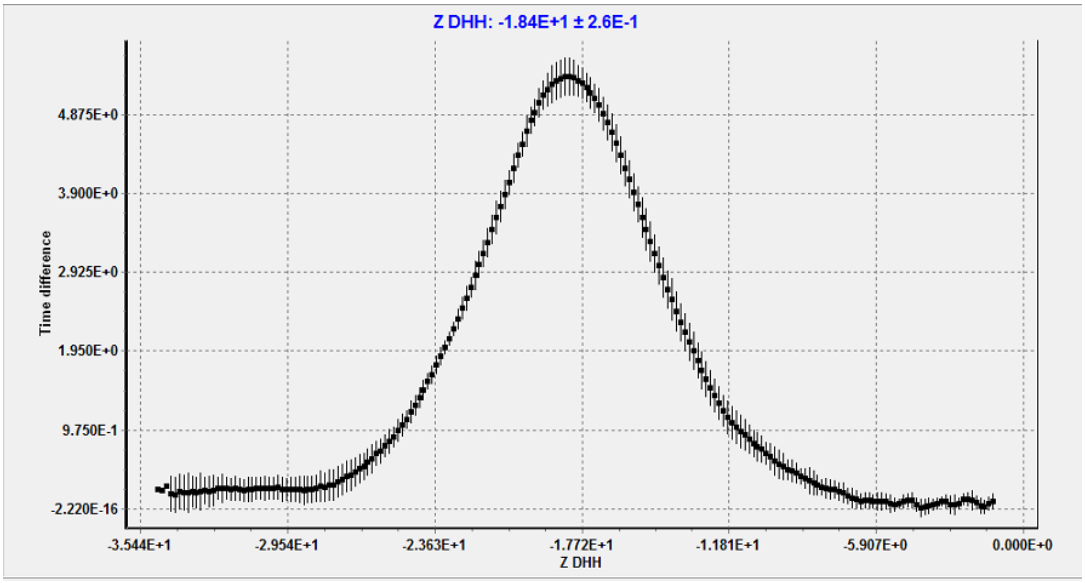

Figure 28 The Z_{DHH} distribution curve for MSP1D1 10PIP$_2$ Nanodiscs in the presence of 3 mM Ca^{2+} transformed from the raw intensity scans.

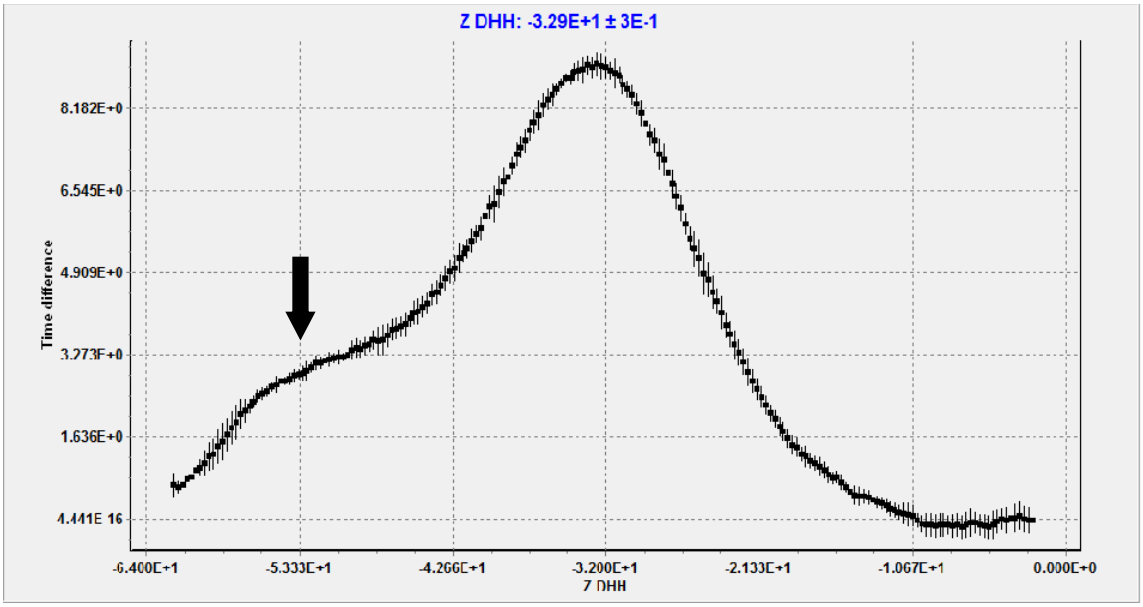

Figure 29 The Z_{DHH} distribution curve for MSP1D1 10PIP$_2$ Nanodiscs in the presence of 3 mM Mg^{2+} transformed from the raw intensity scans. Notice that the peak in **Figure 29** is nearly two times more negative than the peak in **Figure 28**. Also, there is a strong shoulder ~ -53 (indicated by the arrow), suggesting further aggregation.

Nanodisc™ Sample	Buffer	Z_{DHH}
MSP1D1 10PIP$_2$	100mM NaCl, 50mM Tris, pH 7.4	-40.3 ± 0.9
MSP1D1 10PIP$_2$	100mM NaCl, 50mM Tris, 3mM $CaCl_2$ pH 7.4	-17.9 ± 0.8
MSP1D1 10PIP$_2$	100mM NaCl, 50mM Tris, 3mM MgCl pH 7.4	ND

Table 8 The Z_{DHH} of PIP$_2$ Nanodiscs calculated from the measured electrophoretic mobilities using MCE in the absence and presence of divalent cations.

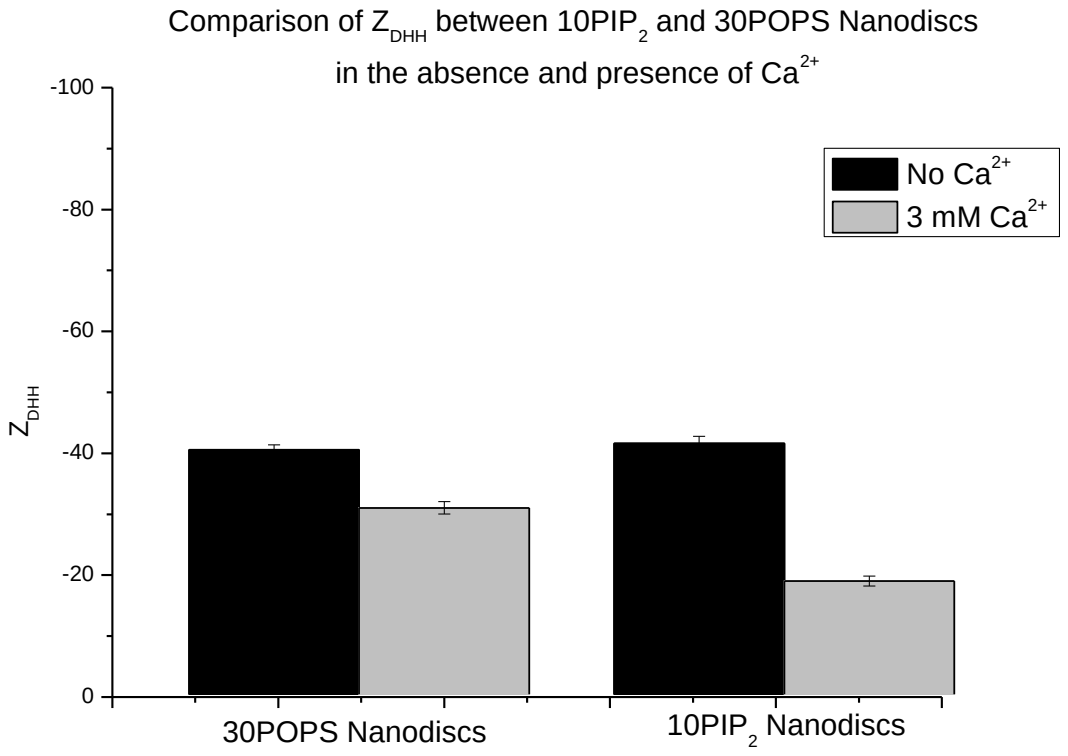

Figure 30 A comparison of the Z_{DHH} of 30POPS Nanodiscs and $10PIP_2$ Nanodiscs in the absence (black) and presence (gray) of 3 mM Ca^{2+}. In this graph, the fractional charge is the ratio of the Z_{DHH} in the presence of 3 mM $CaCl_2$ to the Z_{DHH} in the absence of 3 mM $CaCl_2$. In the presence of Ca^{2+}, the charge magnitude of $10PIP_2$ Nanodiscs decreases by ~ 50%. In the presence of Ca^{2+}, the charge magnitude of 30POPS Nanodiscs decreases by ~ 25%.

MSP1D1 Nanodisc™ sample	10 uM Ca^{2+}	3 mM Ca^{2+}	10 uM Mg^{2+}	3 mM Mg^{2+}
POPC	-	-	-	-
POPE	ND	ND	ND	ND
POPS	-	-	-	-
POPA	-	+	-	-
PIP_2	-	-	-	+

Table 9 shows the behavior of MSP1D1 Nanodiscs in the presence of divalent cations Ca^{2+} and Mg^{2+}. (–) means that aggregation was not observed and (+) means that aggregation was observed. POPE Nanodisc™ behavior in the presence of divalent cations was not determined.

pH. Even though the pH in the bulk solution in a cell is kept nearly constant, short-lasting local pH changes can occur at reaction sites. Many receptors in cell-signaling processes, which are located at the membranes, induce currents through the membrane upon binding of a signaling molecule [Alberts et al., 2002]. Often, the signaling molecule is thereby hydrolyzed, so that a proton is released and the pH locally changed. This is especially important in mitochondria, where proton gradients play an important role in energy transduction pathways [Alberts et al., 2002]. Thus, a series of experiments was undertaken to explore the effect of pH on Nanodisc^{TM} charge. Please note, for MCE analysis of Nanodiscs, a reference pH of 7.4 will be used for the discussion in this section. Therefore, $\Delta Z_{PHx} - \Delta Z_{PH7.4} = \Delta Z_{DHH}$, where x is the pH of comparison to the reference standard of pH 7.4

Figure 31 summarizes the pH dependence of Z_{DHH} data for POPC, 10POPE and 30POPS Nanodiscs. Across the three different lipids, the ΔZ_{DHH} was 6 from pH 7.4 to 8.0. From pH 8.0 to 8.5, the ΔZ_{DHH} was unchanged.

POPC and POPS Nanodiscs were observed to behave similarly for pH changes from 7.0 to 8.5. At pH 7.0, ΔZ_{DHH} was 0 (**Figure 31**). At pH 8.0, ΔZ_{DHH} was 6 for both POPC and POPS Nanodiscs and Z_{DHH} remained unchanged from pH 8.0 to 8.5. The choline portion of a PC head group is non-titratable and therefore it is unlikely PC lipid head groups contribute to this increase in Z_{DHH}. In addition, the serine portion of a PS head group does contain an ammonium cation that can potentially ionize over this pH range. However, this is unlikely since there was no significant difference in ΔZ_{DHH} between POPC and POPS Nanodiscs. This suggests that the increase in magnitude of Z_{DHH} for POPC and POPS Nanodiscs is most likely due to the ionization of amino acids on the MSPs.

POPE Nanodiscs showed similar behavior to that of POPC and POPS Nanodiscs at pHs above 7.4. At pH 8.0, ΔZ_{DHH} was 6 and Z_{DHH} remained unchanged when the pH was increased to 8.5. However, electrophoretic mobility measurements could not be made at pH 7.0. The reason for this is unclear, as sedimentation velocity data on 10POPE Nanodiscs at pH 7.0 show a monodisperse size population (**Figure A4**).

Figure 32 summarizes the pH dependence of Z_{DHH} data of MSP1D1 30POPA and MSP1D1 10PIP_2 Nanodiscs. Unlike POPC, 30POPS and 10POPE Nanodiscs, ΔZ_{DHH} was >6 from pH 7.4 to 8.5 for 30POPA and 10PIP_2 Nanodiscs. 30POPA Nanodiscs were much more sensitive to pH changes, as Z_{DHH} increases as the pH was increases. 10PIP_2 Nanodiscs did not see a significant ΔZ_{DHH} from pH 7.0 to 7.4. At pH 8.0, ΔZ_{DHH} of 10PIP_2 was 4. At pH 8.5, ΔZ_{DHH} was 15.

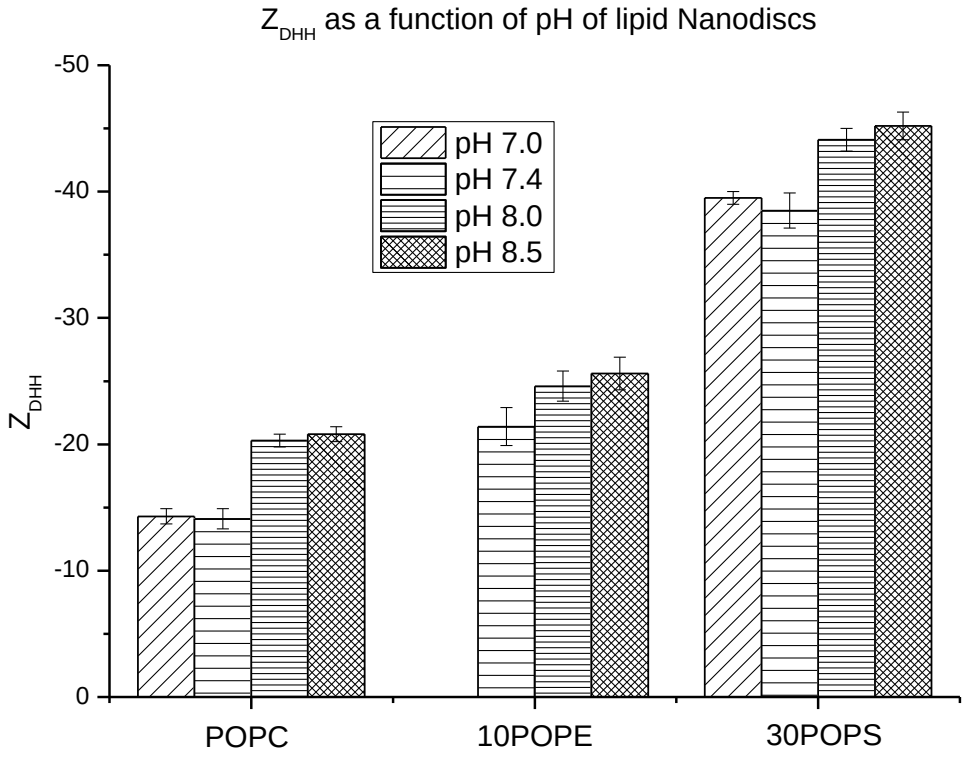

Figure 31 pH dependence of Z_{DHH} for MSP1D1 POPC, MSP1D1 10POPE and MSP1D1 30POPS Nanodiscs. Electrophoretic mobility measurements on 10POPE Nanodiscs at pH 7.0 could not be made. The reason for this is unclear, as sedimentation velocity data on 10POPE Nanodiscs at pH 7.0 show a monodisperse size population. Please note therefore, that in **Figure 31**, 10POPE Nanodiscs do not have a Z_{DHH} plotted at pH 7.0.

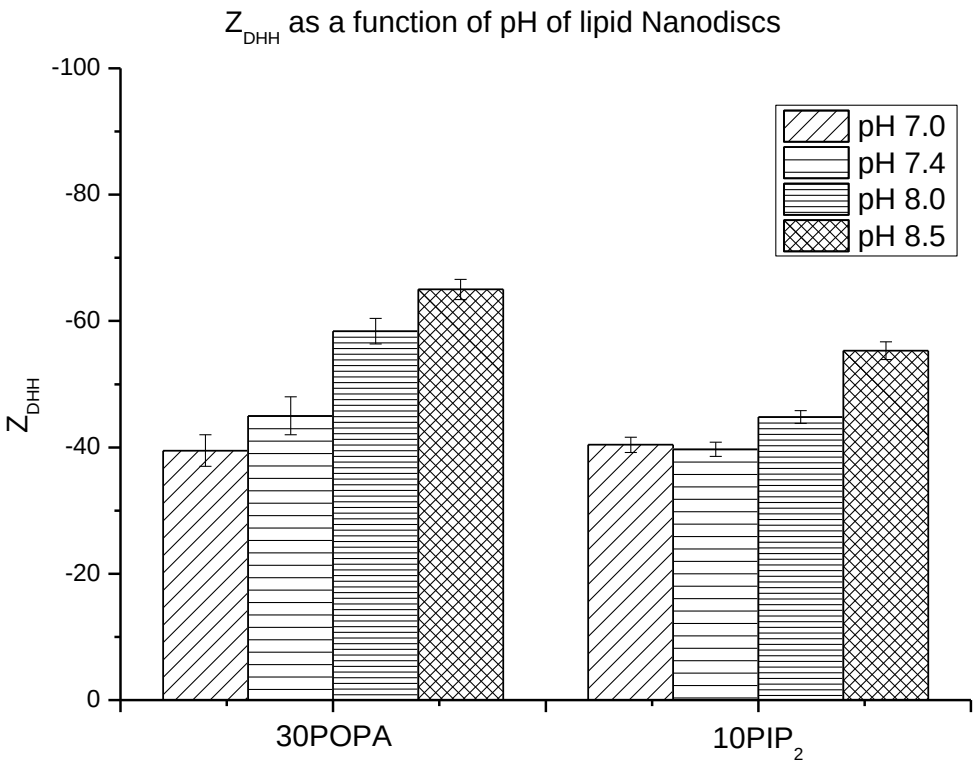

Figure 32 pH dependence of Z_{DHH} for MSP1D1 30POPA and MSP1D1 10PIP_2 Nanodiscs.

Temperature. **Figure 33** summarizes the Z_{DHH} of MSP1D1 POPC, 30POPS and 30POPA Nanodiscs measured at different temperatures. Measurements were made at 20°C, 25°C and 35°C in standard buffer.

Temperature differences can have a wide variety effects on lipid microenvironments, depending on the lipid components present. For example, the phase transition temperature of different lipids can vary depending on which fatty acids are present, which in turn affects the fluidity of the lipid bilayer [Marsh, 1990]. In this study, the primary concern is how temperature affects the electrophoretic mobility and Z_{DHH}. POPA lipids in particular, have a phase transition temperature ~ 28°C, while POPC and POPS lipids have phase transition temperatures of ~ -2°C and ~ 14°C respectively. It was important to normalize the charge measurements by making charge measurements above the phase transition temperatures of the lipids analyzed.

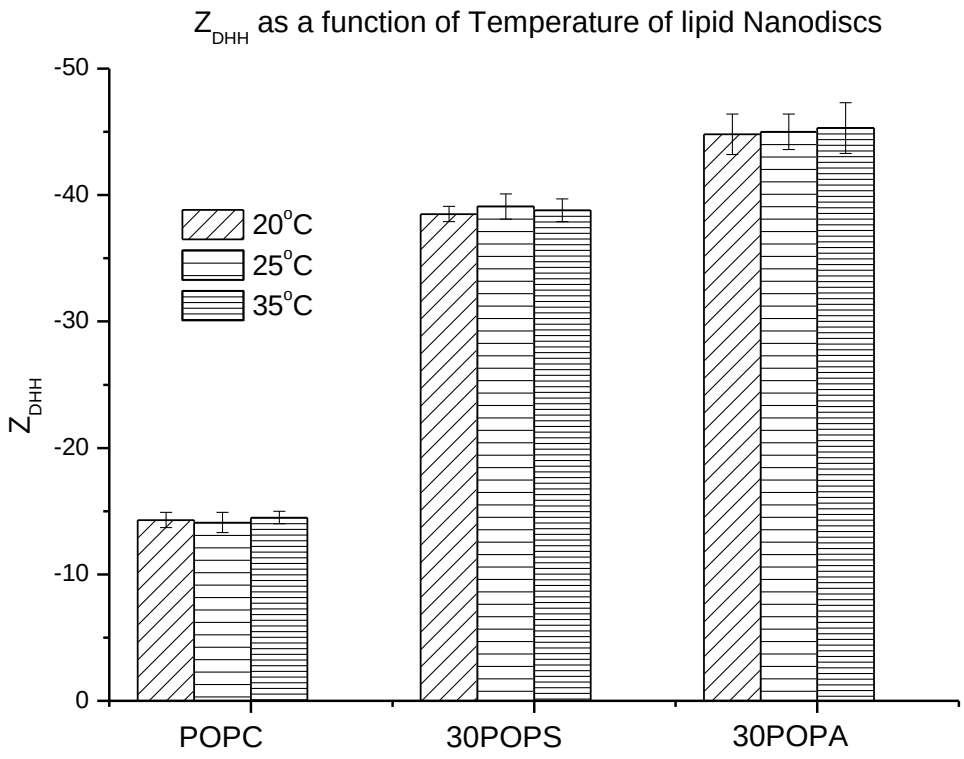

Figure 33 Z_{DHH} as a function of temperature data on MSP1D1 POPC, MSP1D! 30POPS and MSP1D1 30POPA Nanodiscs. Z_{DHH} is insensitive to temperature changes up to 35°C for POPC, 30POPS and 30POPA Nanodiscs. This suggests that the enthalpy of ionization is very low and entropy driven. Temperature experiments were not made with 10POPE or 10PIP_2 Nanodiscs due to lack of sample.

Anion binding. **Figure 34** summarizes the data on anion binding for POPC and POPS Nanodiscs in the presence of 100 mM Na_2S0_4.

It has been shown that proteins can preferentially interact with anions [Collins 2004; Gokarn et al., 2011]. Studies have suggested that these preferential interactions with anions occur at the site of positively charge amines and backbone amide nitrogens [Collins, 2004]. PS lipids have a positively charged ammonium cation group and PC lipids have a positively charged nitrogen in the choline group. Therefore, if anion binding were to occur on lipids, it would most likely be with these two lipids (of the lipids studied), since POPA and PIP_2 contain no positively charged groups in their lipid head group, although it is possible that the MSP could bind anions.

No anion binding was observed, as the Z_{DHH} was not significantly different in the presence of 100 mM Na_2SO_4 for POPC and POPS Nanodiscs.

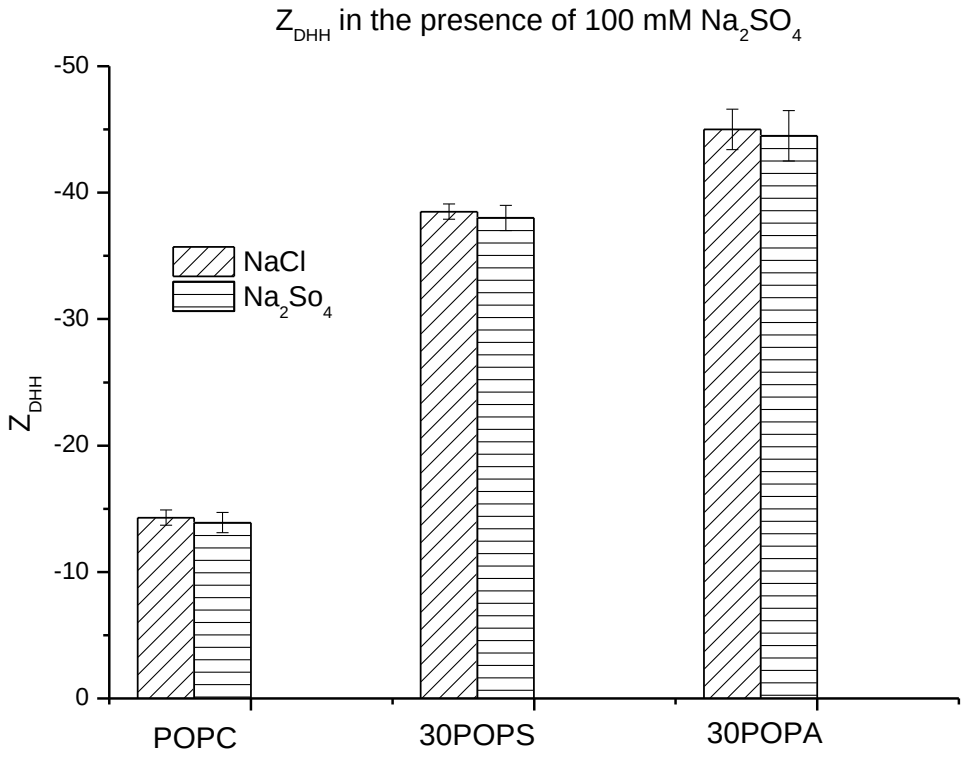

Figure 34 Z_{DHH} of MSP1D1 POPC, MSP1D1 30POPS and MSP1D1 30POPA Nanodiscs in the presence of 100 mM Na_2SO_4. The Z_{DHH} is insensitive to the addition of sulfate ions and suggest that anion binding does not occur with POPC, 30POPS and 30POPA Nanodiscs.

DISCUSSION

Feasibility of measuring Nanodisc™ charge using MCE

As shown in **Figure 1**, Nanodiscs form a single, distinct boundary that moves from the top membrane to the bottom membrane when an electric field is applied. The results indicate that it is possible to determine the electrophoretic mobility, and from that, calculate the Z_{DHH} of Nanodiscs. One advantage of this combination of technique (MCE) and technology (Nanodiscs), is that neither the sample nor the equipment needs to be modified for Nanodiscs to be visualized as they migrate from one membrane to the other.

Nanodiscs were generally stable over a pH range from 7.0 to 8.5 (**Figures 31** and **32**), a temperature range from 20.0 ^{o}C to 35.0 ^{o}C (**Table 33**), and provided good results in different ionic environments and salt concentrations. Except for POPA Nanodiscs in Ca^{2+} (**Figures 23b and 24)** and PIP_2 Nanodiscs in Mg^{2+} (**Figure 29**), Ca^{2+} and Mg^{2+} concentrations up to 10 mM did not cause aggregation or self-association of the Nanodiscs used in this study.

Reproducibility of charge measurements

Nanodisc™ electrophoretic mobility measurements from MCE were reproducible to within ±10%. This level of precision is consistent with that observed for BSA [Jordon, 2014]. Nanodisc™ samples, run two years apart still generate similar though not identical electrophoretic mobilities and Z_{DHH} (**Table 10**).

Date	MSP1D1 POPC Nanodisc™ Charge (Z_{DHH})[a]	Date	MSP1D1 30POPS Nanodisc™ Charge (Z_{DHH})[a]
10/08/2012	-13.6 ± 0.4	09/12/2012	-38.2 ± 0.1
02/01/2014	-14.5 ± 0.3	6/19/2014	-39.8 ± 0.2

Table 10 The Z_{DHH} from MSP1D1 POPC and 30POPS Nanodiscs measured ~2 years apart. These measurements were made on the same sample batches containing POPC and 30POPS Nanodiscs, respectively.

[a] Precision shown is for the individual measurements. The overall reproducibility is closer to ±10% (**Table 4**).

Sedimentation velocity experiments on Nanodiscs also show stability after being stored for two years at 4°C (**Figure 35**). Quantitatively, the sedimentation coefficients are within 1% (Sedanal [Stafford, 2003] and DC/DT$^+$ [Philo, 2000]) and qualitatively show similar symmetric g(s) distributions (**Figure 35**); **likewise**, c(s) analysis [Schuck, 2000], which has higher resolution than Sedanal and DC/DT+, yields a single peak.

In addition, different sample batches of Nanodiscs, with the same lipid composition show similar charge data (**Table 11**). For example, 3 different batches of MSP1D1 and MSP1E3D1 POPC and POPS Nanodiscs, and 2 different batches of MSP1D1 POPA Nanodiscs were characterized by MCE and provided nearly identical results (**Table 11**). These results indicate that other groups should be able to reproduce our data and that data obtained by other groups may be interpreted in light of our data.

Sample Batch	MSP1D1 POPC Nanodisc™ Charge (Z_{DHH})[a]	Sample Batch	MSP1D1 30POPS Nanodisc™ Charge (Z_{DHH})[a]
1	-13.6 ± 0.4	1	-38.2 ± 0.1
2	-13.4 ± 0.1	2	-37.3 ± 0.3
3	-14.1 ± 0.1	3	-37.9± 0.6

Table 11 Z_{DHH} of 3 sample batches of MSP1D1 POPC and MSP1D1 30POPS Nanodiscs received from the Sligar group at the University of Illinois at Urbana-Champaign.

[a] Precision shown is for the individual measurements. The overall reproducibility is closer to ±10% (**Table 4**).

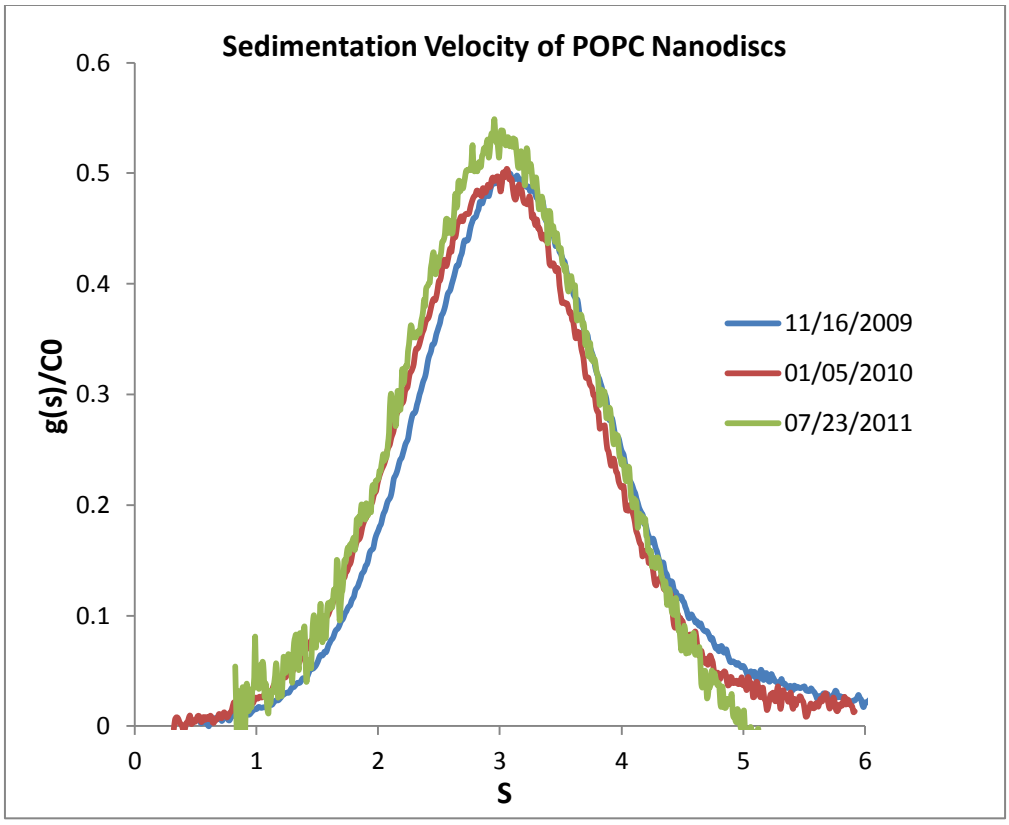

Figure 35 Sedimentation velocity profile of POPC Nanodiscs run at three different intervals generated using Sedanal [Stafford, 2003]. First on November 16, 2009, again on January 5, 2010 and July 23, 2011. After each velocity run, samples were recovered and aliquot into microentrifuge tubes and placed back into a 4°C refrigerator for storage. The sedimentation coefficient distributions are symmetrical and overlay. Small differences (<1%) are within error of the analytical ultracentrifuge. POPC Nanodiscs used for this analysis were provided by Dr. Sandy Ross at the University of Montana.

One thing to consider in making comparisons between analyses is that the electric field calculation is based on the conductivity of the solution. While the MCE uses a constant current, it is most useful to normalize the electric field across solvent conditions to make a direct comparison of the mobilities. When calculating the electric field and Z_{DHH}, it is crucial to use the correct parameters (solution viscosity, R_s, conductivity, etc.) for the charge calculation, since the error can propagate significantly if an error is made in obtaining these parameters. For example, during early experiments, the water used in making solvents was from a Nanopure™ water system resulted in the standard buffer having conductivities ranging from 12.4-12.6 mS.

Later experiments used a Milli-Q^{TM} system resulting in a solvent conductivity ranging from 12.0-12.2 mS. Using the wrong conductivity (e.g. by 0.5 mS) will result in a >10% difference in the Z_{DHH}. However, using the measured conductivities reduced the discrepancy to less than the uncertainty of the measurements.

Uncertainty and limitations of charge measurements

The uncertainty and limitations of Nanodisc^{TM} charge measurements may be separated into those that are a consequence of Nanodiscs, and those that result from MCE. Most limitations were related to electrophoresis and MCE.

Nanodiscs: In general, Nanodiscs provided well-behaved lipid solutions. In fact, the only solution conditions where charge measurements could not be made were: 1) POPA Nanodiscs in the presence of Ca^{2+} and 2) PIP_2 Nanodiscs in the presence of Mg^{2+}, where aggregates were observed. While these results generated limited quantitative data, they still provide information about the interaction of PA and PIP_2 lipids with divalent cations. In addition, there was some difficulty running 10POPE Nanodiscs at pH 7.0 and in the presence of divalent cations. Some studies have observed PE lipids aggregating at pHs below 7.0 [Duzgunes et al., 1985]. However, sedimentation velocity experiments of POPE Nanodiscs at pH 7.0 showed a mono-disperse size distribution (**Figure A4**). There is no current explanation as to why this behavior was observed with POPE Nanodiscs.

MCE: While MCE is a useful tool to observe the electrophoretic mobility of proteins, it does have some limitations inherent to the technique and in electrophoresis in general [Filoti et al. 2015].

The processes involved in electrophoresis are made complex by the coupled flow of ions in the electric field and the effect the coupling has on the electric field [Henry, 1931; Moody and Shepard, 2004]. Macromolecules also can contribute to the electric field by carrying a portion of the electrical current. Furthermore, the fraction of the current carried by the molecule, hence its velocity, depends on both the solvent's ion concentration and the charge on the molecule itself [Schmitt-Koplin, 2008]. Experiments at low salt concentrations will force the molecule to carry a greater fraction of the charge, thereby diminishing the accuracy of the mobility determination [Filoti et al. 2015]. Even for a molecule with a low magnitude of Z_{DHH} (<10), monovalent salt concentrations >20 mM are required to avoid this problem [Heiger, 1992].

In MCE, as charged macromolecules move in the external electric field, their concentration builds up at the bottom membrane [Laue et al., 1998]. The concentration of macromolecules localized at the bottom membrane can often be one to two orders of magnitude greater than the loading concentration. As a result, a Debye layer forms, in which the macromolecule forms the surface charge layer and counter-ions attracted via the coulomb force, form a second layer, electrically screening the first layer [Tadmor et al., 2002]. At high salt concentrations, there is sufficient counter-ion interaction to minimize the influence of the electric field coming from the macromolecules that form the surface charge layer. At low salt concentrations, counter-ions cannot sufficiently screen the surface charge layer, and as a result, the electric field of this Debye layer extends into the solution and can affect the molecules in the external electric field. The net electric field is smaller toward the bottom membrane, decreasing exponentially as the electric field of the Debye layer increases exponentially toward the bottom membrane [Yeh and Hsu, 2011]. This variation in the net electric field results in a buildup of

macromolecules at the boundary where the net electric field is small. Macromolecules to the left of the boundary move faster than those to the right.

Nanodiscs contain a high charge density that, at low salt concentrations, can cause issues with mobility measurements. **Figures 9-12** show electrophoretic mobility experiments at ionic strengths of 50 mM to 225 mM. Experiments run at ionic strengths lower than 50 mM resulted in Nanodiscs forming asymmetric velocity gradients (**Figure 36**). This effect is more pronounced with increasing anionic lipid content. Due to the membrane scaffolding proteins, this effect is even seen in neutral lipids such as POPC at ionic strengths <50 mM.

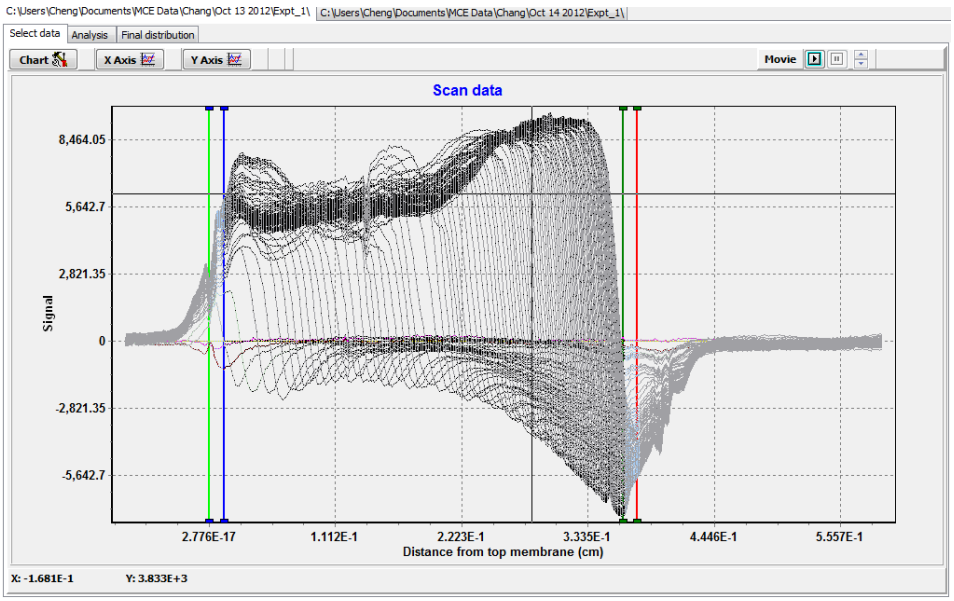

Figure 36 MCE raw data profile of POPC Nanodiscs run at a Na^+ concentration of 15 mM. Notice the asymmetric velocity gradients forming during the duration of the experiment.

There are other experimental conditions to consider that can affect the quality and accuracy of the data, such as extreme pH (3>pH>11), mismatched mobilities of solvent ions, and formation of concentration gradients [Filoti et al., 2015].

Membranes

Unfortunately, there does not currently exist any membranes that are prepared solely for MCE [Laue et al. 1989]. The membranes used are regenerated cellulose dialysis membranes that must be cut to specific sizes in order to fit into the cuvette for cell assembly. With respect to proteins, biotech grade dialysis membranes tend to work much better than regular grade dialysis membranes. This is due to the manufacturing process of biotech membranes that eliminates the use of metal salts. Metal salts can induce cellulose oxidation, which in turn, reduces the anionic charge from the carboxylate formation, leading to unbalanced anion/cation fluxes of the membranes [Spectrapor manufacturer's notes]. For reasons unknown, regular grade dialysis membranes tend to work much better with Nanodiscs than biotech grade dialysis membranes, giving much more consistent and clean data. Biotech grade membranes often result in inconsistent data and irregular behavior. In addition, lower molecular weight cut-off membranes tend to work better with Nanodiscs. The most consistent data came with using 6-8 kDa MWCO membranes with increasing inconsistency up to 25 kDa MWCO membranes. Membrane batches from the manufacturing company can also vary significantly. Suitability experiments have shown that some batches work much better than others and generally there is no way to predict which batches will be compatible for MCE analysis.

Comparison of mobility data to literature

Monovalent alkali cation interactions with PC lipids: Electrophoretic mobility measurements on PC lipids have been made by Klasczyk et al. (2010), McLaughlin et al. (1978) and Pincet et al. (1999). These groups have reported measurements for:

1) POPC liposomes in 100 mM NaCl, 15 mM HEPES, 2 mM KOH at pH 7.0 were observed to have an electrophoretic mobility of 1 x 10^{-5} $cm^2/V \cdot s$. Furthermore, it was calculated that the measured electrophoretic mobility resulted in an approximation of a +1 charge per 605 POPC lipids. An ELS apparatus, a Zetasizer (Malvern Instruments), was used in this study [Klasczyk et al., 2010].
2) Egg PC vesicles in 100 mM NaCl, 15 mM HEPES at pH 7.4 were observed to have an electrophoretic mobility of -1 x 10^{-11} $cm^2/V \cdot s$. Furthermore, it was concluded that the measured electrophoretic mobility resulted in an approximation of a -1 charge per 600 egg PC lipids. A Micro-electrophoresis apparatus Mk II (Rank Brothers LTD) was used in this study [McLaughlin et al., 1978].
3) SOPC vesicles in pure water were observed to have an electrophoretic mobility of 4 x 10^{-11} $cm^2/V \cdot s$. Furthermore, it was concluded that the measured electrophoretic mobility resulted in an approximation of a +1 charge unit per 1100 SOPC lipids. A Surface forces apparatus was used in this study [Pincet et al., 1999].

Our charge measurements results will be compared to these electrophoretic results, as well as for ion binding results using non-electrophoretic methods.

MSP1D1 POPC Nanodiscs in 100 mM NaCl, 50 mM Tris at pH 7.4 were observed to have an electrophoretic mobility of -4.2 x 10^{-5} ± 3.8 x 10^{-6} $cm^2/V \cdot s$ using MCE, resulting in a calculated Z_{DHH} of -14.1 ± 1.0 (**Table 4**). A consequence of the difference between the calculated and measured charge for the MSPs leads to some uncertainty in the interpretation of the Nanodisc™ charge. For example, there is a +1.9 charge difference between the calculated charge for the MSP and the charge on POPC Nanodiscs. Do we attribute the charge differences to an error in the calculated MSP charge, or is the difference a consequence of residual charge on the POPC

head groups? While there is no definitive way to answer this question, the +1.9 charge difference is within the uncertainty/accuracy of MCE analysis [Durant, 2002], and well within the uncertainty of protein charge calculation from the amino acid composition [Filoti et al., 2015]. If the MSP charge in solution is assumed to be that calculated from the amino acid composition (**Table 6**), then POPC lipids would contribute a +1.9 charge (resulting in the Z_{DHH} of -14.1 reported in **Table 5**). Thus, from this assumption, the calculated charge per POPC lipid would be approximately a +1 charge per 63 POPC lipids. If the MSP charge in solution is assumed to be the measured Z_{DHH} for POPC Nanodiscs, then the PC lipids would contribute a net charge of 0. For the remainder of this discussion, it will be assumed that the MSP1D1 protein charge contribution to Nanodiscs is -14.1 and for MSP1E3D1 protein, the contribution is -18.0 (**Table 4**).

Electrophoretic mobility measurements on POPC Nanodiscs using MCE generally agree with the reported observations of Klasczyk et al. (2010), McLaughlin et al. (1978) and Pincet et al. (1999). Previous electrophoretic mobility measurements have shown POPC liposomes, SOPC liposomes and egg PC lipid vesicles to have a zero or very low non-zero magnitude of electrophoretic mobilities, on the order of 1×10^{-5} $cm^2/V \cdot s$ and lower. Klasczyk et al. (2010) observed electrophoretic mobilities on the order of 1×10^{-5} $cm^2/V \cdot s$ and Pincet et al. (1999) and McLaughlin et al. (1987) observed electrophoretic mobilities on the order of 1×10^{-11} $cm^2/V \cdot s$, and yet each study concluded that PC lipids were neutral in the presence of Na^+ ions. In addition, the electrophoretic mobility of POPC Nanodiscs was also found to be on the order of 1×10^{-5} $cm^2/V \cdot s$. However, that includes the charge contribution from the MSPs. The discrepancy in the electrophoretic mobility value obtained by MCE to the values obtained by Pincet et al (1999) and McLaughlin et al. (1978) is probably due to differences in the frictional

coefficient (which is important, since the electrophoretic mobility depends on its charge to frictional coefficient ratio) of these particular PC liposomes in comparison that of POPC Nanodiscs. Liposomes tend to be very large (on the order 1 x 10^3 nm or higher) and so the charge to frictional coefficient ratio will be very low for these large electrically neutral molecules. Nanodiscs on the other hand, have a relatively large charge to frictional coefficient ratio, due to the charge contribution from the MSPs, as well as their small size (~ 10 nm in diameter).

One reason for the discrepancy in the electrophoretic mobility data from our work and that of Klasczyk et al. (2010) concerns electro-osmotic flow and its influence on the behavior of ions in solution as acted upon by an electric field [Heiger, 1992]. The result of electroendosmosis is bulk fluid flow that superimposes on the electrophoretic motion. In ELS, the laser beam is focused to a spot where a neutral object does not move (and the effects of electroendosmosis are minimized) when the field is applied. This calibration is done occasionally as part of a routine service (provided by a service technician), but will drift with time, leading to skewed apparent mobilities. For the apparent mobilities reported by Klasczyk et al. (2010), timely and proper re-calibration is essential to data acquisition. It must be noted that Klasczyk et al. (2010) makes no mention of the frequency of re-calibration between measurements, and when their Zetasizer was calibrated. In general, ELS has a lower precision than that of MCE [Filoti et al. 2015]. In **Figure D1**, as the salt concentration increases, the uncertainty of the electrophoretic mobility increases to ~ 66% in Li^+, ~ 100% in K^+ and cannot be determined from the figure for Na^+ at 100 mM. At 150 mM, the uncertainty increases to ~ 138% in Li^+, ~ 300% in K^+ and ~ 100% in Na^+. The uncertainty of the electrophoretic

mobility observed by Klasczyk et al. (2010) makes it very difficult to compare electrophoretic mobility data.

In addition, Klasczyk et al. (2010) also observed the electrophoretic mobility of POPC liposomes in the presence of different monovalent alkali cations (**Figure D1**). Klasczyk et al. (2010) observed significantly different electrophoretic mobilities in the presence of different monovalent alkali cations. The electrophoretic mobility of POPC liposomes in the presence of K^+ was three times greater (and negative in magnitude) than the electrophoretic mobility of POPC liposomes in the presence of Na^+, which corresponds to a -1 charge unit per 61 PC lipids. Furthermore, in the presence of Li^+, the electrophoretic mobility of POPC liposomes also was found to be three times greater (but positive in magnitude) than the electrophoretic mobility of POPC liposomes in Na^+, corresponding to a +1 charge unit per 20 PC lipids. POPC liposomes were also observed to undergo a charge inversion (reversal of sign) in the presence of very low Li^+ concentration. **Figure D1** shows that in the presence of no ions, the electrophoretic mobility of the POPC liposomes was -5×10^{-5} $cm^2/V \cdot s$. At 10 mM Li^+ concentration, the electrophoretic mobility decreases in magnitude to near zero. These results suggest that PC lipids may have specific interactions with Li^+ ions. Klasczyk et al. (2010) also observed POPC liposomes in Cs^+ and Rb^+, but saw no significant differences to the electrophoretic mobility until ~ 350 mM salt concentrations. Even then, the uncertainty at 350 mM Rb^+ is significantly larger, ~ 500% greater than the reported electrophoretic mobility value. Note that, in general, ELS results are unreliable at salt concentrations greater than 100 mM due to the effects of thermal convection [Filoti et al., 2015]. Given this limitation, the large uncertainty in the electrophoretic mobility at salt concentrations greater than 100 mM in observed by Klascyzk et al. (2010) most likely arises from this convection.

Comparison to non-electrophoretic methods. Binder and Zschornig (2001) studied ion binding to PC lipids using IR spectroscopy to observe how monovalent alkali cations affected the position of the phosphate and carbonyl groups. They found that center of gravity (COG) of the absorption bands was only weakly affected by Li^+ ions and that Na^+ and K^+ ions had no effect on the shape of the spectra (**Figure D2**). They attribute the slight interaction by Li^+ as a solvation effect at the site of interest (either the phosphate or carbonyl group), rather than specific binding. This is reflected in the binding constants of Na^+ (~ 0.15 M^{-1}), K^+ (~ 0.15 M^{-1}), and Li^+ (~ 0.30 M^{-1}) being significantly less than Mg^{2+} (~ 30 M^{-1}) and Ca^{2+} (~ 40 M^{-1}) to PC lipids [Tatulian, 1987]. A similar study was done using NMR spectroscopy by Altenbach and Seelig (1984) with Na^+ and K^+ ions on POPC liposomes. With respect to the signal spectra of PC lipids, monovalent alkali cations (excluding Li^+, which was not tested in the investigation by Altenbach and Seelig, 1984) did not significantly perturb the NMR signal. **Figure 5** shows that the electrophoretic mobility and Z_{DHH} in the presence of different monovalent alkali cations did not differ by >10% for POPC Nanodiscs. While the measured electrophoretic mobilities using MCE generally agree with the current literature that POPC is a neutral lipid, our results show that POPC Nanodisc™ behavior in the presence of different monovalent alkali cations is inconsistent with some reported observations. This is in contrast to the reported observations of Klasczyk et al. (2010), showing vastly different electrophoretic mobilities in the presence of Li^+, K^+, and Na^+ ions. Our data does however, agree with:

1) NMR data by Altenbach and Seelig (1984) that show no significant shift to the PC lipid signal in the presence of Na^+ and K^+ ions

2) IR spectroscopy data Binder and Zschornig (2001) that show Na^+ and K^+ have no affect on the absorption band of PC lipids and Li^+ only weakly affects the absorption band of PC lipids (**Figure D2**).
3) Binding constants obtained by Tatulian (1987) that show Na^+, K^+ and Li^+ have weak binding constants to PC lipids. Although Li^+ binding constants were slightly greater than those of Na^+ and K^+.

The Z_{DHH} of Nanodiscs in the presence of Li^+ was generally lower in magnitude (~ 3%) to that of the Z_{DHH} in the presence of Na^+. This agrees with the observations of Binder and Zschornig (2001) and Tatulian (1987) that Li^+ does seem to have a relatively stronger interaction with PC lipids than Na^+ and K^+; although the charge change is still insignificant when compared to interactions between PC lipids and divalent cations [McLaughlin et al., 1978; Altenbach and Seelig, (1984); Sou and Tsuchida, 2008].

Monovalent alkali cation interactions with PE lipids: Electrophoretic mobility measurements on PE liposomes have been made by Woodle et al. (1992), Davidson et al. (1994) Roy et al. (1998) and Disalvo and Bouchet (2014). These groups have reported measurements for:

1) Methylated PEG-DSPE modified liposomes in 10 mM phosphate buffer at pHs 5.2, 7.3 and 9.2. At pH 7.3, the electrophoretic mobility was found to be:
    a. $-4.5 \times 10^{-6} \pm 4 \times 10^{-7}$ $cm^2/V \cdot s$ at a lipid molar ratio of 7.5%
    b. $-6.5 \times 10^{-6} \pm 2 \times 10^{-6}$ $cm^2/V \cdot s$ at molar ratio of 5%
    c. ND at molar ratios of 10%.

An ELS instrument (Coulter Electronics DELSA) was used in this study [Woodle et al., 1992]

2) POPC/bovine liver PE reconstituted HDL particles in 150 mM NaCl, 10 mM Tris at pH 8.6. No electrophoretic mobilities were reported. However, zeta potentials were calculated from electrophoretic mobilities. The zeta potential of reconstituted HDL particles containing POPC and bovine liver PE was found to be -8.9 mV. Agarose gel electrophoresis was used in this study to determine the reported zeta potential [Davidson et al., 1994].
3) Egg yolk phosphatidylethanolamine in 1 mM phosphate buffer, 1 mM NaCl at pH 7.4. No electrophoretic mobility quantities were reported. However, zeta potentials were calculated and PE lipids were found to have a zeta potential at 10% lipid molar ratios (**Figure D4-D6)**. of:
    a. -16 mV for extruded PE liposomes
    b. -9 MV for sonicated PE liposomes
    c. -12 mV for multi-lamellar PE vesicles

An ELS (a Zetasizer 4 from Malvern Instruments) was used in this study [Roy et al., 1998].

4) DMPE vesicles in 1 mM KCl, at pH 7.0. No electrophoretic mobility values were reported. However, zeta potentials were calculated and PE lipids were found to have a zeta potential of -45 mV and -15 mV (**Figure D7** and **D8**; molar ratios not reported). A microelectrophoresis apparatus (a Zeta-Meter System 3.0) was used in this study [Disalvo and Bouchet, 2014].

Our charge measurements results will be compared to these electrophoretic results.

10POPE Nanodiscs in 100 mM NaCl, 50 mM Tris at pH 7.4 were observed to have an electrophoretic mobility of $-6.5 \times 10^{-5} \pm 5.3 \times 10^{-6}$ $cm^2/V \cdot s$ using MCE. In **Table 4**, the Z_{DHH} for 10POPE Nanodiscs is -21.4 ± 1.5. In addition, since two out of the three studies mentioned only reported zeta potentials [Roy et al. 1998 and Disalvo and Bouchet 2014] (and did not report the measured electrophoretic mobilities used to calculate the zeta potentials), zeta potentials obtained

by MCE will be mentioned only for the sake of comparison. Keep in mind, that the purpose of this investigation was to determine Z_{DHH} and not zeta potential and therefore any zeta potentials mentioned will be found in **Table B1**. The zeta potential calculated from the MCE mobility data of POPE Nanodiscs was -10.8 ± 0.7 mV.

The electrophoretic mobility and Z_{DHH} of 10POPE Nanodiscs from MCE is inconsistent with some reported observations. In general, the current literature show that PE lipids are neutral or slightly anionic [Roy et al., 1998, Davidson et al., 1994, Woodle et al., 1992)] or inconclusive [Disalvo and Bouchet, 2014]. In contrast, MCE data show that 10POPE Nanodiscs, (Z_{DHH} of -21.4 ± 1.5, **Table 6**), are anionic in this system. Taking the MSP charge contribution into account, it was calculated that the charge per lipid contribution of PE lipids is ~ -1 charge units per 2 PE lipids. Roy et al. (1998) observed that at 10% lipid molar ratios of PE liposomes, the zeta potential was -16 mV (**Figure D4**). When compared with the control (~ -9 mV), it only shows a magnitude increase of ~ 7 mV. In comparison, at 10% lipid molar ratios, PS liposomes in the same study showed a magnitude increase ~ 30 mV (from the control), an increase slightly greater than four times that of PE liposomes. Furthermore, at 50% PE lipid molar ratios, the zeta potential increased to ~ -25 mV, a magnitude increase of only 9 mV (**Figure D4**). At 50% PS lipid ratios, the zeta potential was ~ -58 mV, a magnitude increase of ~ -20 mV (**Figure D4**). Roy et al. (1998) concluded, that, assuming PS lipids in the study were contributing a -1 charge unit per lipid, and given the much lower zeta potentials observed for egg yolk PE liposomes, PE lipid charge was more similar to PC lipids, than PS lipids. Similar observations were made with different batches of PS and PE liposomes (**Figures D5** and **D6**) by Roy et al. (1998).

Similar conclusions were reached by Davidson et al. (1994) and Woodle et al. (1992). Based on the electrophoretic mobility and calculated zeta potential of reconstituted POPC-bovine

liver PE HDL particles using agarose gel electrophoresis, Davidson et al. (1994) calculated that the zeta potential of reconstituted POPC HDL particles was -7.6 mV. In comparison, the zeta potential of reconstituted POPC-bovine liver PE HDL particles was found to be -8.9 mV. This 1.3 mV difference they concluded, only resulted in a less than 0.5 charge unit difference between the POPC and bovine liver PE liposomes. As a result, Davidson et al. (1994) came to a similar conclusion as Roy et al. (1998); that PE lipids were much closer to PC lipids in charge, than PS lipids. Woodle et al. (1992) observed similar but not identical electrophoretic mobilities of modified PE liposomes to Nanodiscs obtained by MCE. Woodle et al. (1994) analyzed PE lipids that were modified so that the ammonium cation was replaced with a methylated poly-ethylene glycol group, anionic in nature. They expected to observe negative electrophoretic mobilities and zeta potentials due to the modification of PE lipids from a zwitterionic structure, to a fully anionic lipid. Indeed, Woodle et al. (1994) observed negative electrophoretic mobilities and calculated zeta potentials. However, the magnitude of these quantities for the methylated PEG-DSPE modified liposomes were still much lower than that of PG, another anionic lipid that was considered to be similar to the PEG-modified PE lipids. The electrophoretic mobility and calculated zeta potential of PG lipids were three times greater than that of the modified PE lipids at pH 7.3 (**Figure D3**).

General observations of PE lipids. PE lipids tend to be much more difficult to work with than other lipids, given its non-lamellar phase behavior (**Figure D9**). As a result, there are significant inconsistencies regarding reported charge data for PE lipids. Similar to POPE Nanodisc™ charge data from MCE, Disalvo and Bouchet (2014) observed negative electrophoretic mobilities and zeta potentials for DMPE liposomes. However, within a single study, they reported two significantly different zeta potentials for two different batches of DMPE liposomes. **Figure D7**

shows their calculated zeta potential for one batch of DMPE liposomes of -15 mV. **Figure D8** shows the zeta potential for a second batch of DMPE liposomes that was found to be -45 mV. The uncertainty in **Figure D7** looks to be >10% of the zeta potential value, and is not reported in **Figure D8**. The electrophoretic technique used was microelectrophoresis and it has the same limitations as ELS pertaining to electroendosmosis. Both techniques also apply a similar solution in dealing with electroendosmosis. In microelectrophoresis, the microscope is focused on a stationary layer where fluid does not move. By focusing the microscope on these stationary layers, it is possible to observe particle motion that is not affected by electroendosmosis. In addition, measurements in microelectrophoresis require very dilute solutions (both sample and salt), and thus have low electrical conductivity and require high electric fields [Gittens and James, 1960]. At these electric fields, thermal convection can reduce accuracy and precision. These effects are exacerbated given that the measurements were made in 1 mM KCl solutions. At these experimental conditions, the solvent does not contain enough ions, thereby diminishing the accuracy of these mobility measurements.

Furthermore, while Roy et al. (1998) observed that PE lipids are slightly anionic, there is some uncertainty about the ELS measurements, possibly due to the sample preparation. Roy et al. (1998) prepared three different batches of PE liposomes in their study:

1) Batch 1 included liposomes that were extruded through 400 and 200 nm membranes (**Figure D4**).
2) Batch 2 included liposomes that were sonicated during lipid preparation **(Figure D5**)
3) Batch 3 included mechanical dispersion liposomes (**Figure D6**)

When the electrophoretic mobility of each batch was measured, it resulted in significantly different quantities of zeta potential (**Figures D4-D6**). In addition, the uncertainty of the majority of the data points obtained by Roy et al. (1998) was >10% of the measured quantity. The electrophoretic mobility values obtained by Woodle et al (1994) also contained uncertainties that were >10% of the measured quantity. With this level of inconsistency observed in: 1) solvent conditions, 2) lipid vesicle types, 3)liposome sample batches and 4) using different electrophoretic techniques, it is difficult to make comparisons across reported literature values from different studies.

Comparison to non-electrophoretic methods: That PE lipids are anionic in native membrane-like Nanodiscs is also supported by studies that show "neutral" PE lipids better support protein-protein and lipid-protein (similar to anionic lipids) interactions than neutral PC lipids [O'Toole et al., 2000; Morrisey et al., 2008]. For example, factor X (FX) activation by tissue factor - factor VIIa (TF-FVIIa) interactions occur in the presence of anionic lipids, most importantly PS [Heemskerk et al., 2002]. Morrisey et al. (2011) observed that TF embedded Nanodiscs required at least 30% of the lipids to be PS for optimal FX activation by TF-FVIIa. However, PS only make-up ~ 10% of the total lipids found in platelet cells; and they are mostly localized to the inner leaflet, where they make up ~ 15% of lipids found on the inner leaflet [Yague-Sanchez and Llanillo, 1986]. When other anionic lipids (PA, PG, PI) were incorporated into these TF embedded PS Nanodiscs, it decreased the PS requirement for FX activation by TF-FVIIa (i.e. lower lipid molar ratios of PS were able to better support clotting activity). When neutral PC lipids were incorporated, they did not act synergistically with PS lipids to increase FX activation. However, when "neutral" PE lipids were incorporated, they saw similar FX activation to that of anionic lipids PA, PG and PI. Morrisey et al. (2011) generalized that since "neutral" PE lipids

were observed to have the same effect as anionic lipids on FX activation, the phenomena occurring was independent of charge considerations since "neutral" PE shared no charge similarities to the other anionic lipids. They postulated, that one reason PC lipids did not support protein-protein interactions was mainly due to the bulky choline group which may sterically hinder binding TF-FVIIa interactions.

A similar study was done on spectrin:lipid interactions and it was found that spectrin bound to PE/PC lipid vesicles similarly to that of PC/PS vesicles [O'Toole et al. 2000]. However, that study also concluded that since "neutral" PE lipids and anionic PS lipids both bind spectrin similarly, the interactions are charge independent. In both cases, while structural considerations are important, charge considerations should not be overlooked.

Unfortunately, since PE lipids have such small head group and are non-lamellar lipids (**Figure D9**), it makes it difficult to produce Nanodiscs with higher compositions of PE lipids and therefore 30% and 70% POPE Nanodiscs were not analyzed within this study due to the inability to prepare stable 30% and 70% POPE Nanodiscs in standard buffer.

Electrophoretic mobility measurements of anionic lipids using MCE

General comments about anionic lipids. Our data show that as more anionic lipids are incorporated into Nanodiscs, the magnitude of the electrophoretic mobility and Z_{DHH} increases (**Table 1**). Furthermore, as more anionic lipids are incorporated, the less each lipid contributes to the overall charge (**Table D1)**. This is in agreement with some reported observations [Kato et al., 2011; Roy et al., 1998]. In particular, as the Nanodisc^{TM} charge becomes more anionic, these results suggest that more counterions are associated with the Nanodisc^{TM} and move with it. While the mechanism of binding is not revealed in these measurements, the results are consistent

with the counterions being bound territorially (i.e. as "condensed ions" [Manning, 1969]). The results, then, are consistent with the Nanodiscs exhibiting increasing polyelectrolyte behavior as the anionic lipid content of Nanodiscs increases (**Table D1**).

Monovalent alkali cation interactions with anionic lipids. The variation of monovalent alkali cation ion-types did not affect the electrophoretic mobility of anionic lipid Nanodiscs across, Na^+. K^+ and Li^+ ions (**Figures 6-8**). This finding is inconsistent with some reported observations. The next sections on POPS, POPA, and PIP_2 Nanodiscs will go into more detail on the monovalent ion interactions with those specific lipids.

Monovalent ion interactions with PS lipids: Electrophoretic mobility measurements on PS liposomes have been made by Roy et al. (1998), Kato et al. (2011) and Martin-Molina et al. (2012), and these groups have reported measurements for:

1) Bovine spinal cord phosphatidylserine in 1 mM phosphate buffer, 1 mM NaCl at pH 7.4. No electrophoretic mobility values were reported. However, zeta potentials were calculated and PE lipids were found to have zeta potentials of -39, -52 and -58 mV at 10% lipid molar ratios (**Figure D4-D6)**. An ELS apparatus (a Malvern Zetasizer 4) was used in this study [Roy et al., 1998].
2) PS liposomes containing calcein in 1X PBS at pH 7.4 were observed to have an electrophoretic mobility of -1.5×10^{-4} $cm^2/V \cdot s$ at 10% PS lipid molar ratios (**Figures D11** and **D12**). An ELS apparatus (a Malvern zetasizer) was used in this study [Kato et al. 2011].
3) Bovine brain 3-*sn*-phosphatidyl-L-serine liposomes in 100 uM $Ca(NO_3)_2$ at pH 5.5 observed to have an electrophoretic mobility of -3×10^{-4} $cm^2/V \cdot s$ (**Figure D13**). A phase-analysis

light scattering apparatus (ZetaPALS, Brookhaven Instruments Corporation) was used in this study [Martin-Molina et al. 2012].

Our charge measurements will be compared to these electrophoretic results, as well as for ion binding results using non-electrophoretic methods.

POPS Nanodiscs in 100 mM NaCl, 50 mM Tris at pH 7.4 were observed in this work to have electrophoretic mobilities of:

1) $-7.1 \times 10^{-5} \pm 2.9 \times 10^{-6}$ $cm^2/V \cdot s$ at a 10:90, POPS:POPC composition.
2) $-1.2 \times 10^{-4} \pm 5.7 \times 10^{-6}$ $cm^2/V \cdot s$ at a 30:70, POPS:POPC composition.
3) $-1.7 \times 10^{-4} \pm 3.8 \times 10^{-6}$ $cm^2/V \cdot s$ at a 70:30, POPS:POPC composition.

Corresponding Z_{DHH} values are provided in **Table 4**. In addition, since Roy et al. (1998) only reported zeta potentials (and did not report the measured electrophoretic mobilities used to calculate the zeta potentials), the zeta potential of MSP1D1 10POPS, 30POPS and 70POPS Nanodiscs will be mentioned for the sake of comparison. Zeta potentials calculated from the electrophoretic mobilities by MCE were:

1) -12.3 ± 0.3 mV at a 10:90, POPS:POPC composition.
2) -20.0 ± 0.9 mV at a 30:70, POPS:POPC composition.
3) -29.1 ± 0.7 mV at a 70:30, POPS:POPC composition.

The measured electrophoretic mobility and Z_{DHH} of POPS Nanodiscs using MCE agrees qualitatively with some reported observations. In general, the current literature shows that PS lipids are much more anionic than PC and PE lipids [Kato et al., 2011; Martin-Molina et al., 2012; and Roy et al., 1998]. POPS Nanodiscs were also observed to be more anionic than POPC

and POPE Nanodiscs (**Table 4**). Furthermore, the electrophoretic mobilities of PS liposomes observed by Kato et al. (2011) and Martin-Molina et al. (2012) were on the same order of magnitude (1×10^{-4} $cm^2/V\text{-}s$) as the electrophoretic mobilities observed for POPS Nanodiscs, with the exception of 10POPS Nanodiscs (1×10^{-5} $cm^2/V \cdot s$; a one order of magnitude difference) by MCE. However, it should be mentioned, that while the electrophoretic mobilities observed by Kato et al. (2011) were on the same order of magnitude as ours, the electrophoretic mobilities observed by Kato et al. (2011) were generally larger than the electrophoretic mobilities obtained by MCE. Even though Kato et al. (2011) did not prepare lipid molar ratios of PS liposomes greater than 25%, the observed electrophoretic mobility at molar ratios of 25% was still greater than that observed by MCE for lipid molar ratios of 70% for POPS Nanodiscs. This discrepancy in electrophoretic mobility for PS lipids may be attributed to the use of calcein (at 0.2 mM concentration) for fluorescent labeling. Calcein contains six ionizable (4 carboxylic acids and 2 alcohol groups) groups whose pKa values are: pKa_1=2.1, pKa_2=2.9, pKa_3=4.2, pKa_4=5.5, pKa_5=10.8 and pKa_6=11.7 [Powl et al., 2008]. In PBS, at pH 7.4, the calcein molecules should have a -4 charge in solution, making it very anionic and contributing to a high charge to frictional coefficient ratio, that can result in relatively higher electrophoretic mobilities, like those observed in PS liposomes by Kato et al. (2011).

MCE data showed an increase in the electrophoretic mobility of POPS Nanodiscs as a function of PS content up to 70% incorporation. Kato et al. (2011) observed that PS liposome electrophoretic mobility reached a plateau ~ 25% incorporation, with the greatest increase in electrophoretic mobility observed from 0 to 10% PS composition. At >10% PS content, increases in the magnitude of the electrophoretic mobility of PS liposomes became insensitive to PS content (mobility increases significantly from 0 - 2×10^{-4} $cm^2/V \cdot s$ from 0-10% PS content

and increases from 2 x 10^{-4} cm/Vs to 2.5 x 10^{-4} $cm^2/V \cdot s$ from 10-20% PS content). This may be another consequence of using a highly charged fluorescent tag in calcein. Due to the high charge density of calcein molecules, the charge attributed to PS liposomes prepared by Kato et al. (2011) may not be due solely to PS. The highly anionic liposome may incorporate less PS than the expected molar ratios due to the electrostatic repulsion that can occur between PS lipids and any associated calcein. This electrostatic repulsion between PS lipids is why pure PS liposomes cannot be prepared and must contain supporting neutral lipids (such as PC). In addition, the electrophoretic mobilities of the PS liposomes obtained by Kato et al. (2011) were averaged for four different liposome batches, which differed in diameter (**Figure D12**). This increases the uncertainty of the measurements due to the ability of larger liposomes to incorporate more calcein. Therefore, the charge to frictional coefficient ratio of the liposomes will not be consistent from batch to batch due to the difference in calcein concentrations within each liposome population.

Martin-Molina et al. (2012) also observed electrophoretic mobility values much greater in magnitude than the electrophoretic mobility values obtained by MCE. This discrepancy in electrophoretic mobilities may be due to Martin-Molina et al. (2012) making the charge measurements in a 100 uM $Ca(NO_3)_2$ solution, with no other supporting electrolyte present. Considerations of ELS as a technique have already been mentioned in previous sections and therefore will not be expanded upon here. Similarly, differences in the zeta potentials calculated by Roy et al. (1998) and the zeta potentials obtained from electrophoretic mobility measurements by MCE already have been discussed with respect to PE lipids. All of the discussion relative to the zeta potential data on PE lipids by Roy et al. (1998) applies to zeta potential data on PS lipids in the same study. Roy et al. (1998) also observed monotonically increasing zeta potentials as

more PS lipids were incorporated into the prepared liposomes. This generally agrees with the electrophoretic mobility data obtained by MCE.

Comparison to non-electrophoretic methods. While no comparable mobility data exist for the different monovalent ions studied in this dissertation, there are some indirect data of interest. Na^+ and K^+ have been shown to have general adsorption interactions with anionic lipids, similar to that seen in POPC. In addition, these interactions are not strong enough to show up on NMR or IR spectra. Binding constants generated from ITC experiments are on the order of 0.15 - 0.44 M^{-1} for Na^+ and K^+ [Knecht and Klasczyk, 2013]. Such low binding constants suggest adsorption, not binding to the lipid membrane. This is seen in the electrophoretic mobility measurements using MCE (**Figure 5**), since the electrophoretic mobility and Z_{DHH} are not perturbed in the presence of different monovalent alkali cations. This is in agreement with Eisenberg et al. (1979; **Figure D15**), in which zeta potentials of PS lipids in the presence of Na^+, Li^+ and K^+ did not differ significantly. However, Li^+ has been shown to interact with anionic lipids, specifically phosphatidylserine [**Figures D16** and **D17**; Loosley-Millman et al., 1982]. Loosley-Millman et al. (1982) observed, using x-ray scattering, that Li^+ and Na^+ had significantly different interactions, as seen by the d_w (where d_w is the distance of interbilayer separation) of POPS bilayers in the presence of Na^+ being two times the d_w of POPS bilayers in the presence of Li^+ (**Figure D16**). Furthermore, there is structural data using Li^+ and H NMR relaxation data that show evidence for Li^+ and PS lipid interaction [Srinivasan et al. 1999].

With respect to Na^+ and K^+ interactions with lipid bilayers, our results generally agree with the reported observations of Eisenberg et al. (1979), Loosley-Millman et al. (1982) and Knecht and Klasczyk (2013). However, the charge data of POPS Nanodiscs on MCE in the presence of Li^+ is somewhat inconsistent with some reported observations. Qualitatively, the

Z_{DHH} of POPS Nanodiscs was generally lower in magnitude (although still within the uncertainty of the MCE apparatus) for POPS Nanodiscs in the presence of Li^+ (**Figure 6**). This suggests that Li^+ may have a slightly greater affinity with PS lipids than Na^+ and K^+, in agreement with Eisenberg et al. (1979), Loosley-Millman et al. (1982) and Klasczyk et al. (2010). Quantitatively however, our results do not agree with the reported observations of Loosley-Millman et al. (1982) and Klasczyk et al. (2010). Loosley-Millman et al. (1982; **Figures D16** and **D17**) and Klasczyk et al. (2010; **Figure D1**) observed strong interactions between PS lipids and Li^+. However, the charge data of POPS Nanodiscs on MCE in the presence of Li^+ showed a <10% change in the electrophoretic mobility and Z_{DHH}. Differences between our results and the results of Klasczyk et al. (2010) have already been discussed and will not be further discussed in this section. Loosley-Millman et al. (1982) disclose that quantitative comparisons between their calculated d_w and electrophoretic mobility data is difficult because the relationship between the hydrodynamic plane of shear in zeta potential measurements and how the authors treat the plane of charge is unknown. Inconsistencies with the reported observations of PS lipids in the presence of different monovalent alkali cations make comparison of our data to the literature difficult.

Monovalent alkali cation interactions with PA lipids: Electrophoretic mobility measurements on PA liposomes have been made by Piret et al. (2005), who reported measurements for:

1) PA vesicles in 40 mM citrate, 40 mM phosphate buffer at pH 5.4 were observed to have an electrophoretic mobility of:
    a. -3.5×10^{-4} $cm^2/V \cdot s$ at 10% PA incorporation
    b. -4.2×10^{-4} $cm^2/V \cdot s$ at 30% PA incorporation.

A CE apparatus (a Bio-Rad HPETM 100 CE System) was used in this study [Piret et al., 2005].

Our charge measurements will be compared to these electrophoretic results, as well as for ion binding results using non-electrophoretic methods.

POPA Nanodiscs in 100 mM NaCl, 50 mM Tris at pH 7.4 were observed to have electrophoretic mobilities of:

1) $-7.5 \times 10^{-5} \pm 1.7 \times 10^{-6}$ $cm^2/V \cdot s$ at a 10:90, POPA:POPC composition.
2) $-1.4 \times 10^{-4} \pm 1.6 \times 10^{-5}$ $cm^2/V \cdot s$ at a 30:70, POPA:POPC composition.
3) $-2.1 \times 10^{-4} \pm 1.0 \times 10^{-5}$ $cm^2/V \cdot s$ at a 70:30, POPA:POPC composition.

The measured electrophoretic mobility and Z_{DHH} of POPA Nanodiscs using MCE qualitatively agrees with reported observations of Piret et al. (2005). Piret et al. (2005) reported that PA lipids have similar, but not identical electrophoretic mobilities to that of PS lipids. Similar to POPS Nanodiscs, the electrophoretic mobilities obtained by MCE were of a lower magnitude than the reported electrophoretic mobilities of PA lipid vesicles in the literature. Specifically, where the MCE data disagree with Piret et al. (2005), is the comparison of the electrophoretic mobility and Z_{DHH} of PA lipids to other anionic lipids. Piret et al. (2005) observed an electrophoretic mobility of PA lipid vesicles <10% to those of PS and PI lipid vesicles. As seen in **Figure D18**, the data points overlay and plateau at lipid molar ratios of ~ 30%. From the results, they conclude that PS, PI and PA have similar surface charge densities. MCE data also show that there is a <10% difference between the electrophoretic mobilities of 10POPS and 10POPA Nanodiscs. However, at molar ratios of 30% and 70%, the difference in the electrophoretic mobility of POPS and POPA Nanodiscs is closer to ~ 20%.

This apparent discrepancy can be explained by the different solvent conditions of both studies. Piret et al. (2005) ran their liposomes at pH 5.4, while experiments using MCE were performed at pH 7.4. PA lipids contain a phosphate group that can undergo two ionization events, with one pKa ~ 3.0 and the second pKa at ~ 8.0. At pH 7.0, POPA Nanodiscs had similar electrophoretic mobility and Z_{DHH} values to that of POPS Nanodiscs from MCE (**Figure 32**). The MCE data suggest that in standard buffer at pH 7.4 however, PA lipids may contribute closer to -1.25 charge units per head group, which is supported by the titration curve of PA lipids (**Figures C7** and **C8**; [Marsh, 1990]). Slight changes in pH near physiologic solvent conditions, had a larger effect on POPA Nanodisc^{TM} charge than other lipids, most likely due to the pKa of the second ionizable group (~ 8.0) being closer to physiologic pH. As seen in **Figure 32**, the Z_{DHH} of POPA Nanodiscs at pH 7.0 is more identical to the Z_{DHH} of POPS Nanodiscs at a pH range of 7.0 - 7.4. pH considerations will be explained in more detail below, however this section will focus solely on the behavior of POPA lipids as a function of monovalent cation type.

Taking this evidence, along with titration curves by Marsh (1990; **Figures C7** and **C8**), it may be more correct to assume that the charge of each PA lipid is closer to -1.25 near physiologic conditions and not -1 as observed by Piret et al. (2005). This can be problematic, as many studies, most especially those that develop theoretical models and molecular dynamics simulations, assume PA lipids have identical charge behavior to other anionic lipids with -1 charge such as PS, PG, and PI at physiologic pH. If a PA lipid head group charge of -1.25 is assumed, the $\Delta z/\Delta PL$ values for PA lipids becomes much more similar, although not identical, to the $\Delta z/\Delta PL$ for PS lipids (**Tables D3** and **D5**).

Comparison to non-electrophoretic methods. Similar to PS lipids, no comparable mobility data for PA lipids exist for the different monovalent alkali cations studied in this dissertation.

However, there are some indirect data of interest. Loosley-Millman et al. (1982) used x-ray diffraction to study monovalent ion binding to PA lipids by determining the intermembrane forces (d_w) between phospholipid bilayers in monovalent ionic solutions. In short, the greater the distance (in Å) of this intermembrane force, the less interaction occurring between lipids and the particular monovalent ion (**Figure D16**).

Loosley-Millman et al. (1982) observed that Li^+ and Na^+ had similar binding properties, as seen by the near identical values of d_w (**Figure D16**). The d_w in the presence of K^+ was slightly greater (resulting in less interaction), although not significantly greater than in the presence of Na^+ and Li^+. Loosely-Millman et al. (1982) concluded that these d_w values for PA lipids were not significantly different enough to warrant further experiments, as the focus of the work shifted toward the significant difference in d_w values between Li^+ and other monovalent ions on PS lipids; due to the significant difference in d_w between PS lipids and Li^+ in comparison to other monovalent alkali cations.

MCE data of POPA Nanodiscs in the presence of different monovalent alkali cations generally agree with the x-ray diffraction data of Loosely-Millman et al. (1982). The electrophoretic mobility and Z_{DHH} values of POPA Nanodiscs were generally insensitive to the different monovalent alkali cations present, as the electrophoretic mobility and Z_{DHH} values were not significantly different (<10%) in the presence of Na^+, K^+ or Li^+.

Monovalent alkali cation interactions with PIP_2 lipids: Electrophoretic mobility measurements on PC liposomes have been made by Gabev et al. (1989) and Toner et al. (1988). These groups have reported measurements for:

1) Egg PC/PIP_2 monolayers in 100 mM KCL, 1 mM MOPS at pH 6.0, 7.0 and 8.0. No electrophoretic mobility quantities were reported. However, zeta potentials were calculated and PIP_2 lipids were found to have a zeta potential of -43 mV at all pHs for 20% PIP_2 lipid molar ratios (**Figure D19)**. Gabev et al. (1989) also calculated a valence of -1.8 charge units per PIP_2 lipid. A Micro-electrophoresis apparatus Mk II (Rank Brothers LTD) was used in this study [Gabev et al. 1989].
2) Egg PC/PIP_2 lipid vesicles in 100 mM KCl, 1 mM MOPS at pH 7.0. No electrophoretic mobility quantities were reported. However, zeta potentials were calculated and PIP_2 lipids were found to have a zeta potential of -43 mV at all pHs for 10% PIP_2 lipid molar ratios (**Figure D20).** Toner et al. (1988) also calculated a valence of -3 charge units per PIP_2 lipid. A Micro-electrophoresis apparatus Mk I (Rank Brothers LTD) was used in this study [Toner et al. 1988].

Our charge measurements will be compared to these electrophoretic results, as well as for ion binding results using non-electrophoretic methods.

10% PIP_2 Nanodiscs in 100 mM NaCl, 50 mM Tris at pH 7.4 were observed to have an electrophoretic mobility of $-1.2 \times 10^{-4} \pm 3.6 \times 10^{-6}$ $cm^2/V \cdot s$ using MCE. In **Table 4**, the Z_{DHH} for $10PIP_2$ Nanodiscs is -39.7 ± 1.1. In addition, since Gabev et al. (1989) and Toner et al. (1988) only reported zeta potentials (and did not report the measured electrophoretic mobilities used to calculate the zeta potential), the zeta potential of PIP_2 Nanodiscs will be mentioned for the sake of comparison. The calculated zeta potential of $10PIP_2$ Nanodiscs was -20.6 ± 0.9 mV.

Electrophoretic mobility, Z_{DHH} and zeta potential values for PIP_2 Nanodiscs using MCE qualitatively agree with the current literature. Similar to other anionic lipids, measured

electrophoretic mobilities and calculated zeta potentials found in the literature are much higher in magnitude than the electrophoretic mobilities and zeta potentials obtained by MCE. The calculated zeta potential of PC/PIP_2 monolayers obtained by Gabev et al. (1989) and of egg PC/PIP_2 lipid vesicles Toner et al. (1988) were identical (both ~ -43 mV) and twice that of the calculated zeta potential obtained from MCE. In addition, our data agree with the assessment of Toner et al. (1988) that there is a valence of -3 charge units per PIP_2 lipid. They reached this conclusion by comparing the zeta potentials of PI lipid vesicles to PIP_2 lipid vesicles. The zeta potential of PIP_2 lipid vesicles was found to be three times greater than the zeta potential of PI lipid vesicles. Similarly, the MCE data show that 10PIP_2 Nanodiscs have a similar electrophoretic mobility and Z_{DHH} values to 30POPS Nanodiscs, which also leads us to the same conclusion that PIP_2 lipids on Nanodiscs contribute quantitatively, a -3 charge per lipid head group.

Comparison to non-electrophoretic methods. Toner et al. (1988) also performed ^{31}P NMR experiments in order to calculate association constants of Na^+ (not reported) and K^+ ions to the PC/PIP_2 lipid vesicles. From these association constants, they predict that 0.7 K^+ ions are bound to each PIP_2 molecule (assuming a fixed surface potential of the PC/PIP_2 lipid vesicles of -30 mV and the absence of other monovalent or divalent cations). They further calculated that when Mg^{2+}, but not Ca^{2+} is present, the number of or K^+ ions bound to each PIP_2 molecule decreases to 0.4. Based on the reported data, it is difficult to compare these results to those obtained by MCE, given the different ion concentrations observed in this study. Toner et al. (1988) calculated only 0.01 Ca^{2+} ions per PIP_2 molecule at 1 uM, in comparison to that of 0.2 and 1.3 for Mg^{2+} at 100 uM and 1 mM, respectively. However, that does not give any insight as to whether or not PIP_2 lipids have a higher binding affinity of Mg^{2+} over Ca^{2+}, since the Ca^{2+} concentration was lower

by two and three orders of magnitude. This is an important factor to take into account, since a one order of magnitude increase in concentration for Mg^{2+}, results in a six-fold increase in the amount of Mg^{2+} bound per PIP_2 lipid. Furthermore, Toner et al. (1988) mention measurements made in the presence of Na^+, but do not report those measurements and calculations. Therefore, there is no frame of reference for comparison to monovalent ions. Is the value for the number of Na^+ ions bound per PIP_2 lipid similar or identical to the value in the presence of K^+? Considerations of divalent cation binding with PIP_2 lipids will be discussed later in the section below

Divalent cations

Divalent cation interactions *with PC and PS lipids:* Electrophoretic mobility measurements on PC and PS liposomes in the presence of divalent cations have been made by McLaughlin et al. (1978), Sinn et al. (2005), Sou and Tsuchida (2008) and Martin-Molina et al. (2012). These groups have reported measurements for:

1. Egg PC liposomes in 100 mM NaCl, at pH 7.5. No electrophoretic mobility quantities were reported. However, zeta potentials were calculated and egg PC liposomes were found to have a zeta potential of:
    a. 0 mV in the absence of divalent cations
    b. 11.0 ± 1 mV in the presence of 50 mM Mg^{2+}
    c. 10.0 ± 1 mV in the presence of 50 mM Ca^{2+}

A Micro-electrophoresis apparatus Mk II (Rank Brothers LTD) was used in this study [McLaughlin et al., 1978].

2. DOPC and DOPS lipid vesicles in 10 mM NaCl, pH not reported. In addition, no electrophoretic mobility quantities were reported. However, zeta potentials were calculated and egg PC liposomes were found to have a zeta potential of:
    a. DOPC lipid vesicles
        i. 3 mV in the absence of Ca^{2+}
        ii. 2 mV in the presence of 1.25 mM Ca^{2+}
        iii. 12 mV in the presence of 40 mM Ca^{2+}
    b. DOPS lipid vesicles
        iv. -42 mV in the absence of Ca^{2+}
        v. -35 mV in the presence of 1.25 mM Ca^{2+}

Electrophoretic mobilities were determined using a Malvern Zetasizer 3000 HS [Sinn et al., (2005)].

3. DMPC lipid vesicles in 20 mM NaCl, 10 mM HEPES, and 3 mM $CaCl_2$ at pH 7.4. No electrophoretic mobility quantities were reported. However, zeta potentials reported were:
    a. -6 mV in the absence of Ca^{2+}
    b. 0 mV in the presence of 3 mM Ca^{2+}

Zeta potentials were determined by Laser Doppler Velocimetry (Zeta-sizer Nano ZS, Malvern Instruments) [Sou and Tsuchida, 2008].

4. Bovine PS liposomes in varying concentrations of $Ca(NO_3)_2$ and $Mg(NO_3)_2$ at pH 5.5. The electrophoretic mobilities reported were:
    a. -3.0×10^{-5} $cm^2/V \cdot s$ in the presence of 100 uM of divalent cations
    b. -2.5×10^{-5} $cm^2/V \cdot s$ in 3 mM $Mg(NO_3)_2$

c. -2.0×10^{-5} $cm^2/V \cdot s$ in 3 mM $Ca(NO_3)_2$

Electrophoretic mobilities were determined by phase analysis light scattering (ZetaPALS, Brookhaven) [Martin-Molina et al. 2012].

Divalent cation interactions with POPC and POPS Nanodiscs. Since identical results were observed for POPC and POPS Nanodiscs in the presence of divalent cations Ca^{2+} and Mg^{2+}, they will be discussed together. Our observations of POPC and POPS Nanodiscs in the presence of divalent cations were as follows:

1. In 100 mM NaCl, 50 mM Tris, 3 mM $CaCl_2$ at pH 7.4, the Z_{DHH} was observed to decrease in magnitude by ~ 25% in comparison to the Z_{DHH} of POPC and POPS Nanodiscs in the absence of Ca^{2+} (**Figure 22a** and **22b**).
    a. In the presence of 10 uM $CaCl_2$, the Z_{DHH} of POPC and POPS Nanodiscs was not significantly different from the Z_{DHH} of POPC and POPS Nanodiscs in the absence of Ca^{2+} (**Figures B1** and **B2**).
    b. In the presence of 10 mM $CaCl_2$, the Z_{DHH} of POPC and POPS Nanodiscs was not significantly different from the Z_{DHH} of POPC and POPS Nanodiscs in the presence of 3 mM Ca^{2+} (**Figures B1** and **B2**).
2. In 100 mM NaCl, 50 mM Tris, 3 mM MgCl at pH 7.4, the Z_{DHH} was not significantly different from the Z_{DHH} of POPC and POPS Nanodiscs in the absence of Mg^{2+} at concentrations from 10 uM - 10 mM (**Figure 22a**).

The data obtained by MCE of Nanodisc^{TM} charge in the presence of divalent cations is inconsistent with some reported observations. McLaughlin et al. (1987), Sinn et al. (2005) and Sou and Tsuchida (2008) all observed a decrease in magnitude of the zeta potentials, and Martin-

Molina et al. (2012) observed a decrease in magnitude of the electrophoretic mobilities as Ca^{2+} and Mg^{2+} concentration increased. Perhaps a more accurate description would be that they observed increasing cationic zeta potentials and electrophoretic mobilities with increasing divalent cation concentration. In our experiments, the Z_{DHH} of Nanodiscs becomes more cationic in the presence of Ca^{2+}, but not Mg^{2+}. However, the magnitude of the cationic increase differs between groups due to the different solvent conditions used:

1. McLaughlin et al. (1978) observed a zeta potential change of +10 mV in the presence of 40 mM Ca^{2+} and a zeta potential change of +11 mV in the presence of 40 mM Mg^{2+}.
2. Sinn et al. (2005) observed a ~ 12% change in the zeta potential in the presence of 1.25 mM Ca^{2+} for DOPS liposomes. Sinn et al. (2005) also observed a more negative zeta potential (by ~ 33%) at 1.25 mM $Ca2^{+}$, but observed a more positive zeta potential (~ 400%) at 40 mM Ca^{2+}.
3. Sou and Tsuchida (2008) observed a zeta potential change of +6 mV in the presence of 3 mM Ca^{2+}.
4. Martin-Molina et al. (2012) observed a decrease in the electrophoretic mobility of PS liposomes by ~ 33% in 3 mM Ca^{2+} and a decrease in the electrophoretic mobility by ~ 17% in the presence of 3 mM Mg^{2+}.

Since the experiments conducted by McLaughlin et al. (1987), Sinn et al. (2005), Sou and Tsuchida (2008) and Martin-Molina et al. (2012) differ in solvent conditions and measured quantities, this section will focus on a qualitative comparison of the general behavior observed in divalent cation-lipid interactions.

Calcium. From this work we see that addition of 3 mM Ca^{2+} results in nearly identical fractional charges across both POPC and POPS Nanodiscs (**Figure 22b**), consistent with polyelectrolyte theory [Manning, 1969]. The Ca^{2+} results are consistent with a model in which the divalent Ca^{2+} does not interact with a fully exposed PS lipid layer, but instead displaces existing monovalent Na^{+} ions on the surface. That is, the difference in Z_{DHH} in the presence of 3 mM Ca^{2+} represents the difference in preferential solvation by 100 mM Na^{+} and 3 mM Ca^{2+}. This model implies that Ca^{2+} does not have a specific interaction with PS head groups, contrary to some models [Altenbach and Seelig, 1984]. It also could be that the Ca^{2+} is interacting with some common feature of the Nanodiscs, e.g. either the phosphate group or the protein belt. However, these data do not specifically rule out PS providing a Ca^{2+}-specific binding site.

Magnesium. For POPC and POPS Nanodiscs, addition of 3 mM Mg^{2+} did not significantly affect the electrophoretic mobility and Z_{DHH} values (**Figure 7**). It is difficult to gauge whether this agrees with some reported observations. Martin-Molina et al. (2012) reported that Mg^{2+} decreases the magnitude of the electrophoretic mobility of both PC and PS liposomes and with a charge inversion (sign reversal) at 100 mM Mg^{2+}. Their results were obtained in a $Mg(NO_3)$, rather than $MgCl_2$. However, there is no reason to suspect that the nitrate ion would account for the difference between their data, and ours, which show that Mg^{2+} does not affect the electrophoretic mobility and Z_{DHH} relative to Na^{+}. Concentrations of Mg^{2+} did not exceed 3 mM for our analysis because the intracellular (~5 x 10^{-4} M) and extracellular (~1 mM) Mg^{2+} concentrations generally do not exceed 3 mM in normal conditions [Jahnen-Dechent and Kettler, 2012]. Perhaps the discrepancy with the reported observations of Martin-Molina et al. (2012) results from the much higher [Mg^{2+}] used in their studies.

General comments. For POPC and POPS Nanodiscs, the charge magnitude decreases when 3 mM Ca^{2+} is present in the solvent. It may seem somewhat surprising that pure POPC Nanodiscs interact with Ca^{2+}. However, although the magnitude of the charge change is relatively small, this may reflect preferential solvation effects [Gokarn et al., 2011]. Perhaps more surprising, is that Ca^{2+} neutralizes the same fraction of the expected charge regardless of PS content (**Figure 8**). At this time, we cannot explain this observation. Our results disagree with NMR studies that observe perturbations within the lipid head group environment suggesting Ca^{2+} becomes deeply buried in the membrane, to a much greater extent than monovalent ions [Altenbach and Seelig, 1984]. Other stability and binding studies [Ekerdt and Papahadjopoulos, 1982; Nir et al. 1983], also suggest specific binding is occurring between Ca^{2+} and the phosphate portion of the phospholipid [Altenbach and Seelig, 1984; Roux and Bloom, 1990]; in disagreement with our observations.

Divalent ion interactions with PA lipids: No equivalent electrophoretic mobility measurements on PA lipids in the presence of divalent cations have been reported in the literature. There are however, non-electrophoretic studies of PA lipids in the presence of divalent cations that may help shed some light on the charge data of POPA Nanodiscs from MCE.

Calcium. In the presence of Ca^{2+}, POPA aggregates (**Figures 9a and 10**), in a manner that cannot be reversed by dilution, suggesting an irreversible association. These observations agree with the literature concerning the induced aggregation of PA bilayers in the presence of Ca^{2+} [Serhan et al. 1983]. However, the electrophoretic mobility of POPA Nanodiscs obtained by MCE, in the presence of Ca^{2+} is still anionic. This suggests that complete neutralization of the surface charge may not be what allows the lipid bilayers to approach one another on the order of an Å, which is necessary for aggregation to occur [Papahadjopoulos et al., 1990]. Perhaps a

bridging interaction is occurring where Ca^{2+} that is bound one Nanodisc^{TM} bridges to and binds with another Nanodisc^{TM} thus aggregating. It must be noted that the stoichiometry is not one Ca^{2+} ion bridging two phosphates on separate bilayers. At Ca^{2+} concentration on the order of 10 uM, no aggregation was observed (**Figure B3**), showing that ion binding is not occurring. If tight binding is the mode of interaction between PA lipids and Ca^{2+}, even at lower Ca^{2+} (on the order of uM) concentrations, some of these aggregation behaviors should have been observed, which were not. It wasn't until Ca^{2+} concentrations were on the order of mM that aggregates were observed, suggesting preferential solvation may be the mode of interaction.

Magnesium. With respect to POPA behavior in the presence of Mg^{2+}, there is limited literature data available on Mg^{2+}/POPA interactions that suggest Mg^{2+} induced aggregation [Leventis et al., 1986]. We did not observe Mg^{2+} induced aggregation **(Figure 11**); although an interaction is implied by the reduced magnitude of Z_{DHH}. It has been observed, that the presence of Mg^{2+} does not typically lead to bilayer fusion, but does lead to aggregation [Schultz et al., 2009]. Therefore the interaction of Mg^{2+} and lipids is fundamentally different from that between Ca^{2+} and lipid, since Ca^{2+} was observed to induce aggregation of POPA Nanodiscs by MCE, while Mg^{2+} did not.

MCE experiments showed that POPA Nanodiscs remains monodisperse in the presence of 3 mM Mg^{2+} (**Figure 24b)**. The interaction with Mg^{2+} must be with the exposed phosphate group on PA lipids, since Mg^{2+} did not have an effect on POPC and POPS Nanodiscs, which contain the MSPs. Furthermore, the data suggests that Mg^{2+} also does not have a significant interaction with the carboxylate anion on the PS lipid head group, as the electrophoretic mobility of POPS Nanodiscs was not significantly different in the presence of Mg^{2+}. Mg^{2+} does have binding interactions with phosphate, and this data may suggest that the phospho-L-serine head

group of PS lipids may also prevent molecules and ions from interacting with the phosphate group in PS lipids, similarly to the bulky choline head group of PC lipids.

As seen in **Figure 11**, the fractional charge of POPA Nanodiscs in the presence of Mg^{2+} is similar to the fractional charge of POPS Nanodiscs in the presence of Ca^{2+}, which suggests that there may be an underlying cause such as preferential solvation. What then might account for the different consequences of Ca^{2+} and Mg^{2+} interacting with POPA Nanodiscs? One possibility is the differences in the hydration properties of Ca^{2+} and Mg^{2+}. Ca^{2+} has a weaker association with its hydration shell, resulting in a more variable hydration shell per Ca^{2+} ion, and leads to Ca^{2+} more readily shedding its water molecules during interactions with the lipid head groups [Ikeda et al., 2007]. The dehydration of the Ca^{2+} may be why lipid bilayers can get to the distance (on the order of an Å) that is required for the first step in bilayer fusion. Mg^{2+} on the other hand has a stable and tightly associated hydration shell consisting of six water molecules [Maguire and Cowan, 2002]. Unlike Ca^{2+}, this hydration shell requires a much greater energy of interaction for Mg^{2+} to shed its hydration shell. If Mg^{2+} ions interact with the lipid head group and the interaction is not strong enough to displace the water molecules associated with Mg^{2+}, at the distance of a few Å, these bound water molecules are more than enough to cause bilayers to strongly repel at these distances [Yeagle, 1993]. The different hydration properties of Ca^{2+} and Mg^{2+} may explain why Ca^{2+} causes aggregation in POPA Nanodiscs, while Mg^{2+} does not.

Divalent ion interactions with PIP_2 lipids: No equivalent electrophoretic mobility measurements on PIP_2 liposomes in the presence of divalent cations have not been reported in the current literature. There are however, numerous non-electrophoretic studies of PIP_2 lipids in the presence of divalent cations that may help shed some light on the MCE electrophoretic mobility and Z_{DHH} data of PIP_2 Nanodiscs.

PIP_2 Nanodiscs, like POPA Nanodiscs, were observed to interact with both Ca^{2+} and Mg^{2+} (**Figure 12**). However, the nature of these interactions was opposite to that observed with POPA Nanodiscs. Unlike POPA Nanodiscs, PIP_2 Nanodiscs aggregated in the presence of Mg^{2+}, but not Ca^{2+}. In the presence of Ca^{2+} ions, the Z_{DHH} of PIP_2 Nanodiscs decreased in magnitude. Furthermore, the charge neutralization by Ca^{2+} ions was of a much greater magnitude than that observed in all other Nanodisc^{TM} samples. Whereas the Z_{DHH} was neutralized ~ 25% for POPC and POPS Nanodiscs in the presence of Ca^{2+} (and for POPA Nanodiscs in the presence of Mg^{2+}), the Z_{DHH} was neutralized by ~ 50% for PIP_2 Nanodiscs in the presence of Ca^{2+} (**Figure 30**).

The results here are inconsistent with some reported observations. First, studies have shown that PIP_2 Nanodiscs bind Ca^{2+} and Mg^{2+} differently [Wang et al., 2012]. Some have observed PIP_2 lipids binding Ca^{2+} more strongly and some have observed PIP_2 lipids binding Mg^{2+} more strongly [Wang et al, 2012; Gwanyanya et al, 2006]. While the MCE data of PIP_2 Nanodiscs implies some interaction to both divalent cations, the electrophoretic data cannot give conclusive quantities for the strength of those interactions. **Figure 29** shows that while some aggregation occurs in the presence of Mg^{2+}, the Z_{DHH} is of a higher magnitude (nearly double) than that of PIP_2 Nanodiscs in the presence of Ca^{2+} ions. This suggests that a greater number of Ca^{2+} ions may be interacting with PIP_2 lipids. However, Ca^{2+} also has been observed to induce more aggregation behavior and stronger aggregation behavior than Mg^{2+} [Wang et al, 2012; Serhan et al. 1983]. We did not observe Ca^{2+} induced aggregation in PIP_2 Nanodiscs. Furthermore, Mg^{2+} only neutralized the charge on PIP_2 lipids ~ 25% (as opposed to ~ 50% in the presence of Ca^{2+}) and yet showed aggregation behavior. This also suggests that aggregation behavior is due in part to both the chemical and electrostatic structure of the lipids within a cellular membrane.

A qualitative comparison of POPA and PIP_2 lipid behavior in the presence of divalent cations. Phosphatidic acid is a much smaller lipid than phosphatidylcholine, and its cone shape decreases its head group exposure to the lipid bilayer surface (**Figure D9**). Mg^{2+} is known to chelate polyphosphates, the best example being the Mg-ATP complex (**Figure D22**). However, if Mg^{2+} chelates one PA lipid, the PC lipids are large enough to sterically hinder the chelation of another PA lipid on another lipid bilayer (**Figure D9**). This may be one reason why Mg^{2+}, which was observed to interact with the POPA Nanodiscs, does not induce aggregation. PIP_2 on the other hand, has an asymmetric shape opposite that of PA lipids, with a much larger head group relative to that of the fatty acid tails (**Figure D10**). As a result, if a Mg^{2+} ion did chelate a phosphate on the inositol group of one PIP_2 lipid, that Mg^{2+} is far out enough into the surface to chelate another PIP_2 phosphate group on a separate bilayer, without being sterically hindered by the PC lipids surrounding it. Chelation at multiple PIP_2 lipids could disrupt the membrane by forcing PIP_2 lipids to adopt a more rigid, extended conformation, which might lead to aggregation. In addition, this chelation could also bring separate bilayers into close enough proximity with one another (on the order of an Å), leading to aggregation/fusion.

The PIP_2 MCE data in the presence of Ca^{2+} is a little more difficult to interpret, as no aggregation was observed in PIP_2 Nanodiscs, but aggregation has been observed previously in PIP_2 liposomes in the presence of Ca^{2+} and Mg^{2+} [Wang et al., 2012]. One possible reason may be due to the large PIP_2 head group relative to the fatty acid structure. Of all the lipids observed, only PA aggregated in the presence of Ca^{2+}. The other lipids characterized here (PE lipids excluded) have large head groups that can potentially prevent interaction with the phosphate group in the ester bond. Therefore, access to this particular phosphate may be important for aggregation to occur. For PIP_2 lipids, the head group extends out further from the membrane

surface than neighboring PC lipid head groups and the larger area also pushes neighboring PC lipids further away. Any Ca^{2+} interactions may be isolated to the PIP_2 head group and may not be significant enough to induce aggregation behavior due to the distance between the Ca^{2+} ions and the neighboring positive charge on PC lipids.

However, with respect to PIP_2 Nanodiscs in the presence of Ca^{2+}, the data here are not in agreement with data found in literature and at the current time, there is no physical data that can conclusively prove these possible explanations for the behavior observed with PIP_2 and divalent cations are occurring.

Lipid charge as a function of Na^+ concentration: Electrophoretic mobility measurements on PC liposomes have been made by Klasczyk et al. (2010). Klasczyk et al. (2010) have reported ELS measurements for:

1) POPC liposomes in concentrations ranging from 0-500 mM NaCl, LiCl, KCl, CsCl and RbCl, 15 mM HEPES, 2 mM KOH at pH 7.0. Klasczyk et al. (2010) observed that as the salt concentration increased, the magnitude of the electrophoretic mobility decreased. In the presence of Li^+, as salt concentration increased, the electrophoretic mobility decreased in magnitude until charge inversion ~ 10 mM. At higher salt concentrations, the electrophoretic mobility increased in magnitude in the positive direction. At higher salt concentrations, the electrophoretic mobility became insensitive to additional salt.

Na^+ concentration dependence of POPC Nanodiscs. POPC Nanodisc™ charge was generally insensitive to the changes in Na^+ concentration (**Figure 9**). At ionic strengths of 50 mM to 250 mM, the Z_{DHH} did not change significantly, in contrast to anionic Nanodiscs. This finding, in

conjunction to the salt concentration data of anionic lipids (including POPE Nanodiscs) reinforces the assertion that PC lipids are neutral.

Na^+ concentration dependence of POPE Nanodiscs. POPE Nanodisc^{TM} charge behaved most similarly to anionic lipids as a function of Na^+ concentration. This observation, in conjunction with the Z_{DHH} measurements of POPE Nanodiscs, reinforces that PE lipids are anionic, as the Z_{DHH} increased as Na^+ concentration decreased. However, POPE Nanodisc^{TM} charge did plateau at higher Na^+ concentrations (**Figure 9**).

Na^+ concentration dependence of anionic Nanodiscs. POPS, POPA and PIP_2 Nanodiscs behaved similarly to POPE Nanodiscs (**Figures 10-12**). As Na^+ concentration decreases, the ZDHH increases in magnitude. However, POPS, POPA, PIP_2 Nanodisc^{TM} charge plateaued at higher Na^+ concentrations.

Extrapolated values at zero Na^+ concentration. It is not surprising that the extrapolated values at zero salt for 70POPS, 70POPA and 10PIP_2 Nanodiscs were lower in magnitude than the calculated charge estimates. This observation agrees with polyelectrolyte theory [Manning, 1969]. At high charge densities, more ions must adsorb unto the surface charge of the macromolecule in order to bring the electrostatic potential back to k_BT. With 70POPS and 70POPA, this charge reduction is essential due to the sheer number of anionic lipids present in the Nanodisc^{TM}. If 10-30% of the lipids are anionic lipid, they can still be oriented so that no charged groups (on average) are adjacent to one another (**Figure D23a-D23f**). There can be one, two or three PC lipids in between them at any one time, stabilizing the electrostatic potential by keeping the distance between charged lipid head groups greater than the $l_{B\text{aqueous}}$. At 70% incorporation of anionic lipids, the anionic lipids saturate the Nanodisc^{TM}, so that the majority of

anionic lipids are adjacent to one another. As a result, more counter-ions are needed to adsorb unto the surface in order to keep the distance between charged lipid head groups greater than $l_{B\text{aqueous}}$. Head group repulsion is why pure anionic lipids are not feasible to prepare and constantly fall back into solution unless PC lipids (or positively charge modified molecules) are incorporated to stabilize the lipid structure. As seen in **Table 7**, this neutralization is so great in 70POPS and 70POPA Nanodiscs that each lipid head group only expresses <50% of its charge.

That PIP_2 Nanodiscs have a lower extrapolated Z_{DHH} value than the calculated charge estimates also agrees with polyelectrolyte theory. While 10% incorporation allows the 13 PIP_2 lipids to be spaced far enough apart, as to keep the distance between intermolecular PIP_2 head groups greater than $l_{B\text{aqueous}}$, it is the intramolecular charge distribution that contributes to its high electrostatic potential. The spacing between the 4' and 5' phosphates on the inositol group has been estimated to be less than $l_{B\text{aqueous}}$ [Levental et al., 2008], requiring much more ion adsorption than required by 10POPS or 10POPA Nanodiscs. However, due to there being only 13 PIP_2 lipids, the effect is not as dramatic that seen in 70POPS and 70POPA due to the greater spacing between intermolecular PIP_2 lipids and therefore, the extrapolated Z_{DHH} at zero salt was only slightly lower than the calculated charge estimate.

Polyelectrolyte behavior. In general, lipid Nanodiscs exhibit polyelectrolyte behavior. As the Na^+ concentration decreases, Z_{DHH} increases. In addition, the charge plateaued at higher Na^+ concentrations (**Figures 9-12**).

pH dependence of lipid charge. Electrophoretic mobility measurements on lipid vesicles have been made by Gabev et al. (1989) and Woodle et al. (1992). They have reported measurements for:

1. PC liposomes in 10 mM phosphate buffer at pHs 5.2, 7.3 and 9.2.
    a. At pH 5.2, the electrophoretic mobility was found to be $0.5 \times 10^{-7} \pm 0.4 \times 10^{-7}$ $cm^2/V \cdot s$
    b. At pH 7.3, the electrophoretic mobility was found to be $0.9 \times 10^{-7} \pm 0.1 \times 10^{-7}$ $cm^2/V \cdot s$
    c. At pH 9.2, the electrophoretic mobility was found to be $0.6 \times 10^{-7} \pm 0.2 \times 10^{-7}$ $cm^2/V \cdot s$

    An ELS apparatus (Coulter Electronics DELSA) was used in this study [Woodle et al., 1992]
2. Methylated PEG-DSPE modified liposomes in 10 mM phosphate buffer at pHs 5.2, 7.3 and 9.2.
    a. At pH 5.2, the electrophoretic mobility was found to be:
        i. $-6.0 \times 10^{-6} \pm 3.0 \times 10^{-7}$ $cm^2/V \cdot s$ at a molar ratio of 7.5%
    b. At pH 7.3, the electrophoretic mobility was found to be:
        i. $-4.5 \times 10^{-6} \pm 4.0 \times 10^{-7}$ $cm^2/V \cdot s$ at a molar ratio of 7.5%
    c. At pH 9.2, the electrophoretic mobility was found to be:
        i. $-4.5 \times 10^{-6} \pm 3.0 \times 10^{-7}$ $cm^2/V \cdot s$ at a molar ratio of 7.5%

    An ELS apparatus (Coulter Electronics DELSA) was used in this study [Woodle et al., 1992]
3. Egg PC/PIP_2 monolayers in 100 mM KCl, 1 mM MOPS at pH 6.0, 7.0 and 8.0. No electrophoretic mobility data were reported. However, zeta potentials were calculated and PIP_2 lipids were found to have a zeta potential of -43 mV at all pHs for 20% PIP_2 lipid molar ratios (**Figure D19)**. A Micro-electrophoresis apparatus Mk II (Rank Brothers LTD) was used in this study [Gabev et al. 1989].

While Woodle et al. (1992) did study different lipid molar ratios of methylated PEG-DSPE modified liposomes, only the data at a lipid molar ratio of 7.5% will be considered since it was the only lipid molar ratio to have meaningful measurements across the three pHs observed. No equivalent electrophoretic mobility measurements on lipid vesicles as a function of pH have been reported in the current literature for PA or PIP_2 lipids. Woodle et al. (1992) did measure the electrophoretic mobility of PG lipids, which have been observed in literature to have similar surface charge estimates (of -1 charge unit per lipid). However, the chemical structures of PG and PS lipids are different and therefore, only a qualitative comparison will be made

pH dependence of POPC and POPS Nanodisc^{TM} charge. POPC and POPS Nanodiscs exhibit similar charge behavior as a function of pH. Please note, for MCE analysis of Nanodiscs, a reference pH of 7.4 will be used for the discussion in this section. Therefore, $\Delta Z_{PHx} - \Delta Z_{PH7.4} = \Delta Z_{DHH}$, where x is the pH of comparison to the reference standard of pH 7.4. As pH decreases to 7.0, the ΔZ_{DHH} of POPC and POPS Nanodiscs is ~ 0 (**Figure 31**). However, as the pH increases to 8.5, the ΔZ_{DHH} is ~ 6 for POPC and POPS Nanodiscs. It is unlikely that this increase in Z_{DHH} is due to the ionization of PC or PS head groups. The choline group of PC lipids is non-titratable and due to the carboxylate anion on the serine group of PS lipids, the measured pKa of the adjacent ammonium cation (**Figure C6**) on PS lipids is ~ 11.6 [Marsh, 1990]. Therefore, the increase of Z_{DHH} observed in POPC and POPS Nanodiscs at pH 8.0 must be coming from the amino acid composition of the MSPs, suggesting that the charge of the PC and PS lipids themselves, are insensitive to pH changes from a pH range of 7.0 – 8.5. Within a single MSP are 5 histidines, 7 tyrosines and 17 lysines, which are the most likely candidate amino acids that are ionized in the pH range tested.

As seen in **Table D6**, ΔZ_{DHH} of two the MSPs is 3 at pH 8.5 and at pH 7.0, ΔZ_{DHH} is 2. Assuming that the ΔZ_{DHH} in POPC and POPS Nanodiscs at pH 8.5 is solely contributed by the MSPs, the measured ΔZ_{DHH} of the MSPs at pH 8.5 is twice that of the calculated ΔZ_{DHH} of the MSPs at the same pH. This isn't surprising given that the charge estimates assume all the amino acid residues have pKa values that are equivalent to the isolated residues. For a folded protein, this assumption is not valid and therefore deviations from the calculated charge based off the amino acid sequence are not uncommon [Edsall and Wyman, 1958]. The pKas of amino acid side chains are heavily environment dependent and vary considerably. Histidine in particular has one of the most variable pKa of the 20 common amino acids, so the difference in the measured ΔZ_{DHH} for from the calculated ΔZ_{DHH} is not too surprising.

POPC Nanodisc^{TM} charge behavior as a function of pH is inconsistent with reported observations of Woodle et al. (1992). Woodle et al. (199) observed significantly different electrophoretic mobilities at pH 5.2, 7.3 and 9.2. From pH 5.2 to 7.3, the electrophoretic mobility increases ~ 80%. From pH 7.3 to 9.2, the electrophoretic mobility decreases by ~ 60%. Since the choline group on lipid head groups is non-titratable, and the phosphate group has already ionized, it is difficult to pinpoint what is causing these fluctuations in this pH dependence of PC liposome electrophoretic mobility. No relevant literature concerning pH dependence of PS lipids with respect to Z_{DHH} was found.

pH dependence of POPE Nanodiscs. POPE Nanodiscs also followed the trend of increasing ΔZ_{DHH} as pH increases to 8.5, which agree with the reported observations of Woodle et al. 1992. Woodle et al. (1992) observed no change to the electrophoretic mobility of Methylated PEG-DSPE modified liposomes from pH 7.3 – 9.2. Similarly to POPC and POPS Nanodiscs, the ΔZ_{DHH} was ~ 6 for 10POPE Nanodiscs at pH 8.0 and remained unchanged at pH 8.5. This also

suggests that the ΔZ_{DHH} is most likely due to the ionization of the MSPs and that the Z_{DHH} of POPE Nanodiscs is insensitive to changes in pH at pH 8.5, in agreement with Woodle et al. (1992). Unfortunately, electrophoretic mobility measurements for POPE Nanodiscs in MCE could not be made at pH 7.0. At pH 7.0 POPE Nanodiscs was observed migrating toward the bottom membrane, only to reverse and start moving back up the cell. Some studies have observed PE lipids aggregating at pHs <7.0 [Connor et al., 1984]. However, at pH 7.0, no aggregation was observed on POPE Nanodiscs using AUC (**Figure A4**). At this time, there is no explanation for this behavior observed with POPE Nanodiscs at pH 7.0.

pH dependence of POPA Nanodiscs. POPA Nanodiscs were observed to be pH sensitive, with significantly different Z_{DHH}s at pH 7.0, 7.4, 8.0 and 8.5. In general, as the pH increases, the Z_{DHH} increases and vice versa, for the pH range of 7.0 – 8.5. Furthermore, at pH 7.0, the Z_{DHH} of POPA Nanodiscs was identical to the Z_{DHH} of POPS Nanodiscs (**Figure 32**). This isn't surprising given that the pKa for the second ionizable group on the phosphate group for PA lipids is ~ 8.0 (**Figures C7** and **C8**). The MCE data also show that the charge per PA lipid is closer to -1.25 charge units, rather than a -1 charge unit at pH 7.4, which is supported by the titration data of PA lipids (**Figures C7** and **C8**). In comparison to POPC, POPS and POPE Nanodiscs, the ΔZ_{DHH} of POPA Nanodiscs is >6 from pH 7.4 – 8.5, signifying that the amino acids on the MSPs are not the only groups ionizing and contributing to the observed increased in Z_{DHH} of POPA Nanodiscs.

Physiological impact of PA sensitivity to pH. The sensitivity of PA lipids to pH changes makes it a good pH biosensor, as its charge is sensitive to slight changes at physiologic pH. This is reflected in PA lipids being most commonly found in the mitochondrial membranes, where proton gradients are common during cellular respiration [Porter and Brand, 1995]. However, the

amount of PA in lipid bilayers is still very low (~ 1-3%). PA is synthesized by the endoplasmic reticulum and mitochondria. PA synthesized by the ER is usually converted in diacylglycerol which is then converted to PC, PE, PS, PG, PI, PIP, PIP_2 and PIP_3 lipids. PA that is synthesized in mitochondria is typically incorporated into a cardiolipin molecule or incorporated into the lipid bilayer itself.

pH dependence of PIP_2 Nanodiscs. PIP_2 Nanodiscs were also observed to be pH sensitive. However, this was only observed at pHs greater than 7.4, as ΔZ_{DHH} was ~ 0 at pH 7.0 and was within the uncertainty of the measurement at pH 8.0 (ΔZ_{DHH} ~ 4). At pH 8.5 the ΔZ_{DHH} was 15. While there is currently no reliable titration data on PIP_2 lipids, there have been estimates that the pKa of the second ionization on the 4' and 5' phosphates found on the inositol group ranging from 6.7 to 7.7 [McLaughlin et al., (2002)]. These estimates seem low considering the chemical environment of the PIP_2 lipid at pH 7.4. The environment around a PIP_2 head group is very anionic, due to the -3 charge from 3 phosphate groups. As a result, one would expect a pKa shift greater than that observed in PA lipids, which has only one ionized phosphate group. In addition, due to the reverse cone structure of PIP_2 lipids (**Figure D10**), it would seem less likely that the bulky choline groups of PC lipids have an influence on ionization of PIP_2 lipids. If the pKas obtained from NMR titrations were taken into consideration, it would be expected that PIP_2 lipids should have a similar pH sensitivity to PA lipids. However, that was not observed and therefore the MCE data for PIP_2 lipids as a function of pH does not agree with the estimated pKas of McLaughlin et al. (2002).

There is evidence that PIP_2 lipid sensitivity to pH plays an important role in the regulation of mechanisms in the physiology of inwardly-rectifying K^+ (Kir) channels [Yang et al., 2000]. Yang et al. (2000) observed that at pH 8.5, PIP_2 associated Kir channels were open

for a much longer period of time and closed for shorter periods of time. In addition, at pH 6.5 and below, PIP_2 associated Kir channels were observed to be closed over longer periods of time and opened for shorter periods of time. These observations are congruent with our observations that show PIP_2 increasing in Z_{DHH} as the pH increases to 8.5 by MCE.

Anion binding to lipids. Electrophoretic mobility measurements have been made by Martin-Molina et al. (2012) and Tatulian (1983). Martin-Molina et al. (2012) and Tatulian (1983) have reported measurements for:

1) Bovine brain 3-*sn*-phosphatidyl-L-serine liposomes in varying concentrations of $Ca(NO_3)_2$ and $Mg(NO_3)_2$ at pH 5.5 (**Figure D13**). Martin-Molina et al. (2012) observed that magnitude of the electrophoretic mobilities of the PS liposomes decreased, suggesting that more cations are binding to lipids than are anions. A phase-analysis light scattering apparatus (Zetapals, Brookhaven Instruments Corporation) was used in this study (Martin-Molina et al., 2012).
2) DMPC liposomes in 10 mM KCl, 5 mM Tris-HCl at pH 7.4 at varying concentrations of picric acid (**Figure D24**). Tatulian (1983) observed that up to 10 uM of picric acid, the zeta potential of DMPC liposomes was not affected by picric acid. At concentrations greater than 10 uM of picric acid however, the charge magnitude started to increase significantly. Electrophoretic mobility measurements were carried out on an automatic apparatus Parmoquant-2 cell electrophoresis system [Tatulian, 1983].

Anion binding to lipid Nanodiscs. **Figure 34** shows that in the presence of 100 mM Na_2S0_4, 50 mM Tris at pH 7.4, the Z_{DHH} was not significantly different from the Z_{DHH} in standard buffer for POPC, 30POPS and 30POPA Nanodiscs. This finding is generally inconsistent with some

reported observations. There have not been many studies with respect to anion binding using electrophoretic methods. In the mentioned studies, Martin-Molina et al. (2012) observed that nitrate did not have an effect on the electrophoretic mobilities, as Ca^{2+} or Mg^{2+} had greater interactions with PS lipids; as seen by the decrease in magnitude of the electrophoretic mobility. Tatulian (1983) observed the exact opposite, with the zeta potential more negative as the concentration of picric acid increased. Indeed, the literature in general does not seem to agree on anion binding to any macromolecule. Rydall and Macdonal (1991) observed that sulfate had minimal interactions with POPC bilayers due to a low quadrupole splitting spectra by NMR. However, they observed a large signal splitting in the presence of thiocyanate, perchlorate and nitrate, which signifies a much higher association with PC lipids than that observed by Tatulian (1983). This trend of increasing association of macromolecules (not unique to Nanodiscs) being proportional to solvation effects of these anions agrees with the trend seen in the Hofmeister series on anions.

Macdonald and Seelig (1988) observed that thiocyanate did not bind as strongly to POPC membranes as was observed by Rydall and Macdonald (1991) and Tatulian (1983). However, when the PC lipids were modified with dihexadecyldimethylammonium bromide, making the lipid bilayer more positively charged, thiocyanate association constants were three times greater than that of neutral POPC bilayers. Furthermore, with respect to sulfate, Gokarn et al. (2011) observed the opposite, with sulfate having the strongest association with hen egg-white lysozyme, lowering the effective charge the greatest, in comparison to NaCl.

These discrepancies may be attributed to many factors that mostly involve normalizing solvent conditions. Rydall and Macdonald (**Figure D25;** 1992) observed anion binding to POPC lipids in 500 mM concentrations of the sodium form of the anionic salts. Tatulian (**Figure D26;**

1983) observed anion binding to DMPC lipids in only 10 mM concentration of the K^+ form of the anionic salts. Martin-Molina et al. (2012, **Figure D13**) observed anion binding at various concentrations, but used the Ca^{2+} forms of the anionic salts. It should be noted that the weak apparent binding may be describing solvation effects (and not specific interactions), that may account for the shifts in the NMR signal observed by Rydall and Macdonald (1991) and Macdonald and Seelig (1988).

Charge as a function of temperature. Electrophoretic mobility measurements on PC liposomes have been made by McLaughlin et al. (1978) and Tatulian (1983). They have reported measurements for:

1) Egg PC liposomes in 100 mM NaCl, at pH 7.5. No electrophoretic mobility quantities were reported. However, zeta potentials were calculated and egg PC liposomes were found to have a zeta potentials:
    a. In the presence 50 mM Mg^{2+}
        i. at 15^oC, 13.0 ± 0.5 mV
        ii. at 25^oC, 10.0 ± 1.0 mV
        iii. at 35^oC, 13.5 ± 1.0 mV
    b. In the presence of 50 mM Ca^{2+}
        i. at 15^oC, 20.5 ± 1.0 mV
        ii. at 25^oC, 11.0 ± 1.0 mV
        iii. at 35^oC, 16.0 ± 1.0 mV

    Against a zeta potential of 0 mV (within error) for Egg PC liposomes in the absence of divalent cations. A Micro-electrophoresis apparatus Mk II (Rank Brothers LTD) was used in this study [McLaughlin et al. 1978].

2) DMPC liposomes in 10 mM KCl, 5 mM Tris-HCl at pH 7.4 at varying concentrations of picric acid (**Figure D28**). Tatulian (1983) observed a gradual decrease in the magnitude of the electrophoretic mobility as the temperature increased. Then, a sharp decrease in magnitude of the electrophoretic mobility was observed at the phase transition temperature of DMPC lipids (~ 24^{o}C). After the sharp decrease of the electrophoretic mobility, the electrophoretic mobility gradually decreases at temperatures above the phase transition temperature. Electrophoretic mobility measurements were carried out on an automatic single cell electrophoresis apparatus (Parmoquant-2) [Tatulian, 1983].

POPC, POPS and POPA Nanodiscs in 100 mM NaCl, 50 mM Tris at pH 7.4 showed no significant change in electrophoretic mobility and Z_{DHH} values at a temperature range of 20^{o}C to 35^{o}C (**Figure 33**). This does not agree with some reported observations, as McLaughlin et al. (1987) observed significant differences to the zeta potential as a function of temperature; and Tatulian (1983), observed significant differences in the electrophoretic mobility as a function of temperature. It must be noted however, that the lipids used in MCE, have different phase transition temperatures. POPC (~ -2^{o}C) and POPS (~ 14^{o}C) were measured at temperatures above their phase transition temperatures, while POPA (~ 28^{o}C) was measured both under and over its phase transition temperature.

DMPC lipids used by Tatulian (1983) have a phase transition temperature of ~ 24^{o}C. In addition, naturally derived lipids, such as those from egg, bovine or soybean typically contain significant levels of polyunsaturated fats and therefore have lower phase transition temperatures [Tatulian, 1983]. While Tatulian (1983) observed a sharp decrease at the phase transition temperature of DMPC liposomes, POPA Nanodiscs was did not have a similar sharp decrease at its phase transition temperature. Since PA lipids have a pKa ~ 8.0, one would expect from the

data obtained by Tatulian et al. (1983) that the $\Delta H_{ionization}$ may drive POPA Nanodiscs toward being more anionic. However, that was not observed and agrees with $\Delta H_{ionization}$ values reported by Bernard (**Figure D29**; 1955). This is seen by the formation of negative charge when the ionization of the phosphate occurs. The enthalpy of ionization would however, be significant for a lipid like PE, in which no net ion is formed as a result of ionization; similar to Tris (**Figure D29**). It should also be mentioned, that Tatulian (1983) observed a sharp decrease in the electrophoretic mobility quantity. The electrophoretic mobility does not take into account the viscosity of the solution. At increased temperatures, the decrease in viscosity is significant (seen in the calculated viscosities at 25 and 35^{o}C in **Table 3**) and most likely account for the increase in magnitude of the electrophoretic mobilities observed by Tatulian (1983). Unfortunately, due to lack of sample, no measurements were made on 10POPE Nanodiscs at different temperatures.

CONCLUSION

While there are literature data that characterize lipid electrophoretic mobility, there is little consistency in the charge estimates from the various techniques. Each technique requires specific modifications to ensure optimal conditions for experimentation, but these changes cannot be accounted for or duplicated in other techniques. As we are interested in the details of membrane charge and ion binding to lipid membranes, it is important to develop a simple, reproducible way to analyze lipid charge in a way that can clarify inconsistencies between data obtained using various techniques, membrane systems and experimental conditions. The technique of MCE combined with the technology of Nanodiscs gives us the ability to systematically measure lipid charge in physiologically relevant conditions.

REFERENCES

1. Altenbach, C. and Seelig, J. Ca^{2+} Binding to Phosphatidylcholine Bilayers As Studied by Deuterium Magnetic Resonance. Evidence for the Formation of a Ca^{2+} Complex with Two Phospholipid Molecules. *Biochemistry* **23,** 3913-3920 (1984).
2. Altria, D. K. Capillary Electrophoresis Guidebook: Principles. Operation and Applications, Volume 52. *Hurman Press Inc.* 1996.
3. Bayburt, T. H. and Sligar, S. G. Membrane protein assembly into Nanodiscs. *FEBS Letters*. **584**. 1721-172 (2010).
4. Bernard, A. S. Ionization Constants and Heats of Tris(hydroxymethylamiomethane and Phosphate Buffers. *J. Biol. Chem.* **218**. 961-969 (1955).
5. Binder, H. and Zschornig, O. The effect of metal cations on the phase behavior and hydration characteristics of phospholipid membranes. *Chem. Phys. Lipids*. **115(1-2)**. 39-61 (2002).
6. Blanck J. S., Smettan, G., Ristau O., Ingelman-Sundberg, M and Ruckpaul, K. Mechanism of rate control of the NADPH-dependent reduction of cytochrome P-450 by lipids in reconstituted phospholipid vesicles. *Eur J Biochem* 144:509–513 (1984).
7. Boettcher, J. M., Davis-Harrison, R. L., Clay, M. C., Nieuwkoop, A. J., Ohkubo, Y. Z., Tajkhorshid, E., Morrisey, J. H. and Rienstra, C. M., Atomic View of Calcium-Induced Clustering of Phosphatidylserine in Mixed Bilayers. *Biochemistry*. **50(12)**. 2264-2273 (2011).
8. Brundin, P., Melki, R. and Kopito, R. Prion-like transmission of protein aggregates in neurodegenerative diseases. *Nat. Rev. Mol. Cell. Biol.* **11(4).** 301-307 (2010).
9. Clark, J. R. Effect of lipid structure on the dipole potential of phosphatidylchoine bilayers. *Biochimica et Biophysica Acta (BBA) - Biomembranes*. **1327(2).** 269-278 (1997).
10. Cole, J. L. and Hansen, J. C. Analytical Ultracentrifugation as a Contemporary Biomolecular Research Tool. *J Biomol Tech.* **10(4).** 163-176 (1999).
11. Collins, D. K. Why continuum electrostatics theories cannot explain biological structure, polyelectrolytes or ionic strength effects on ion-protein interactions. *Biophysical Chemistry*. **167**. 43-59 (2012).
12. Connor, J., Yatvin, M. B. and Huang, L. pH-sensitive liposomes: Acid induced liposome fusion. Proc. Natl. Acad. Sci. USA. 81. 1715-1718 (1984).
13. Conrad, J., Troll, M. and Zimm, B. H. Ions Around DNA: Monte Carlo Estimates of Distribution with Improved Electrostatic Potentials. *Biopolymers*. **27**. 1711-1732 (1988).
14. Ornstein L. and Davis, B. J. Disc electrophoresis I: Background and Theory. *NY Academy of Sciences*. 1964.
15. Demchenko, A. P. and Yesylveskyy, S. O. Nanoscopic description of biomembrane electrostatics: results of molecular dynamics simulations and fluorescence probing. *Chemistry and Physics of Lipids*. **160.** 63-84 (2009).
16. Dessinges, N. M., Maier, B., Zhang, T., Peliti, M., Bensimon, D. and Croquette, V. Stretching Single Stranded DNA, A Model Polyelectrolyte. *Physical Review Letters*. **89(24)**. 248102-1 - 248102-4 (2002).
17. Durant, J. (2003) *Free Solution Electrophoresis Measurement and their Theoretical Relationships to Net Protein Valence.* PhD Dissertation. University of New Hampshire (2003).
18. Duzgnes, N., Straubinger, R. M., Baldwin, P. A., Friend, D. S. and Papahadiopoulos, D. Proton-induced fusion of oleic acid-phosphatidylethanolamine liposomes. *Biochemistry*. **24(13)**. 3091-3098 (1985).

19. Edsall, J. T. and Wyman, J. *Biophysical Chemistry Volume I*: *Thermodynamics, Electrostatics, and the Biological Significance of the Properties of Mater*. Academic Press Inc. (1958).
20. Ekerdt, R., and Papahadjopoulos, D. Intermembrane contact affects calcium binding to phospholipid vesicles. *Proc. Natl. Acad. Sci. USA*. **79**. 2273–2277 (1982).
21. Fearnley, J. C., Roderick, L. H. and Bootman, D. M. Calcium Signaling in Cardiac Myocytes. *CSH: Perspectives in Biology*. 1-22 (2011).
22. Filoti, D.I., Shire, S. J., Yadav, S. and Laue, T. M. Comparative study of analytical techniques for determining protein charge. *Journal of Pharmaceutical Sciences* (2015).
23. Flach, C. R., Brauner, J. W. and Mendelsohn, R. Calcium Ion Interactions with Insoluble Phospholipid Monolayer Films at the A/W Interface. External Reflection-Absorption IR Studies. *Biophysical Journal*. **65.** 1994-2001 (1993).
24. Gokarn, Y. R., Fesinmeyer, R. M., Saluja, A., Razinkov, V., Chase, S. F., Laue, T. M. and Brems, D. N. Effective charge measurements reveal selective and preferential accumulation of anions, but not cations, at the protein surface in dilute salt solutions. *Protein Sci*. **20(3)**, 580-587 (2011).
25. Goldberg, E. M., Lester, D. S., Borchardt, D. B. and Zidovetzki, R. Effects of Diacylglycerols and Ca^{2+} on structure of Phosphatidylcholine/Phosphatidylserine Bilayers. *Biophysical Journal*. **56**. 382-393 (1994).
26. Granyanya, A., Sipido, K. R., Vereecke, J. and Mubagwa, K. ATP and PIP2 dependence of the magnesium-inhibited, TRM7-like cation channel in cardiac myocytes. American Journal of Physiology. 291(4). C627-C635 (2006).
27. Gurtovenko, A. A. and Vattulainen, I. Effect of NaCl and KCl on Phosphatidylcholine and Phosphatidylethanolamine Lipid Membranes: Insight from Atomic-Scale Simulations for understanding Salt-Induced Effects in the Plasma Membrane. *J. Phys. Chem. B.* **112.** 1953-1962 (2008).
28. Haddadian, F., Shamsi, S. A., Schaeper, J. P. and Danielson, N. D. Capillary Electrophoresis of Phospholipids with Indirect Photometric Detection. *Journal of Chromatographic Science*. **36**. 395-400 (1998).
29. Hagge, S. O., Hammer, M. U., Wiese, A., Seydel, U. and Gutsmann, T. Calcium adsorption and displacement: characterization of lipid monolayers and their interaction with membrane-active peptides/proteins. *BMC Biochemistry*. **7(15).** 1-13 (2006).
30. Hauser, H. and Dawson, R. M. C. The Binding of Calcium at Lipid-Water Interfaces. *European Journal of Biochemistry*. **1.** 61-69 (1967).
31. Hautala, J. T., Wiedmer, S. K. and Riekkola M. L. Anionic liposomes in capillary electrophoresis: Effect of calcium on 1-palmitoyl-2-oleyl-sn-glycero-3-phosphatidylcholine/phosphatidylserine-coating in silica capillaries. *Anal. Bioanal. Chem.* **378.** 1769-1776 (2004).
32. Heiger, D. N. High Performance Capillary Electrophoresis: An Introduction. *Hewlett-Packard GmbH*. 1992.
33. Henry, D. C., The Cataphoresis of Suspended Particles. Part I. - The Equation of Cataphoresis. *Proc.Roy.Soc.A*. **133**. 106-140 (1931).
34. Ikeda, T., Boero, M. and Terakura, K. Hydration of magnesium and calcium ions from constrained first principle molecular dynamics. J. Chem. Phys. 127(7). 2-7 (2007).
35. Immordinom M. L., Dosiom F. and Cattel, L. Stealth liposomes: review of the basic science, rational and, clinical applications, existing and potential. *International Journal of Nanomedicine*. **1(3).** 297-315 (2006).
36. Inagaki, S., Ghirlando, R. and Grisshammer, R. Biophysical characterization of membrane proteins in Nanodiscs. *Methods* **59**, 287-300 (2013).
37. Jahnen-Dechent, W. and Ketteler, M. Magnesium basics. *Clinical Kidney Journal*. **5(1)**. i3-i14 (2012).

38. Jordon, K. (2014) *Real-time Electrophoretic Mobility in Membrane Confined Electrophoresis.* Master's Thesis. University of New Hampshire (2014).
39. Kato, K., Koido, M., Akagi, T. and Ichiki, T. (2011) *Precise Evaluation of Electrophoretic Mobility Distribution of Nanoliposomes using Microcapillary Electrophoresis Ships with Sensitive Fluorescent Imaging.* Protocol. School of Engineering, The University of Tokyo (2011).
40. Klasczyk, B., Knecht, V., Lipowsky, R. and Dimova, R. Interactions of Alkali Metal Chlorides with Phosphatidylcholine Vesicles. *Langmuir*. **26(24).** 18951-18958 (2010).
41. Knecth, V. and Klasczyk, B. Specific Binding of Chloride Ions to Lipid Vesicles and Implications at Molecular Scale. *Biophysical Journal*, 104. 818-824 (2013).
42. Kourennyi, D. E. and Barnes, S. Depolarization-induced calcium channel facilitation in rod photoreceptors is independent of G proteins and phosphorylation. *J. Neurophysiol*. **1.** 133-138 (2000).
43. Krylov, S. N. and Dovichi, N. J. Capillary Electrophoresis for the Analysis of Biopolymers. *Anal. Chem.* **72.** 111R-128R (2000)
44. Laue, T. M., Hazard, A. L., Ridgeway, T. M. and Yphantis, D. A. Direct Determination of Macromolecular Charge by Equilibrium Electrophoresis. *Anal. Biochem.* **182,** 377-382 (1989).
45. Laue, T. M., Shah, B. D., Ridgeway, T. M. and Pelletier D. L. Analytical Ultracentrifugation in Biochemistry and Polymer Science: Computer-Aided Interpretation of Analytical Sedimentation Data for Proteins. *Royal Society of Chemistry*. 1992.
46. Levental, I., Janmey, P. A. and Cebers, A. Electrostatic Contribution to the Surface Pressure of Charged Monolayers Containing Polyphosphoinositides. *Biophysical Journal*. **95(3)**. 1199-1205 (2008).
47. Leventis, R., Gagne, J., Fuller, N. and Silvius, J. Divalent Cation Induced Fusion and Lipid Lateral Segregation in Phosphatidylcholine-Phosphatidic Acid Vesicles. Biochemistry. 25(22). 6978-6987 (1986).
48. Macdonald, M. P., and Seelig, J. Anion Binding to Neutral and Positively Charged Lipid Membranes. *Biochemistry*. **27**. 6769-6775 (1988).
49. Maguire, M. E. and Cowan, J. A. Magnesium in chemistry and biochemistry. BioMetals. 15. 203-210 (2002).
50. Majhi, P. R., Ganta, R. R., Vanam, R. P., Seyrek, E., Giger, K. and Dubin, P. L. Electrostatically Driven Protein Aggregation: β-Lactoglobulin at Low Ionic Strength. *Langmuir*. 1-10 (2006).
51. Makino, K., Yamada, T., Kimura, M., Oka, T., Ohshima, H. and Kondo, T. Temperature and ionic strength-induced conformational changes in the lipid head group region of liposomes as suggested by zeta potential data. *Biophysical Chemistry*. **41.** 175-183 (1991).
52. Manning, G. S. Limiting Laws and Counterion Condensation in Polyelectrolyte Solutions I. Colligative Properties. *The Journal of Chemical Physics*. **51(3).** 924-933 (1969).
53. Manning G. S. Counterion Condensation on Charged Spheres, Cylinders, and Planes. J. Phys. Chem. B **111**. 8554-8559 (2007).
54. Marassi, F. M. and Macdonald, P. M. Response of the Phosphatidylcholine Headgroup to Membrane Surface Charge in Ternery Mixtures of Neutral, Cationic and Anionic Lipids: A Deuterium NMR Study. *Biochemistry*. **31.** 10031-10036 (1992).
55. Masrh, D. Handbook of Lipid Bilayers: Second Edition. *CRC Press*. 1990.
56. Martin-Molina, A., Rodriguez-Beas, C. and Faraudo, J. Effect of Calcium and Magnesium on Phosphatidylserine Membranes: Experiments and All-Atomic Simulations. *Biophysical Journal*. **102**. 2095-2013 (2012).
57. May, C. (2007) *Valence and Structure Relationships in Oligonucleotides.* PhD Dissertation. University of New Hampshire (2007).

58. McLaughlin, A., Grathworth, C. and McLaughlin, S. The Adsorption of Divalent Cations to Phosphatidylcholine Bilayer Membranes. *Biochimica et Biophysica Acta.* **513.** 338-357 (1978).
59. McLaughlin, C. A., Lau L.Y. A, Macdonald C. R. and McLaughlin, G.A. S. The Adsorption of Alkaline Earth Cations to Phosphatidyl Choline Bilayer Membranes: A Unique Effect of Calcium. *Bioelectrochemistry: Ions, Surfaces, Membranes*. **Chapter 3**. 49-56 (1980).
60. McLaughlin, S., Wang, J., Gambhir, A. and Murray, D. PIP_2 and Proteins: Interactions, Organization, and Information Flow. *Annu. Rev. Biophys. Biomol. Struct.* **31.** 151-175 (2002)
61. Merolli, A. and Satin, M. Role of Phosphatidyl-Serine in Bone Repair and Its Technological Exploitation. *Molecules.* **14.** 5367-5381 (2009).
62. Moody, T. P. and Shepard, H. K. Nonequilibrium thermodynamics of membrane-confined electrophoresis. *Biophys Chem*. **108**. 51-76 (2004).
63. Moody, T. P., Kingsbury, J. S., Durant, J. A., Wilson, T. J., Chase, S. F. and Laue, T. M. Valence and anion binding of bovine ribonuclease A between pH 6 and 8. *Anal. Biochem.* **336**, 243-252 (2005).
64. Morfin, I., Horkey, F., Basser, J. P., Bley, F., Hecht, A., Rochas, C. and Geissler, E. Adsorption of Divalent Cations on DNA. *Biophysical Journal*. **87(4)**. 2897-2904 (2004).
65. Nath, A., Atkins, W. M. and Sligar, S. G. Applications of Phospholipid Bilayer Nanodiscs in the Study of Membranes and Membrane Proteins. *Biochemistry.* **46(8).** 2059-2069 (2007).
66. Newton, A. Regulation of Conventional and Novel Protein Kinase C Isozymes by Phosphorylation and Lipids: Chapter 2. *Current Cancer Research*. (2010).
67. Nir, S., Duzgunes N. and Bentz, J. Binding of monovalent cations to phosphatidylserine and modulation of Ca^{2+} and Mg^{2+} induced vesicle fusion. *Biochim. Biophys. Acta*. **735**. 160–172 (1983).
68. Onaka, T., Miyajima, T. and Ohashi, S. On the binding of magnesium to long-chain polyphosphate ions. *Journal of Inorganic and Nuclear Chemistry*. **43(12)**. 3323-3327 (1981).
69. Ohnishi, T. Properties of Double-Stranded DNA as a Polyelectrolyte. *Biophysical Journal*. **3.** 459-468 (1963).
70. O'Shaughnessy, B. and Yang, Q. Manning-Oosawa Counterion Condensation. *PRL*. **94,** 048302-1-048302-4 (2005).
71. Owen, R. L., Strasters, J. K. and Breyer, E. D. Lipid vesicles in capillary electrphoretic techniques: Characterization of structural properties and associated membrane-molecule interactions. *Electrophoresis*. **26.** 735-751 (2005).
72. Papahadjopoulos, D., Nir, S. and Duzgunes, N. Molecular mechanisms of calcium-induced membrane fusion. Journal of Bioenenergetics and Biomembranes. 22(2). 157-179 (1990).
73. Philo, J.S. A method for directly fitting the time derivative of sedimentation velocity data and an alternative algorithm for calculating sedimentation coefficient distribution functions. *Analytical Biochemistry*. **279**. 151-163 (2000).
74. Pincet, F., Cribier, S. and Perez, E. Bilayers of neutral lipids bear a small but significant charge. *The European Physical Journal B.* **11.** 127-130 (1999).
75. Porter, R. K. and Brand, M. D. Mitochondrial proton conductance and H+/O ratio are independent of electron transport rate in isolated hepatocytes. Biochem J. 310(2). 379-382 (1995).
76. Record, M. T., Jr, Anderson C. F., Lohman, T. M. Thermodynamic analysis of ion effects on the binding and conformational equilibria of proteins and nucleic acids: the roles of ion association or release, screening, and ion effects on water activity. *Q Rev Biophys.* **11(2**):103–178. (1978).

77. Ridgeway, T. M., Hayes, D. B., Moody, T. P., Wilson, T. J., Anderson, A. L., Levasseur, J. H., Demaine, P. D., Kenty, B. E. and Laue, T. M.. An apparatus for membrane-confined electrophoresis. *Electrophoresis.* **19**, 1611-1619 (1998).
78. Ritchie, T. K., Grinkova, Y. V., Bayburt, T. H., Denisov, I. G., Zolnerciks, J. K., Atkins, W. M. and Sligar, S. G.. Reconstitution of Membrane Proteins in Phospholipid Bilayer Nanodiscs. *Methods in Enzymology*.**464**, 211-231 (2009).
79. Roux, M., and Bloom, M. Ca^{2+}, Mg^{2+}, Li^{+}, Na^{+}, and K^{+} distributions in the headgroup region of binary membranes of phosphatidylcholine and phosphatidylserine as seen by deuterium NMR. *Biochemistry*. **29**. 7077–7089 (1990).
80. Roy, M. T., Gallardo, M. and Estelrich, J. Influence of Size on Electrokinetic Behavior of Phosphatidylserine and Phosphatidylethanolamine Lipid Vesicles. *Journal of Colloid and Interface Science*. **206**. 512-517 (1998).
81. Rydall, R. J., Macdonald, M. P. Investigation of Anion Binding to Neutral Lipid Membranes using ^{2}H NMR. *Biochemistry*. **31**. 1092-1099 (1992).
82. Saiz, L. and Klein, M. L. Electrostatic interactions in a neutral model phospholipid bilayer by molecular dynamics simulations. *Journal of Chemical Physics.* **116(7).** 3052-3057 (2002).
83. Serhan, C. N., Broekman, M. J., Korchak, H. M., Smolen, J. E., Marcus, A. J. and Weissman, G. Changes in phosphatidylinositol and phosphatidic acid in stimulated human neutrophils. Relationship to calcium mobilization, aggregation and superoxide radical generation. *Biochim Biophys Acta*. **762(3).** 420-428 (1983).
84. Scherer, P. G. and Seelig, J. Electric Charge Effects on Phospholipid Headgroups. Phosphatidylcholine in Mixtures with Cationic and Anionic Amphiphiles. *Biochemistry.* **28.** 7720-7728 (1989).
85. Schuck, P. Size distribution analysis of macromolecules by sedimentation velocity ultracentrifugation and Lamm equation modeling. *Biophysical Journal.* **78**:1606-1619 (2000).
86. Schultz, Z. D., Pazos, I. M., McNeil-Watson, F. K., Lewis, E. N. and Levin, I.W. Magnesium-induced lipid bilayer microdomain organizations: Implications for membrane fusion. J. Phys. Chem. B. 113(29). 9932-9941 (2009).
87. Schwartz, H. and Guttman, A. Separation of DNA by Capillary Electrophoresis Volume VII. *Beckman Coulter* (1995).
88. Serhan, C. N., Broekman, M. J., Korchak, H. M., Smolen, J. E., Marcus, A. J. and Weissman, G. Changes in phosphatidylinositol and phosphatidic acid in stimulated human neutrophils. Relationship to calcium, mobilization, aggregation and superoxide radical generation. *Biochim Biophys Acta*. **762(3).**
89. Smetjtek, P., Satterfield, E. L., Word, C. R. and Abramson, J.J. Electrophoretic mobility of sarcoplasmic reticulum vesicles is determined by amino acids of A + P + N domains of Ca^{2+} -ATPase. *Biochimica et Biophysica Acta*. **1798**. 1689-1697 (2010).
90. Srinivasan, C., Minadeo, N., Geraldes, F. G. C. ad Mota de Freitas, D. Competition between Li^{+} and Mg^{2+} for red blood cell membrane phospholipids. A ^{31}P, ^{78}Li and ^{6}Li nuclear magnetic resonance study. *Lipids.* **34(11).** 1211-1221 (1999).
91. Stafford, W. F. Analytical Ultracentrifugation: Sedimentation Velocity Analysis *Current Protocols in Protein Science*, **20.7**, 1-11 (2003).
92. Strobel, H. W., Lu A. Y., Heidema, J and Coon, M. J. Phosphatidylcholine requirement in the enzymatic reduction of hemoprotein P-450 and in fatty acid, hydrocarbon, and drug hydroxylation. *J Biol Chem.* **245(18).** 4851-4 (1970).
93. Takahashi, A., Camacho, P., Lechleiter, D. J. and Herman, B. Measurement of Intracellular Calcium. *American Physiological Society: Physiological Reviews*. **(79)4.** 1089-1125 (1999).

94. Tatulian A. S. Effects of Lipid Phase Transition on the Binding of Anions to Dimyristoylphosphatidylcholine Liposomes. *Biochimica et Biophysica Acta*. **736**. 189-195 (1983).
95. Tatulian, A. S. Binding of alkaline-earth metal cations and some anions to phosphatidylcholine liposomes. *European Journal of Biochemistry*. **170**. 413-120 (1987).
96. Tavoosi, N., Davis-Harrison, R. L., Pogorelov, T. V., Ohkubo, Y. Z., Arcario, M. J., Clay, M. C., Rienstra, C. M., Tajkhorshid, E and Morrisey, J. H. Molecular Determinants of Phospholipid Synergy in Blood Clotting. *Journal of Biological Chemistry*. **286(26).** 23247-23253 (2011).
97. Thomas, S., Kumar, R. S. and Brumeanu, T. D. Role of lipid rafts in T cells. *Arch. Immunol. Ther. Exp.* **52.** 215-225 (2004).
98. Tsui, F.C., Ojcius, D.M., Hubbell, W.L. The intrinsic pKa values for phosphatidylserine and phosphatidylethanolamine in phosphatidylcholine host bilayers. Biophys J. **49**. 459-68 (1986).
99. van Meer, G., Voelker, D. R. and Feigenson, G. W. Membrane lipids: where they are and how they behave. *Nat. Rev. Mol. Cell Biol.* **9(2)**. 112-124 (2008).
100. van Paridon P. A., De Kruijff, B., Ouwerker, R. and Wirtz, K. W. Polyphosphoinositides undergo charge neutralization in the physiological pH range: A 31P-NMR study. *Biohim. Biophys. Acta*. **877.** 216-219 (1986).
101. Vernier, P. T., Ziegler, M. J. and Dimoa, R. Calcium Binding and Head Group Dipole Angle in Phosphatidylserine--Phosphatidylcholine Bilayers. *Langmuir*. **25.** 1020-1027 (2009).
102. Wang, Y., Collins, A., Guo, L., Smith-Dupont, K. B., Gai, F., Svitkina, T. and Janmey, P. A. Divalent cation-induced cluster formation by polyphosphoinositides in model membranes. J. Am. Chem. Soc. 134(7). 3387-3395 (2012).
103. Wilson, D. I. and Poole, C. Methods and Instrumentation in Separation Science: Volume I. *Academic Press: A Harcour Science and Technology Company*. 2000.
104. Wohlert, J. and Edholm, O. The Range and Shielding of Dipole-Dipole Interactions in Phospholipid Bilayers. *Biophysical Journal*. **87.** 2433-2445 (2004).
105. Woodle, M. C., Collins, L. R., Sponsler, E., Kossovsky, N., Papahadjopoulos, D. and Martin, F. J. Sterically stabilized liposomes: Reduction in electrophoretic mobility but not electrostatic surface potential. *Biophysical Journal*. **61.** 902-910 (1992)
106. Wooll, J. (1996) *Investigation of $Pd(A)_{20}$ $Pd(T)_{20}$ in the Analytical Electrophoresis Apparatus.* PhD Dissertation. University of New Hampshire (1996).
107. Yague-Sanchez, J. and Llanillo, M. Lipid composition of subcellular particles from sheep platelets. Location of phosphatidylethanolamine and phosphatidylserine in plasma membranes and platelet liposomes. *Biochim. Biophys. Acta*. **856(2)**. 193-201 (1986).
108. Yeagle, P.L. The Membranes of Cells: 2nd Edition. San Diego Academic Press. 1993.
109. Zimm, B. H. and Le Bret, M. Counter-Ion Condensation and System Dimensionality. *Journal of Biomolecular Structure and Dynamics*. **1**. 461-471 (1983).

APPENDICES

APPENDIX A

SUPPLEMENTARY AUC DATA OF NANODISCS

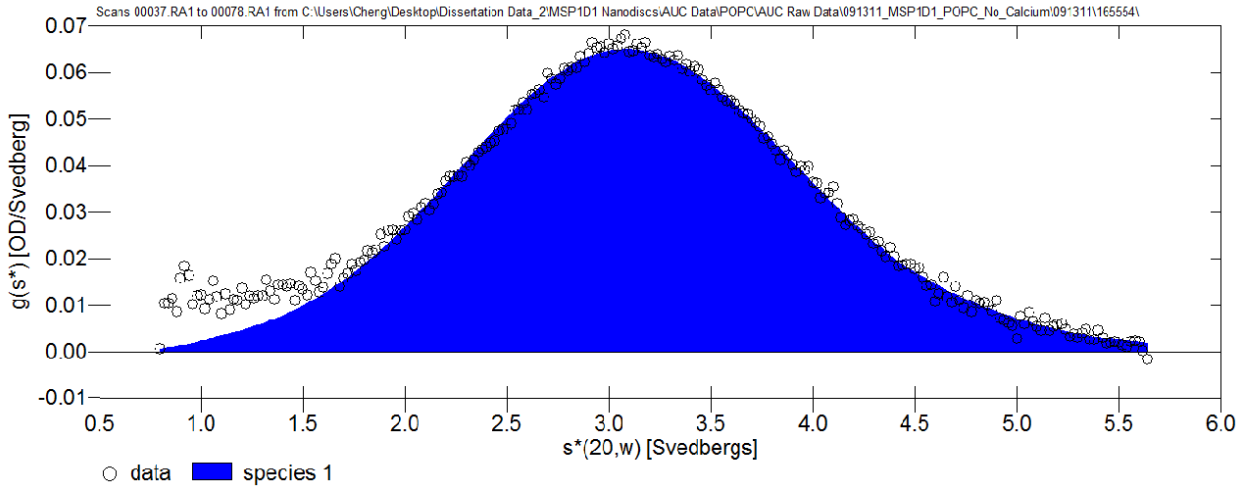

Figure A1 Sedimentation velocity data of POPC Nanodiscs in standard buffer at pH 7.4 using DC/DT+ [Philo, 2000].

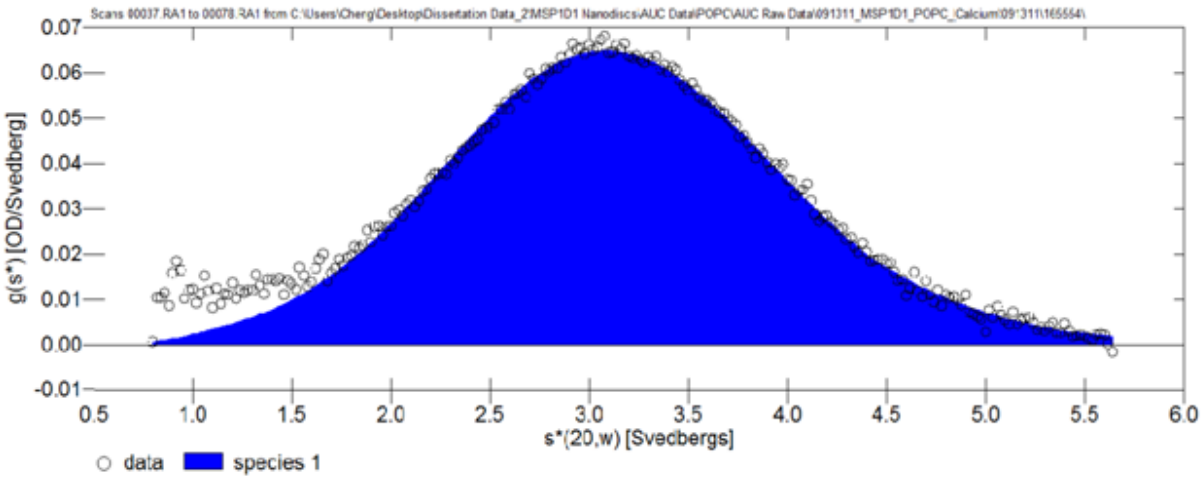

Figure A2 Sedimentation velocity data of POPC Nanodiscs in the presence of 3 mM $CaCl_2$ using DC/DT+ [Philo, 2000].

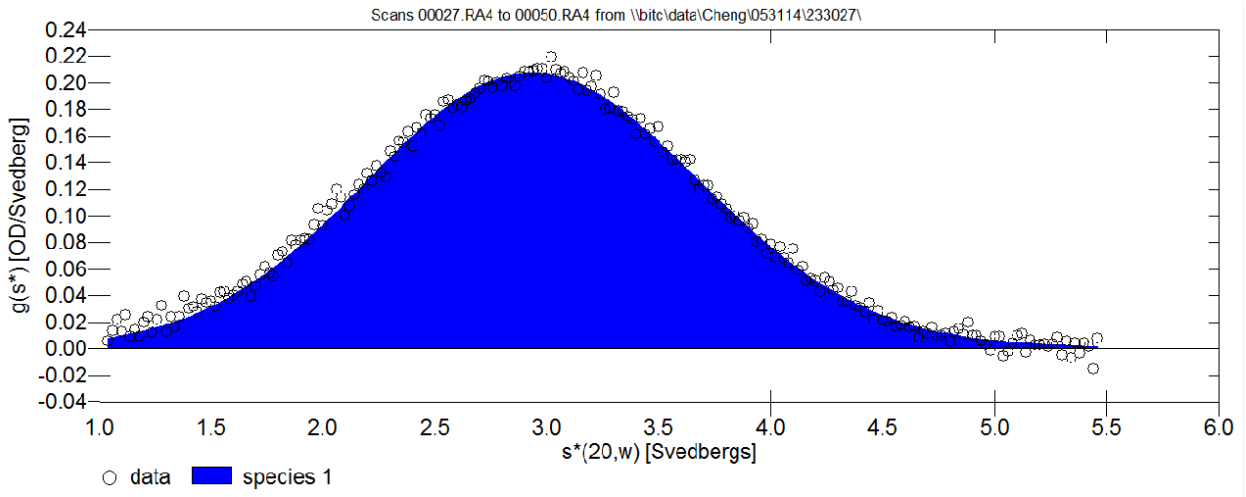

FigureA3 Sedimentation velocity data of 10POPE Nanodiscs in standard buffer at pH 7.4 using DC/DT+ [Philo, 2000].

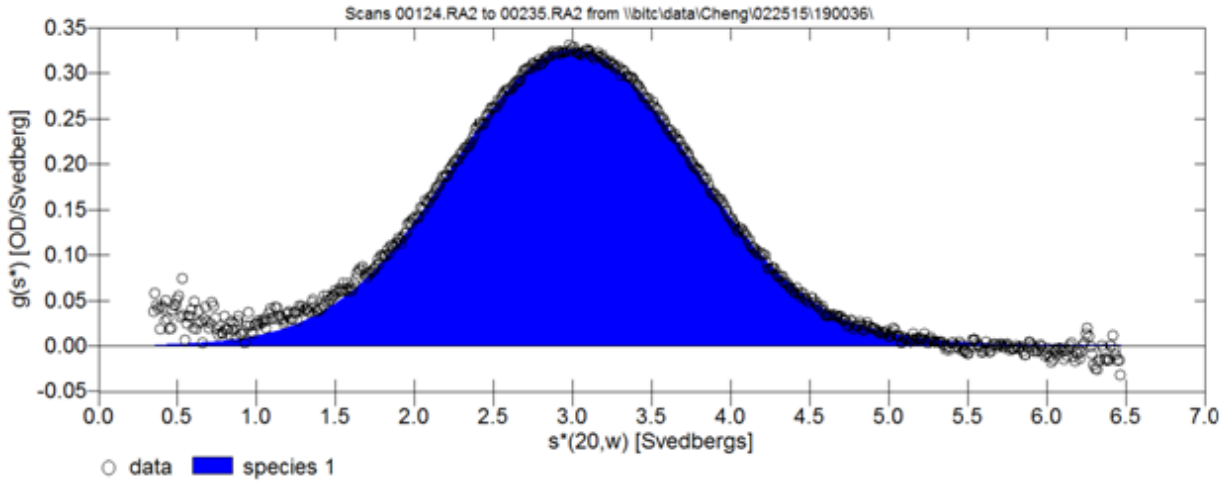

Figure A4 Sedimentation velocity data of 10POPE Nanodiscs in standard buffer at pH 7.0 using DC/DT+ [Philo, 2000].

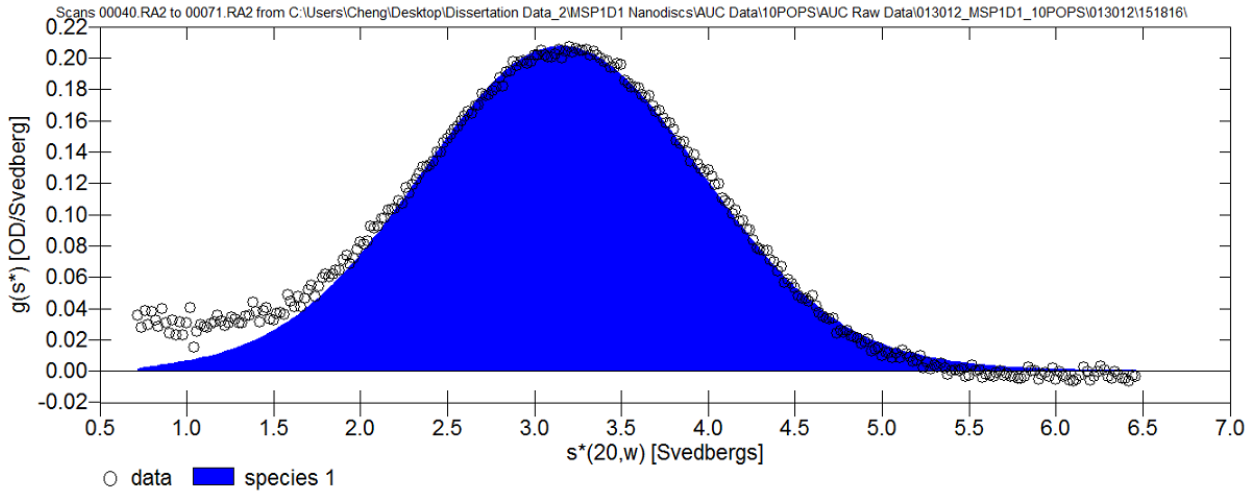

Figure A5 Sedimentation velocity data of 10POPS Nanodiscs in standard buffer at pH 7.4 using DC/DT+ [Philo, 2000].

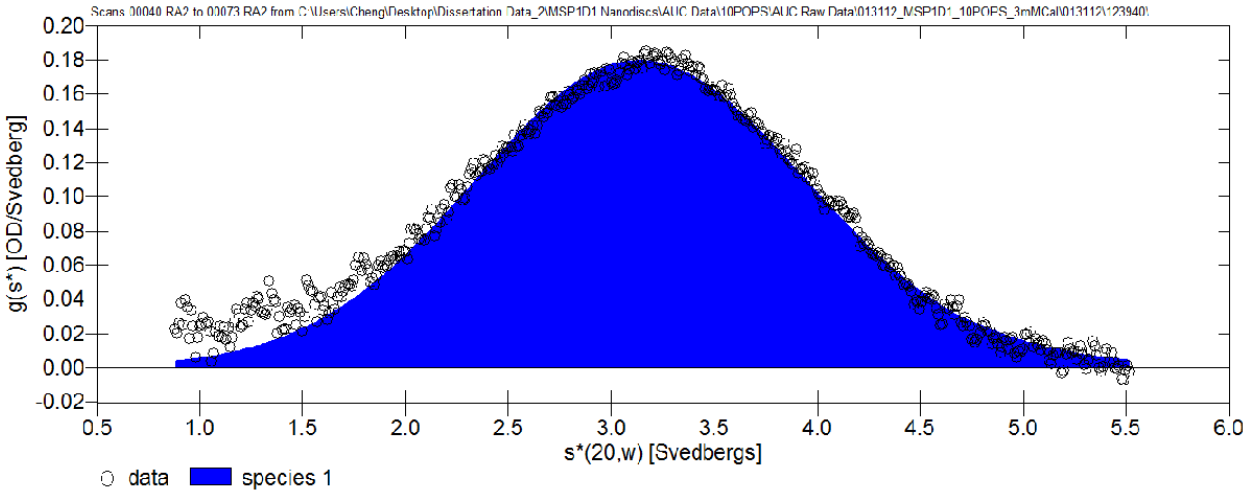

Figure A6 Sedimentation velocity data of 10POPS Nanodiscs in the presence of 3 mM $CaCl_2$ at pH 7.4 using DC/DT+ [Philo, 2000].

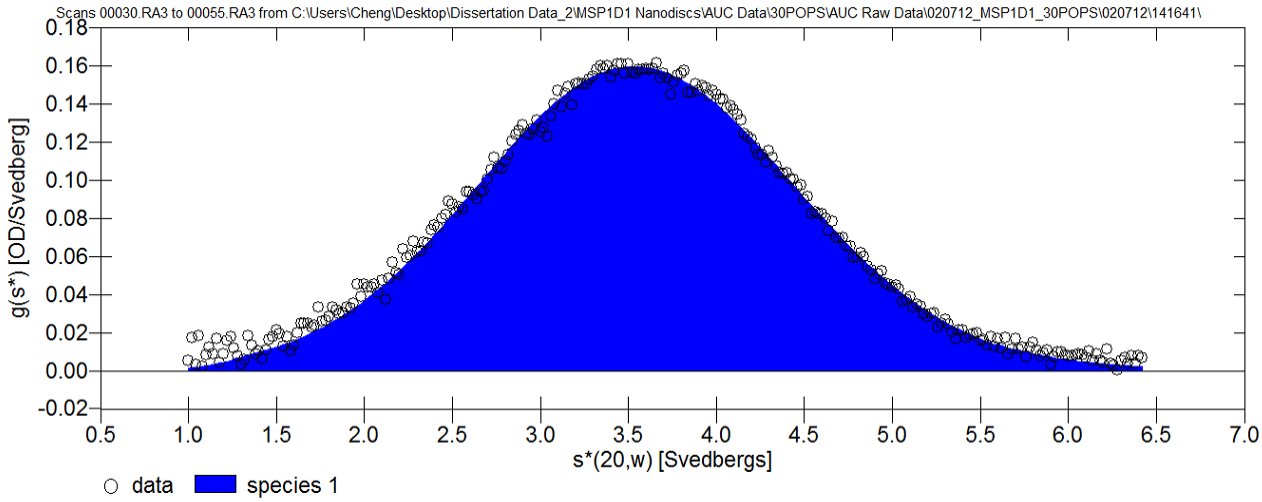

Figure A7 Sedimentation velocity data of 30POPS Nanodiscs in standard buffer at pH 7.4 using DC/DT+ [Philo, 2000].

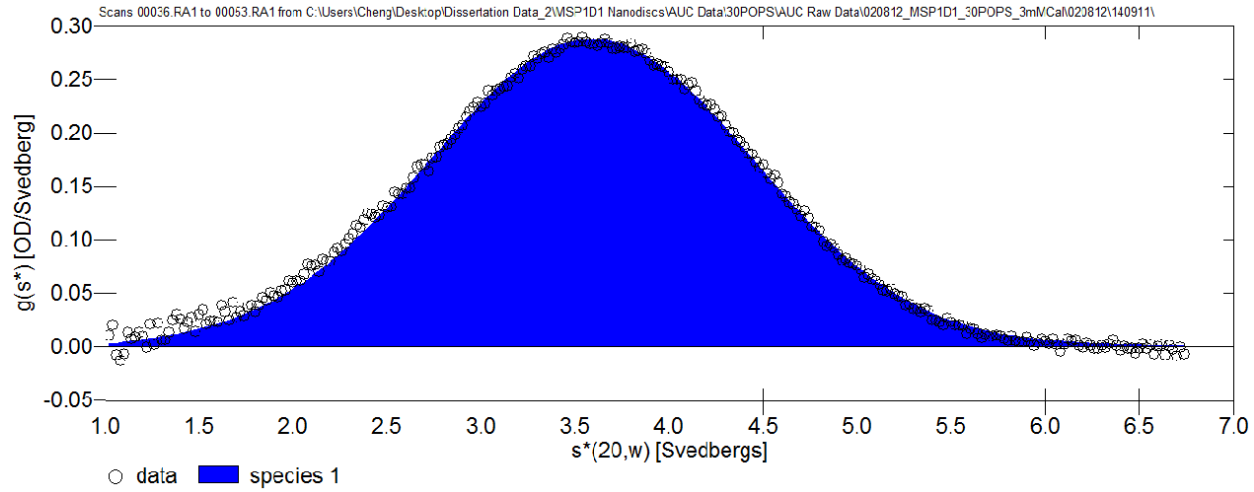

Figure A8 Sedimentation velocity data of 30POPS Nanodiscs in the presence of 3 mM $CaCl_2$ at pH 7.4 using DC/DT+ [Philo, 2000].

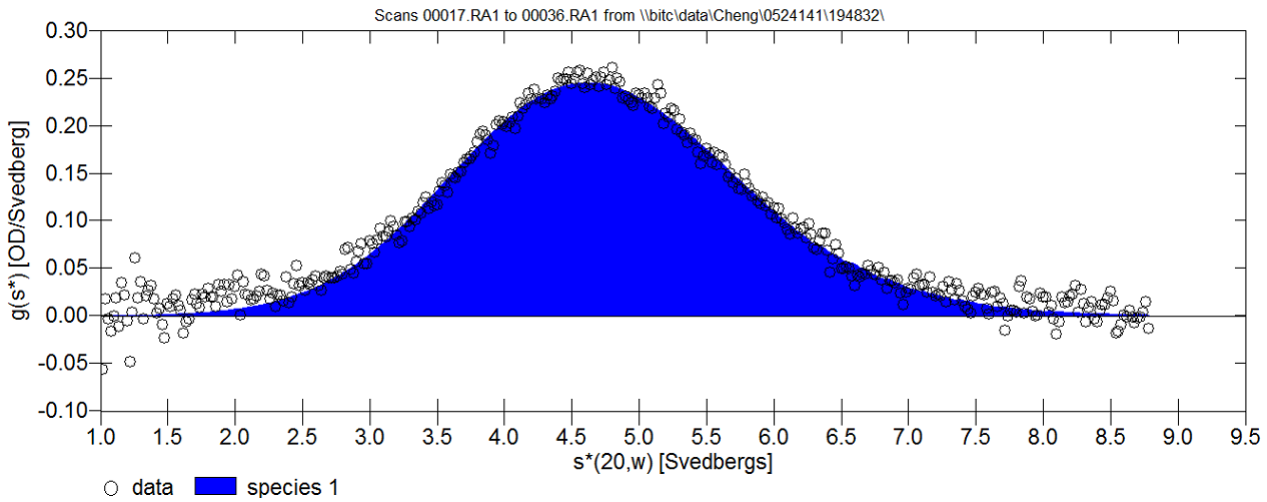

Figure A9 Sedimentation velocity data of 70POPS Nanodiscs in standard buffer at pH 7.4 using DC/DT+ [Philo, 2000].

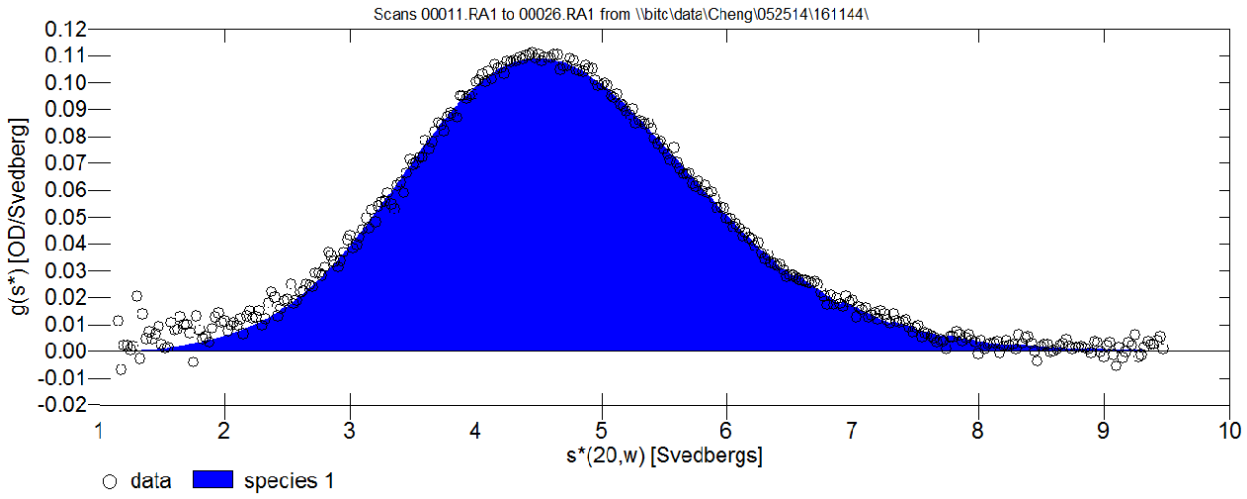

Figure A10 Sedimentation velocity data of 70POPS Nanodiscs in the presence of 3 mM $CaCl_2$ at pH 7.4 using DC/DT+ [Philo, 2000].

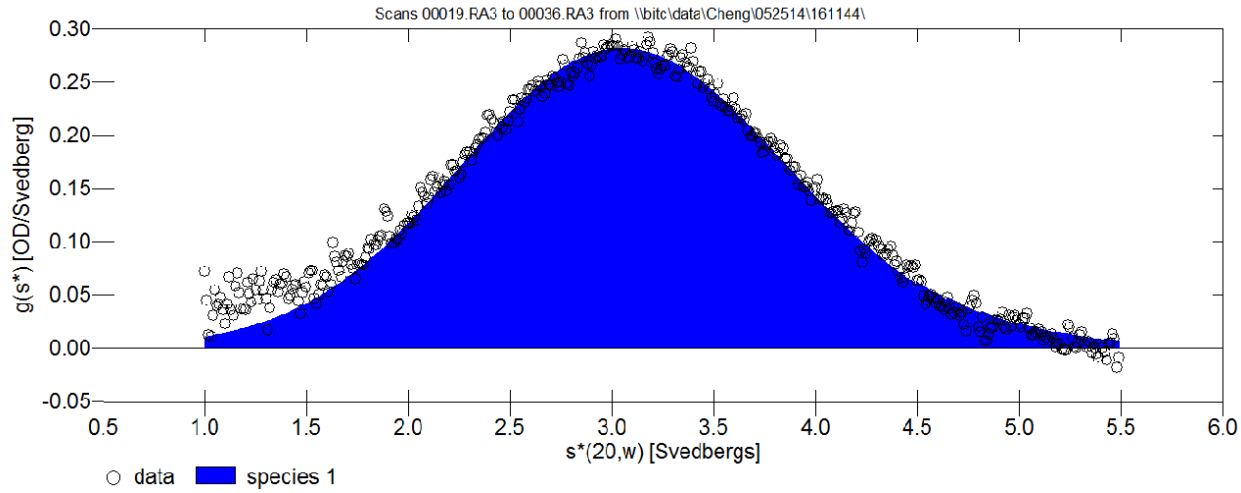

Figure A11 Sedimentation velocity data of 10POPA Nanodiscs in standard buffer at pH 7.4 using DC/DT+ [Philo, 2000].

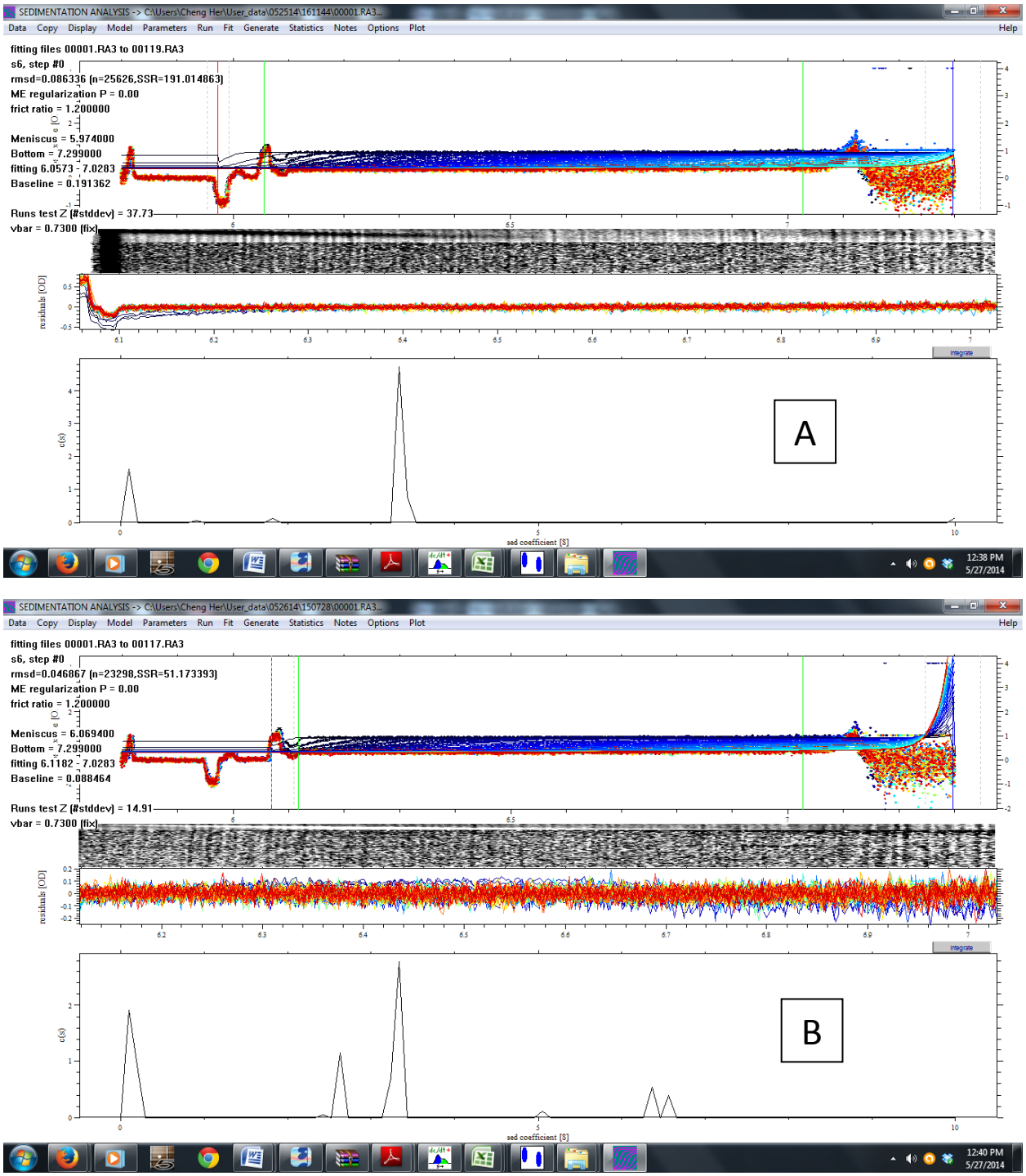

Figure A12 (a) and A12 (b) Sedimentation velocity data of MSP1D1 10POPA in the absence (a) and presence (b) of Ca^{2+}.

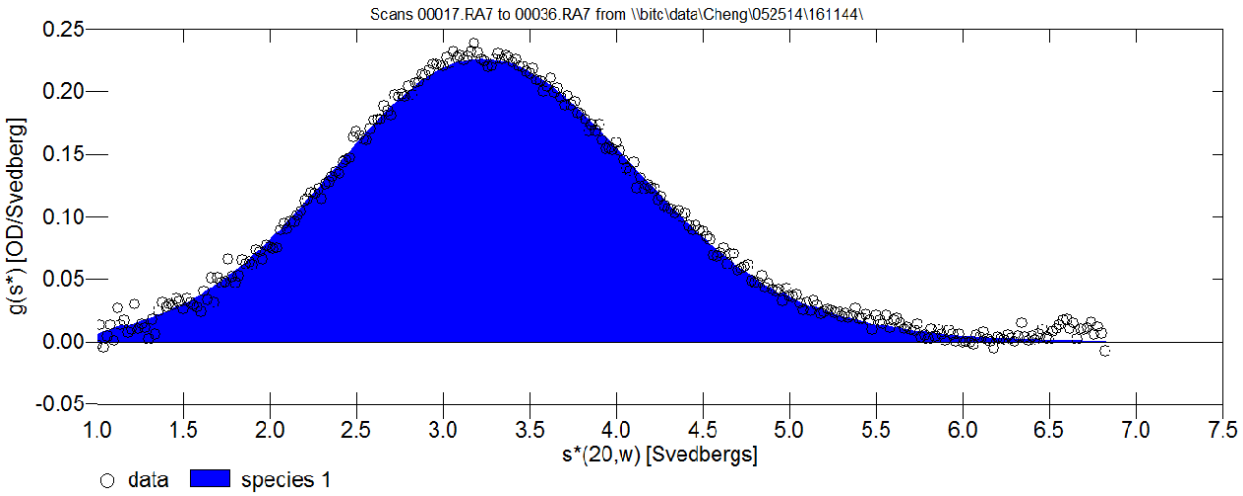

Figure A13 Sedimentation velocity data of 30POPA Nanodiscs in standard buffer at pH 7.4 using DC/DT+ [Philo, 2000].

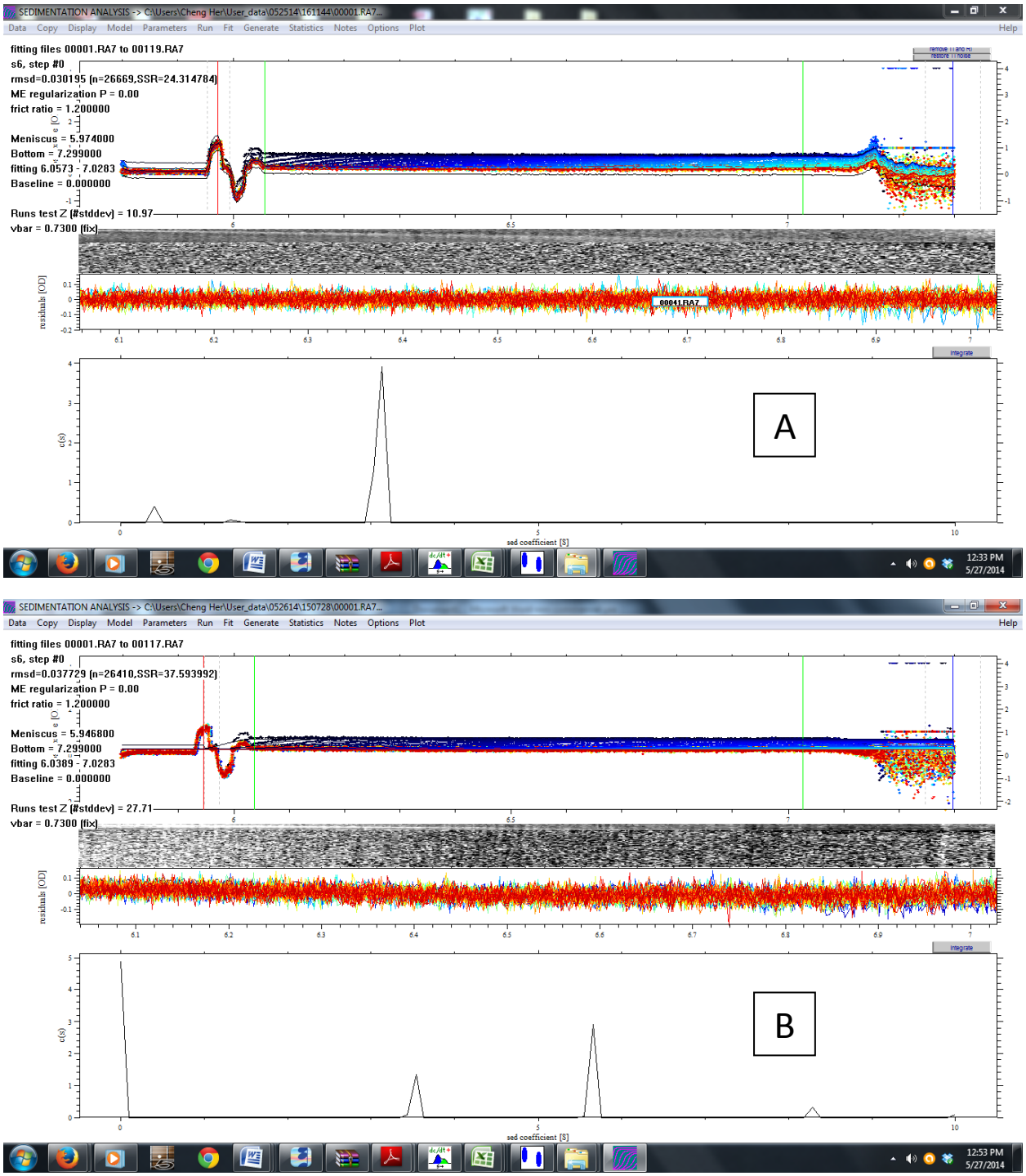

Figure A14 (a) and A14 (b) Sedimentation velocity data of MSP1D1 30POPA in the absence (a) and presence (b) of Ca^{2+}.

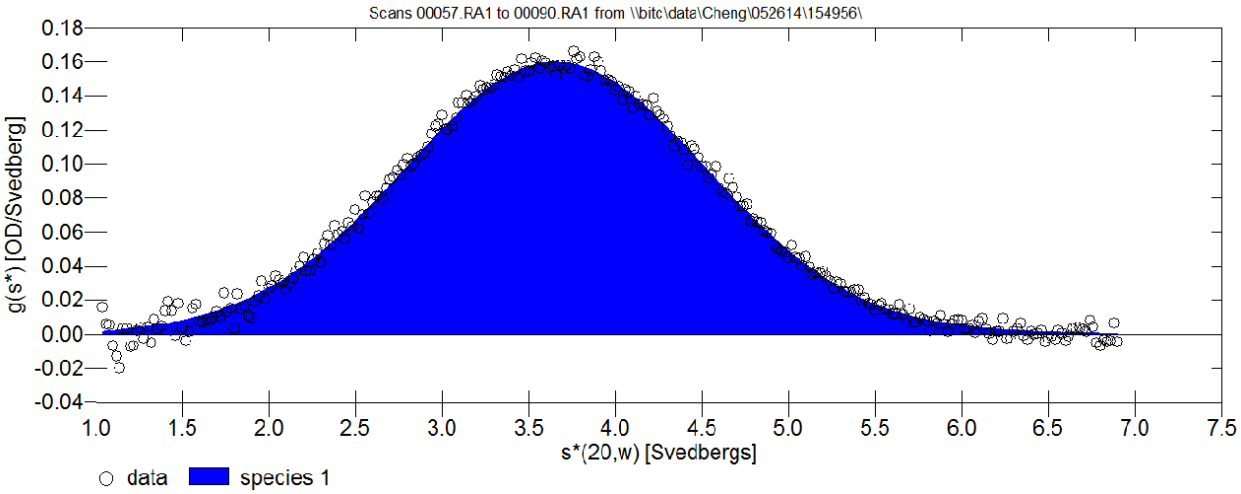

Figure A15 Sedimentation velocity data of 70POPA Nanodiscs in standard buffer at pH 7.4 using DC/DT+ [Philo, 2000].

APPENDIX B

SUPPLEMENTARY MCE DATA FOR NANODISCS

Nanodisc™ Sample	Electrophoretic Mobility ($cm^2/V \cdot s$)	Z_{DHH}	Zeta Potential (mV)
MSP1D1 POPC	$-4.2 \times 10^{-5} \pm 3.8 \times 10^{-6}$	-14.1 ± 1.0	-7.2 ± 0.2
MSP1D1 10% POPS	$-7.1 \times 10^{-5} \pm 2.9 \times 10^{-6}$	-24.6 ± 0.8	-12.3 ± 0.3
MSP1D1 30% POPS	$-1.2 \times 10^{-4} \pm 5.7 \times 10^{-6}$	-38.5 ± 1.4	-20.0 ± 0.4
MSP1D1 70% POPS	$-1.7 \times 10^{-4} \pm 3.8 \times 10^{-6}$	-56.4 ± 2.4	-29.1 ± 0.4
MSP1D1 10% POPA	$-7.5 \times 10^{-5} \pm 1.7 \times 10^{-6}$	-26.2 ± 1.7	-13.7 ± 0.7
MSP1D1 30% POPA	$-1.4 \times 10^{-4} \pm 1.6 \times 10^{-5}$	-45.0 ± 3.0	-24.1 ± 1.0
MSP1D1 70% POPA	$-2.1 \times 10^{-4} \pm 1.0 \times 10^{-5}$	-66.6 ± 4.7	-32.6 ± 1.2
MSP1D1 10% PIP_2	$1.2 \times 10^{-4} \pm 3.6 \times 10^{-6}$	-39.7 ± 1.1	-20.6 ± 0.9
MSP1D1 10% POPE	$6.5 \times 10^{-5} \pm 5.3 \times 10^{-6}$	-21.4 ± 1.5	-10.8 ± 0.7

Figure B1 The calculated zeta potentials of various Nanodiscs in standard buffer containing various phospholipid ratios by MCE. Values of electrophoretic mobility and Z_{DHH} are included for reference.

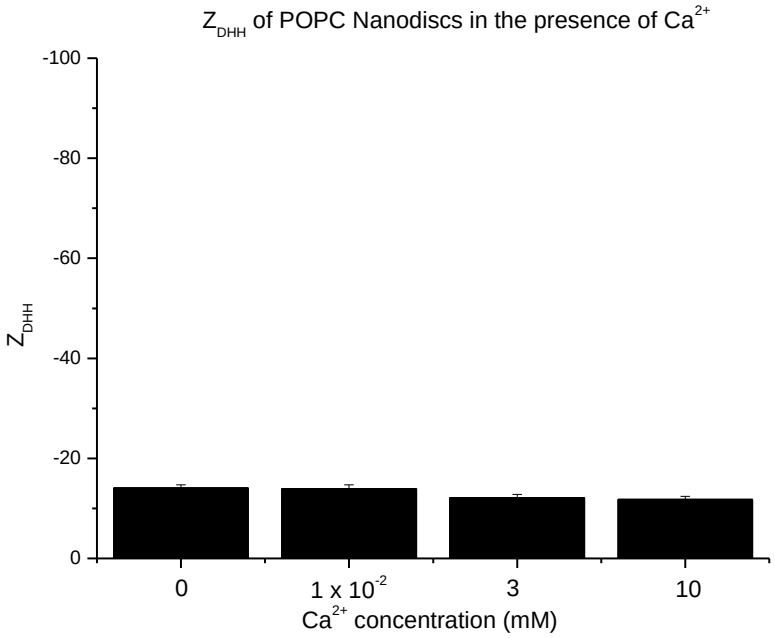

Figure B2 The Z_{DHH} of MSP1D1 POPC Nanodiscs in at varying concentrations of Ca^{2+}. The vertical bars in the figures represent the standard deviations.

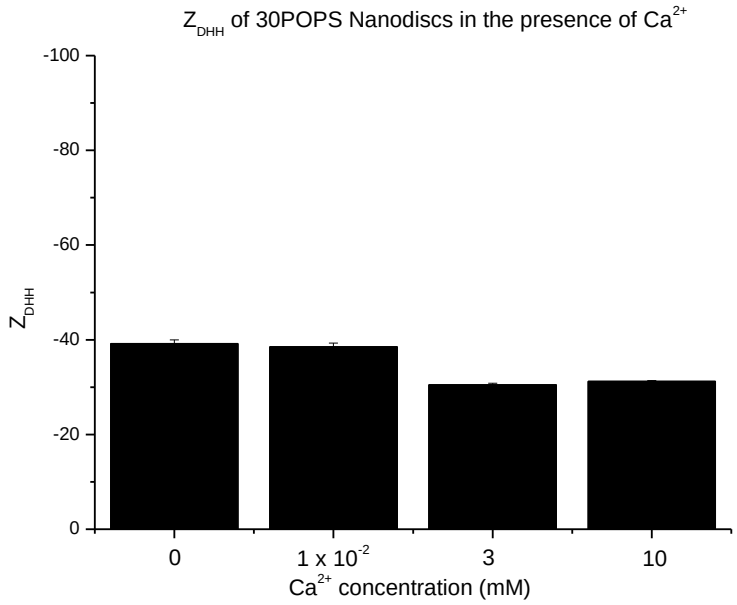

Figure B3 The Z_{DHH} of MSP1D1 30POPS Nanodiscs in at varying concentrations of Ca^{2+}. The vertical bars in the figures represent the standard deviations.

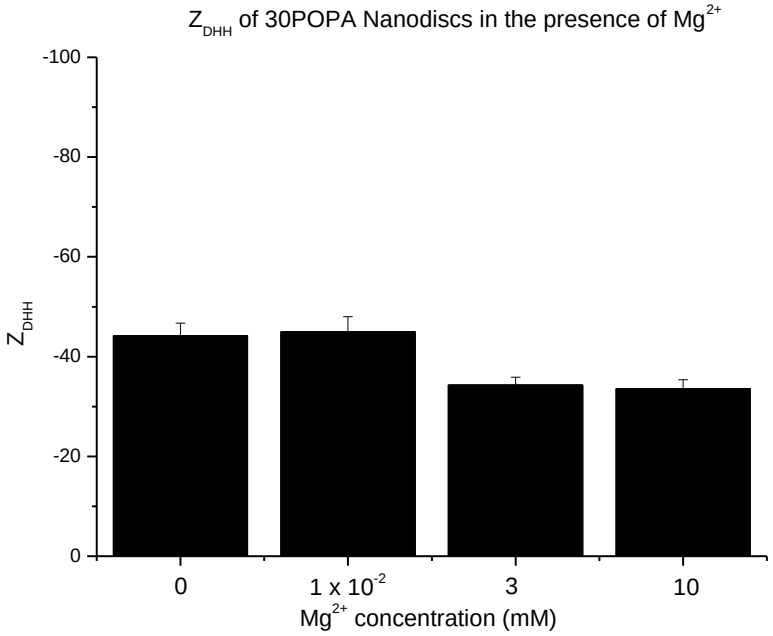

Figure B4 The Z_{DHH} of MSP1D1 30POPA Nanodiscs in at varying concentrations of Mg^{2+}. The vertical bars in the figures represent the standard deviations.

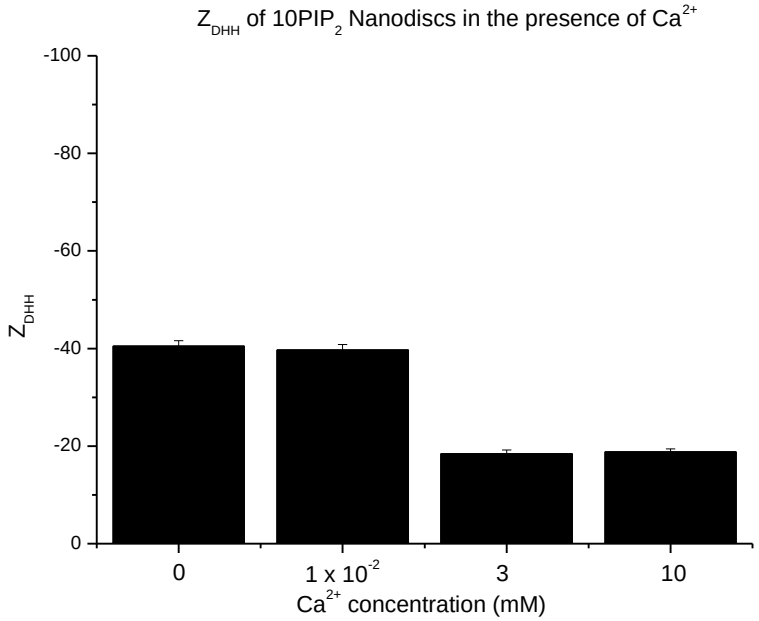

Figure B5 The Z_{DHH} of MSP1D1 10PIP_2 Nanodiscs in at varying concentrations of Ca^{2+}. The vertical bars in the figures represent the standard deviations.

APPENDIX C

TITRATION CURVES FOR PHOSPHLIPIDS

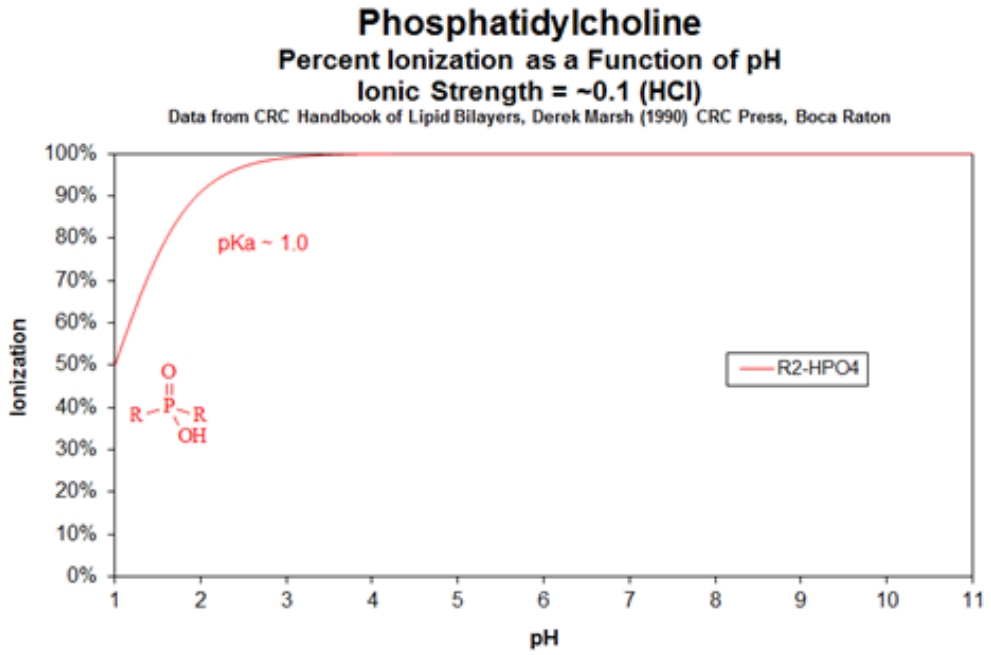

Figure C1 Titration curve of phosphatidylcholine represented as percent ionization as a function of pH [Marsh, 1990]

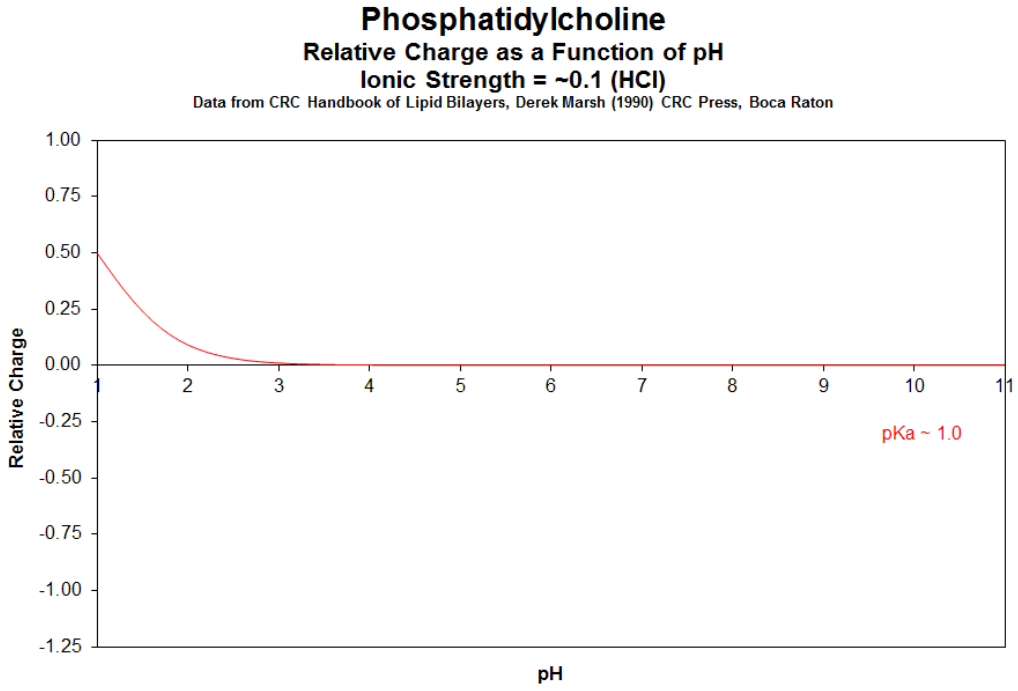

Figure C2 Titration curve of phosphatidylcholine represented as relative charge as a function of pH [Marsh, 1990].

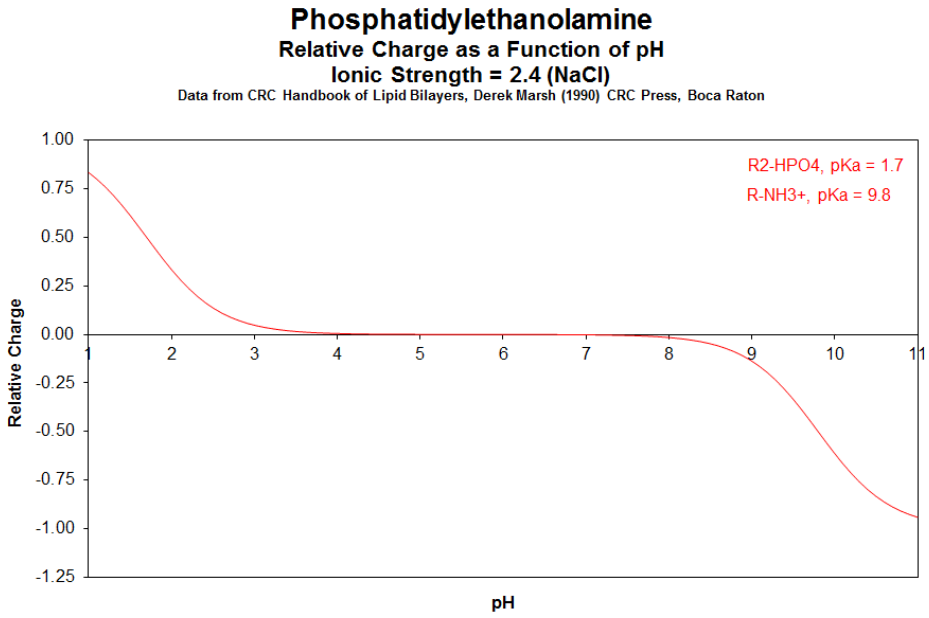

Figure C3 Titration curve of phosphatidic acid represented as relative charge as a function of pH [Marsh, 1990].

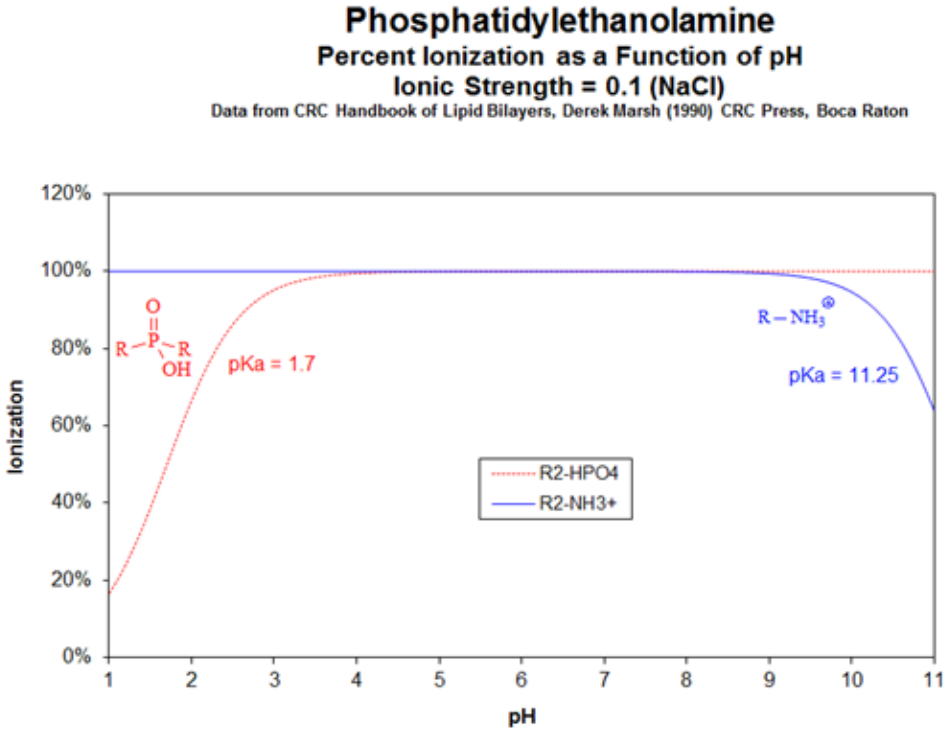

Figure C4 Titration curve of phosphatidic acid represented as percent ionization as a function of pH [Marsh, 1990].

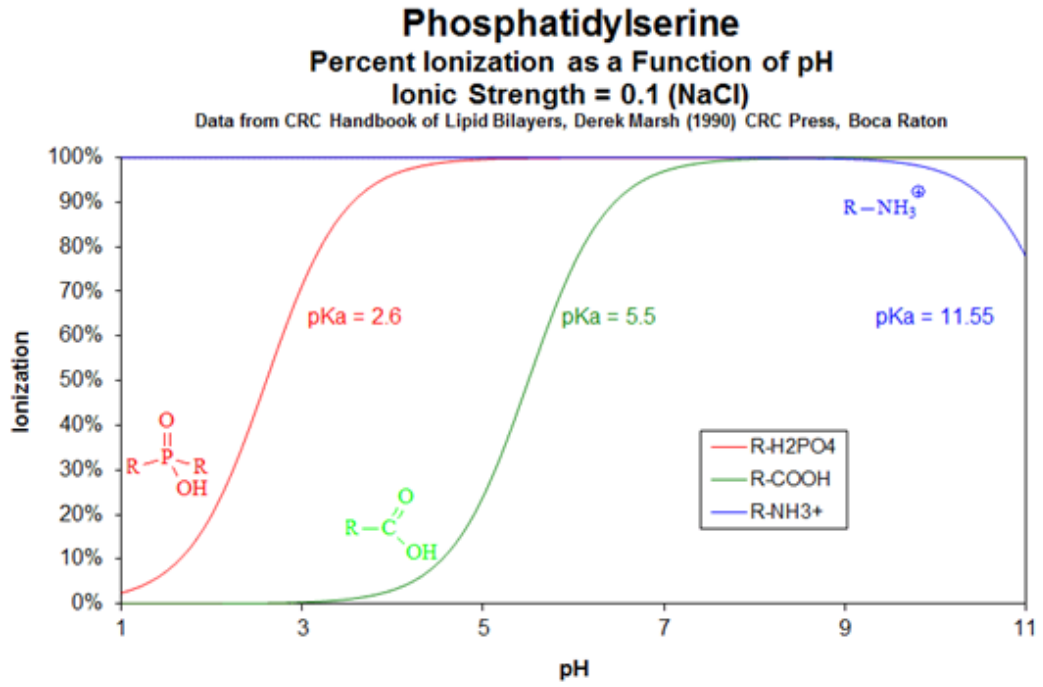

Figure C5 Titration curve of phosphatidylserine represented as percent ionization as a function of pH [Marsh, 1990].

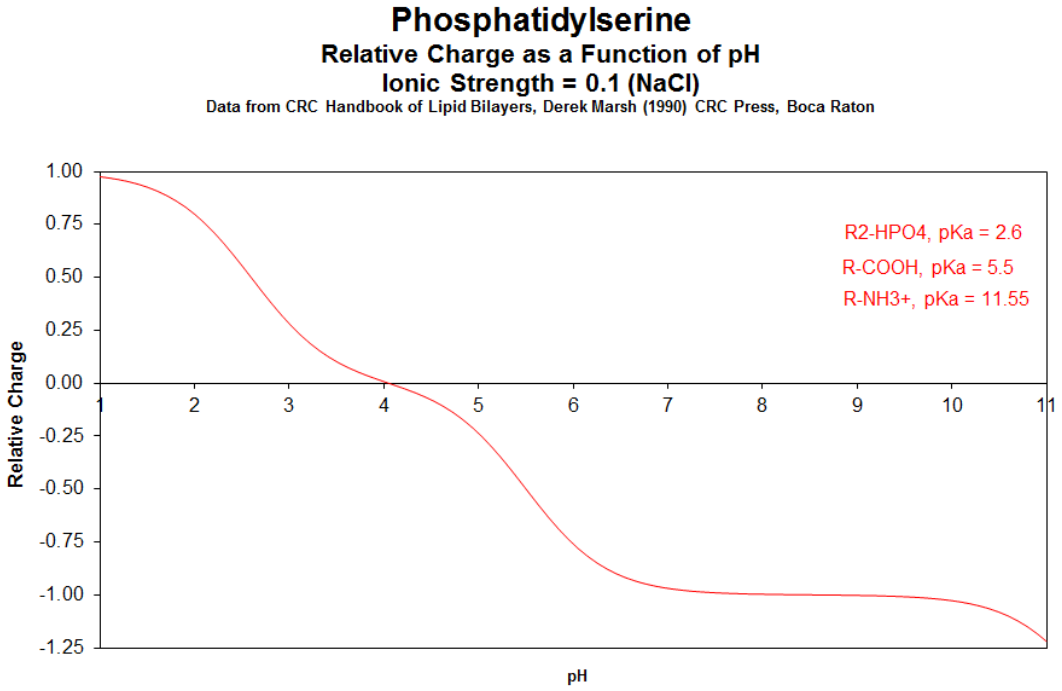

Figure C6 Titration curve of phosphatidylserine represented as relative charge as a function of pH [Marsh, 1990].

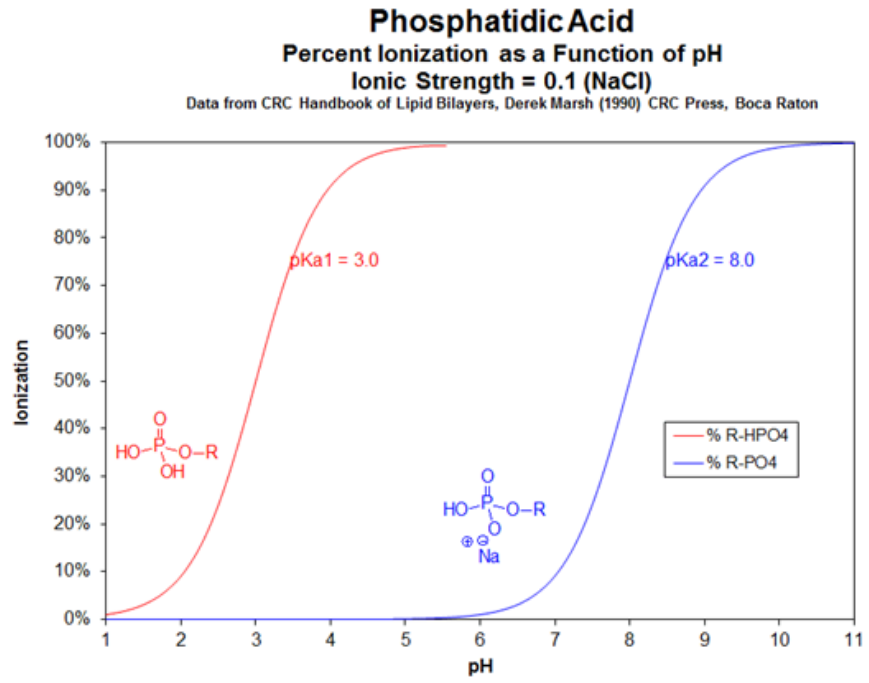

Figure C7 Titration curve of phosphatidic acid represented as percent ionization as a function of pH [Marsh, 1990].

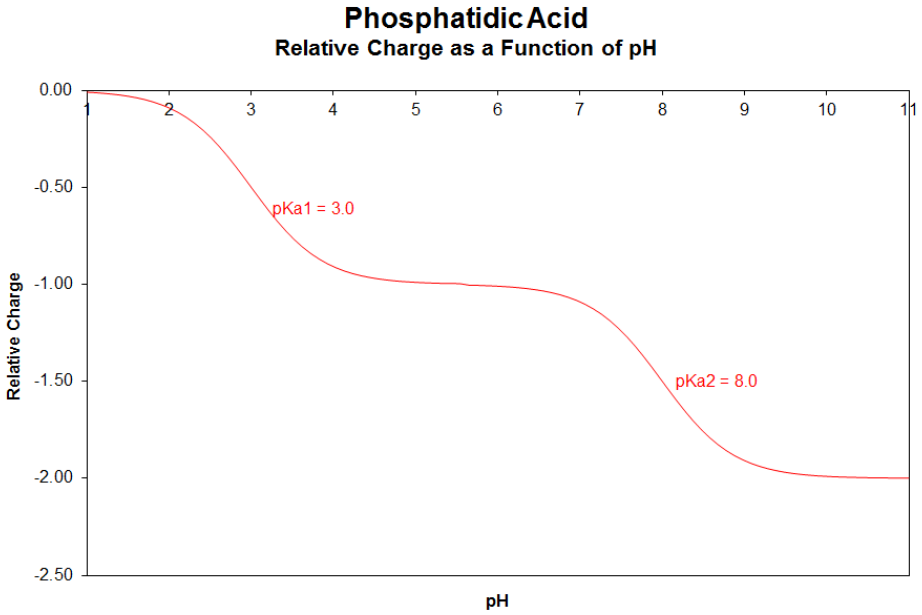

Figure C8 Titration curve of phosphatidic acid represented as relative charge as a function of pH [Marsh, 1990].

APPENDIX D

SUPPLEMENTARY DISCUSSION DATA

Nanodisc™ Sample	Lipid Charge Contribution (Z_{DHH})[a]	Calculated Charge of Lipids
MSP1D1 POPC	0	0
MSP1D1 10% POPS	-10.5	-13
MSP1D1 30% POPS	-24.4	-38
MSP1D1 70% POPS	-42.3	-88
MSP1E3D1 POPC	0	0
MSP1E3D1 10% POPS	-19.0	-25
MSP1E3D1 30% POPS	-39.2	-75
MSP1E3D1 70% POPS	-74.3	-175
MSP1D1 10% POPA	-12.1	-16
MSP1D1 30% POPA	-30.9	-47
MSP1D1 70% POPA	-52.5	-109
MSP1D1 10% PIP_2	-25.6	-38
MSP1D1 10% POPE	-7.3	-13

Table D1 The Z_{DHH} of anionic Nanodiscs assuming that the Z_{DHH} obtained using MCE for POPC Nanodiscs represents the charge contribution of the MSPs.

[a] Calculated assuming that the Z_{DHH} of POPC Nanodiscs, -14.1, is contributed entirely from the MSPs and that PC lipid contribute a Z_{DHH} of 0. The values in the table therefore, are the measured Z_{DHH} of the different lipids, with the protein contribution subtracted from that value. This Z_{DHH} values represents the charge contribution solely from the lipid head groups.

Study	PC lipid type	Charge per PC lipid
Klasczyk et al. 2010[a]	POPC	+1 per 605 PC lipids
Pincet et al. 1999	Egg PC	-1 per 600 PC lipids
McLaughlin et al. 1978	SOPC	+1 per 1100 PC lipids
Nanodiscs with MCE[b]	POPC	+1 per 63 PC lipids
Nanodiscs with MCE[c]	POPC	0 per PC lipid

Table D2 Comparison of calculated charge per PC lipids across different studies.

[a] Not provided by the authors. Calculated separately based on reported liposome diameter of 56.4 nm [Klasczyk et al. 2010] and assumed area of 66 A^2 for POPC lipids [Bayburt and Sligar, 2012]

[b] Assumes that PC lipids in POPC Nanodiscs contribute a +2 charge

[c] Assumes that PC lipids in POPC Nanodiscs contribute a charge of 0

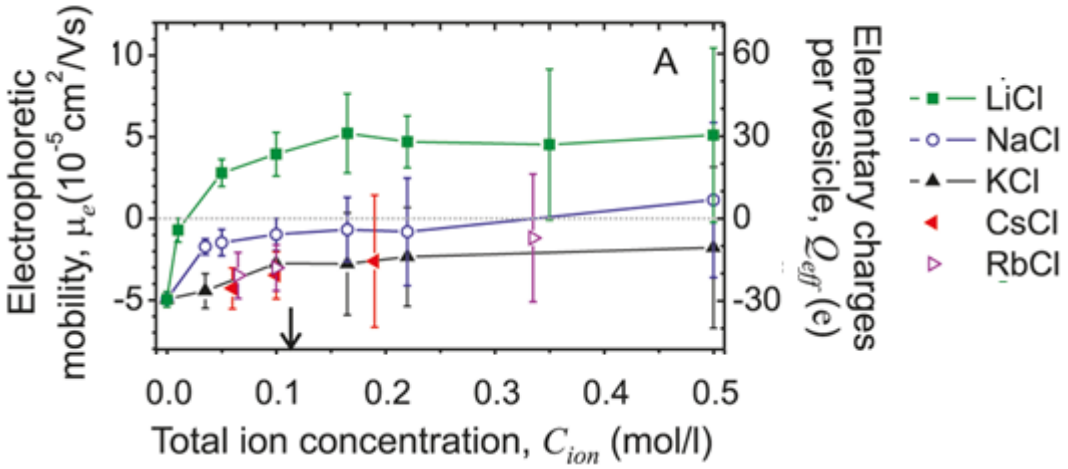

Figure D1 Electrophoretic mobility data on POPC liposomes in the presence of different monovalent cations by Klasczyk et al. (2010) using electrophoretic light scattering.

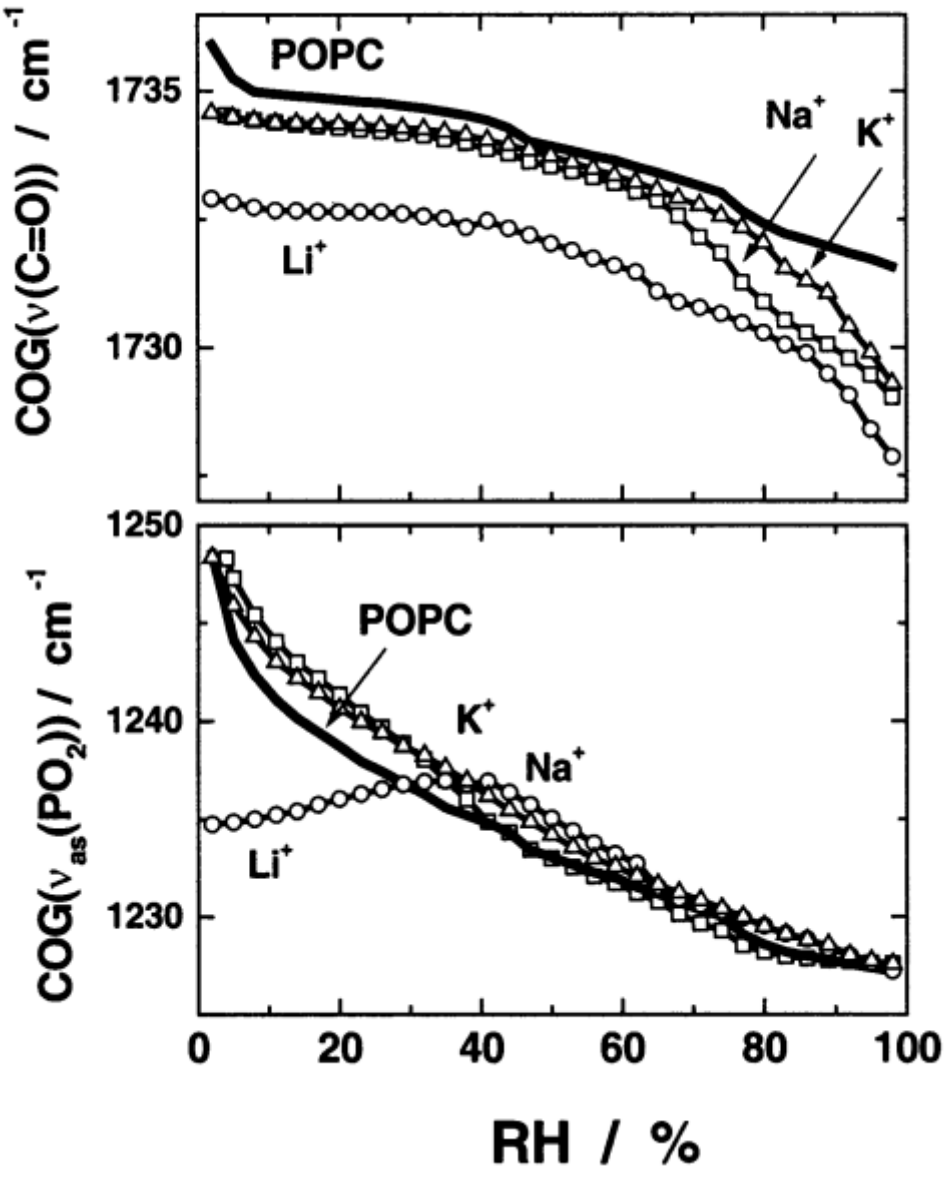

Figure D2 Center of gravity IR spectra of the phosphate (a) and carbonyl (b) absorption bands in the presence of the monovalent alkali cations Li^+, Na^+ and K^+ as a function of relative humidity [Binder and Zschornig, 2002].

TABLE 1 **Electrophoretic mobility and zeta potential of PEG-DSPE containing liposomes**

Lipid composition*	Electrophoretic mobility			Zeta potential		
	pH 5.2	pH 7.3	pH 9.2	pH 5.2	pH 7.3	pH 9.2
		μm-cm/V-s			*mV*	
PC	0.05 ± 0.04	0.09 ± 0.01	−0.06 ± 0.02	0.6 ± 0.2	1.3 ± 0.2	−0.8 ± 0.26
PEG:PC (1:9)	−0.54 ± 0.02			−7.0 ± 0.12		
PEG:PC (0.75:9.25)	−0.60 ± 0.03	−0.45 ± 0.04	−0.45 ± 0.03	−7.4 ± 0.5	−5.4 ± 0.4	−5.7 ± 0.7
PEG:PC (0.5:9.5)		−0.65 ± 0.20			−7.5 ± 2.6	
PG:PC (0.75:9.25)	−1.94 ± 0.07	−1.65 ± 0.06	−1.69 ± 0.05	−24.9 ± 0.8	−21.2 ± 0.8	−21.6 ± 0.5
PC:Chol (10:5)		0.03 ± 0.02			0.8 ± 0.3	
PEG:PC:Chol (0.75:9.25:5)		−0.50 ± 0.06			−6.6 ± 0.8	
PG:PC:Chol (0.75:9.25:5)		−1.96 ± 0.04			−25.2 ± 0.5	

*PC refers to phosphatidylcholine; PG to phosphatidylglycerol, a negatively charged lipid; PEG to PEG-DSPE, a negatively charged lipid; and Chol to cholesterol.

Figure D3 Electrophoretic mobility and zeta potential of PC, PEG-DSPE and PG containing liposomes [Woodle et al. 1992].

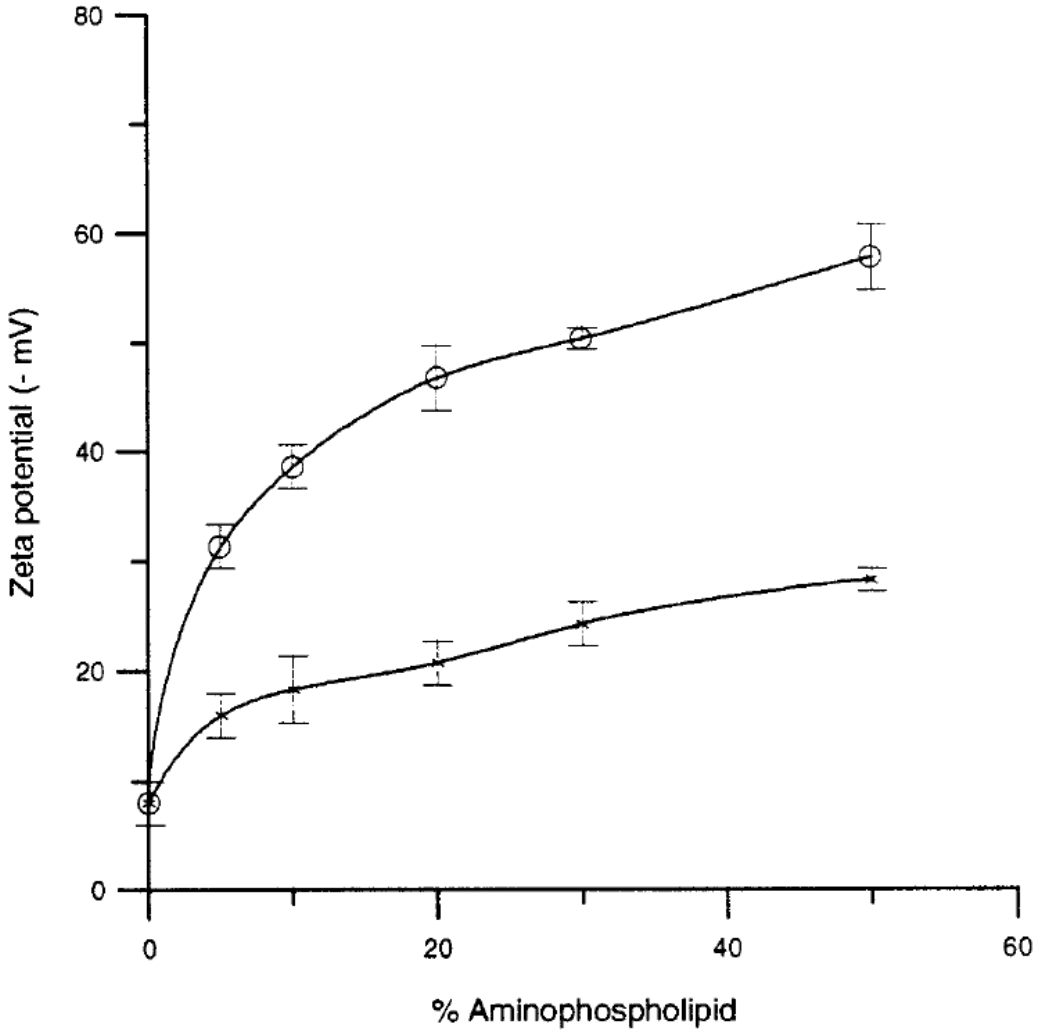

Figure D4 Zeta potential of extruded liposomes. Values are the average of the four sized liposomes at any aminophospholipid composition. Bars point out the standard deviation ($n \geq 3$). PS, (O); PE, (*) [Roy et al. 1998].

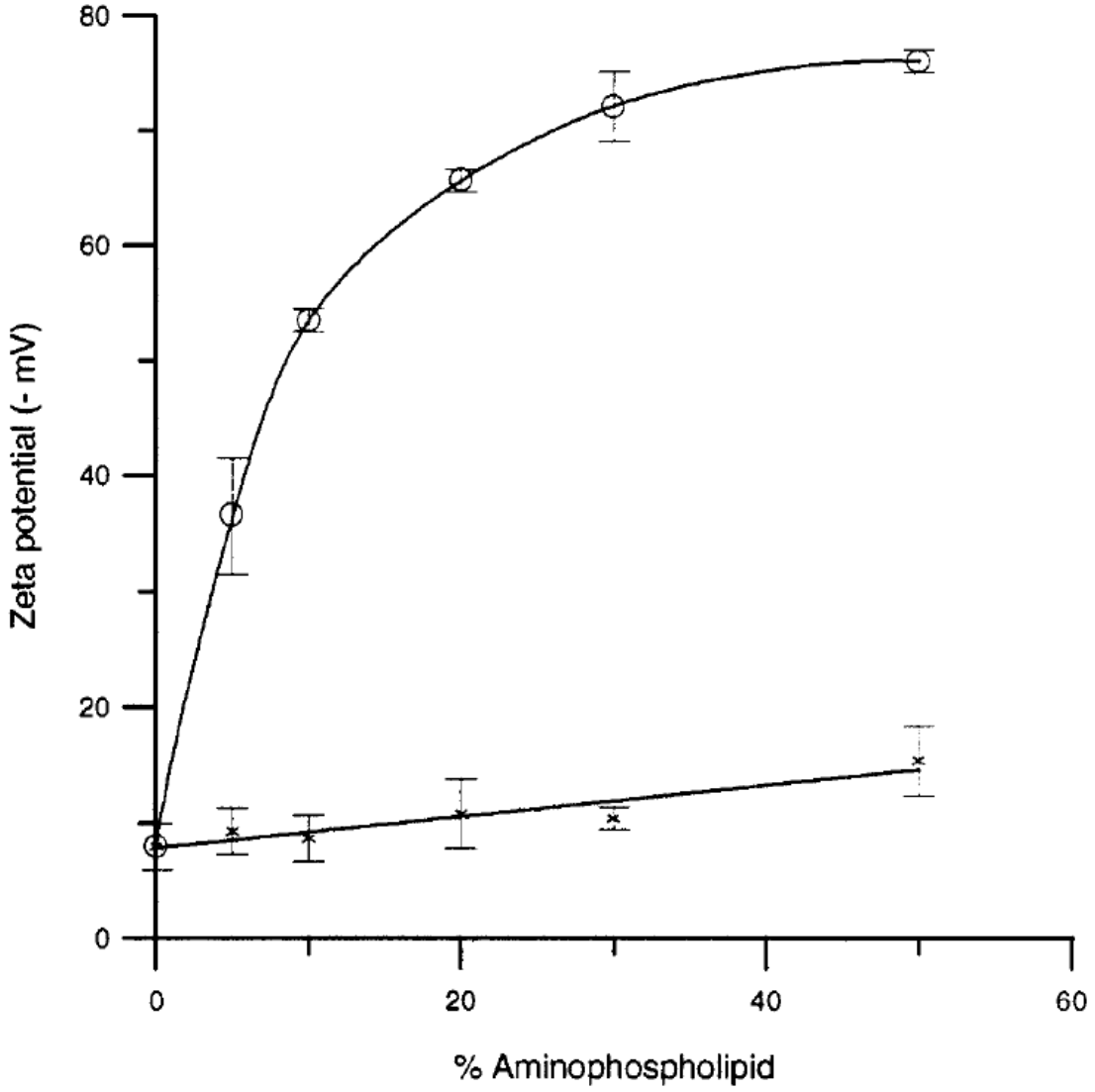

Figure D5 Zeta potential of sonicated liposomes. Bars point out the standard deviation ($n \geq 3$). PS, (O); PE, (*) [Roy et al. 1998].

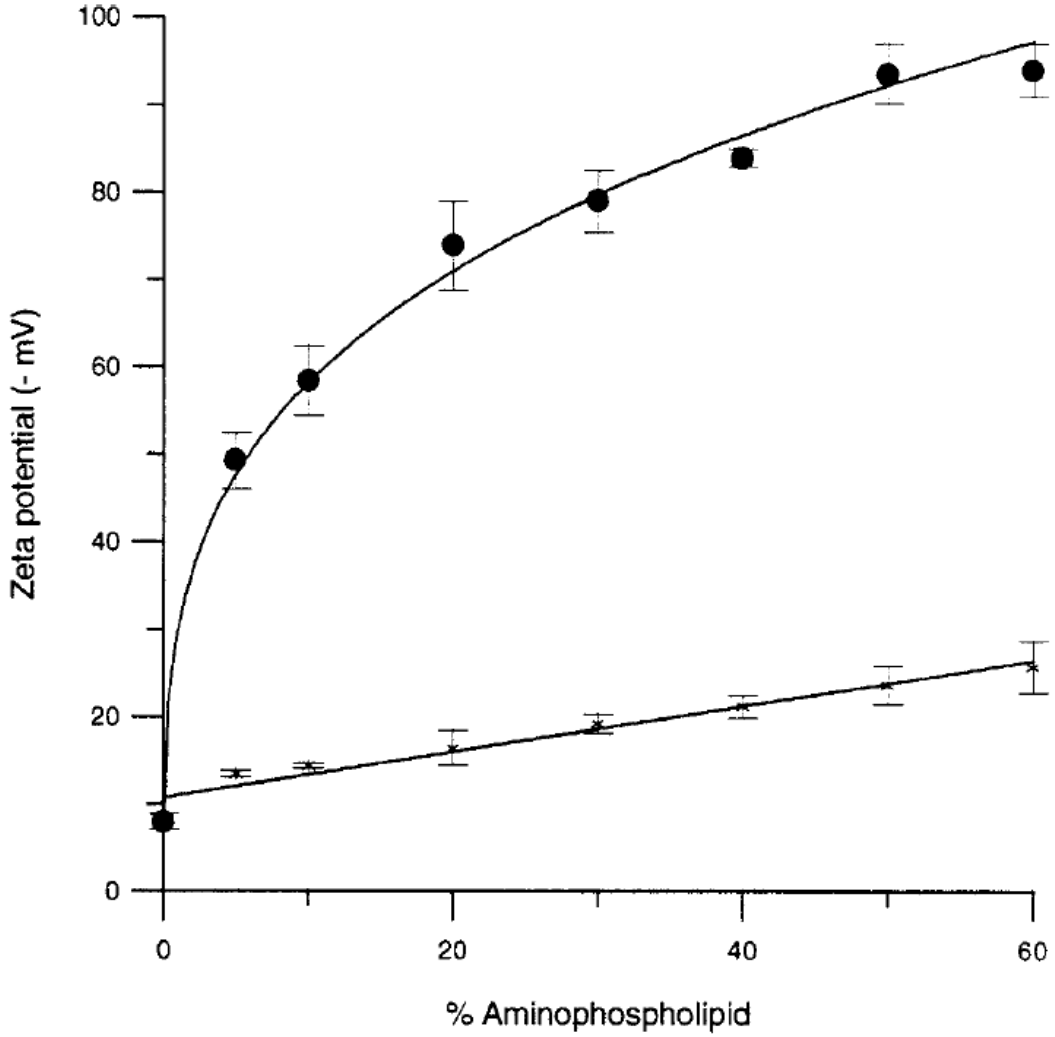

Figure D6 Zeta potential of multi-lamellar vesicle liposomes. Bars point out the standard deviation ($n \geq 3$). PS, (O); PE, (*) [Roy et al. 1998].

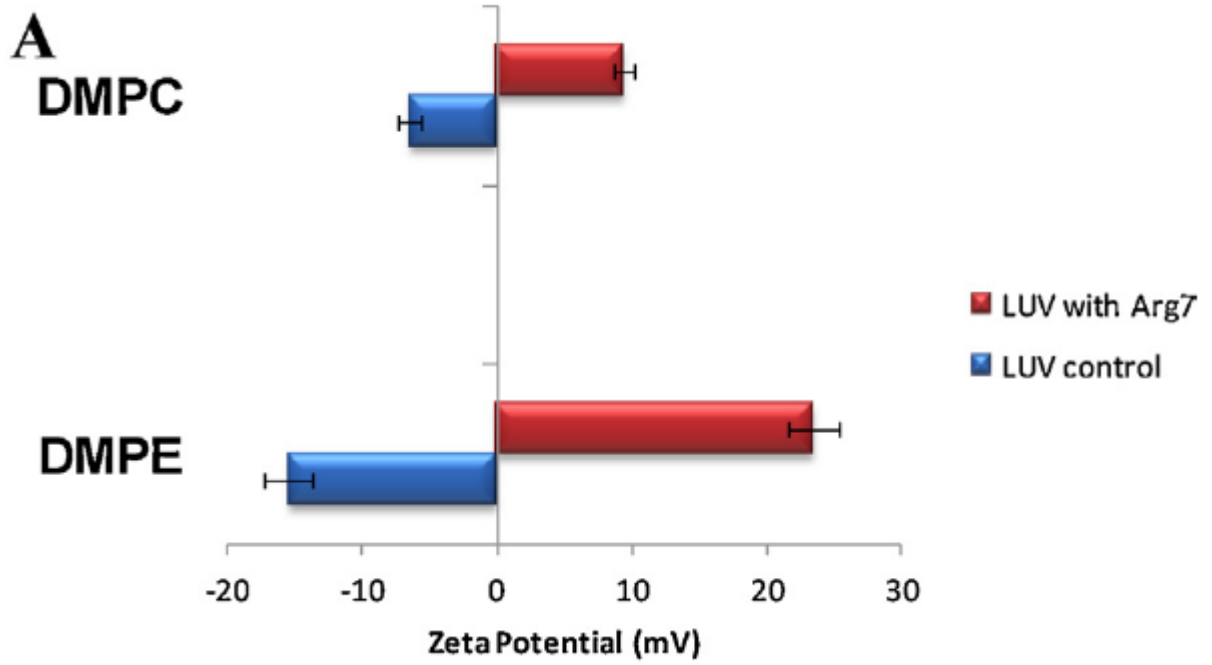

Figure D7 DMPC and DMPE zeta potentials in the absence (blue) and presence (red) of arginine 7 [Disalvo and Bouchet 2014].

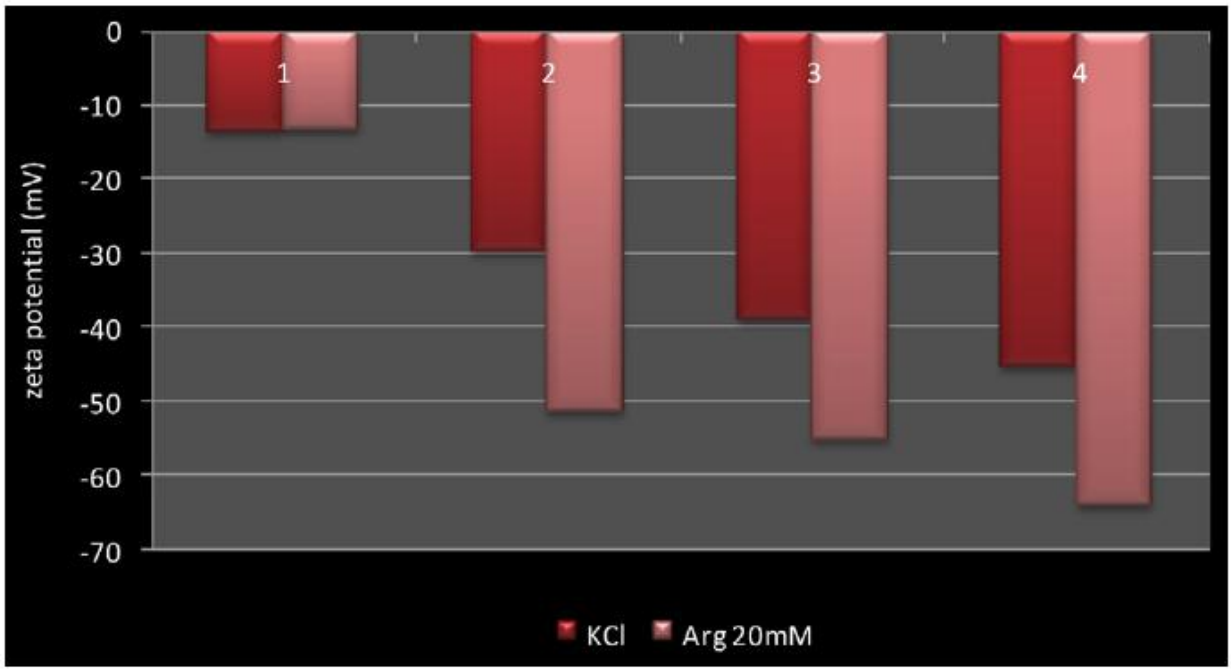

Figure D8 Effects of arginine on DMPC (1), dimethyl-PE (2), monomethyl-PE (3) and DMPE (4). Red columns: Liposomes in 1 mM KCl; pink column: Liposomes in 1 mM KCl and 20 mM arginine [Disalvo and Bouchet 2014].

Figure D9 Diagram of a lipid bilayer that contains phosphatidylcholine (red borders) and phosphatidic acid (purple border).

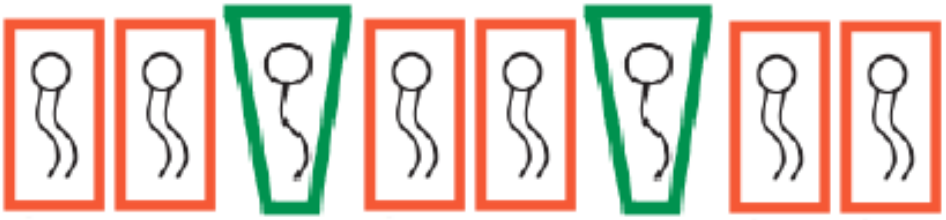

Figure D10 Diagram of a lipid bilayer that contains phosphatidylcholine (red borders) and phosphatidyl inositol 4,5-bisphosphate (green border).

Nanodisc™ Sample	PL^- /Nanodisc™	Z_{DHH} of lipid contribution[b]	Expected charge contribution/Nanodisc™[c]	$\Delta z/\Delta PL$[d]
MSP1D1 10POPS	13	-10.5	-13	0.81
MSP1D1 30POPS	38	-24.4	-38	0.64
MSP1D1 70POPS	88	-42.3	-88	0.48
MSP1E3D1 10POPS	25	-19.0	-25	0.76
MSP1E3D1 30POPS	75	-39.2	-75	0.52
MSP1E3D1 70POPS	175	-74.3	-175	0.42
MSP1D1 10POPA	13	-12.1	-16	0.76
MSP1D1 30POPA	38	-30.9	-47	0.66
MSP1D1 70POPA	88	-52.5	-109	0.48
MSP1D1 10PIP_2	13	-25.6	-38	0.67
MSP1D1 10POPE	13	-7.3	-13	0.56

Table D3 Summary of anionic lipid Nanodisc™ data using MCE in standard buffer.

[a] The number of anionic lipids per Nanodiscs assuming a constant number of lipids per Nanodisc [Ritchie et al., 2009].

[b] The Z^{DHH} contribution solely coming from the lipid head group. Explained in greater detail in **Table D1**

[c] The charge assuming each PS (**Figure C6)** or PA (**Figure C8**) lipid contributes the charge calculated from the pKa values. For PS lipids, the assumption is that each lipid head group contributes a -1 charge. For PA lipids, the assumption is that each lipid head group contributes a -1.25 charge. For PIP_2, the assumption is that each lipid head group contributes a -3 charge.

[d] The charge contribution per lipid head group. This quantity is a ratio of the measured Z_{DHH} lipid contribution (**Table 12**), to that of the calculated charge estimates.

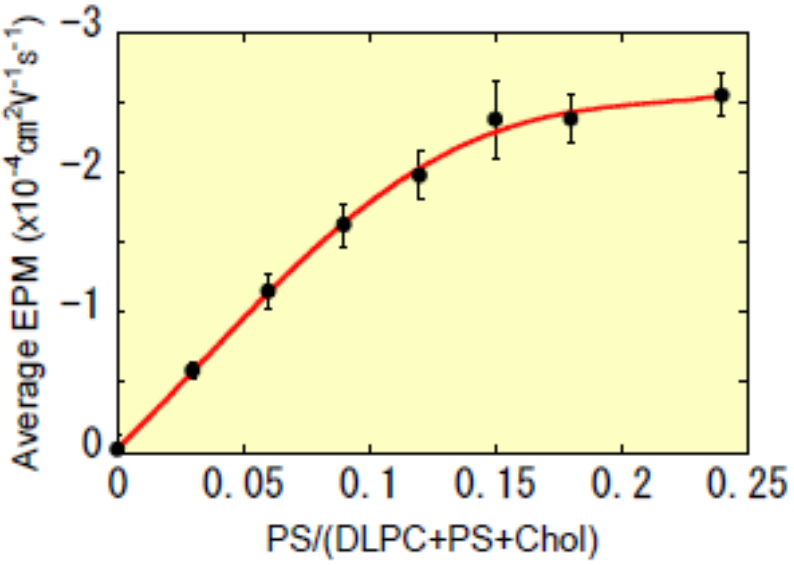

Figure D11 Average electrophoretic mobility of PS liposomes as a function of PS composition [Kato el al., 2011].

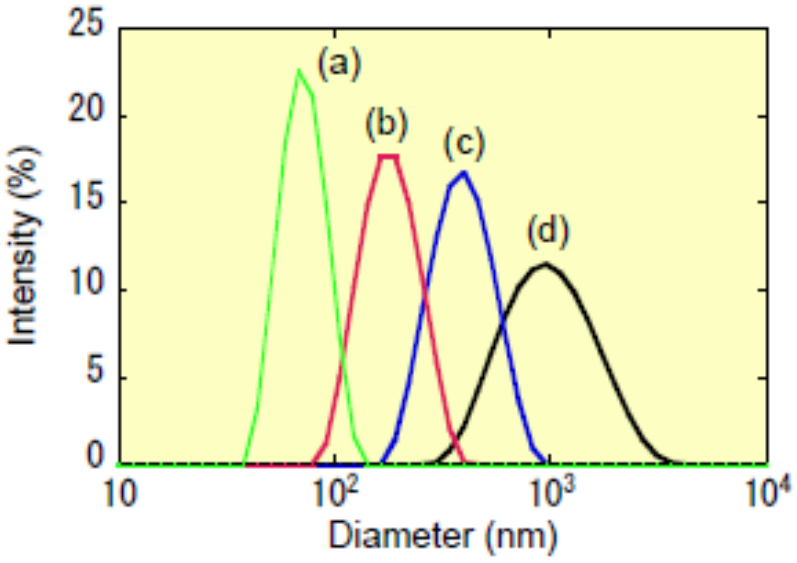

Figure D12 Size distribution of liposomes extruded through membranes with pore sizes of (a) 50 nm, (b) 200 nm, (c) 400 nm, and (d) 1000 nm [Kato et al. 2011].

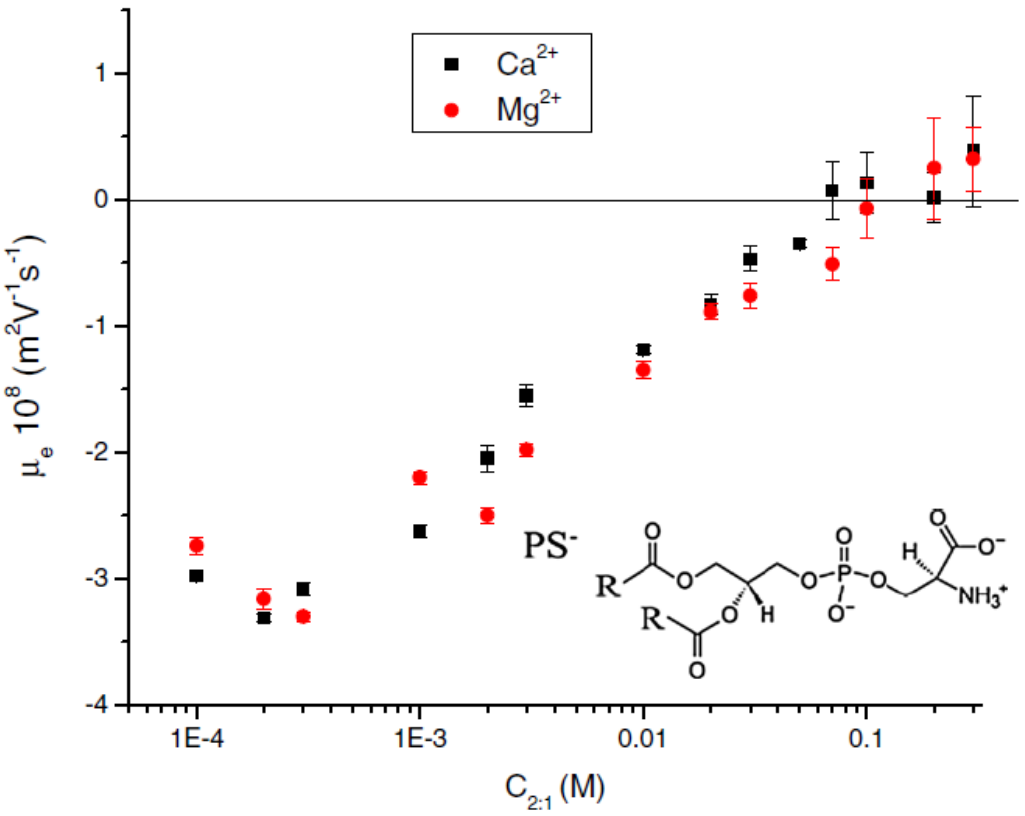

Figure D13 Electrophoretic mobility of PS liposomes as a function of $Na(NO_3)_2$ and $Mg(NO_3)_2$. Squares and circles are $Ca(NO_3)_2$ and $Mg(NO_3)_2$, respectively. Inset: Molecular structure of PS lipids [Martin-Molina et al. 2012].

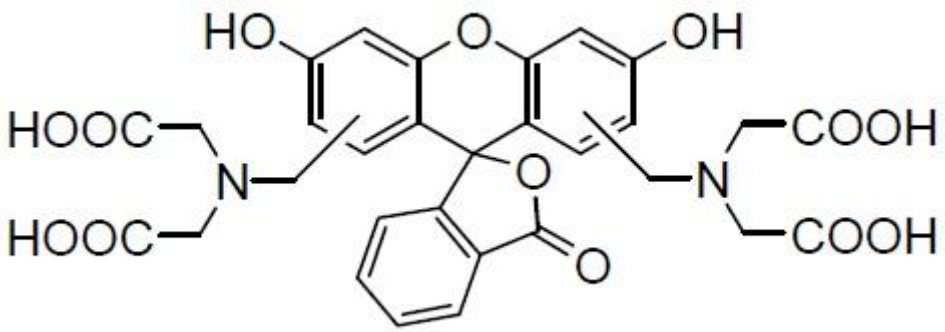

Figure D14 Molecular structure of calcein.

PS liposome/Nanodisc™ composition		Electrophoretic mobility ($cm^2/V \cdot s$)
10% PS liposomes	Kato et al. (2011)	-1.5×10^{-4}
10POPS Nanodiscs	MCE	$-7.1 \times 10^{-5} \pm 2.9 \times 10^{-6}$

PS liposome/Nanodisc™ composition		Electrophoretic mobility ($cm^2/V \cdot s$)
25% PS liposomes	Kato et al. (2011)	-2.5×10^{-4}
30POPS Nanodiscs	MCE	$-1.2 \times 10^{-4} \pm 5.7 \times 10^{-6}$
70POPS Nanodiscs	MCE	$-1.7 \times 10^{-4} \pm 3.8 \times 10^{-6}$

Tables D4a and **D4b Comparison** of electrophoretic mobilities obtained by Kato et al. (2011) using PS liposomes and electrophoretic mobilities obtained by MCE.

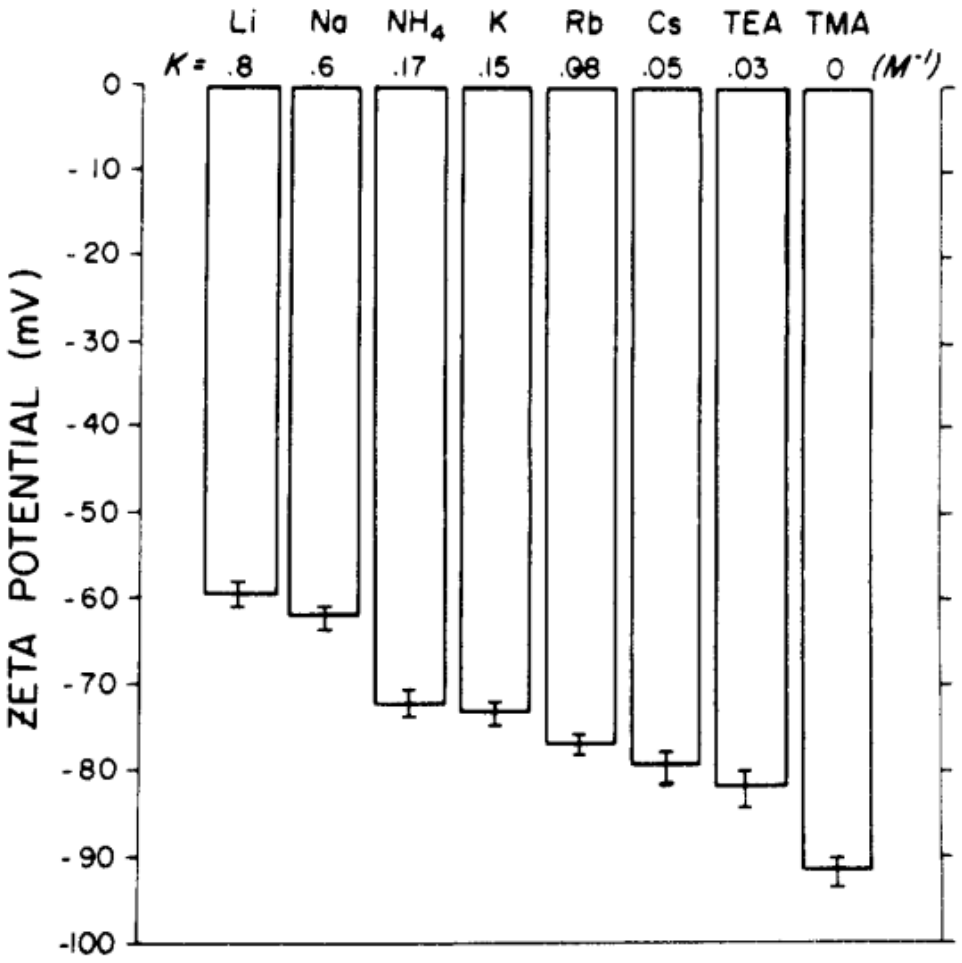

Figure D15 Zeta potentials of multilamellar PS vesicles formed in decimolar chloride solutions of the indicated cations. The solutions also contain 1 x 10^{-4} M EDTA and 1 x 10^{-3} M Tris. The pH was 7.5 and the temperature was 25°C. The error bars indicate the standard deviation of 20 measurements. The values of the intrinsic association constants of the different cations with PS are also shown [Eisenberg et al., 1979].

TABLE I A

SEPARATION OF PS, PG AND PA BILAYERS IN 0.2 M CHLORIDE SOLUTIONS OF Li^+, Na^+, K^+, Cs^+, AND TMA^+ AT CONSTANT OSMOTIC PRESSURE

Ion	PS d_w	log P_π	PG d_w	log P_π	PA d_w	log P
(0.2 M)	*(Å)*	*(dyn/cm²)*	*(Å)*	*(dyn/cm²)*	*(Å)*	*(dyn/cm²)*
Li^+	23.5 ± 0.3	5.3	45.5 ± 0.6	5.4	51.8 ± 1.6	5.2
Na^+	46.9 ± 0.5	5.4	46.4 ± 0.7	5.4	51.7 ± 1.5	5.3
K^+	51.0 ± 1.0	5.3	52.3 ± 0.3	5.3	58.3 ± 1.7	5.2
Cs^+	54.9 ± 0.9	5.3	53.6 ± 2.0	5.3	58.4 ± 1.4	5.3
TMA^+	60.6 ± 0.8	5.3	58.6 ± 0.4	5.3	61.2 ± 0.8	5.2

Figure D16 Separation of PS, PG and PA bilayers in 0.2 M chloride solutions of Li^+, Na^+, K^+, Cs^+ and TMA^+ at constant osmotic pressure. d_w is the distance of interbilayer separation and log P_π is the osmotic pressure [Loosley-Millman et al. 1982].

TABLE I B

ION BINDING AFFINITY SERIES FOR BINDING OF MONOVALENT ALKALI METAL CATIONS TO PS, PG, AND PA BILAYERS

Lipid	Ion adsorption sequence
PS	$Li^+ \gg Na^+ > K^+ > Cs^+ > TMA^+$
PG	$Li^+ \simeq Na^+ > K^+ \simeq Cs^+ > TMA^+$
PA	$Li^+ \simeq Na^+ > K^+ \simeq Cs^+ \geq TMA^+$

Figure D17 Ion binding affinity series for binding of monovalent alkali metal cations to PS, PG, and PA bilayers [Loosley-Millman et al. 1982].

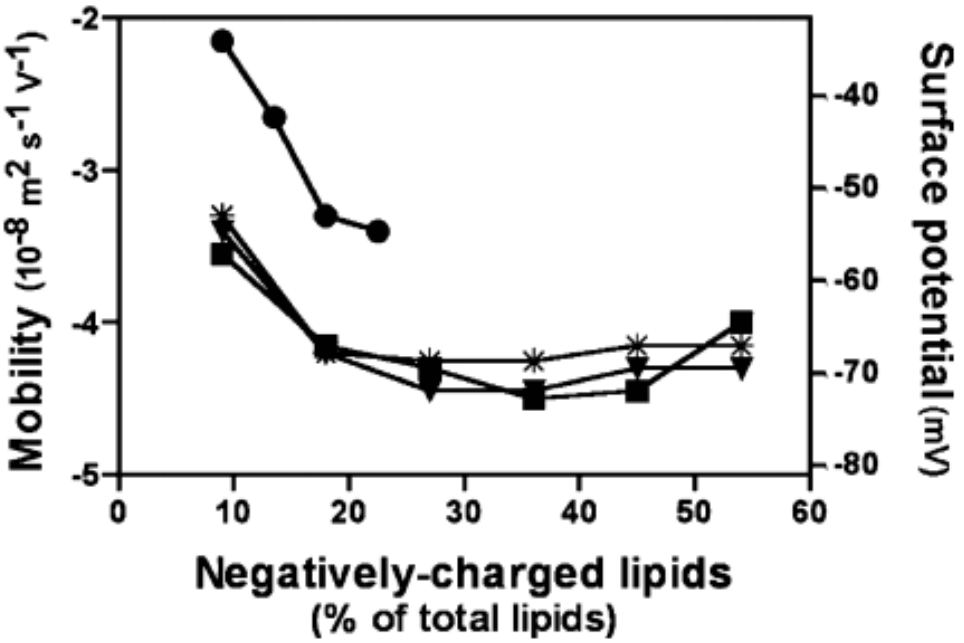

Figure D18 Electrphoretic mobility of liposomes containing increasing amounts of negatively-charged lipids; phosphotidyl inositol (■), phosphatidylserine (▼), phosphatidic acid (*), gangliodside GM1 (●) measured by capillary electrophoresis (12 kV; 30 min). The abscissa shows the percentage of negatively-charged present in liposomes. The left ordinate shows the actual mobility and the right ordinate the corresponding calculated surface potential of each liposome preparation. Each data point shown is the mean of triplicate, with less than 6% variation (S.D. values have not been shown for the sake of clarity) [Piret et al., 2005].

	$\Delta z/\Delta PA^a$	$\Delta z/\Delta PA^b$
MSP1D1 10POPA	0.92	0.76
MSP1D1 30POPA	0.86	0.66
MSP1D1 70POPA	0.64	0.48

Table D5 $\Delta z/\Delta PA$ calculations from the measured electrophoretic mobility of POPA Nanodiscs.

[a] represents the unit of charge per lipid head group if PA lipids contribute a -1 charge per lipid head group.

[b] represents the unit of charge per lipid head group if PA lipids contribute a -1.25 charge per lipid head group.

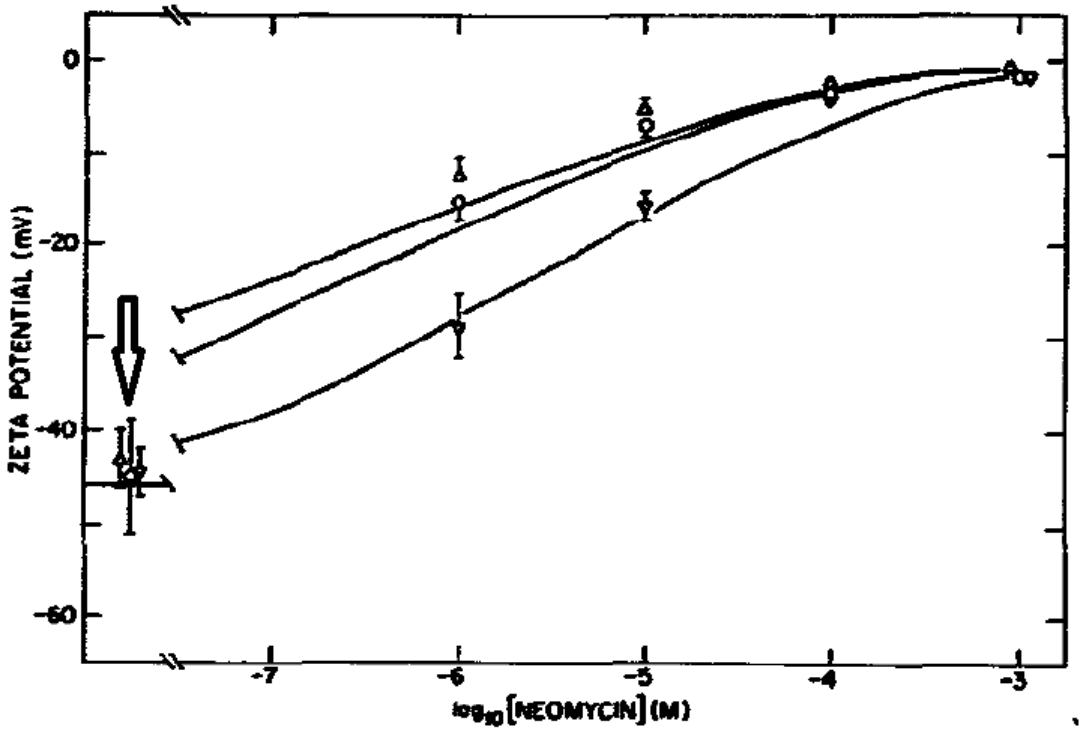

Figure D19 The effect of neomycin on the zeta potential of 10:1 (mol/mol) PC:PIP2 vesicles formed in 0.1 M KCl, 1 mM MOPS at pH 6.0 (triangles), 7.0 (circles), and 8.0 (inverted triangles). The valence of the PIP_2 molecules in the absence of neomycin was calculated to be -1.8 in all cases [Gabev et al. 1989].

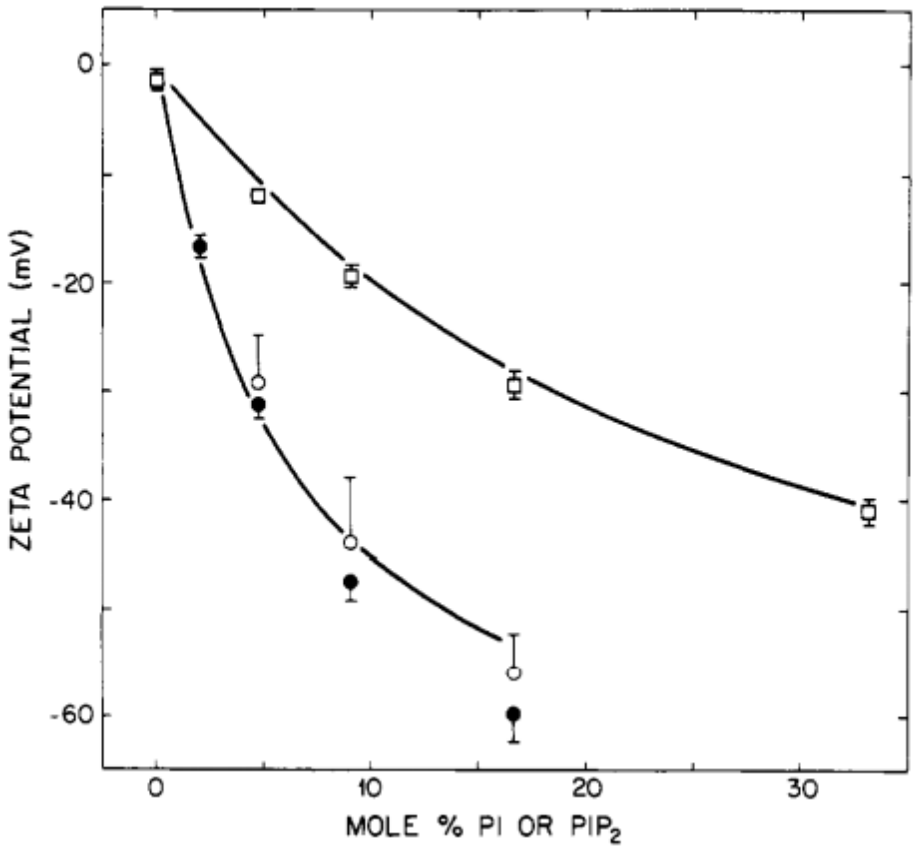

Figure D20 Zeta potential of PC/PIP_2 (circles) and PC/PI (squares) multilamellar vesicles plotted as a function of the mole percent anionic lipid in the vesicle. The solutions contained 0.1 M KCl buffered to pH 7.0 with 1 mM MOPS. The open circles represent data obtained from vesicles formed by using the sodium salt of PIP_2; the closed circles represent data obtained from vesicles formed by using the ammonium salt of PIP_2. The vertical bars in the figures represent the standard deviations when these are larger than the size of the symbols [Toner et al. 1988].

Table I: Number of Cations Bound to PIP_2 in a Bilayer Membrane Exposed to a 0.1 M KCl, pH 7, Solution

cation	concn (M)	no. of cations bound per PIP_2 molecule	
		$\psi_0 = -30$ mV	$\psi_0 = -60$ mV
hydrogen	10^{-7}	0.9	1.3
potassium	10^{-1}	0.7	1.5
calcium	10^{-6}	0.01	0.08
magnesium	10^{-4}	0.2	1.0
magnesium	10^{-3}	1.3	2.5

Figure D21 Number of cations bound to PIP_2 in a bilayer membrane exposed to a 0.1 M KCl, pH 7.0 solution at predicted surface potentials of -30 mV and -60 mV [Toner et al. 1988].

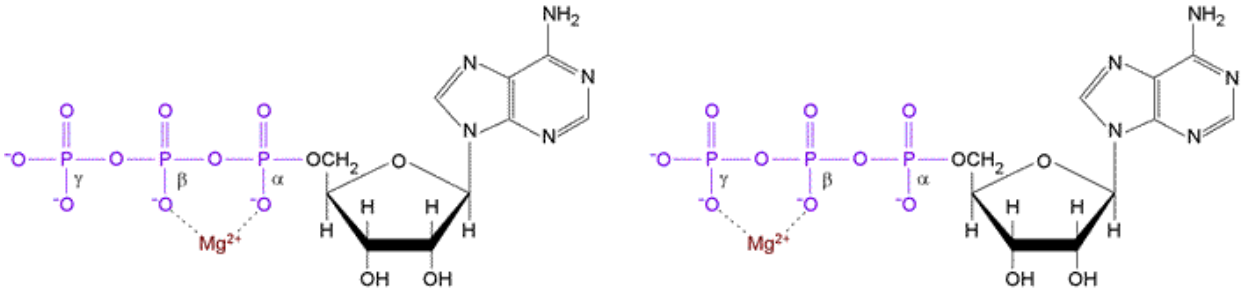

Figure D22 Image of Mg^{2+} chelating polyphosphate groups such as ATP.

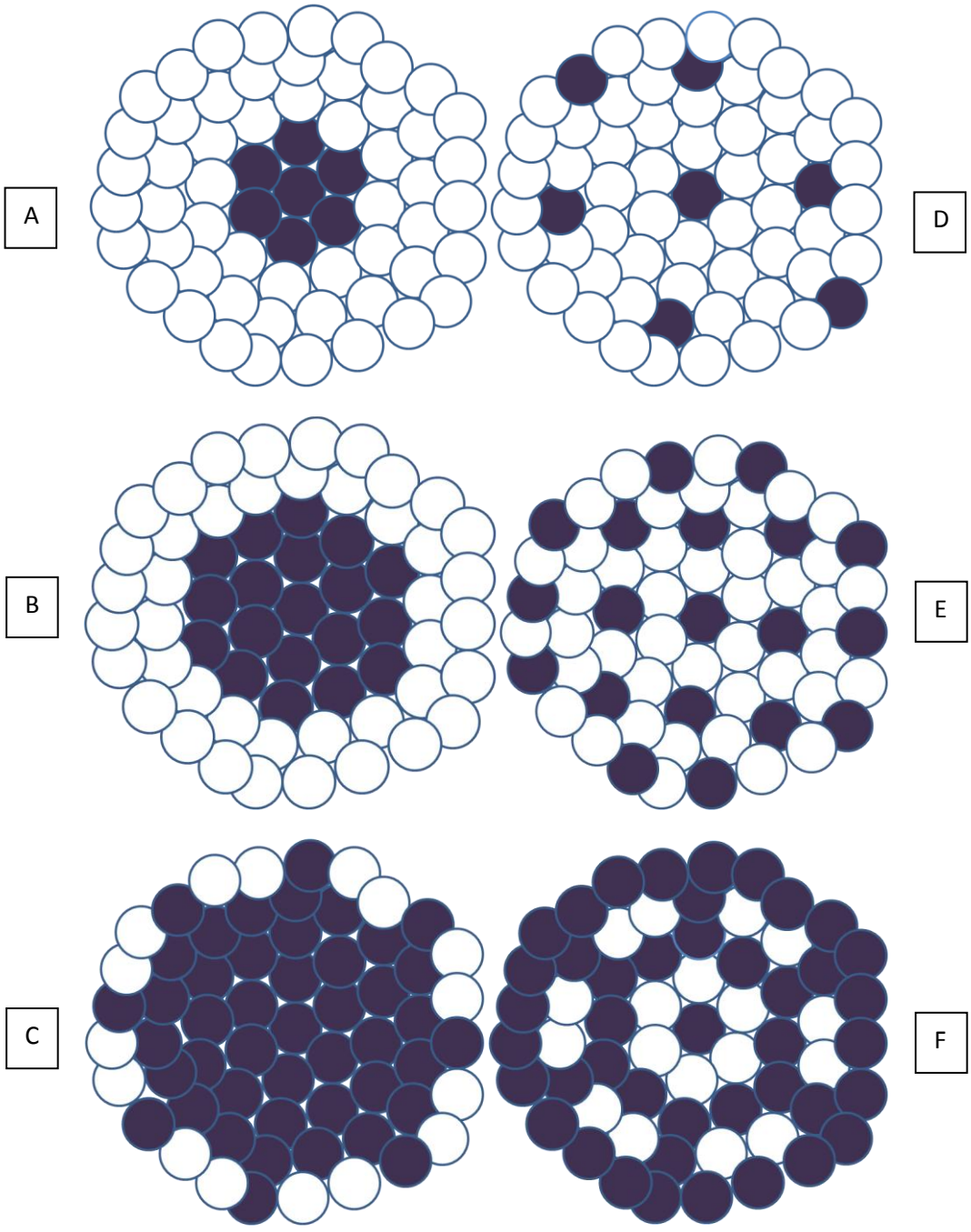

Figures D23a, D23b, D23c, D23d, D23e, D23f Models of the distribution of charged lipids within the Nanodisc^{TM} structure. Figures a, b and c represent an extreme model of lipids in which the charges are packed in very tightly. Figures d, e and f represent a distributed model, in which the charges are more evenly spaced out within the Nanodisc^{TM} bilayer. This model assumes that there is limited electrostatic interaction with the membrane scaffolding protein due to the amphipathic nature of the protein structure, with hydrophobic amino acids dominating the interactions with the hydrocarbon chain of the lipids. Hydrophilic amino acids are more likely faced outward toward the aqueous environment.

	Charge at pH 7.0	Charge at pH 7.4	Charge at pH 8.0	Charge at pH 8.5
MSP1D1 MSP	-13.6	-15.8	-17.2	-18.8

Table D6 The calculated charge estimate of the amino acid composition per two MSPs at various pHs.

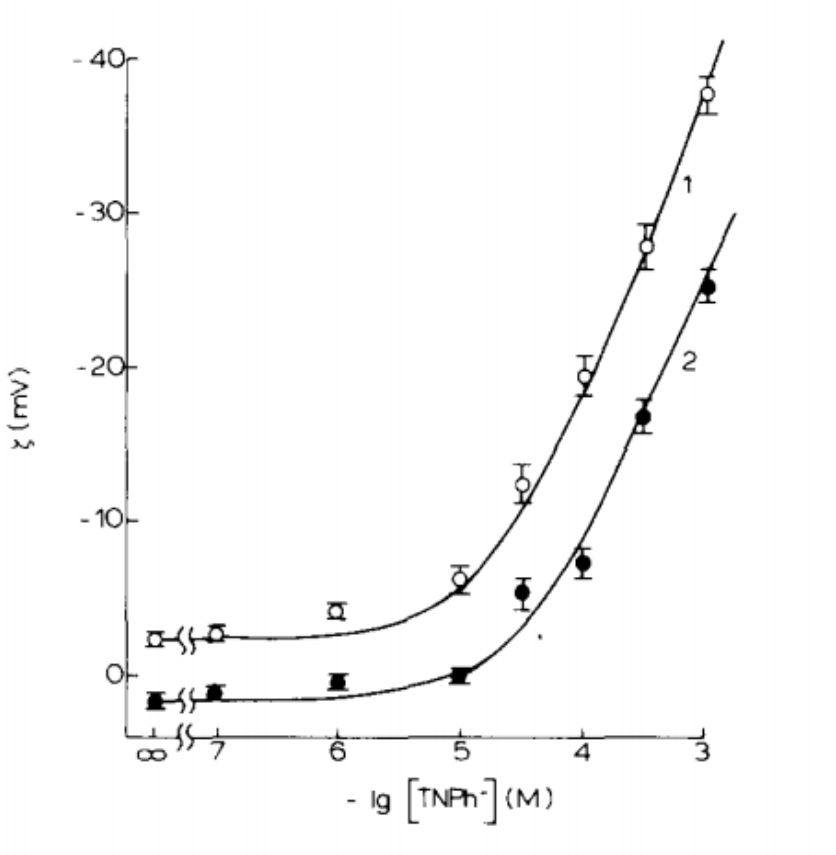

Figure D24 Dependence of the zeta potential of DMPC liposomes on the concentration of $TNPh^-$ at 26°C (○) and 18°C (■). The aqueous solutions were buffered to pH 7.4 with 5 mM Tris-HCl and the ionic strength was held constant at 0.01 M with KCl [Tatulian, 1983].

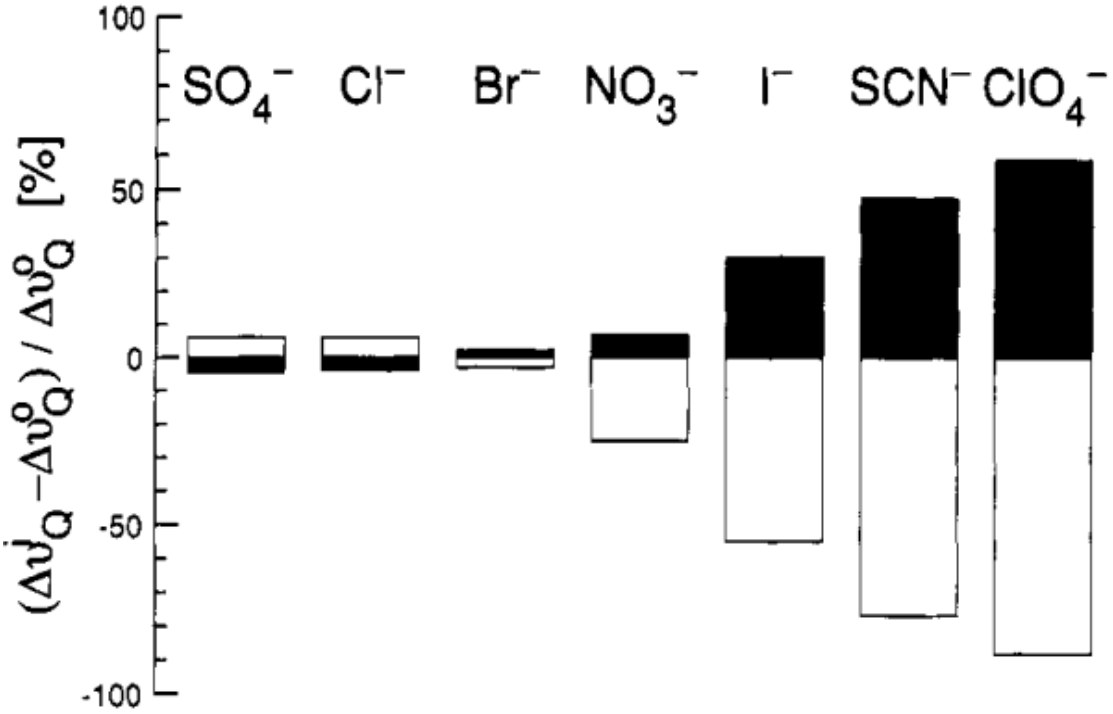

Figure D25 Survey of the effects of various aqueous anions on the quadrupole splitting from α- and *β*-choline-deuterated POPC. The change in value of the quadrupole splitting measured with either POPC-α-d_2 (dark bars) or POPC-β-d_2 (light bars) containing membranes in the presence of 0.5 M of the indicated anion is expressed as the percent change of the quadrupole splitting relative to its value in the absence of anions [Rydall and Macdonald, 1992].

THE PARAMETERS K^{-1} (mM) AND σ_{max} ($\mu C/cm^2$) USED IN Eqn. 6 TO DESCRIBE THE BINDING OF SEVERAL ANIONS TO DMPC LIPOSOMES ABOVE AND BELOW T_c

Anion	$T = 25°C$		$T = 22°C$	
	K^{-1}	σ_{max}	K^{-1}	σ_{max}
$TNPh^-$ [a]	0.20 ± 0.07	2.3 ± 0.7	0.22 ± 0.08	1.4 ± 0.3
ClO_4^-	4.5 ± 0.3	1.0 ± 0.1	4.3 ± 0.3	0.6 ± 0.04
I^-	25 ± 3.5	2.0 ± 0.2	27 ± 4.0	1.2 ± 0.1
SCN^-	100 ± 7.0	5.5 ± 0.4	110 ± 10	3.2 ± 0.2
Br^-	280 ± 25	2.6 ± 0.3	280 ± 25	1.7 ± 0.2
NO_3^-	480 ± 40	1.8 ± 0.2	500 ± 60	1.1 ± 0.1

[a] The parameters presented correspond to 26 (left) and 18°C (right).

Figure D26 The parameters K^{-1} (binding constant, expressed in mM) and σ_{max} (the maximum number of binding sites per unit area, expressed in $\mu C/cm^2$) used to describe the binding of several anions to DMPC liposomes at 25°C and 22°C [Tatulian, 1983].

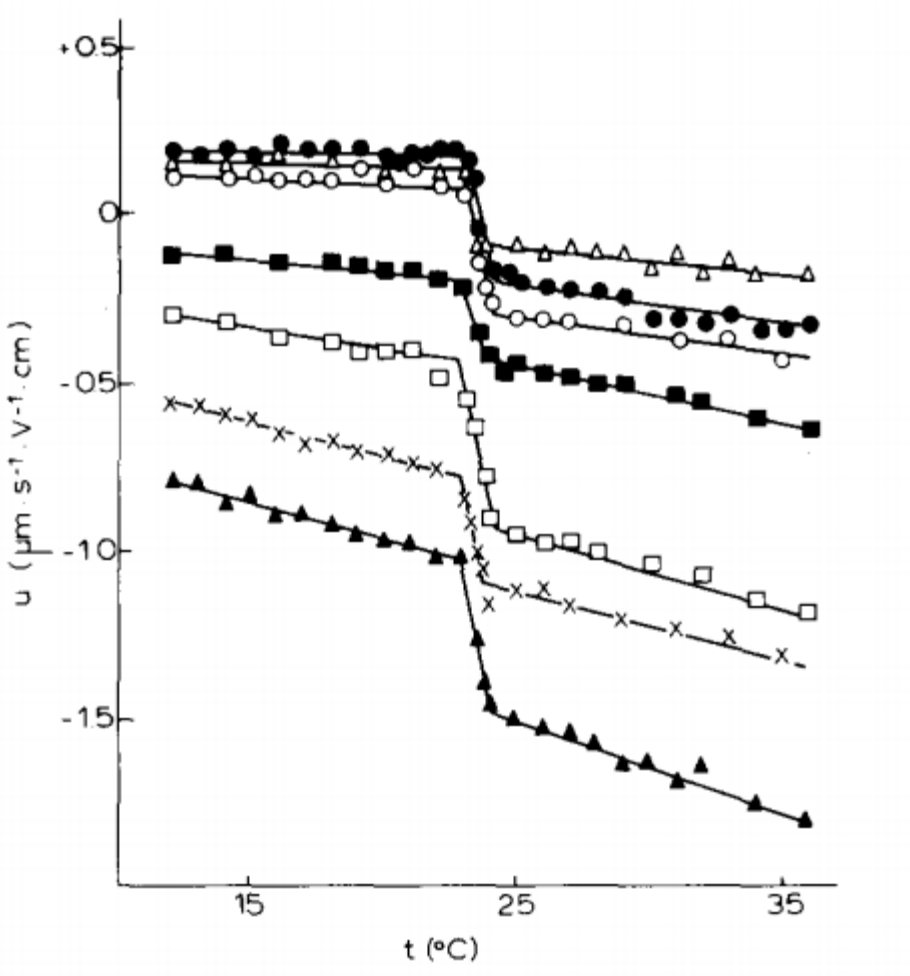

Figure D28 Temperature dependence of the electrophoretic mobility of DMPC liposomes in 0.01 M solutions of K_2SO_4 (Δ), KCl (●), KNO_3 (○), KBr (■), KSCN (□), KI (x), and $KClO_4$ (▲) buffered to 7.4 with 5 mM Tris-HCl [Tatulian, 1983].

TABLE I

Heats of Ionization of $H_2PO_4^-$ at Ionic Strengths of 0 and 0.70 M and of Tris Hydrochloride at 0.65 M*

Temperature	$H_2PO_4^-$; $\mu = 0$†		$H_2PO_4^-$; $\mu = 0.70$		Tris;‡ $\mu = 0.65$	
	pK_A'	$\Delta H°$	pK_A'	ΔH	pK_A'	ΔH
°C.						
5	7.27	1700	6.76	6000 ± 300	8.99	+11,700 ± 200
15	7.23	1400	6.68	2900 ± 300	8.67	+11,700 ± 200
25	7.21	800	6.64	−200 ± 300	8.38	+11,700 ± 200
37	7.19	250	6.68	−4200 ± 300	8.05	+11,700 ± 200
50	7.19	−350			7.71	

Figure D29 Heats of Ionization of H_2PO^{4-} at Ionic Strengths of 0 and 0.70 M and of Tris Hydrochloride at 0.65 M [Bernard, 1955].